Lehrstuhl für Genetik der
Technischen Universität München

Genetic and biochemical characterisation of *Arabidopsis thaliana* pantothenate synthetase

Rafał Kazimierz Jończyk

Vollständiger Abdruck der von der Fakultät Wissenschaftszentrum Weihenstephan für Ernährung, Landnutzung und Umwelt der Technischen Universität München zur Erlangung des akademischen Grades eines

Doktors der Naturwissenschaften (Dr. rer. nat.)

genehmigten Dissertation.

Vorsitzender:	Univ.-Prof. Dr. Kay H. Schneitz
Prüfer der Dissertation:	1. Univ.-Prof. Dr. Alfons Gierl
	2. Univ.-Prof. Dr. Gert Forkmann
	3. Univ.-Prof. Dr. Wilfried Schwab

Die Dissertation wurde am 31. 01. 2007 bei der Technische Universität München eingereicht und durch die Fakultät Wissenschaftszentrum Weihenstephan für Ernährung, Landnutzung und Umwelt am 26. 04. 2007 angenommen.

Zusammenfassung

Pantothenat (Vitamin B_5) ist der universelle Vorläufer von Coenzym A, das essentielle Funktionen im Metabolismus von Kohlenhydraten und Fettsäuren erfüllt. Die Biosynthese von Pantothenat ist auf Pflanzen, Pilze und Mikroorganismen beschränkt, während Tiere das Vitamin mit der Nahrung aufnehmen müssen. Daher sind die Enzyme dieses Synthesewegs interessant als potentielle Targets für neuartige Herbizide, Fungizide und antimikrobielle Wirkstoffe. Darüber hinaus wird die Pantothenatbiosynthese mit dem Ziel bearbeitet, das Vitamin in Mikroorganismen zu produzieren und Pflanzen mit erhöhtem Vitamin B_5-Gehalt zu erzeugen.

Die Biochemie, der Mechanismus und die Regulation der Biosynthese von Pantothenat sind in Mikroorganismen ausführlich untersucht worden, aber das Verständnis dieses Synthesewegs in Pflanzen ist weiterhin unvollständig. In *Arabidopsis thaliana* wird Pantothenat durch das cytosolische Enzym Pantothenat Synthetase (PTS) synthetisiert, das von einem einzigen Gen (*PTS*) kodiert wird. Es gibt Hinweise, dass Pflanzen über einen weiteren, PTS-unabhängigen Syntheseweg für Pantothenat verfügen, der über Pantoyllacton anstelle von Pantoat verläuft. Um die physiologische Rolle von PTS in Arabidopsis näher zu bestimmen, wurden in dieser Arbeit zunächst zwei T-DNA Insertionsmutanten charakterisiert. Beide Insertionsallele von *PTS* verursachten einen rezessiven, Embryo-lethalen Phänotyp. Normale Samenentwicklung und der übrige Lebenszyklus von *pts* Mutanten konnten entweder durch Zugabe von exogenem Pantothenat oder durch Transformation mit dem *E. coli* Gen für PTS wiederhergestellt werden. Diese Ergebnisse weisen stark darauf hin, dass die alleinige Rolle von Arabidopsis PTS in der Synthese von Pantothenat besteht und dass kein weiteres Enzym in der Lage ist, das Vitamin in ausreichender Menge bereitzustellen. Durch konstitutive, cytosolische Überexpression von *E. coli* PTS in Arabidopsis konnte die aus Blattgewebe extrahierbare PTS-Aktivität gegenüber Wildtypkontrollen um das bis zu 660-fache erhöht werden. Damit war jedoch keine signifikante Änderung des Pantothenat-Gehalts in Blättern verbunden. Dieses Ergebnis legt nahe, dass die PTS Aktivität in Arabidopsis nicht limitierend für die Produktion von Pantothenat ist. *PTS*-Promotor::β-glucoronidase Studien und die Analyse von öffentlichen Microarraydaten zeigten, dass das *PTS* Gen in Arabidopsis ubiquitär exprimiert wird, was der fundamentalen Funktion dieses Gens entspricht.

Die Biosynthese von Pantothenat in Pflanzen ähnelt dem entsprechenden Prozess in Bakterien, aber es gibt wichtige Unterschiede sowohl bei den beteiligten Enzymen als auch in

der subzellulären Organisation. Im Gegensatz zu bakteriellen PTS zeigen pflanzliche PTS starke Substratinhibierung durch Pantoat, und dieses Phänomen wurde bisher als Teil eines regulatorischen Mechanismus für Pantothenat in Pflanzen diskutiert. Um die strukturelle Basis und die physiologische Relevanz der Substratinhibierung in pflanzlichen PTS aufzuklären, wurden detaillierte enzymkinetische Untersuchungen mit PTS aus Arabidopsis und *E. coli* durchgeführt. Zunächst wurde gezeigt, dass Arabidopsis PTS ein homodimeres Enzym ist, das demselben zweischrittigen Reaktionsmechanismus folgt, der für *E. coli* PTS bereits etabliert ist. Außerdem besaßen Arabidopsis und *E. coli* PTS nahezu identische pH-Profile für die Pantothenatsynthese (Vorwärtsreaktion) und die Pantothenat:β-Alanin Austauschreaktion, was nahe legt, dass konservierte Aminosäurereste im aktiven Zentrum an den geschwindigkeitsbestimmenden Schritten dieser Prozesse beteiligt sind. Ein Alignment der verfügbaren PTS Aminosäuresequenzen bestätigte, dass die bekannten Reste im aktiven Zentrum von bakteriellen PTS in der gesamten Proteinfamilie konserviert sind. Das Alignment zeigte außerdem eine besondere Dimerisierungsdomäne in PTS aus grünen Pflanzen, die, verglichen mit PTS aus Bakterien oder Pilzen, durch eine Insertion von ca. 20 Aminosäureresten gekennzeichnet ist. Enzymkinetische Untersuchungen von wildtypischen und mutanten Formen der PTS aus Arabidopsis zeigten, dass die Pflanzen-spezifische Dimerisierungsdomäne allosterische Wechselwirkungen der beiden Untereinheiten vermittelt, die Substratinhibierung und andere nicht-hyperbole kinetische Eigenschaften zur Folge haben. Die kinetischen Eigenschaften von Arabidopsis PTS ergeben keinen Hinweis auf eine biochemische Regulation dieses Reaktionsschritts im Syntheseweg von Pantothenat. Allerdings wurde gezeigt, dass der allosterische Mechanismus zu erhöhter katalytischer Effizienz bei niedrigen Pantoat- und β-Alaninkonzentrationen führt, und zwar auf Kosten von verringerter katalytischer Effizienz bei hohen Pantoat- und β-Alaninkonzentrationen. Dieses Ergebnis legt nahe, dass Allosterie in pflanzlichen PTS evolviert ist, um eine Feinabstimmung des Enzyms auf niedrige Substratkonzentrationen zu erreichen.

Aufgrund der vorliegenden Arbeit kann ein verbessertes Modell der Pantothenatbiosynthese in Pflanzen vorgeschlagen werden, in dem die Rate der Pantothenatproduktion durch die Verfügbarkeit von Pantoat oder β-Alanin im Cytosol, aber nicht durch PTS Aktivität limitiert wird. In diesem Modell haben die spezifischen katalytischen Eigenschaften von pflanzlichen PTS keinerlei regulatorische Funktion, sondern erlauben eine robuste Synthese von Pantothenat bei niedrigen Gehalten an Pantoat und β-Alanin. Eine niedrige cytosolische Konzentration von Pantoat würde außerdem bedeuten, dass

Substratinhibierung, also die auffälligste kinetische Eigenschaft von pflanzlichen PTS *in vitro*, keinerlei Bedeutung *in vivo* hätte. Schließlich besagt dieses Modell der Pantothenatbiosynthese, dass PTS kein geeignetes Target für die Erhöhung des Vitamin B_5-Gehalts in Pflanzen ist.

Summary

Pantothenate (vitamin B_5) is the precursor to coenzyme A, an essential cofactor that is required in the metabolism of carbohydrates and fatty acids. As a vitamin, the pathway of its synthesis is confined to plants, fungi, and microorganisms, and animals must obtain it in their diet. Consequently, the enzymes of the pathway are potential targets for novel drugs including herbicides, fungicides, and antimicrobial agents. Furthermore, there is an interest in developing a biotransformation system for the production of pantothenate by microorganisms and to enhance the vitamin B_5 content of plants.

The biochemistry, mechanism and regulation of the biosynthetic pathway of pantothenate have been thoroughly characterized in microorganisms, but our knowledge of this pathway in plants remains fragmented. In *Arabidopsis thaliana*, pantothenate is synthesised by the cytosolic enzyme pantothenate synthetase (PTS) which is encoded by a single gene (*PTS*). It is unclear whether PTS represents the only mode of pantothenate production in plants as two previous reports pointed to the existence of a parallel pathway that proceeds via pantoyl lactone instead of pantoate. To asses the role of PTS in Arabidopsis, two T-DNA insertion mutants were characterized. Both mutant alleles of Arabidopsis *PTS* conferred a recessive embryo-lethal phenotype. Normal seed development and the remaining life cycle could be restored in *pts* mutants either by supplying exogenous pantothenate or by introducing a T-DNA carrying the *E. coli* gene for PTS. This is strong evidence that the sole role of PTS in Arabidopsis is to synthesize pantothenate and that no other enzyme can produce sufficient amounts of the vitamin. Constitutive overexpression of *E. coli* PTS in the cytosol caused the extractable PTS activity in transgenic Arabidopsis leaves to increase by up to 660-fold, but this had no effect on the steady-state levels of pantothenate. This suggests that PTS activity is not limiting for the synthesis of pantothenate in Arabidopsis. *PTS*-promoter::β-glucoronidase reporter activity and analysis of publicly available microarray data showed that *PTS* is expressed throughout the Arabidopsis plant which is consistent with the basal function of this gene.

The process of pantothenate biosynthesis is similar in bacteria and plants, but there are important differences, both in the enzymes involved and in the overall organization of the pathway. In contrast to bacterial PTS, plant PTS show strong substrate inhibition by pantoate, and it has been hypothesised that this property is part of a regulatory mechanism in plants. In order to clarify the structural basis for substrate inhibition in plant PTS and its physiological significance, detailed kinetic studies were carried out with recombinant PTS from Arabidopsis

and *E. coli*. Initially, Arabidopsis PTS was shown to be a homodimeric enzyme and to follow the same two-step reaction mechanism that was previously established for *E. coli* PTS. Also, Arabidopsis and *E. coli* PTS were found to possess near-identical pH profiles for pantothenate synthesis (forward direction) and for the pantothenate:β-alanine exchange reaction. This suggests that conserved active site residues are involved in the rate-limiting steps of these reactions. An alignment of the available PTS amino acid sequences confirmed that the known active site residues of bacterial PTS are highly conserved throughout the protein family. The alignment also revealed a distinct dimerisation domain in PTS from green plants that is characterised by an insertion of approximately 20 amino acids relative to bacterial or fungal PTS. Kinetic analyses of wild type and mutant forms of Arabidopsis PTS showed that the plant-specific dimerisation domain mediates allosteric subunit interactions that cause substrate inhibition by pantoate and other non-hyperbolic responses. The kinetic properties of Arabidopsis PTS provide no basis for a biochemical regulation of this step in the pantothenate pathway. However, it was found that the allosteric mechanism leads to enhanced catalytic efficiency at low pantoate and β-alanine concentrations at the expense of decreased catalytic efficiency at elevated pantoate and β-alanine concentrations. This suggests that allostery arose in plant PTS in order to fine-tune the enzyme to low substrate concentrations.

Based on the results of this work, an enhanced model of pantothenate biosynthesis in plants can be proposed, where the rate of pantothenate production is limited by the availability of pantoate or β-alanine in the cytosol but not by PTS activity. In this model, the specific catalytic properties of plant PTS have no regulatory function but allow robust synthesis of pantothenate from low amounts of pantoate and β-alanine. Low cytosolic concentrations of pantoate would also mean that substrate inhibition, which is the most obvious kinetic property of plant PTS *in vitro*, is negligible *in vivo*. Finally, this model of pantothenate biosynthesis implies that PTS is not a suitable target for improving the pantothenate content in plants.

Acknowledgments

I would like to thank Prof. Dr. Alfons Gierl for providing me the opportunity to carry out my PhD study in his laboratory at the Lehrstuhl für Genetik.

I would like to express my extreme gratitude to my research supervisor, Dr. Ulrich Genschel, for his unceasing support, guidance, research and academic advice during the course of my study. I am also greatly thankful for friendly relationship acquired over the course of my work, his expert, constructive criticism and precise editing of my thesis. Thanks you for teaching me, being patient, and for the many lessons on writing.

I would like to express my genuine appreciation to Verena Kriechbaumer, for her continuous support, understanding and friendship. Her willingness to help, was not confined to academic concerns alone. Special thanks for altruistically shared Giessdienst, life stories, laughs, coffee, junk food and the greatest help with Arbeitsamt.

I would like to express my sincere appreciation to Dr. Monika Frey, Dr. Ramon Torres-Ruiz for support, guidance, kindness, and academic advices.

My work on this dissertation has been aided in direct and indirect ways by numerous colleagues, including Silvia Ronconi, Gerti Spielbauer, Katrin Schullehner, Birgit Treml, Oksana Kortes, Regina Hüttl, Zheng Yu, Regina Stefanek, Regina Schuhegger, Peggy Müller, Miriam Vogg, Annette Martin, Heidi Miller-Mommerskamp, Hedi Kellner, Carolin Ziegler, Petra Wick, Peter Dobos, Ruohe Yin, Thomas Rauhut, Erich Glawischnig, Holger Schmidt, Andreas Fießelmann.

Contents

Zusammenfassung **i**

Summary **iv**

Acknowledgments **vi**

Contents **vii**

Abbreviations **1**

Chapter 1 Introduction **3**

1.1 Nomenclature for pantothenate synthetase used in the literature and in this work 4

1.2 Pantothenate biosynthesis enzymes 4
1.2.1 Ketopantoate hydroxymethyltransferase 7
1.2.2 Ketopantoate reductase 10
1.2.3 Aspartate decarboxylase 14
1.2.4 Pantothenate synthetase 18

1.3 Metabolic engineering of the bacterial pathway 24

1.4 Organization and regulation of plant pantothenate pathway 27

1.5 Pantothenate transport 30
1.5.1 Pantothenate transport in bacteria 30
1.5.2 Pantothenate transport in yeast 30
1.5.3 Pantothenate transport in animal 31
1.5.4 Pantothenate transport in plants 31

1.6 Aims of this work 32

Chapter 2 Materials and Methods **34**

2.1 General 34

2.2 Enzymes and plasmids 34

2.3 Plant material 35
2.3.1 Segregation analysis 36

2.4 Reagents and media 36
2.4.1 Buffers and media 36
2.4.2 Radioactive reagents 36

2.5 Microbiological techniques 37
2.5.1 Bacterial strains 37
2.5.2 Preparation of *E .coli* XL1 Blue competent cells 37
2.5.3 Preparation of *E. coli* BL21 (DE3) competent cell 37
2.5.4 Preparation of *Agrobacterium* (GV3101 MP90) competent cells 37
2.5.5 *Agrobacterium* transformation (electroporation) 38
2.5.6 *E. coli* transformation (heat-shock) 38
2.5.7 *E. coli* growth condition 38
2.5.8 Transformation of Arabidopsis, floral dip 38
2.5.9 Selection of transformed *A. thaliana* 39

2.5.10 Microscopy 39
2.5.11 GUS staining 39

2.6 DNA techniques 39
2.6.1 Preparation of plasmid DNA from *E. coli* 39
2.6.2 Preparation of plasmid DNA from *Agrobacterium tumefaciens* 39
2.6.3 Preparation of plant genomic DNA 40
2.6.4 Agarose gel electrophoresis and isolation of DNA fragments 40
2.6.5 DNA-Sequencing 40
2.6.6 Bioinformatics tools, protein sequences alignment 41

2.7 Constructs for plant overexpression of *E. coli* and *A. thaliana* pantothenate synthetase proteins 41
2.7.1 Cytosolic construct (pUG-DCC) 42
2.7.2 Plastidic construct (pUG-ARC) 42
2.7.3 Mitochondrial construct (pUG-BHC) 42
2.7.4 Reporter construct (pRJ-PSPRO) 43

2.8 Construct for overexpression of *E. coli* pantothenate synthetase proteins in *E. coli* 43
2.8.1 *E. coli* PTS-N-terminal His-tag, ECPTS plasmid 43
2.8.2 Constructs for overexpression of *A. thaliana* wild type and mutagenized pantothenate synthetase proteins in *E. coli* 44
2.8.2.1 *A. thaliana* PTS-Wild-type (PTS) 44
2.8.2.2 PTS- Mut-1 45
2.8.2.3 PTS-E132A 45

2.9 Genotyping of *pts-1* and *pts-2* 46

2.10 Protein techniques 46
2.10.1 Overproduction of *E. coli* PTS and *A. thaliana* PTS proteins 46
2.10.2 Protein purification 47
2.10.3 Protein quantification 47
2.10.4 Preparation of crude protein extract from fresh and lyophilized plant material for western blot analysis 47
2.10.5 SDS-Polyacrylamide-gel-elektrophoresis (SDS-PAGE) 48
2.10.6 MonoQ anion exchange chromatography 48
2.10.7 Gel filtration 49
2.10.8 Thrombin digest of His-tag proteins 49
2.10.9 Western Blotting 49

2.11 Enzyme assays for pantothenate synthetase 50
2.11.1 Spectrophotometric assay 50
2.11.2 Isotopic assay 51
2.11.3 PTS activity in segregating transgenic Arabidopsis overexpressing *panC* 52
2.11.4 Thin layer chromatography (TLC) 52
2.11.5 Quantification of the labelled products in isotopic assays 53
2.11.6 Stability of assayed proteins 53
2.11.7 Pantothenate:β-alanine isotope exchange assay 53
2.11.8 Reverse activity of pantothenate synthetase 53

2.12 Kinetic analysis of *A. thaliana* and *E. coli* PTS proteins 54

Chapter 3 Pantothenate synthesis in *Arabidopsis thaliana* **56**

3.1 Introduction 56

3.2 The *Arabidopsis thaliana* gene for pantothenate synthetase (*PTS*) 57
3.2.1 Molecular characterisation of *PTS* gene (At5g48840) 57
3.2.2 Molecular characterization of Salk T-DNA insertion mutants 58
3.2.3 Phenotypical characterisation of *pts-1* and *pts-2* 59

3.3 Development of *pts-1/pts-1* seeds 62

3.4 Chemical rescue of *pts-1/pts-1* mutants 64
3.4.1 Effect of exogenous pantothenate or pantehteine supplied by spraying on seed development in *PTS/pts-1* plants 65
3.4.2 Effect of exogenous pantothenate supplied in the growth medium 66
3.4.3 Pantothenate supports the complete developmental cycle of *pts-1/pts-1* plants 66

3.5 Overexpression of *E. coli* pantothenate synthetase in Arabidopsis in different compartments 68
3.5.1 Generation of the *A. thaliana* overexpressing constructs 68
3.5.2 Analysis of transgenic *A. thaliana* carrying overexpression constructs 70
3.5.3 Analysis of the expression level of the *E. coli* PTS protein and PTS activity in Arabidopsis plants overexpressing *panC* in the cytosol 71
3.5.4 Analysis of pantothenate level in segregating Arabidopsis overexpressing *E. coli* PTS in cytosol 74

3.6 Genetic complementation of *PTS* knock-out-mutation 76
3.6.1 Generation of *pts-1* knock out plants functionally complemented by *panC* 76
3.6.2 Analysis of the offspring of *pts-1* knock-out plants complemented by the *panC* 77
3.6.3 Western blot analysis of *pts-1* knockout plants complemented by the *panC* gene 79

3.7 Tissue specific expression of the *A. thaliana PTS* gene 80
3.7.1 Analysis of publicly available microarray data 80
3.7.2 *A. thaliana* PTS promoter driven GUS, expression profile 82

3.8 Conclusions 85

Chapter 4 Kinetic analysis of wild type and mutant forms of *A. thaliana* PTS **86**

4.1 Introduction 86

4.2 Alignment of pantothenate synthetases, conserved active site residues and divergent dimerization contacts in the PTS protein family 88
4.2.1 Generation of PTS mutants 91
4.2.2 Sequence analysis of PTS expression plasmids 91
4.2.3 Expression, purification, and properties of *A. thaliana* PTS 92
4.2.4 Expression, purification, and properties of *E. coli* PTS 94
4.2.5 Expression and purification of mutagenised PTS 94
4.2.6 Stability of the enzymes 95

4.3 Radioisotope assays 96
4.3.1 Sensitivity and linearity of ^{14}C-label detection system 96
4.3.2 The effect of pH on *A. thaliana* and *E. coli* PTS activity 97
4.3.3 pH optima of the reverse exchange reaction catalysed by *A. thaliana* and

E. coli PTS 100
4.3.4 Comparison between reaction mechanism of *A. thaliana* and *E. coli* PTS 102
4.3.5 Reverse reaction of PTS 104

4.4 Allosteric properties of *A. thaliana* PTS 105
4.4.1 Initial rate kinetic analysis of *A. thaliana* PTS 106
4.4.2 Consideration of modified mechanisms or allostery to explain the behaviour of *A thaliana* PTS 113
4.4.3 Initial rate kinetic analysis of PTS-Mut1 115
4.4.4 Initial rate kinetic analysis of PTS-E132A 116
4.4.5 Mutation in the subunit interface, conclusions 119

4.5 Conclusions 121

Chapter 5 Discussion **123**

5.1 Pantothenate synthesis in *Arabidopsis thaliana* 123

5.2 Comparison of *pts* with other *emb* mutations 128

5.3 Chemical complementation 130

5.4 Genetic complementation 130

5.5 Plants overexpressing the *E. coli panC* gene 131

5.6 Evolution of allostery in pantothenate synthetases 133

5.7 Is there a parallel pathway to pantothenate? 135

5.8 Overproduction of pantothenate in plants 136

Chapter 6 Bibliography **140**

Abbreviations

Apart from those listed below, the abbreviations used throughout this thesis follow the recommendations of the IUPAC-IUB Joint Commission on Biochemical Nomenclature as outlined in the Biochemical Journal (1992), **281**, 1-19.

AHIR	acetohydroxy acid isomeroreductase
aa	amino acid
ADC	aspartate decarboxylase
AMP	adenosine monophosphate
ATP	adenosine triphosphate
β-Ala	β-alanine
bp	base pairs
ddH_2O	deionised water
DPCK	dephosphocoenzyme A kinase
DTT	dithiotreitol
DW	dry weight
EDTA	ethylenediaminetetraacetica acid
IPTG	isopropylthio-β-D-galactoside
KPHMT	ketopantoate hydroxymethyl transferase
KPR	ketopantoate reductase
α-KIVA	α-ketoisovalerate
NAD	nicotinamide adenin dinucleotide
NADH	dehydronicotinamide adenin denucleotide
NADP	nicotinamide adenin dinucleotide phosphate
NADPH	dehydronicotinamide-adenin-dinucleotide phosphate
ORF	open reading frame
Pa	pantothenate
PANK	pantothenate kinase
PCR	poly chain reaction
PMSF	phenylmethylsulfonyl fluoride
PP_i	inorganic pyrophosphate
PPAT	phosphopantetheine adenylyltransferase

PPCDC	phosphopantothenoylcysteine decarboxylase
PPCS	phosphopantothenoylcysteine synthetase
PTS	pantothenate synthetase
Pt	pantoate
TEMED	N,N,N',N'-tetramethylethylenediamine
THF	tetrahydrofolate
TRIS	tris(hydroxymethyl)-aminomethane
X-Gal	5-bromo-4-chloro-3-indoyl-β-D-galactoside

Chapter 1
Introduction

Pantothenate, also referred to as vitamin B5, is part of the water-soluble B vitamin group, essential for human and animal nutrition. Its biochemical role in all organisms is to form the core of the structure of coenzyme A, an essential cofactor for central pathways of respiration, lipid metabolism, and for the synthesis of many secondary metabolites (Abiko, 1975). In addition, the phosphopantetheine moiety is incorporated into the prosthetic group of acyl carrier proteins in fatty acid synthases, polyketide synthases and non-ribosomal peptide synthetases (Kleinkauf, 2000; Webb *et al*., 2004). The importance of coenzyme A and acyl carrier protein, and thereby pantothenate, in cellular metabolism is demonstrated by the fact that over 100 enzymes in *Escherichia coli* require them as cofactor (Chakauya *et al*., 2006). It is estimated that about 4% of all enzymes utilize coenzyme A, coenzyme A thioesters, or 4'-phosphopantetheine as substrates (Begley *et al*., 2001).

Pantothenate is thought to have existed in the prebiotic world, so the biosynthetic pathways for pantothenate were established early and have not changed subsequently (Miller and Schlesinger, 1993). Coenzyme A synthesis from pantothenate proceeds by the same route in bacteria, eukaryotes, and, in all likelihood, in archea (Genschel, 2004).

Most bacteria, plants, and fungi, synthesize pantothenate, and so pantothenate is found virtually everywhere in biology, in both bound and free forms (Leonardi *et al*, 2005). This is reflected by its name, which is derived from the Greek word "*pantothen*" meaning "from all sides". *E. coli*, for example produces and secretes 15 times more pantothenate than is required for intracellular CoA biosynthesis (Jackowski and Rock, 1981).

Only microbes, fungi and plants synthesize pantothenate *de novo* and form the dietary source of pantothenate for animals (Smith and Song, 1996), which are unable to synthesize pantothenate and are totally dependent on the uptake of exogenous pantothenate. Therefore, the pathway enzymes are attractive target(s) for non-toxic antibiotics, fungicides and herbicides. Moreover, the pathway enzymes for pantothenate are also a target for modifying (elevating) pantothenate levels in crop plants. The process of pantothenate biosynthesis is similar in bacteria and plants, but there are important differences, both in the enzymes involved and in the overall organization of the pathway.

1.1 Nomenclature for pantothenate synthetase used in the literature and in this work

All authors use the term *panC* for the gene encoding pantothenate synthetase in bacteria. The protein encoded by *panC* is termed pantoate-β-alanine ligase (systematic name) or pantothenate synthetase (most common synonym) (Maas, 1952; Miyatake *et al*., 1979; Cronan *et al*, 1982; Primerano and Burns, 1983; Merkel and Nichols, 1996; Sahm and Eggeling, 1999; Zheng and Blanchard, 2001; Williams *et al*., 2003; Chassagnole *et al.,* 2003 Raman and Rathinasabapathi, 2004; Tuck *et al*., 2006).

Common abbreviations for pantothenate synthetase are PS (Genschel *et al*., 1999; von Delft *et al*., 2001; Lobley *et al*., 2003; Wang and Eisenberg, 2003; Merkamm *et al*., 2003 2006; Genschel, 2004; Webb *et al*., 2004; Coxon *et al*., 2005; Chakauya *et al*, 2006), PtS (Ottenhof *et al*., 2004.), or PanC (Elischewski *et al*., 1999).

In this work, the bacterial gene for pantothenate synthetase is termed *panC,* whereas the plant gene for pantothenate synthetase is termed *PTS*. The product of both the bacterial *panC* and the plant *PTS* gene is PTS protein. The *A. thaliana* T-DNA insertion alleles in the *PTS* gene available from the Salk Institute, Salk_101909 and Salk_594477, are named *pts-1* and *pts-2* in this work, respectively.

1.2 Pantothenate biosynthesis enzymes

The pathway to pantothenate was determined piecemeal over a number of years. Although some enzymes of the pathway were identified straightforwardly, others were not and hence the pathway remained uncertain until the 1980s. With the advent of bacterial mutants defective in specific steps of the pathway and the application of molecular biological techniques, the pathway in *eubacteria* has been completely elucidated. Some of the enzymes have also been characterised in fungi and plants.

The pathway is the best understood in *E. coli* where it is comprised of four enzymatic steps (Cronan *et al*., 1982) (Fig.1). Ketopantoate hydroxymethyltransferase (KPHMT; EC; 2.1.2.11; Powers and Snell, 1976) converts *α*-ketoisovalerate into ketopantoate using 5,10-methylene tetrahydrofolate. Subsequently ketopantoate is reduced to pantoate by ketopantoate reductase (KPR; EC 1.1.1.169; Frodyma and Downs, 1998) using NADPH as the hydrogen donor. In a separate branch, β-alanine is synthesized from L-aspartate by the enzyme L-aspartate-α-decarboxylase (ADC; EC 4.1.1.11; Cronan, 1980). Finally, pantothenate is produced in an ATP-consuming condensation reaction between pantoate and β-alanine, catalysed by pantothenate synthetase (PTS; EC 6.3.2.1; Cronan *et al*., 1982).

Already in 1982, using *E. coli* strains auxotrophic for pantothenate, the genes *panB* (encoding KPHMT), *panC* (encoding PTS) and *panD* (encoding ADC) were physically mapped by conjugation experiments and found to be close to one another at 3.1 min on the genome (Cronan *et al.*, 1982). Merkel and Nichols (1996) sequenced a DNA segment containing the *E. coli panBCD* gene cluster, which established the gene order *panD-panC-panB.* The *panB* and *panC* genes lie adjacent to one another, but are separated from *panD* by an open reading frame (ORF) of undefined function (*orf3*; Merkel and Nicholson, 1996), which is orientated in the opposite direction. The authors speculate that this *orf3* is a relative newcomer to this site on the chromosome, having inserted into a pre-existing pantothenate gene cluster, and existence of an ancestral *panBCD* operon has been hypothesised (Merkel and Nicholson, 1996). Also in *B. subtilis* the organisation of the *panB* and *panC* genes is identical (Sorokin *et al*., 1996). In *Corynebacterium glutamicum* the *panB* and the *panC* genes overlap by one nucleotide and are thought to form an operon (Sahm and Eggeling, 1999). All four enzymes from *E. coli* pantothenate biosynthetic pathway have been cloned and overexpressed, and their crystal structures have been solved (von Delft *et al*., 2001; 2003; Zheng and Blanchard, 2000; Schmitzberger *et al*., 2003; Albert *et al*., 1998; Matak-Vinkovic *et al*., 2001).

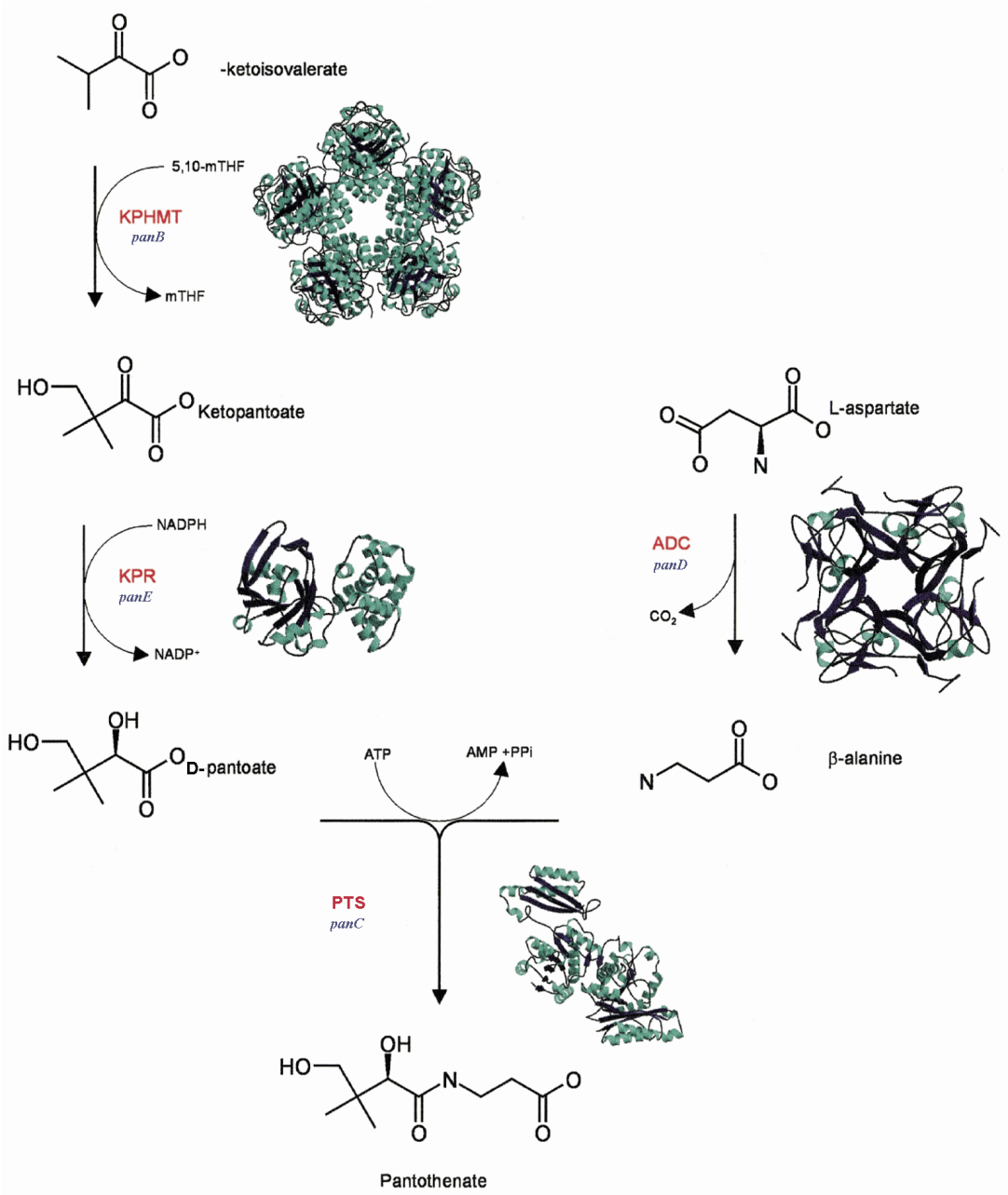

Fig. 1.1 Pantothenate biosynthesis pathway in *E. coli* (reproduced from Lobley *et al*., 2003, modified). Enzyme names are given in red with the corresponding genes in blue. The enzyme structure are: KPHMT, ketopantoate hydroxymethyltransferase (1m3u) (von Delft *et al*., 2003); KPR, ketopantoate reductase (1KS9) (Matak-Vinkovic *et al*., 2001); ADC, aspartate decarboxylase (1AW8) (Albert *et al*., 1998); PTS, pantothenate synthetase (1HLO) (von Delft *et al*., 2001); 5,10-mTHF, 5,10-metylene tetrahydrofolate.

Although all the enzymes involved in pantothenate synthesis have been characterized in microbes, not all the steps in the plant pantothenate synthesis pathway have been studied in detail despite the availability of the Arabidopsis genome sequence. Some evidence suggests that the steps of the pantothenate biosynthesis are probably the same as those in microbes.

The first evidence for the operation of the pantothenate biosynthetic pathway in plants came from the identification of a pantothenate-requiring auxotroph of *Datura innoxia*. This

auxotrophic cell-line could grow in cell culture if supplied with ketopantoate, pantoate or pantothenate (the intermediates in the microbial pathway), but not α-KIVA (Sahi *et al*., 1988), suggesting missing or defective KPHMT, the first enzyme in the *E. coli* pathway. Another evidence, that the plant biosynthetic pathway for pantothenate is similar to that in microbes, came from a radiotracer experiment with pea (*Pisum sativum*) leaves. These studies demonstrated the incorporation of radiolabeled L-[U-^{14}C]valine precursor into α-ketoisovalerate, ketopantoate, and pantoate (Jones *et al*., 1994). The formation of radiolabeled intermediates along each step of the pathway known in *E. coli* suggested the pathway to be similar in plants, and provided support for the existence of the enzymes KPHMT and KPR.

Cloning of the genes for pantothenate biosynthesis enzymes in *E. coli* has resulted in both sequence information and the crystal structures of the proteins, which have subsequently provided valuable tools to search for homologous genes in higher plants. The identification of these genes has afforded further insight into the operation of the plant pathway (Coxon *et al.*, 2005). Two genes (At2g46110 and At3g61530) encoding *KPHMT* and a single gene (At5g48840) encoding *PTS* were identified in Arabidopsis (Ottenhof *et al*., 2004).

1.2.1 Ketopantoate hydroxymethyltransferase

Ketopantoate hydroxymethyltransferase (KPHMT) was first partially purified from *E. coli* and initially characterized in 1957 (McIntosh *et al*.). Teller *et al*. (1976) purified the enzyme to homogeneity. The *panB* gene from *E. coli*, encoding KPHMT was isolated by functional complementation of the corresponding *E. coli* mutant (Jones *et al.,* 1993).

KPHMT is a class II aldolase (*i.e.* metal requiring) that converts α-ketoisovalerate (α-KIVA, the oxoacid of valine) into ketopantoate using 5,10-methylene tetrahydrofolate as a cofactor (Powers and Snell, 1976; Teller 1976). This reaction is the first committed step of pantothenate biosynthesis. The enzyme requires Mg^{2+} for activity; in the absence of Mg^{2+}, the activity of the enzyme is reduced by greater than 10-fold (Powers and Snell, 1976). The enzyme is stable and active over a broad pH range, with an optimum from 7.0 - 7.6, below pH 5 the enzyme is inactive (Powers and Snell, 1976). The apparent K_m values reported by Powers and Snell (1976) (in the forward direction) are 0.18 and 1.1 mM for tetrahydrofolate and α-ketoisovalerate, respectively. Apparent K_m values for ketopantoate and THF assayed in reverse direction were 0.16 and 0.18 mM, respectively.

There are over 100 sequences similar to *E. coli panB* available in online databases of sequenced genomes. The protein encoded by *E. coli* K12 gene has 264 amino acids,

corresponding to a molecular weight of 28.2 kDa. The *panB* gene isolated from the filamentous fungus *Aspergillus nidulans* is 58% similar at the amino acid level to the *E. coil* K12 enzyme but comprises 349 amino acids (37.7 kDa), the extra residues being located mainly as extensions at both N and C termini (Kurtov *et al*., 1999).

Structures of KPHMT from three organisms, *i.e. E. coli* (von Delft *et al.*, 2003)*, M. tuberculosis* (Chaudhuri *et al*., 2003), and *N. meningitides* (unpublished structure PDB entry 1o66), have been solved. *E. coli* KPHMT was shown to be a homodecamer; a pentamer of dimers, with the dimer being the functional unit (von Delft *et al*., 2003). The protein adopts the $(\beta\alpha)_8$ barrel fold and the active site, with a co-ordinated Mg^{2+} ion, is located at the C-terminus of the barrel (von Delft *et al*., 2003). Little is known about the mode of action of KPHMT, except that the addition of the hydroxymethyl group proceeds with retention of configuration (Aberhart and Russell, 1984). Several possible mechanisms for KPHMT have been proposed but further studies are needed to distinguish which of these possible mechanisms is occurring (reviewed by Webb *et al.,* 2004).

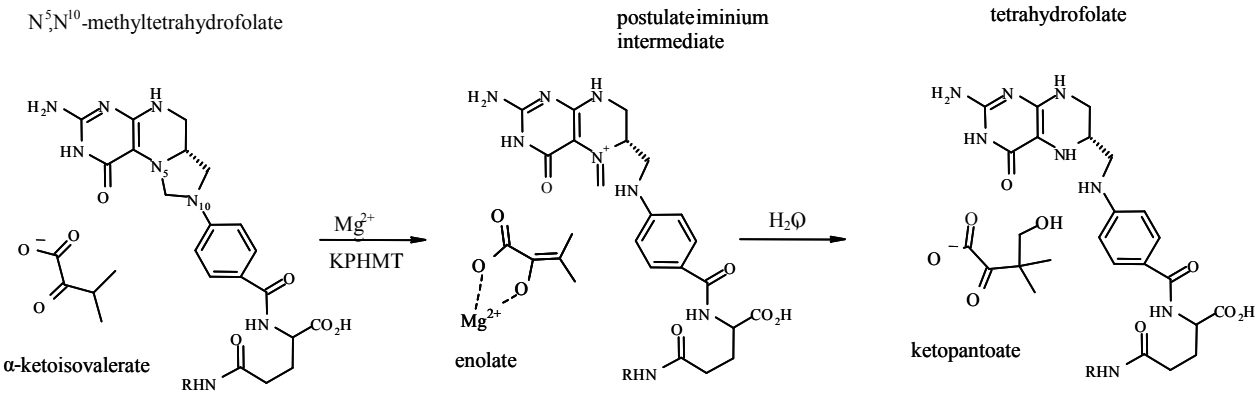

Fig. 1.2 Proposed mechanism for the conversion of α-KIVA and methylene-THF into ketopantoate and TFH catalysed by KPHMT (reproduced from von Delft *et al.,* 2003)

KPHMT is inhibited by pantoate concentrations greater than 50 μM, by pantothenate above 500 μM, and by coenzyme A at concentrations greater than 1 mM (Powers and Snell, 1976). This feedback inhibition, caused by the downstream intermediates pantoate, pantothenate and CoA, leads to a decrease in V_{max}, increase in K_m, and to enhanced cooperativity for substrate (ketopantoate) (Powers and Snell, 1976). Thus, KPHMT has regulatory properties expected of an enzyme catalyzing the first committed step in a biosynthetic pathway.

Searching the Arabidopsis genome for homologues to the *E. coli panB* gene using BLAST, two homologues to the *panB* gene were identified, *i.e*. *panB1* and *panB2*. The two Arabidopsis *panB* genes are 30% identical at the amino acid level to the *E. coli* counterpart, and this is also the case for two *panB* genes identified in rice (Ottenhof *et al*., 2004). The first Arabidopsis *panB1* gene (At2g46110), is located on chromosome II end encodes a polypeptide of 347 amino acids (KPHMT1), whereas the second gene, *panB2* (At3g61530) is situated on chromosome III and encodes for a polypeptide of 354 amino acids (KPHMT2) (Ottenhof *et al*, 2004). The Arabidopsis KPHMT sequences showed 87% similarity to each other at the amino acid level and 79% at the DNA level (Ottenhof *et al.*, 2004). Comparison of their organisation reveals that *panB1* has four exons and three introns, whereas *panB2* has five exons and four introns, but the positions of the shared introns are identical (Fig. 1.3).

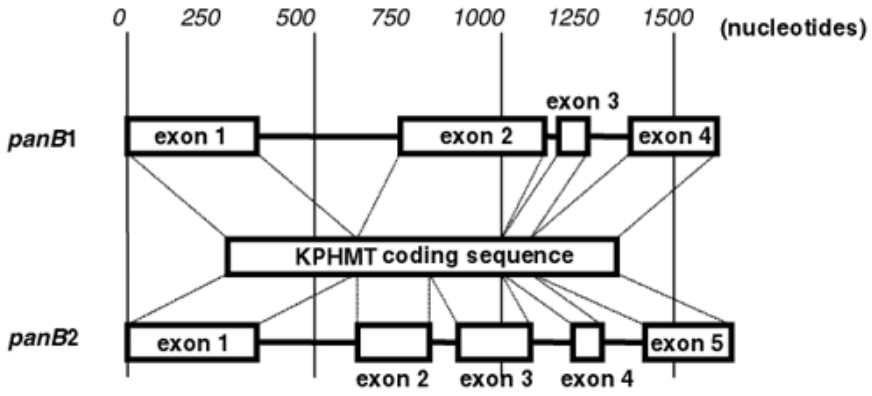

Fig. 1.3 Organisation of Arabidopsis *panB1* and *panB2* genes, encoding for KPHMT (reproduced from Ottenhof *et al*., 2004).

The occurrence of two *panB* genes in the Arabidopsis genome is likely to be the result of genome duplication, since the two genes lie in regions of chromosomes II and III where a duplication event has taken place (Arabidopsis Genome Initiative, 2002). The two *panB* genes were amplified from an Arabidopsis cDNA library, and found to functionally complement the *E. coli panB* mutant, indicating that both genes encode active proteins (Ottenhof *et al.*, 2004). Furthermore, two *panB* genes present in the rice genome, suggest that the presence of two KPHMT isoforms might have functional significance in plants.

The two genes for KPHMT in Arabidopsis and rice both have extensions relative to *E. coli* KPHMT at the N- and C- termini of the enzyme. The reason for the C-terminal extension (about 40- 50 residues) is unknown. The extensions at the N-termini are almost certainly transit peptides for targeting of the enzyme to the mitochondria. Fusion of the full-length Arabidopsis KPHMT precursors to GFP demonstrated that they are capable of translocating

GFP into mitochondria and KPHMT activity was reproducibly measured in mitochondria from pea and Arabidopsis, and was not detectable in purified chloroplasts (Ottenhof *et al*., 2004). From this analysis Ottenhof *et al*. concluded that most plant tissues have two functional KPHMTs, and both are located in the same cell compartment.

Similarity searches for KPHMT isoforms identified two genes in all plant genomes examined, including *Hordeum vulgare* (barley), grape, *Lotus japonicus*, pine, *Sorghum bicolour* (sorghum), *Triticum aestivum* (wheat), soybean, tobacco and onion, suggesting strongly that the presence of two isoforms in plants is widespread, and possibly universal (Chakauya *et al*., 2006). Sequence alignment of the Arabidopsis and rice KPHMTs with yeast, *Aspergillus nidulans, Mycobacterium bovis* and *E. coli*, shows that the plant enzymes all have conserved residues identified from the crystal structure as important in binding the product and coordinating the Mg^{2+} atom required for activity (Chakauya *et al*., 2006). Moreover, Chakauya *et al*. (2006) concluded from phylogentic analysis that the plant enzymes form a separate clade, and they are more similar to the fungal KPHMTs than those from bacteria.

The presence of two expressed genes for KPHMT in Arabidopsis might mean that the two izozymes perform different roles and/or have different kinetic properties. Given the level of sequence similarity between them, they are unlikely to be very different biochemically, but this remains to be tested (Ottenhof *et al*., 2004). An analysis of the microarray data in GENEVESTIGATOR (Zimmermann *et al*., 2004) showed that both *panB* genes are expressed throughout the plant, although *panB2* is upregulated during germination and embryo development (Chakauya *et al*., 2006).

1.2.2 Ketopantoate reductase

The first purification of an enzyme with ketopantoate reductase (KPR) activity was by Shimizu *et al.* (1988) who purified the enzyme from *Pseudomonas maltophilia* and provided evidence for KPR to be responsible for biosynthesis of pantoate. To date no other endogenous KPR enzymes have been purified.

Zheng and Blanchard cloned, overexpressed and purified the *E. coli panE* gene encoding KPR (EC 1.1.1.169). They showed that it is monomeric with a molecular mass of 34 kDa. It catalyzes the NADPH-dependent reduction of α-ketopantoate to D-pantoate (Zheng and Blanchard, 2000) (Fig. 1.4A). The steady state kinetic mechanism is ordered with NADPH binding first followed by ketopantoate binding and $NADP^+$ release following hydroxypantoate release (Fig. 1.4B).

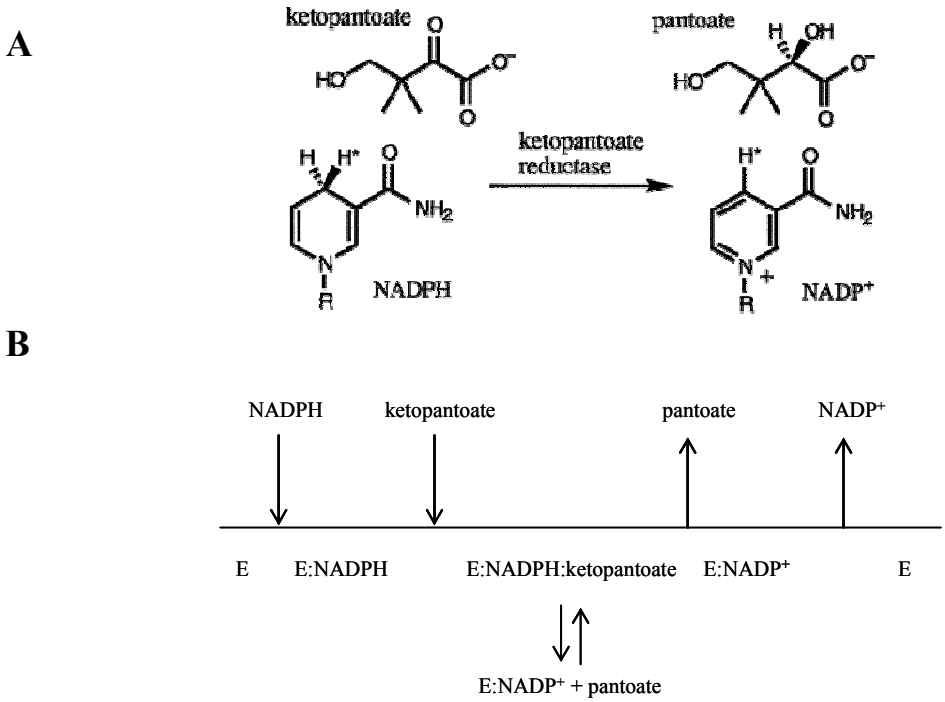

Fig. 1.4 A, NADPH-dependent reduction of ketopantoate catalysed by KPR (reproduced from Matak-Vinkovic *et al*., 2001); **B**, kinetic mechanism of *E. coli* and *Pseudomonas maltophila* KPR (Zheng and Blanchard, 2000, modified).

The forward reaction was shown to be dependent on protonation of a residue with a pK_a between 8.1 and 8.7 and NADPH binding was dependent on dephosphorylation of a residue with a p*K*a of around 6.2. In the reverse direction (pantoate oxidation) the reaction is dependent on deprotonation of a residue with a pK_a between 7.6 and 8.1 (Zheng and Blanchard, 2000). The K_m values reported for *E. coli* KPR are 4.0 μM for NADPH and 120 μM for ketopantoate (Zheng and Blanchard, 2000).

Interestingly, reduction of (α-)ketopantoate can also be catalyzed by *E. coli* acetohydroxy acid isomeroreductase (EC 1.1.1.86), the product of the *ilvC* gene. The *in vitro* function of this enzyme is to catalyzes the formation of α,β-dihydroxy-β-metylvalerate and α,β-dihydroxyisovalerate from α-aceto-α-hydroxybutyrate and α-acetolactate, respectively, in isoleucine and valine biosynthesis (Primerano and Burns, 1982). It has been suggested that both *panE* and *ilvC* are responsible for the biosynthesis of pantoate from ketopantoate *in vivo* (Primerano and Burns, 1982). Moreover, the *panE* gene encoding ketopantoate reductase has been demonstrated to be identical to the *ApbA* gene, which is involved in the alternative pyrimidine biosynthetic (abp) pathway in *Salmonella typhimurium* (Frodyma and Downs, 1988). The his-tagged enzyme from *S. typhimurium* overexpressed in *E. coli* was purified by Frodyma and Downs (1998).

Ketopantoate reductase from *Pseudomonas maltophilia* 845 was found to be specific for ketopantoate, the only alternative substrate was 3-hydroxy-2-ketoisovalerate, which had considerably lower activity (~2% of the ketopantoate activity) (Shimizu *et al*., 1988). Shimizu *et al*. (1988) observed no reaction in the presence of NADH and no metal dependence. The pH dependence showed an optimum rate at pH 6 in the direction of ketopantoate reduction and at pH 8.5 in the direction of pantoate oxidation. The enzyme from *S. typhilium* was found to be less stringent in terms of selectivity for NADPH over NADH, with an approximately four-fold selectivity for the phosphorylated cofactor (Frodyma and Downs, 1998).

KPR from *E. coli* is a member of the family of short-chain oxidoreductases, which form a large, evolutionary old family of NAD(P)(H)-dependent enzymes (Ottenhof *et al.,* 2004). KPR is a monomer, with two clearly defined domains. The N-terminal domain (residues 1-167) is based on the Rossmann fold, eight five β-strands and three α-helices. The C-terminal domain (168-303) has been described as a family-specific and is entirely α-helical (Matak-Vinkovic *et al*., 2001). The active site is thought to lie in the cleft between these two domains and the majority of the strictly conserved residues neighbour this cleft. In a sequence-structure alignment search Lobley *et al.* (2003) identified a large number of proteins with a structure similar to the N-terminal domain, and only three proteins with any significant similarity in the C-terminal domain. This indicates that N-terminal domain has much greater structural similarity than the C-terminal domain. Moreover, complete lack of conservation in the active-site residues suggest that these enzymes diverged a considerable time ago (Lobley *et al*., 2003).

Owing to the identification of the first and final enzymes of the pantothenate pathway in the Arabidopsis genome (section 1.2.1 and 1.2.4) it was concluded that the intermediate enzyme-KPR is also present there (Coxon *et al.,* 2005). Despite searches in the Arabidopsis genome using the BLAST program and the *E. coli panE* sequence as a query, no bacterial homologues of KPR was found. Due to poor *panE* sequence similarity between microorganisms, failure to find a convincing homologue in plants, using a bacterial *panE*, is not astonishing. The level of sequence similarity between *panE* genes from microorganisms is low, of the order of 15% (Matak-Vinkovic *et al*., 2001), and this might therefore preclude its identification using a bacterial enzyme as a query sequence. Lobley *et al*. (2003) identified a large number of proteins and reported complete lack of conservation in the active-site residues suggesting that these enzymes diverged a considerable time ago. KPR is a member of the family of short-chain oxidoreducteses, which form a large, evolutionary old family of NAD(P)H- dependent enzymes. There are an estimated 138 candidates genes for these enzymes in Arabidopsis

genome (Kallberg *et al*., 2002). More than 80, homologous to *E. coli panE* are known as putative sequences for ketopantoate reductases (Webb *et al*., 2004). KPR activity is clearly present in plants, as demonstrated using feeding studies (Jones *et al*., 1994), so it is possible that this enzyme is quite different from KPR encoded by *panE*. Indeed, in *E. coli* there is another enzyme, acetohydroxy acid isomeroreductase (AHIR), encoded by *ilvC*, which is able to reduce ketopantoate to pantoate, albeit much less efficient than it can utilize its natural substrate acetohydroxy acid (Primerano and Burns, 1983). It is unlikely to be involved in pantothenate biosynthesis in *E. coli*, since it can only compensate for a *panE* mutation when it is overexpressed but it is possible that in plants it may play a role (Coxon *et al*., 2005). This enzyme has been shown to be the only enzyme with KPR activity in *Corynebacterium glutamicum* (Merkamm *et al.,* 2003) leading to the suggestion that a similar situation may prevail in plants (Chakauya *et al*., 2006). In spinach and Arabidopsis, there is a single gene for AHIR, and the spinach enzyme has been purified from chloroplasts and its crystal structure has been solved (Biou *et al*., 1997). However, whether it is involved in pantothenate biosynthesis remains unexplored. Another candidate enzyme was partially purified from spinach chloroplasts (Julliard, 1994). It could catalyse the reduction of ketopantoyl-lactone to pantoyl-lactone but could not use ketopantoate. Recently Rathinasabapathi and Raman (2005) reported a significant increase in pantothenate levels in tomato leaf discs fed with pantoyl-lactone. An alternative, parallel pathway, which could operate via pantoyl-lactone, located in chloroplasts, was considered (Julliard, 1994). The reported by Julliard (1994) enzyme had low specific activity for the substrates tested (common substrates of short chain dehydrogenase/reductase). Chakauya *et al*. (2006), concluded that the enzyme is probably a non-specific dehydrogenase. Moreover, as its product is pantoyl-lactone, it is unlikely to be involved in pantothenate biosynthesis mediated by plant pantothenate synthetase, because the latter cannot use pantoyl-lactone as a substrate (Genschel *et al*., 1999). Chakauya *et al*. (2006) discuss that ketopantoyl-lactone spontaneously ring-opens to form ketopantoate, but pantoyl-lactone is stable under the conditions found in the cell, therefore additional pathway leading to pantothenate via the lacton form they consider to be unlikely.

Reverse-FUGUE (a search strategy in which a solved crystal structure is used as the query) identified a possible homologue of *panE* in Arabidopsis. It is 41.6 kDa (compared to 33.9 kDa for *E. coli*) and contains a putative nucleotide-binding motif and the conserved Ser244 thought to be important in the binding of ketopantoate, although the glutamate associated with catalytic activity of the enzyme was not conserved (Ottenhof *et al*., 2004). The veracity of this candidate protein being KPR requires further investigation and is currently underway (Coxon

et al., 2005). The identity of the enzyme that carries out the reduction step in pantothenate biosynthesis in plants remains elusive. The fact that the Arabidopsis genome encodes an estimated 138 short chain dehydrogenases means it will be necessary to carry out careful biochemical analysis to resolve this question (Chakauya *et al*., 2006).

1.2.3 Aspartate decarboxylase

L-aspartate-α-decarboxylase (ADC), encoded in *E. coli* by *panD*, converts L-aspartate to β-alanine and carbon dioxide. ADC provides the major route of β-alanine production in *E. coli* (Cronan, 1980). This route appears to be unique to prokaryotes and absent in eukaryotes including yeast and plants (Rathinasabapathi *et al.,* 2000; White *et al.,* 2001). β-Alanine is found in all living organisms and is essential for normal growth because it is a precursor for pantothenate (Raman and Rathinasabapathi, 2004). Bacterial and yeast mutants deficient in β-alanine biosynthesis are not viable (Cronan, 1980; Merkel and Nichols, 1996; White *et al.,* 2001). The mechanism of bacterial ADC has been reported by Saldanha *et al.* (2001) (Fig. 1.5).

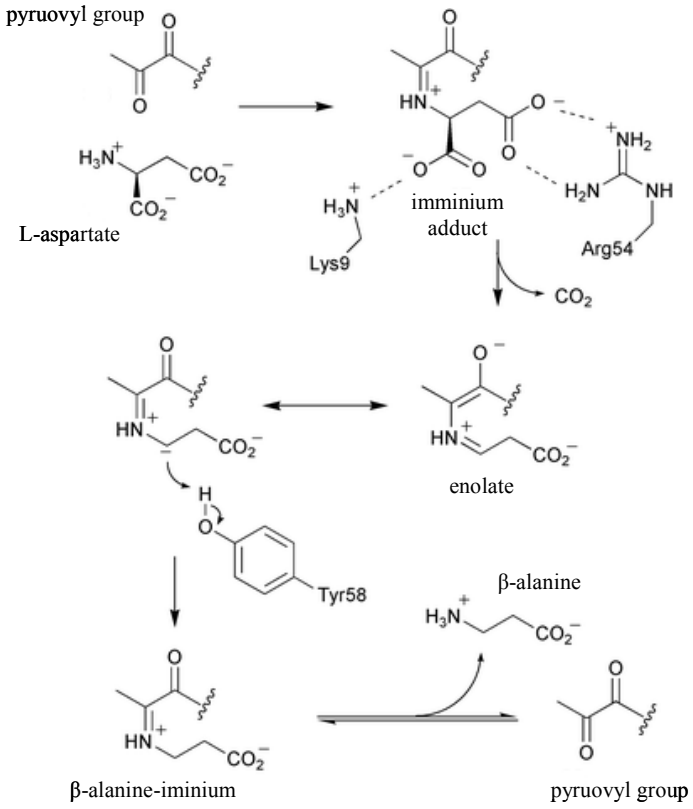

Fig. 1.5 Catalytic mechanism of ADC (reproduced form Webb *et al*., 2004). The figure shows the ADC-catalysed decarboxylation of L-aspartate which leads to the formation of β-alanine. The mechanism of ADC depends upon the formation of an iminium ion adduct between the substrate L-aspartate and the pyruvoyl group. The decarboxylation step gives enolate, which is reprotonated by Tyr58 what leads to formation of the β-alanine iminium species, which is then hydrolysed to regenerate the active site pyruvoyl group.

Native *E. coli* ADC has a molecular weight of 59 kDa (Williamson and Brown, 1979). This enzyme is unusual in that it contains a covalently bound pyruvoyl group involved in catalysis (Williamson and Brown, 1979). It is initially translated as an inactive proenzyme (designated the π-protein), which self-processes, by cleavage between Gly-24 and Ser-25 to produce a β-subunit with XHO at its C-terminus and α-subunit with a pyruvoyl group at its N-terminus (Ramjee *et al*., 1997) (Fig. 1.6). The pyruvoyl group is formed by intramolecular, non-hydrolytic serinolysis, in which the side-chain oxygen of Ser25 attacks the carbonyl carbon of Gly24 (Fig. 1.5) (Schmitzberger *et al*., 2003). The reaction, which is also known as an N→O acyl shift, (*via* oxyoxazolidine intermediate) results in the formation of an ester intermediate (Recsei *et al.*, 1983). β-elimination of the ester produces dehdroalanine, which hydrolyses to form the pyruvoyl group. This process yields an α-chain of 11 kDa with the pyruvoyl group at the N-terminus and a β-chain of 2.8 kDa with Gly24 at the C-terminus (Ramjee *et al*., 1997).

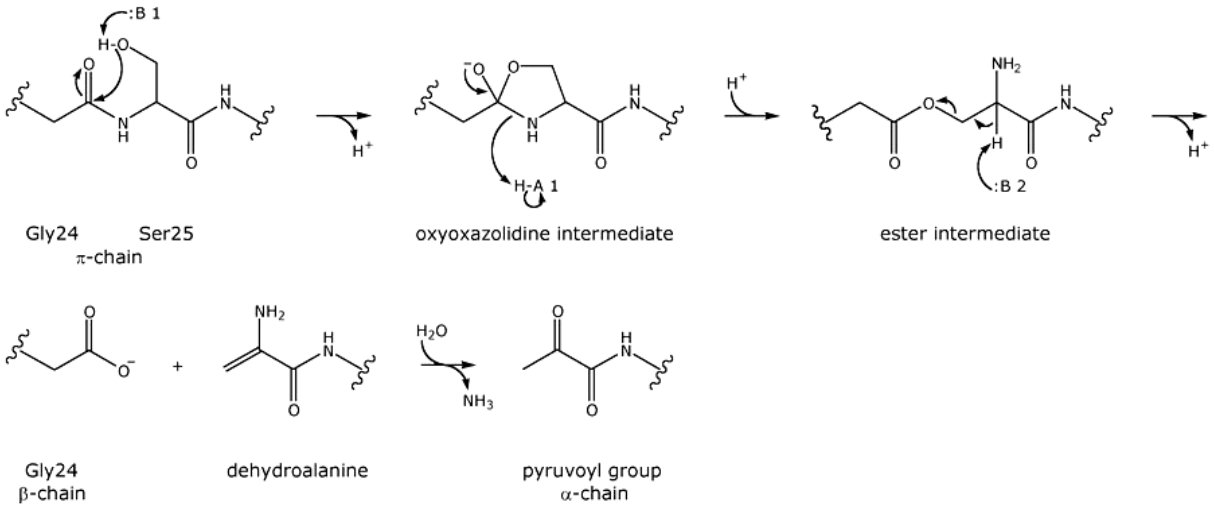

Fig. 1.6 Schematic representation of the self-processing reaction (reproduced form Schmitzberger *et al*., 2003). Base 1, acid 1 and base 2 are designated as B 1, H-A 1 and B 2, respectively.

The mechanism of ADC processing is thought to be characteristic of self-catalysed backbone rearrangements in general, an important post-translational modification for protein maturation that is observed in a number of often evolutionary and structurally unrelated proteins (Schmitzberger *et al*., 2003). Moreover, Blast alignment of ADC shows a strong conservation of the residues implicated in the mechanisms of auto-processing and catalysis (Lobley *et al*., 2003).

The purified recombinant enzyme comprises principally the unprocessed π-subunit (of 13.8 kDa), with a small proportion of the α- and β-subunits (11 kDa and 2.8 kDa respectively)

(Ramjee *et al*., 1997). Several crystal structures of *E. coli* ADC have been solved. These have included a structure of the processed enzyme, with the catalytic pyruvoyl group as well as a structure of the ester intermediate observed in the processing reaction (Albert *et al*., 1998). *E. coli* ADC is a homotetramer, with a tertiary structure comprised of a six-stranded β-barrel (Albert *et al.,* 1998). The crystal structure of the *E. coli* ADC demonstrated that the active enzyme is a multimer containing three each of α-and β-subunits and an incompletely processed π-protein (Albert *et al*., 1998).

Williamson and Brown (1979), who first purified the *E. coli* enzyme to homogeneity, reported the K_m value for L-aspartate to be 0.16 mM. The pH optimum for the action of the enzyme is rather broad, between pH 6.5 and 7.5, but the enzyme functions half-maximally or greater between pH 5.3 and pH 8.6. The enzyme also acts over a relatively wide range of temperature, with half-maximal activity at 26°C and 78°C and an optimum at 55°C (Williamson and Brown 1979). Ramjee *et al*. (1997) determined the activity of ADC both directly after overexpression and purification and after subsequent processing. This demonstrated a 10- fold increase in the specific activity of the enzyme. The fully processed enzyme shows a specific activity of 2400 nmol min^{-1} mg^{-1}, as compared to 100-250 nmol min^{-1} mg^{-1} for newly prepared overexpressed enzyme and 650 nmol min^{-1} mg^{-1} for the native enzyme as determined by Williamson and Brown. ADC is not subject to feedback inhibition by β-alanine, pantothenate, coenzyme A or acetyl coenzyme A (Williamson and Brown, 1979; Cronan, 1980). This is consistent with the increase in β-alanine level in transgenic tobacco plants that overexpressed the *panD* (Fouad and Rathinasabapathi, 2006).

β-Alanine is the only naturally occurring β-amino acid and, despite its central role in pantothenate synthesis and in environmental stress adaptation, little is known about its source in plants. In plants, β-alanine synthesis has been hypothesized to proceed by degradation of spermine, propionate, or uracil (reviewed by Raman and Rathinasabapathi, 2004). No homologue of *E. coli* ADC could be identified using either BLAST or searches with the program FUGUE in which the 3D structure of the *E. coli* ADC was compared with all the annotated proteins in Arabidopsis (Ottenhof *et al*., 2004). Furthermore, functional complementation of the *E. coli panD* mutant DM 3498 using an Arabidopsis cDNA expression library resulted in no positive clones (Coxon *et al*., 2005).

No ADC homologue was identified in *Saccharomyces cerevisiae* by the FUGUE approach, indicating that the gene may not have traversed the prokaryotic–eukaryotic border (Ottenhof *et al*., 2004). Instead, like other eukaryotes, it is likely that plants have alternative methods by which β-alanine is produced (Fig. 1.7).

In yeast, β-alanine for pantothenate biosynthesis appears to come from the polyamine spermine (White *et al*., 2001). Plant polyamine oxidases have been characterized from a variety of sources, and an enzyme catalyzing the oxidation of 3-aminopropionaldehyde to β-alanine was identified in millet (*Setaria italica*) (Awai *et al*., 1995, 2004) (Fig. 1.7, enzyme 2). However, spermine appears not to be essential for Arabidopsis as it can survive without the ability to make spermine (Coxon *et al*., 2005).

Catabolism of uracil, leading to β-alanine, NH_3 and CO_2, involves the reduction of the pyrimidine ring catalysed by dihydropyrimidine dehydrogenase (Fig. 1.7, enzyme 3), followed by the opening of the ring by dihydropyrimidinase (Fig. 1.7, enzyme 4) and finally the hydrolysis of the resulting ureide group by β-ureidopropionase (Fig. 1.7, enzyme 5) (sometimes called β-alanine synthetase). Evidence for the existence of this pathway in plants comes from feeding studies. [^{3}H]uracil was efficiently incorporated into β-alanine when fed to leaves of the *Limonium latifolium*, which accumulates β-alanine beatine, and *Limonium sinuatum*, a non-accumulator (Duhaze *et al*., 2003). Genes for dihdrouracil dehydrogenase have been isolated from several leguminous plants, and the Arabidopsis gene encoding dihydropyrimidinase was cloned and functionally characterised (reviewed by Chakauya *at al*., 2006). β-Ureidopropionase was purified from maize seedlings, and the corresponding gene was cloned from Arabidopsis (reviewed by Chakauya *at al*., 2006). Together, these results suggest that uracil degradation is a credible source of β-alanine for pantothenate production in plants. Rathinasabapathi (2002) reported that β-alanine in plants could be derived from propionate metabolism (Fig 1.7, enzymes 6-9). However, whether any of those pathways provides β-alanine for pantothenate synthesis in higher plants remains unknown.

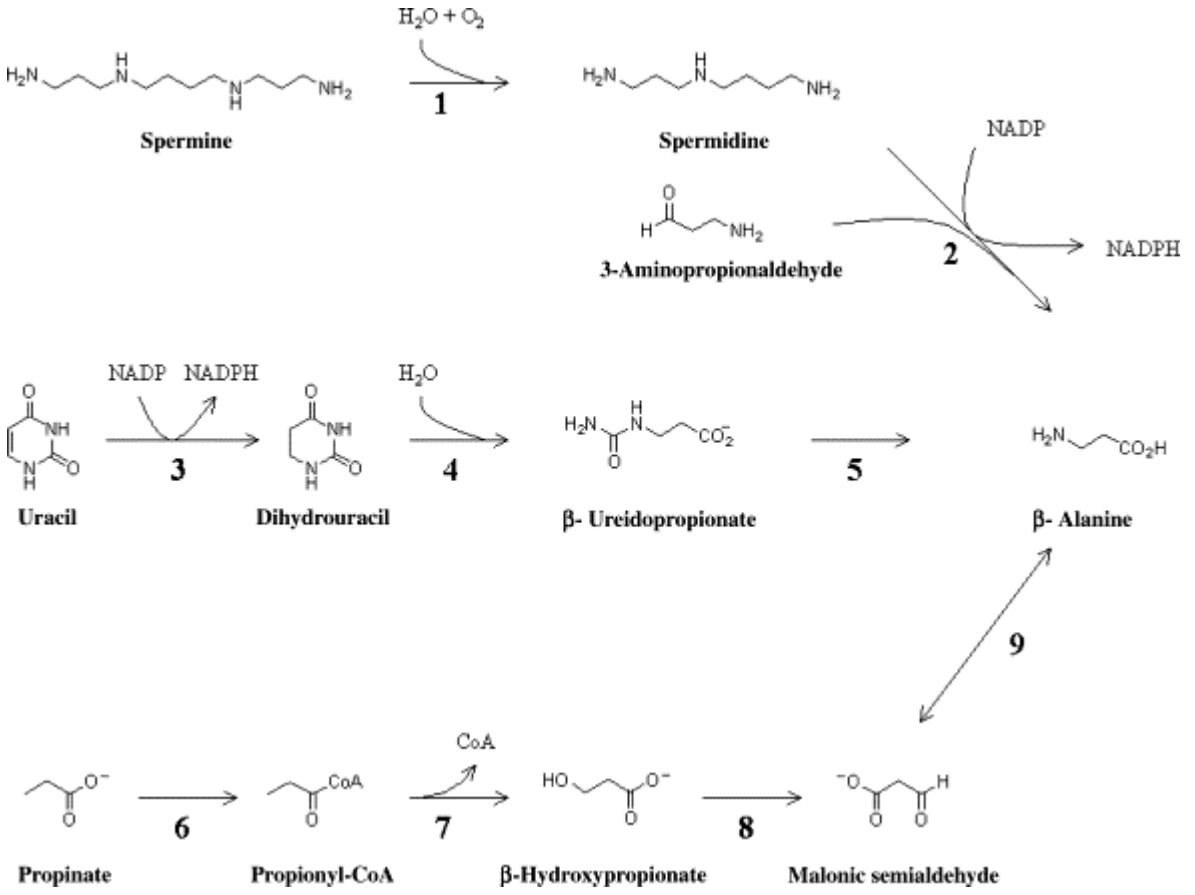

Fig. 1.7 Multiple routes of β-alanine in plants (reproduced from Raman and Rathinasabapathi, 2004) (**1**) Polyamine oxidase; (**2**) 3-amino propanal dehydrogenase; (**3**) dihydropyrimidine dehydrogenase; (**4**) dihydropyrimidinase; (**5**) β-uredіopropionase; (**6** and **7**) acylCoA transferases; (**8**) 3-hydroxy propionate dehydrogenase; (**9**) transaminase.

1.2.4 Pantothenate synthetase

Pantothenate synthetase (PTS) catalyses the condensation of pantoate and β-alanine to form pantothenate. The reaction requires ATP and proceeds via a pantoyl-adenylate intermediate (Mass, 1960; Wieland *et al.,* 1963). *E. coli* PTS was purified to homogeneity and characterized by Miyatake *et al.* (1979). It had a high pH optimum of 10, with K_m values of 150 μM for β-alanine, 63 μM for pantoate, and 100 μM for ATP. Pfleiderer *et al*. (1960) have reported lower affinities of substrates for the enzyme, but their results were apparently due partly to the erroneous pH and temperature optima they employed. The enzyme requires a divalent cation, Mg^{2+} or Mn^2, and a monovalent cation, K^+ or NH_4^+, as activators (Miyatake *et al.,* 1979). Miyatake *et al*. (1979) proposed PTS to be a tetramer of 18-20 kDa protomers, but they were probably dealing with a degradation product, since *panC* from *E. coli* encodes a 31.5 kDa protein similar in size to the many *panC* orthologs that, at ~50% pairwise sequence identity, are readily identified in various sequenced bacterial genomes and have also been

isolated from the eukaryote *Saccharomyces cerevisiae* (Genschel *et al*., 1999) and the higher plants *Oryza sativa* and *Lotus japonicus* (Genschel *et al*., 1999). The PTS enzymes from *E. coli* (von Delft *et al.*, 2001), higher plants (Genschel *et al*., 1999), *Mycobacterium tuberculosis* (Zheng and Blanchard, 2001) and *Fusarium oxysporum* (Perez-Espinosa *et al.,* 2001) form dimers in solution.

The kinetic mechanism of *E. coli* PTS was determined by Miyatake *et al*. (1978), who analysed the patterns of product inhibition by AMP and pantothenate on steady state enzyme activity. The observed pattern of inhibition was explained by a Bi Uni Uni Bi Ping Pong mechanism (Fig. 1.8) in which ATP is bound first, followed by pantoate, followed by pyrophosphate release. Subsequent β-alanine binding is followed by pantothenate release, with AMP release being the last step. The same kinetic mechanism has been shown for *Mycobacterium tuberculosis* pantothenate synthetase (Zheng and Blanchard, 2001).

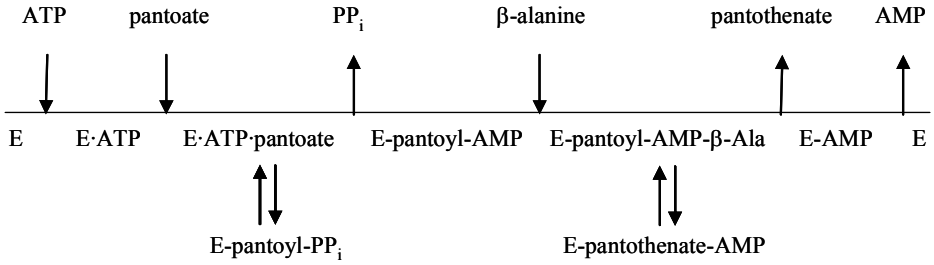

Fig. 1.8 The Bi Uni Uni Bi Ping Pong kinetic mechanism of *E. coli* and *M. tuberculosis* pantothenate synthetases (Miyatake *et al*., 1978; Zheng and Blanchard, 2001).

The *E. coli* pantothenate synthetase enzyme exists as a homodimer. Each subunit has two well-defined domains. The N-terminal domain forms a Rossmann fold, which contains the active site cavity and, the C-terminal domain forms a hinged lid for this cavity (von Delft, 2001). In the structure of pantothenate synthetase there are two sequence motif: HIGH and KMSKS (von Delft *at al*., 2001), that are important in binding of ATP in tRNA synthetases. The HIGH motif is at the N-terminus (residues 21-60 in *E. coli*), whereas the KSMKS motif is not conserved at the sequence level in PTS enzymes, but it is evident from structural alignments (von Delft *et al*., 2001). PTS belongs to the HIGH superfamily of nucleotidyltransfereses and is, thus, related to class I aminoacyl-tRNA synthetases (Aravind *et al*., 2002). Aminoacyl-tRNA synthetases attach amino acids to their cognate tRNAs in a two-step process by ATP activation of the amino acid and subsequent transfer to the tRNA (Fersht, 1999). The first half-reactions of bacterial PTS and aminoacyl-tRNA synthetase are

analogous in that both enzymes utilize ATP to form an acyl adenylate intermediate and release PP_i.

The Bi Uni Uni Bi Ping Pong mechanism involving acyl adenylate intermediate formation has been documented for other ATP-dependent synthetases, including malonyl-CoA synthetase, fatty acyl-CoA synthetase and some aminoacyl-tRNA synthetases (reviewed by Zheng and Blanchard, 2001). Malonyl-CoA synthetase has been shown to use a Bi Uni Uni Bi Ping Pong kinetic mechanism, consisting of an adenylation step followed by a thioesterification step. Although aminoacyl-tRNA synthetase-catalysed reactions similarly involved acyl adenylate formation, different kinetic mechanisms have been claimed for different enzymes. For example, the Bi Uni Uni Bi Ping Pong kinetic mechanism was proposed for *E. coli* proline- and rat liver threonine-tRNA synthetases, while *E. coli* and yeast arginyl-tRNA synthetases were reported to use a sequential mechanism (reviewed in Zheng and Blanchard, 2001).

The crystal structure of the apoenzyme forms of pantothenate synthetase from *E. coli* (von Delft *et al*., 2001) and *M. tuberculosis* (Wang and Eisenberg, 2003; 2006) have been reported, as well as several very important complexes of the *M. tuberculosis* enzyme including the pantoyl adenylate bound at the active site (Wang and Eisenberg, 2003, 2006). *M. tuberculosis* pantothenate synthetase has a nearly identical structure to that of the *E. coli* pantothenate synthetase and their sequence identity is 46% at the amino acid level. Sequence alignment revealed that *M. tuberculosis* PTS has 10 more residues at the N-terminus and about 20 more residues at the C-terminus than *E. coli* PTS. The N-terminal residues form a coli before first β-strand in the crystal structure, the C-terminal residues are away from the active site cavity, and are unlikely to have catalytic function, but may be involved in interactions with other proteins (Wang and Eisenberg, 2003). Even though the residues at the dimer interface are poorly conserved in the PTS family (von Delft *et al*., 2001) residues at the dimer interfaces are quite similar in the PTS proteins form *E. coli* and *M. tuberculosis* (Wang and Eisenberg, 2003). Moreover the C-terminal domain of *M. tuberculosis* covers the active site cavity with only a small opening (closed conformation), while that of *E. coli* PTS is away from the active site cavity (open conformation) (Wang and Eisenberg, 2003).

It has been shown that ATP binds into the Rossmann-fold domain of the enzyme, and pantoate binds into a pocket, deep in the active site cavity (von Delft *et al*., 2001; Wang and Eisenberg, 2006). For *E. coli* pantothenate synthetase, it has been proposed that the binding of ATP is accompanied by a hinge bending action that moves the two domains of the enzyme closer together and, leads from an open apo-structure to a closed structure (von Delft *et al*.,

2001). Wang and Eisenberg (2003), however, only found the closed conformation for the *M. tuberculosis* enzyme. They therefore suggested that ATP is bound into this closed structure *via* small-scale motions of a loop (residues 75 to 88), which acts as a gate to the active site cavity, rather than by a hinge-bending action. Pantoyl adenylate is highly unstable in solution due to rapid lactonization (Wieland *et al*., 1963). However inside the active site of the enzyme the molecule is tightly bound with hydrogen bonds to the active site residues, thereby preventing lactonization (from occurring) (Wand and Eisenberg, 2003). Binding of β-alanine occurs only after the reaction intermediate is formed (Wand and Eisenberg, 2003) (Fig. 1.9). Nucleophylic attack on the intermediate by β-alanine, brakes down the intermediate with concomitant formation of pantothenate and AMP. Once the intermediate brakes down to form AMP and pantothenate, the planarity of the peptide bond in pantothenate forces the molecule to have a conformation that cannot have favourable interactions with the side chains that bind pantoate and β-alanine (Wang and Eisenberg, 2006). In addition, there are steric clashes with the phosphate group of AMP and the Asp161 side chain. Therefore, pantothenate will leave the active site once it is formed (Wang and Eisenberg, 2006). Moreover, the enzyme has a very low affinity for pantothenate. Wang and Eisenberg (2006), failed to obtain a pantothenate-enzyme complex, when soaking or growing crystals with this compound. This is consistent with the finding that pantothenate is a poor inhibitor of the enzyme (Zheng and Blanchard, 2001). The AMP molecule, on the other hand, has good binding interactions in the active site (Wang and Eisenberg, 2006). However, it typically is present at a low concentration in the cell and thus can easily diffuse out of the active site. Moreover, ATP has many favourable interactions in the active site of the enzyme, and it can readily displace AMP (Wang and Eisenberg, 2006).

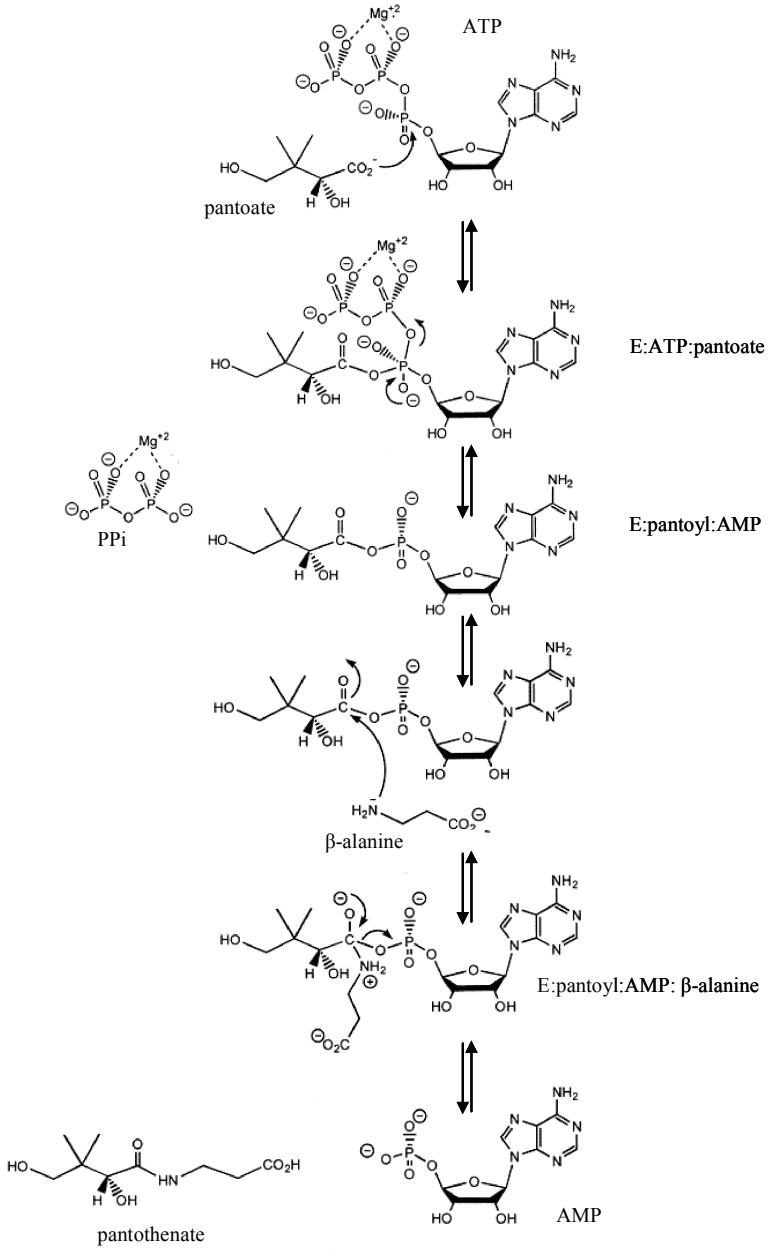

Fig. 1.9 Condensation between pantoate and β-alanine, catalysed by *E. coli* and *M. tuberculosis* pantothenate synthetase (reproduced from Zheng and Blanchard, 2001). The reaction starts with ATP binding to the active site. Pantoate initiates a nucleophylic attack on the α-phosphate. The Mg^{2+} ion and the positively charged side chains around the β- and γ-phosphate groups draw the negative charges toward the leaving pyrophosphate. This favours the formation of the pantoyl adenylate intermediate. The subsequent attack of β-alanine requires the deprotonation of the β-amino group to allow nucleophylic attack on the carboxylate of the pantoyl adenylate intermediate. The intermediate breaks down do to form AMP and pantothenate.

Pantothenate is thought to have existed in the prebiotic world, so the biosynthetic pathways for pantothenate were established early and have not changed subsequently (Miller and Schlesinger, 1993). It is thus of considerable interest that pantothenate synthetase is a member of the superfamily that includes aminoacyl-tRNA synthetases (tRSs), another group of enzymes of ancient origin, and phosphopantetheine adenyltransferase (PPAT), an enzyme involved in the synthesis of coenzyme A, which is itself derived from pantothenate (von Delft *et al*., 2001).

Using assays developed to measure the activity of *E. coli* PTS, several groups have tried to detect activity in crude plant extracts, but without success (Sahi *et al*., 1988; Genschel *et al*., 1999). The first plant pantothenate biosynthesis enzyme to be cloned was a cDNA encoding PTS from *Lotus japonicus*, which was isolated by functional complementation of the corresponding *E. coli* mutant (Genschel *et al*., 1999). This provided the first conclusive evidence for the pantothenate biosynthesis pathway in plants. The *Lotus japonicus* and *Oryza sativa* cDNAs encoded proteins of approximately 34 kDa that are 65% similar to each other at the amino acid level. The *PTS* gene from, yeast, *L. japonicus* and *O. sativa* were able to functionally complement an *E. coli* mutant lacking *PTS*, therefore *PTS* genes seems to be conserved across phylogenetically distant organisms (Genschel *et al*., 1999).

The recombinant pantothenate synthetase from *Lotus*, overexpressed in *E. coli* required D-pantoate, β-alanine and ATP for activity and had a higher affinity for pantoate (K_m = 45 μM) than for β-alanine (K_m = 990 μM). Neither ketopantoate nor pantoyl-lactone could replace pantoate as substrate. Interestingly, pantoate inhibits the *L. japonicus* PTS enzyme at concentration greater than 0.5 mM (Genschel *et al*., 1999), whereas the *E. coli* PTS has normal Michaelis kinetics with this substrate (Miyatake *et al*., 1979). The significance of the inhibition of plant PTS by pantoate is not currently understood, but it has been suggested that it may be involved in regulation of the pantothenate pathway in plants (Genschel *et al*., 1999). Recently, Ottenhof *et al*. (2004) identified the Arabidopsis gene encoding for pantothenate synthetase (At5g48840). In all plants examined so far, there is a single gene for PTS.

The Arabidopsis PTS is 310 amino acid long and has 39% amino acid sequence similarity to the *E. coli* orthologue (Merkel and Nichols, 1996). It is 66 and 62% similar to those from *Lotus* and rice, respectively (Genschel *et al*., 1999). In common with PTS from other plants, there is no N-terminal extension compared with the *E. coli* protein (Ottenhof *et al*., 2004). This led to the conclusion that the enzymes are cytosolic, which was confirmed by GFP-targeting experiments with the Arabidopsis enzyme (Ottenhof *et al*., 2004). This is in contradiction to an earlier report on pantothenate biosynthesis in spinach by Julliard (1994),

who reported the detection of pantothenate synthetase activity in chloroplast stroma. This activity could only be demonstrated with pantoyl-lactone. In contrast, both *E. coli* PTS and *Lotus* PTS have a strict requirement for the open form of pantoate, and do not use pantoyl-lacton as a substrate (Genschel *et al*., 1999). It is possible that there is another PTS in plant cells that is located in chloroplast, but it is considered to be unlikely, as extensive homology searching in the Arabidopsis genome with both conventional and structure-based methods (FUGUE) have identified a single PTS gene only (Ottenhof *et al*., 2004).

1.3 Metabolic engineering of the bacterial pathway

Vitamin B5, precursor of coenzyme A, is synthesised by microorganisms and plants but not by animals. This vitamin is, therefore, required in pharmacy and animal feeding. Now, the synthesis of pantothenate is principally chemistry based. Biotechnological alternatives are considered for *Escherichia coli* (Moriya *et al*., 1997) and *Corynebacterium glutamicum* (Sahm and Eggeling, 1999). The latter, a Gram positive aerobic bacteria, is already extensively used for the production of a number of amino acids and nucleotides, including the branched chain amino acids sharing the same initial pathway as pantothenate (Fig. 1.10). A genetically engineered strain has been elaborated indicating that this bacterium can accumulate pantothenate in the medium, albeit at levels actually much lower than described for *E. coli* (Sahm and Eggeling, 1999).

Mass (1960) observed that the *in vitro* rate of pantothenate production by the pantothenate synthetase of *E. coli* is 100 times faster than the maximal in-vivo rate. The high levels of activity of pantothenate synthetase in *E. coli* suggest that the supply of either pantoate or β-alanine is rate-limiting in pantothenate biosynthesis *in vivo* (Powers and Snell, 1976; Cronan, 1980). Miyatake *et al*. (1979) suggested that the rate-limiting step in pantothenate synthesis is probably also the rate-limiting step in CoA synthesis because supplementation of *E. coli* growth media with pantothenate increases the intracellular coenzyme A pool by 10- to 20-fold. Based on *in vitro* pantoate and coenzyme A inhibition of KPHMT, Powers and Snell (1976) proposed that this enzyme was limiting, whereas Cronan (1980) suggested that the formation of β-alanine was the limiting step. Jackowski and Rock (1981) demonstrated that neither of these metabolites were limiting for coenzyme A biosynthesis although the supply of β-alanine was limiting for the biosynthesis of pantothenate. This was observed when a β-alanine auxotrophic *E. coli panD*$^-$ strain was grown in increasing concentrations of β-alanine. Whilst the intracellular concentration of coenzyme A was initially dependent on the extracellular supply of β-alanine, this reached plateau at 8 mM. Above this concentration, the

extracellular concentration of pantothenate increased as the cell exported excess pantothenate (Jackowski and Rock, 1981). In wild type *E. coli,* the intracellular pantothenate pool is small, less than 1 μM (Jackowski and Rock, 1981; Vallari and Rock 1985), but this bacterium exports pantothenate into the growth medium, indicating that *E. coli* produces 15-fold more pantoate than is required and pantothenate production is not limiting for coenzyme A production (Jackowski and Rock, 1981). The level of coenzyme A in *E. coli* is controlled by feedback inhibition of pantothenate kinase by coenzyme A and coenzymes A thioesters, and by the rate of degradation of coenzyme A to phosphopantetheine (Vallari *et al*., 1987; Vallari and Jackowski, 1988). Physiological, biochemical, and genetic evidence points to feedback inhibition of pantothenate kinase as a key regulated step in the biosynthetic pathway of coenzyme A synthesis (Vallari *et al*., 1987; Vallari and Jackowski, 1988).

Elischewski *et al*. (1999) found that 3-fold overexpression of *panE* in *E. coli* led to a corresponding 3.5-fold increase in pantothenate excretion. Since the level of pantothenate production was further enhanced by the addition of ketopantoate this indicate that KPR is no longer limiting in this system, but was in the wild-type bacterial strain. The limiting factor in pantothenate production in *Corynebacterium glutamicum* is β-alanine synthesis (Dusch *et al.*, 1999). Overexpression of *C. glutamicum panD* lead to an increase in pantothenate excretion to the same levels as were achieved by β-alanine supplementation. Overexpression of *E. coli panD* did not lead to the same observation. Aspartate and ketoisovalerate (KIVA) are metabolite common to both the pantothenate pathway and the valine pathway (Fig.1.10). The ketopantoate reductase activity, normally attributed to a specific enzyme encoded by *panE*, has been shown to be catalysed only by the acetohydroxy acid isomeroreductase (*ilvC*) in *C. glutamicum* (Merkamm *et al*., 2003) (Fig. 1.10). Apart from this particularity, the genetic organization of *C. glutamicum* metabolic pathway is similar to that found in many bacteria. The *ilvBN* product has, therefore, a double role being essential for the upstream pathway transforming pyruvate to α-KIVA, common precursor to both valine and pantothenate biosynthesis (Fig. 1.10). In addition to α-KIVA the biosynthetic pathway for pantothenate also requires CH_2-THF (cofactor for KPHMT), presumably generated by the glycine-(serine)-hydroxy-methyl transferase, and β-alanine synthesised naturally at low rates by the aspartate decarboxylase (*panD*) (Dusch *et al*., 1999). Glycine accumulates in parallel to pantothenate, this might indicate that CH_2-THF availability may be a potential limiting factor (Chassagnole *et al*., 2003).

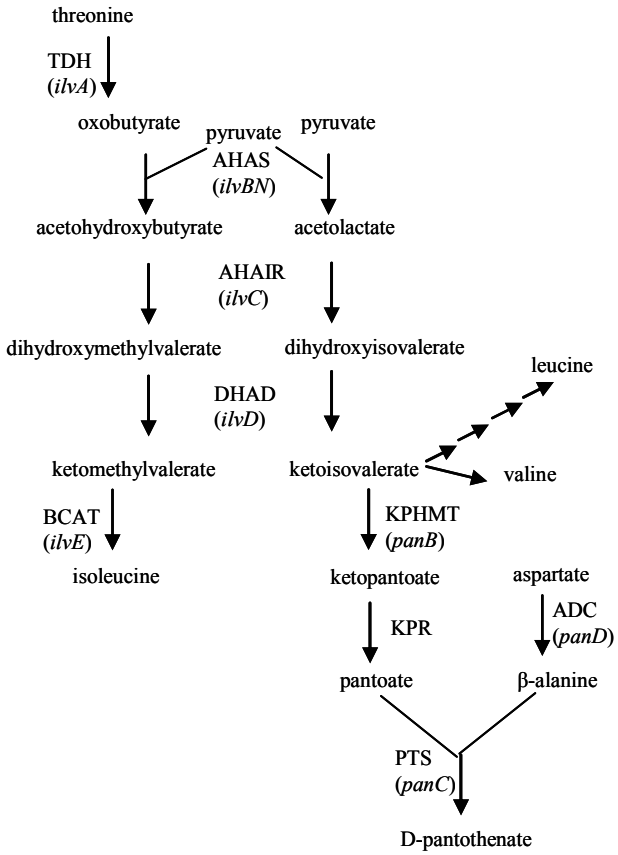

Fig. 1.10 Scheme of the pantothenate biosynthetic pathway and its integration into the synthesis of branched-chain amino acids (reproduced from Merkamm *et al*., 2003). The enzymes involved in the biosynthetic steps are TDH, threonine deaminase; AHAS, acetohydroxy acid synthase; AHAIR, acetohydroxy acid isomeroreductase; DHAD, dihydroxyacid dehydratase; BCAT, branched-chain amino acid aminotransferase; KPHMT, ketopantoate hydroxymethyl transferase; KPR, ketopantoate reductase; ADC, aspartate decarboxylase; PTS, pantothenate synthase. When identified in *C. glutamicum*, the corresponding genes are indicated between brackets (see text for details).

Studies of pantothenate biosynthesis in *C. glutamicum* have demonstrated that competition for α-KIVA from amino acid biosynthesis is the main limiting factor for pantoate biosynthesis (Sahm and Eggeling, 1999). The deletion of *ilvA* (threonine decarboxylase) which is essential for L-isoleucine synthesis increased the yield of pantothenate by reducing the competition for the enzymes required for α-KIVA synthesis (Dusch *et al.*, 1999). Overexpression of *panB* and *panC,* both with and without overexpression of the genes for branched chain amino acids biosynthesis, also lead to an increased yield of pantothenate (Dusch *et al.*, 1999). In general, the activities of the enzymes of pantothenate biosynthesis are two or three orders of magnitude lower than those of branched-chain amino acid biosynthesis and central metabolism. This considerably limits the flux through the pathway due to competition with alternative pathways (Chassagnole *et al*., 2003). α-KIVA provides a branch point between the pathways of pantothenate and valine biosynthesis. Studies have indicated that the flux to valine is ten-fold higher than that to pantothenate from this point leading to

significant dissipation of the metabolic flux in this undesired direction (Chassagnole *et al*., 2002; 2003). It has been reported by Moriya *et al*. (1997) that engineered *E. coli* can produce pantothenate reaching concentration of 66 g l^{-1}, but it is not known to what extent *C. glutamicum* is subject to such phenomena.

The catabolism of pantothenate has been described in *Pseudomonas* P-2 by Goodhue and Snell (1966). In this organism, pantothenate is hydrolysed to pantoate and β-alanine. The hydrolytic enzyme, pantothenase (EC 3.5.1.22), has been subsequently characterised and it has been found that the enzymes from different strains of *Pseudomonas* lead either to pantolactone or to pantoate or to both (Airas, 1988). The enzyme is unusual in its sensitivity to heat, it functions optimally at 28°C and is rapidly inactivated at temperatures above 30°C (Nurmikko *et al*., 1966). The K_m value for pantothenate reported was 3 mM and interestingly, the enzyme shows relatively high rate of the reverse reaction raising the question whether this enzyme could function also in pantothenate synthesis when no pantothenate is present in the growth medium (Airas, 1988). The author speculates that, if the pantoyl lactone concentration is 1 mM and the β-alanine concentration 1 mM, then the pantothenate concentration at the equilibrium would be 13 μM, therefore a role of the pantothenase in pantothenate synthesis was not excluded by Airas (1988).

1.4 Organization and regulation of the plant pantothenate pathway

Despite the common enzymatic steps, compartmentalization of the plant pantothenate biosynthesis pathway makes it more complex than its bacterial counterpart. The compartmentalization of the pathway in plants is likely to have some influence on the regulation of pantothenate biosynthesis, but the effect of this or any other point of control are as yet unclear (Chakauya *et al*., 2006). As pantothenate synthesis in plants occurs in different compartments, the transport of pathway intermediates between them could be of regulatory and functional significance.

As expected from sequence analysis of KPHMT1 and KPHMT2, subcellular localization demonstrated that both isoforms are targeted exclusively to mitochondria whereas pantothenate synthetase is located in the cytosol (Ottenhof *et al*., 2004). Moreover, KPHMT activity was detected in pea and Arabidopsis mitochondria (Ottenhof *et al*., 2004) and was not detectable in purified chloroplasts. KPHMT converts α-ketoisovalerate into ketopantoate using 5,10-methylene tetrahydrofolate (CH_2-THF) as a cofactor (Powers and Snell, 1976; Teller, 1976). In plant cells the synthesis of THT, occurs in the mitochondria (Ravanel *et al.,* 2001) and the estimated concentration of folates in mitochondria is 100-150-fold higher than

in chloroplasts (reviewed by Ravanel *et al*., 2001). This argument supports the view that plant cells do not produce ketopantoate in the chloroplasts.

Further investigation of the pantothenate biosynthesis pathway in plants requires identification of the enzymes responsible for the reduction of ketopantoate to pantoate, and for the synthesis of β-alanine. No ADC homologue was identified in the Arabidopsis genome, nor in that of the yeast *S. cerevisiae*, suggesting that ADC has not made the transition across the prokaryote-eukaryote border. The pathway providing β-alanine for pantothenate synthesis is, as yet unknown, although several routes are considered (see above). A possible homologue of *E. coli panE* in Arabidopsis was identified (Ottenhof *et al*., 2004; Coxon *et al*., 2005), but it has not been demonstrated whether this Arabidopsis protein has KPR activity, and thereby whether it has a role in pantothenate biosynthesis *in vivo*. In a study of Huh *et al*. (2003), yeast KPR was found to be cytosolic. Whether or not the reductase has a similar location in plants, there is clearly a need to transport either ketopantoate or pantoate across the mitochondrial membranes into the cytosol, implicating a specific transporters protein (Chakauya *et al*., 2006).

The only known function of pantothenate is its use in the synthesis of coenzyme A and acyl carrier protein, the principal biologically active form of the vitamin (Leonardi *et al*., 2005). The five enzymatic steps converting pantothenate to coenzyme A have been described in plants and the pathway was reconstituted *in vitro* (Kupke *et al*., 2003). Analysis of the coding sequence for the coenzyme A synthesis enzymes (starting from pantothenate) suggests that they are all likely to be cytosolic. This strongly suggests that pantothenate is presumably metabolized further in the cytosol. In a study of Guerra (1993) in spinach, the enzyme catalysing the first committed step towards coenzyme A, pantothenate kinase, was found to be localised in the cytosol and predominantly in the chloroplasts. Recently, Tilton *et al*. (2006) showed that Arabidopsis possess two functional PANK (AtPANK1, AtPANK2) isoforms. In the same study it was demonstrated that only one isoform of pantothenate kinase is necessary and sufficient for producing adequate coenzyme A levels, and that no other enzyme can compensate for the loss of both isoforms. Analysis of N-terminal sequences of both *PANK* isoforms revealed that neither enzyme was predicted to contain chloroplast or mitochondrial transit peptides (Tilton *et al*., 2006). Although experimental evidence on the cellular location of PANK enzymes is lacking, the absence of targeting sequence supports the scenario in which coenzyme A is produced in the cytosol and shuttled into the organelles according to metabolic demands. It further suggests that *PANK1* and *PANK2* are not paralogs of the two pantothenate kinases partially purified from spinach chloroplast (Falk and Guerra, 1993).

Nevertheless, a plastidic site of coenzyme A synthesis is plausible because of the extensive requirement for coenzyme A in the chloroplast, especially for *de novo* fatty acid synthesis and lipid metabolism (Falk and Guerra, 1993). This view is supported by the endosymbiotic origin of plant chloroplasts (Margulis, 1970). Moreover, many important biosynthetic pathways localized to the chloroplast are duplicated in the cytosol. Nevertheless, in the light of the work of Tilton *et al*. (2006) this does not seem to be the case for PANK.

Coenzyme A is found in the majority of cellular compartments (plastids, mitochondria, cytosol, endomembrane system), implying that there must be transporters present, responsible for shuttling coenzyme A and coenzyme A precursors of these pathways between different compartments. A transporter for coenzyme A has been reported in potato mitochondria (Neuburger *et al*., 1984; Yang *et al*., 1994). Since coenzyme A is transported into mitochondria a mitochondrial site of coenzyme A synthesis may not be necessary. Evidence exists that chloroplasts also have coenzyme A import capability (Yang *et al*., 1994).

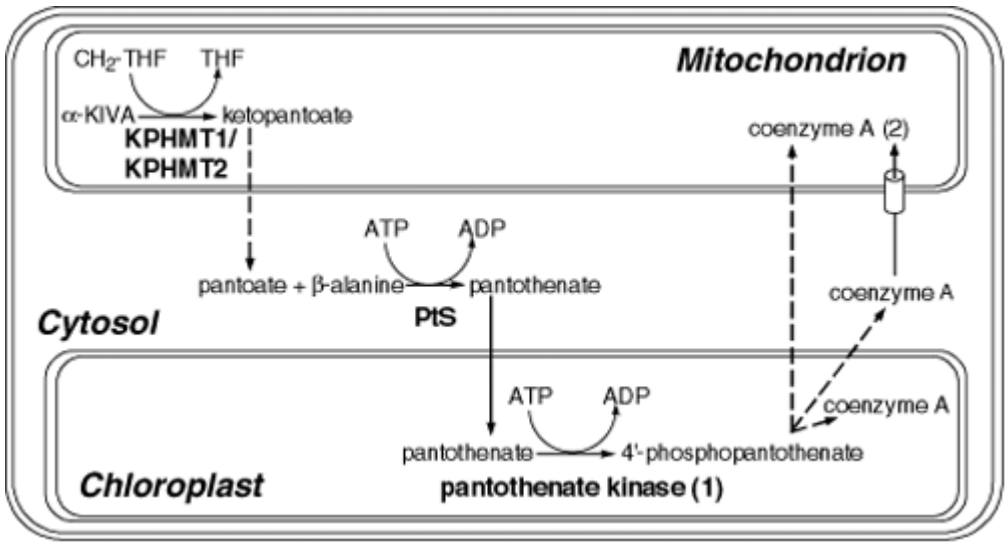

Fig. 1.11 Schematic model of the subcellular distribution of the enzymes of pantothenate and coenzyme A biosynthesis in higher plants (reproduced from Ottenhof *et al*., 2004). Ketopantoate hydroxymethyltransferase (KPHMT) is in the mitochondrion, whereas pantothenate synthetase (PtS) is in the cytosol. Depending on the location of plant ketopantoate reductase either ketopantoate or pantoate must be exported from the mitochondrion. The source of β-alanine in plants remains unestablished. (1): Falk and Guerra (1993) reported that the first committed step to coenzyme A biosynthesis, pantothenate kinase, was localised in chloroplasts of spinach; (2): coenzyme A can be imported into plant mitochondria by a specific carrier in potato (Neuburger *et al*., 1984).The five enzymes responsible for the synthesis of coenzyme A have all been identified in plants (Kupke *et al*., 2003), and none of them appear to have transit peptides, suggesting that they are all found in the cytosol.

1.5 Pantothenate transport

1.5.1 Pantothenate transport in bacteria

Many organisms, as well as being capable of *de novo* synthesis of pantothenate, are capable of absorbing preformed pantothenate from their local environment. This uptake is mediated by an Na^+:pantothenate transporter, pantothenate permease. Pantothenate is taken up by virtually all bacteria and is essential for those lacking *de novo* pantothenate biosynthesis, such as *Streptococcus pneumoniae*, *Lactobacillus lactis* and *Hemophilus influenzae* (Gerdes *et al*., 2002). In *E. coli*, pantothenate uptake is mediated by pantothenate permease, also termed the PanF protein, encoded by the *panF* gene. PanF uses a sodium-cotransport mechanism to concentrate pantothenate from the medium (Jackowski, 1990; Vallari and Rock, 1985). The transport system is highly specific for pantothenate, with a K_t of 0.4 μM and a maximum velocity of 1.6 pmol/min/10^8 cells. Although the transport system has a high affinity for pantothenate, the maximum velocity is 100-fold less than that of typical amino acid transport processes, indicating that the permease is not an abundant protein (Vallari and Rock, 1985). Overexpression of the PanF protein in *E. coli* produces a 10-fold increase in the rate of pantothenate uptake and concomitant elevation of the steady-state intracellular concentration of pantothenate (Jackowski and Alix, 1990). However, the coenzyme A levels remain unaffected, indicating that PanF activity does not regulate coenzyme A biosynthesis (Jackowski and Alix, 1990).

Pantothenate is effluxed from *E. coli*, which excretes large amounts of pantothenate that it has synthesized *de novo* (Jackowski and Rock, 1981). *E. coli* produces and secretes 15 times more pantothenate than required for intracellular CoA biosynthesis (Jackowski and Rock, 1981). Pantothenate excretion is still active in *panF* mutants, which are unable to take up the vitamin (Vallari and Rock, 1985), showing that the uptake is unidirectional, and pointing to the existence of a distinct and uncharacterized efflux system. Constitutive production of pantothenate combined with transporter-mediated efflux of excess pantothenate may constitute a bacterial mechanism for pantothenate homeostasis which is required for efficient allosteric regulation of coenzyme A synthesis.

1.5.2 Pantothenate transport in yeast

Yeast is naturally capable of *de novo* pantothenate biosynthesis (White *et al*., 2001). Yeast have all the enzymes required for pantothenate biosynthesis except for aspartate decarboxylase, the enzyme necessary for β-alanine biosynthesis in *E. coli*. β-Alanine in yeast is formed from spermine via the amine oxidase encoded by *FMS*1 gene (White *et al*., 2001).

Pantothenate uptake is mediated by the product of the *FEN2* gene of *Saccharomyces cerevisiae.* It is a hydrogen ion-pantothenate symporter belonging to the major facilitator superfamily localized on the plasma membrane (Stolz and Sauer, 1999). The Fen2p primary sequence bears no resemblance to the PanF transporter from *E. coli* or the mammalian multivitamin transporter (Leonardi *et al*., 2004). The Fen2p transporter has high affinity for pantothenate with a K_t of 3.5 μM. It is most active at low extracellular concentration of pantothenate and does not transport β-alanine. β-Alanine was able to complement the pantothenate auxotrophy of a *fen2*$^-$ mutant and is probably imported by the general amino acid permease Gap1 (Stolz and Sauer, 1999). The *liz1* gene of *Schizosaccharomyces pombe* encodes an active transport protein for pantothenate, which is homologous with the Fen2p protein of *S. cerevisiae* (Stolz *et al*., 2004). Both the Fen2p and Liz1 transporters are required for pantothenate uptake at low extracellular concentrations.

1.5.3 Pantothenate transport in animals

In animals, pantothenate as well as biotin and lipoate, transport depends on a sodium-dependent multivitamin transporter. This transporter was cloned from three sources, *i.e.* rat placenta, a human choriocarcinoma cell line, and rabbit intestine (reviewed by Leonardi *et al*., 2004). The cDNAs of the cloned transporters predict almost identical proteins of about 69 kDa consisting of 635 amino acids. Expression of the cloned cDNAs in either mammalian cells or *Xenopus laevis* oocytes results in the appearance of sodium-dependent transport of pantothenate with K_t of 2-5 μM that is inhibited by either biotin or lipoic acid. (reviewed by Leonardi *et al*., 2004). The mammalian pantothenate transporter belongs to the sodium-coupled glucose transporter family and the proteins in this family share a common core of 13 transmembrane helices (reviewed by Leonardi *et al*., 2004).

1.5.4 Pantothenate transport in plants

Pantothenate transport in plants has not been investigated yet. Nevertheless it can be concluded that plants are capable to take up pantothenate if supplied. Evidence for that came from a pantothenate-requiring auxotroph of *Datura innoxia*. This auxotrophic cell line could grow in cell culture if supplied with ketopantoate, pantoate, or pantothenate (Sahi *et al.*, 1988). The nature of this transport is unknown and has not been investigated.

1.6 Aims of this work

The biosynthetic pathway for pantothenate in bacteria, comprising four enzymatic reactions, is well established, and the enzymes from *E. coli* have been fully characterised, including overexpression and purification of recombinant enzymes and the determination of their crystal structure. The absence of pantothenate biosynthesis in animals makes these enzymes an attractive target for non-toxic antibiotics, fungicides and herbicides. Therefore, the pantothenate pathway, like many other microbial pathways of vitamin biosynthesis is an area of growing academic and industrial interest. There has already been some success in the industrial production of pantothenate using recombinant bacterial strains with enhanced expression of *panC* and *panD* (Dusch *et al*., 1999, Chassagnole *et al*., 2003). Metabolic engineering of pantothenate production in plants requires a much more complete understanding of the endogenous pathway than we currently have. Generation of crop plants overproducing the vitamin seems to be more complicated than in the bacterial system. Successful engineering of the pantothenate biosynthetic pathway requires complete understanding of its organisation and enzymes itself. At the moment our knowledge is fragmented. The synthesis of pantothenate and coenzyme A, the metabolically active form of the vitamin, in plants takes places in different compartments. Comprehensive understanding of the plant pantothenate synthetic pathway requires detailed characterisation of all enzymes on the pathway as well as their cellular location.

The overall goal of this work was to characterise the physiological role of pantothenate synthetase in *A. thaliana*, and to assess its possible participation in the regulation of pantothenate production. It has been proposed that plants possess an alternative, chloroplast-localised pathway leading to coenzyme A (Falk and Guerra, 1993; Julliard, 1994), but its contribution to the synthesis of coenzyme A biosynthesis has not been investigated. During the course of these study two T-DNA knock-out mutations of *A. thaliana PTS* were characterised to shed light on the significance of the hypothetical pathway in Arabidopsis development.

Pantothenate is thought to have existed in the prebiotic world. Consequently, the biosynthetic pathways for pantothenate were established early and have not changed subsequently (Miller and Schlesinger, 1993). It has been proposed that plant and bacterial pantothenate biosynthetic pathways proceed via the same route. This raised the question, whether *A. thaliana* and *E. coli* PTS are functionally conserved. This was investigated by heterologous expression of *E. coli* PTS. Moreover, an attempt to generate transgenic *A.*

thaliana plant overproducing pantothenate was undertaken. This enabled to address the question whether pantothenate levels can be modified by altering the PTS activity.

The bacterial PTS enzyme exhibits normal Michaelis-Menten kinetics with respect to its natural substrates, pantoate, β-alanine, and ATP (Pfleiderer, 1960; Miyatake, 1979), whereas plant PTS shows substrate inhibition by pantoate (Genschel *et al*., 1999). However, the physiological relevance or the structural basis for the distinct kinetic behaviour of *A. thaliana* PTS were not investigated. These open question were addressed by comparative analysis of PTS sequences and detailed kinetic analyses of wild-type and mutant forms of *A. thaliana* PTS.

Chapter 2
Materials and Methods

2.1 General

All laboratory reagents used in this work are obtained commercially (analytical grade) from the companies BioRad (USA), Fluka (Switzerland), Merck (Darmstadt), Roth (Karlsruhe), Serva (Heidelberg), Sigma-Aldrich (USA).

Oligonucleotides were obtained from Biomers (Ulm, Germany) or Sigma ARK (Germany).

The molecular biology protocols, unless otherwise stated, were as described by Sambrook and Russell (2001).

2.2 Enzymes and plasmids

Restriction enzymes were purchased from Gibco BRL (USA), New England Biolabs (USA), Quiagen (Hilden), Roche (Schweiz), Serva (Heidelberg), Sigma-Aldrich (USA) and Stratagene (USA).

Myokinase, lactate dehydrogenase, pyruvate kinase from rabbit muscle were purchased from Sigma-Aldrich.

DNA purification was performed using the GFX^{TM} DNA and Gel Band Purification Kit from Amersham Pharmacia Biotech (Freiburg). Purification of recombinant His-tag proteins overexpressed in *E. coli* was done using Ni-NTA-Agarose from Amersham Pharmacia Biotech (Freiburg).

Pfu DNA polymerase was from Promega. DNA size marker and protein molecular mass standards were from Invitrogen, Bovine serum albumin was purchased from New England Biolabs (USA).

Vectors: pGEM-T (Promega), pBluescript KS- (Stratagene), pCambia1201 and pCambia1305.1 (Cambia, Australia) pET28-a plasmid and *E. coli* strain BL21 (DE3) were obtained from Novagen.

2.3 Plant material

Arabidopsis thaliana plants (ecotype Col-0) as well as transgenic Arabidopsis plants were grown on autoclaved soil. Seeds were vernalized for 5 days at 4°C in the dark; growth was continued in a growth chamber at 18°C under continuous light.

In *in vitro* cultures, seedlings were germinated aseptically on agar medium containing half-strength Murashige and Skoog salts and 1% sucrose (w/v), vernalized as above.

Growth stages of Arabidopsis in analysis of *PTS* expression using Genevestigator (section 3.7.1) were determined according to Boyes *et al*., 2001; table 2.1 (below).

Stage	Description	Days[a]	sd	CV[b]
Principal growth stage 1	Leaf development			
1.02	2 rosette leaves >1 mm in length	12.5	1.3	10.7
1.03	3 rosette leaves >1 mm in length	15.9	1.5	9.5
1.04	4 rosette leaves >1 mm in length	16.5	1.6	9.8
1.05	5 rosette leaves >1 mm in length	17.7	1.8	10.2
1.06	6 rosette leaves >1 mm in length	18.4	1.8	9.8
1.07	7 rosette leaves >1 mm in length	19.4	2.2	11.1
1.08	8 rosette leaves >1 mm in length	20.0	2.2	11.2
1.09	9 rosette leaves >1 mm in length	21.1	2.3	10.8
1.10	10 rosette leaves >1 mm in length	21.6	2.3	10.9
1.11	11 rosette leaves >1 mm in length	22.2	2.5	11.2
1.12	12 rosette leaves >1 mm in length	23.3	2.6	11.3
1.13	13 rosette leaves >1 mm in length	24.8	3.2	12.8
1.14	14 rosette leaves >1 mm in length	25.5	2.6	10.2
Principal growth stage 3	Rosette growth			
3.20	Rosette is 20% of final size	18.9	3.0	16.0
3.50	Rosette is 50% of final size	24.0	4.1	17.0
3.70	Rosette is 70% of final size	27.4	4.1	15.0
3.90	Rosette growth complete	29.3	3.5	12.0
Principal growth stage 5	Inflorescence emergence			
5.10	First flower buds visible	26.0	3.5	13.3
Principal growth stage 6	Flower production			
6.00	First flower open	31.8	3.6	13.3
6.10	10% of flowers to be produced have opened	35.9	4.9	13.6
6.30	30% of flowers to be produced have opened	40.1	4.9	12.3
6.50	50% of flowers to be produced have opened	43.5	4.9	11.2
6.90	Flowering complete	49.4	5.8	11.7
Principal growth stage 8	Silique ripening			
8.00	First silique shattered	48.0	4.5	9.3
Principal growth stage 9	Senescence			
9.70	Senescence complete; ready for seed harvest	ND[c]	ND	ND

Table 2.1. *Arabidopsis thaliana* (Col-0) growth stages for the soil-based phenotypic analysis (reproduced from Boyes *et al*., 2001) Table used as a reference for figure 3.18 A.

[a] Average day from date of sowing, including a 3-day stratification at 4°C to synchronize germination.

[b] CV, coefficient of variation, calculated as (SD/days) x 100.

[c] ND, not determined

2.3.1 Segregation analysis

The χ^2 statistical test was used to determine how well a set of segregation data fits a particular hypothesis.

The formula is $\frac{(O-E)^2}{E}$ over all classes, where *O* is the observed number of plants (or seeds) in a category and *E* is the expected number of plants (or seeds) in a category. *O* end *E* are the actual number of plants (or seeds) scored. The classes are different phenotypic groups. The degrees of freedom (*df*) = (number of classes) – 1. Two phenotypical classes were analysed, therefore, there is 2 – 1 = 1 degree of freedom. A hypothesis was considered acceptable if the calculated value of χ^2 is was less then the value for χ^2_{95}. With one degree of freedom $\chi^2_{95} = 3.841$.

2.4 Reagents and media

2.4.1 Buffers and media

Typical buffers and media were prepared according to Sambrook and Russell (2001).

Stock solutions of 100 mM potassium pantoate were prepared by incubating pantoyl-lactone with an equal molar amount of KOH (King *et al*., 1974). The solution was left at room temperature for an hour, adjusted to pH 7-8 with KOH.

X-Gluc solution (for 10ml): 6.15 ml 0.1 M Na_2HPO4; 3,85 ml NaH_2PO_4; 0.1 ml 100 mM potassium ferrocyanide (pH 7.0); 0.1 ml 100 mM potassium ferricyanide (pH 7.0); 30 µl Triton X-100; 20 µl 0.5 M EDTA; 5.2 mg X-Gluc in 50 µl DMF.

2.4.2 Radioactive reagents

Radiolabeled [3-^{14}C]β-alanine was purchased from ARC (American Radiolabeled Chemicals) ([3-^{14}C]β-alanine 55mCi/mmol; 0.1 mCi/ml.

[3-^{14}C]Pantothenate (55 mCi/mmol) was synthesized by incubating 0.5 mM [3-^{14}C]β-alanine (55 mCi/mmol) with 0.7 mM D-pantoate. 5 mM Na_2ATP, 10 mM $MgSO_4$. 10 mM $(NH_4)_2SO_4$, 100 mM Tris-HCl (pH 8.0), and 0.4 µg/µl *E. coli* PTS at 25°C until completion of the reaction (30min). Reaction products were separated by TLC chromatography. Silica gel spots containing [3-^{14}C]pantothenate were scraped from the TLC plate and extracted with 5 mM Tris-HCl (pH 8.0). The extract was centrifuged, and the supernatant was lyophilized and resuspended in 30 µl H_2O. This preparation had a concentration of 50 µCi/ml and > 99% of total ^{14}C-label were associated with pantothenate.

2.5 Microbiological techniques

2.5.1 Bacterial strains

Strain	Genotype	Application
E. coli XL1 Blue	*supE44 hsdR17 recA1 endA1 gyrA46 thi relA1 lac-lac [F' proAB+ lacIq lacZΔM15 Tn10(Tetr)]*; (Bullock *et al*., 1987)	Standard-cloning
E. coli BL21 (DE3)	F^- *ompT hsdS*$_B$ (r_B^- m_B^-) *gal dcm* (DE3) (Studier and Mofat, 1986)	Protein expression

Agrobacterium tumefaciens strain GV3101::pMP90RK with resistance marker rifampicin (chromosomal marker), kanamycin and gentanamycin (Ti plasmid marker) (Koncz and Schell, 1986) was used for *Agrobacterium*-mediated gene transfer.

2.5.2 Preparation of *E. coli* XL1 Blue competent cells

100ml dYT medium was inoculated with 5 ml overnight culture (containing tetracycline 15 mg/l) of *E.coli* XL1 Blue. The cells were grown to an $OD_{600} < 0.5$, and then were pelleted by centrifugation for 20 min in 4°C with 4,500 rpm. Pellet was suspended and incubated in cold TBF I buffer (30 mM KAc, 50 mM MnCl, 100 mM RbCl, 10 mM $CaCl_2$, 15% glycerol, pH 5.0 with acetic acid, sterilized by filtration) for 20 min on ice. Next, the cells were again pelleted by centrifugation in 4°C for 5 min with 4,000 rpm. Pellet was resuspended in 3.6 ml of cold TBF II buffer (10 mM NaMOPS pH 7.0, 10 mM RbCl, 15 mM $CaCl_2$, 15% glycerol, sterilized by filtration), aliquoted, snap frozen in liquid nitrogen. Aliquots were stored in -70°C.

2.5.3 Preparation of *E. coli* BL21 (DE3) competent cells

E. coli strain BL21 (DE3) competent cells were prepared as described for *E. coli* XL1 Blue.

2.5.4 Preparation of *Agrobacterium* (GV3101 MP90) competent cells

500 ml of LB medium was inoculated with 5 ml of saturated culture of *Agrobacterium* (strain GV3101::MP90). Culture was incubated at 28°C with vigorous agitation. At log phase (OD_{550} 0.5-0.8), the culture was chilled on ice and cells were pelleted by centrifuging at 4000 g for 10 min at 4°C in a prechilled rotor. Cells were washed 3 times by suspending in 500 ml,

250 ml and 50 ml of ice-cold ddH_2O respectively. After washing cells the pellet was finally suspended in 5 ml of 10% (v/v) ice-cold, sterile glycerol. 50 µl aliquots were snap frozen in liquid nitrogen and stored in -70°C.

2.5.5 *Agrobacterium* transformation (electroporation)

An aliquot of competent *Agrobacterium* cells (50 µl) was thawed on ice. 1-3 µg of plasmid DNA was added, mixed and incubated for 2 min on ice. The cell suspension was transferred into a prechilled 2 mm electroporation cuvette. Electroporation was carried out in the BioRad Gene-Pulser using the following conditions: resistance 400 Ω, capacitance 25 µF, capacitance extender 125 µF, voltage 2.5 kV, 5 s pulse length. Immediately after electroporation 1 ml of YEP medium (10 g/l pepton, 5 g/l yeast extract, 5 g/l NaCl, pH 7.0) was added and the bacterial suspension was transferred into a 15-ml culture tube. The culture was incubated for 4 hours in 28°C with gentle agitation. A 50 µl aliquot of the culture was plated on YEP-agar plates containing 25 mg/l gentamicin (Ti-plasmid marker) and 100 mg/l rifampicin (chromosomal marker). Plates were sealed with parafilm and incubated in 28°C for 2-3 days.

2.5.6 *E. coli* transformation (heat-shock)

An aliquot of competent E. coli cells (50 µl) was thawed on ice. 100-500 ng of plasmid DNA was added, mixed and incubated for 20 min on ice. An eppendorf containing transformation mix was then heated to 42°C for 1 min and then immediately cooled on ice for 2 min. 400 µl of dYT medium was added and probe was incubated in 37°C for an hour.
50-200 µl transformed bacteria suspensions were plated on dYT plates with addition of appropriate antibiotic.

2.5.7 *E. coli* growth conditions

Standard bacteria cultures were grown in volume of 3 ml (dYT or LB) at 37°C over night in a shaker incubator (120 rpm). Cultures were inoculated with a single colony from the plates. Cultures 500 ml or 1000 ml were inoculated from the 3 ml cultures.

2.5.8 Transformation of Arabidopsis, floral dip

A 5 ml liquid preculture, inoculated from single colony of *Agrobacterium,* carrying the appropriate binary vector, were grown with vigorous agitation for 2 days at 28°C with appropriate antibiotics. 200 ml of LB medium was inoculated with 1 ml of the preculture and

incubated for a further 24 h at 28°C. The cells were pelleted by centrifugation at RT, 6000 rpm for 10 min. The cells were resuspended in infiltration medium (½ Murashige and Skoog salts; 1x Gamborg's B5 vitamins; 5 % sucrose; 0.044 µM benzylamino purine; 50 µl/l Silvet L-77). Inflorescence shoots from 5-7 plants of *Arabidopsis thaliana* (wild type Col-0) were dipped into the suspension and soaked for 30 sec. After dipping plants were sealed with transparent plastic bags for the next 24 h, then the cover was removed, plants were rinsed with water and returned to their normal growing conditions. After about 4 weeks seeds were collected.

2.5.9 Selection of transformed *A. thaliana*

Selection was carried out by germinating seeds collected from transformed plants on ½ MS plates containing 1% sucrose and 25 mg/l hygromicin.

2.5.10 Microscopy

Immature seeds of wild-type, *pts-1* and *pts-2* plants were harvested from the siliques, cleared in Hoyer's solution (7.5 g gum Arabic, 100 g chloral hydrate, 5 ml glycerol, 60 ml water), observed under microscope with Nomarski optics and photographed.

2.5.11 GUS staining

Plant material from transgenic *A. thaliana* carrying P_{AtPTS}GUS driven construct was incubated in X-Gluc solution at 37°C over night. Next day, chlorophyll was removed form tissue by incubating in 70% ethanol for few hours. Etiolated material was photographed.

2.6 DNA techniques

2.6.1 Preparation of plasmid DNA from *E. coli*

Plasmid DNA was prepared from *E. coli* by the alkaline lysis method (Sambrook and Russell, 2001).

2.6.2 Preparation of plasmid DNA from *Agrobacterium tumefaciens*

10 ml YEP medium-cultures were inoculated from single colonies and grown in 28°C for 2-3 days. 3 ml cultures were pelleted and pellet was suspended in 150 µl Lysis-buffer (50 mM Glucose, 25 mM Tris-HCl, pH 8.0, 10 mM EDTA, 20 µg/ml RNase). Next with 300 µl buffer II (0.2 N NaOH, 1% SDS) bacteria were lysed for 5 min on ice, then 225 µl of 7.5 M ammonium acetate was added. After 10 min incubation on ice probes were centrifuged 14,000

rpm, 15 min in 4°C. Supernatant was then transferred into a new eppendorf tube and mixed with phenol/chloroform 1:1 (v/v) and chloroform/isoamylalkohol (24:1). DNA from aqueous phase was precipitated with 800 µl of isopropanol alcohol, centrifuged for 20 min, 14,000 rpm at RT. DNA pellet was rinsed with 70% ethanol, dried and suspended in 30 µl TE buffer.
Such prepared DNA was PCR analyzed as well as used for *E. coli* transformation to confirm the presence of the proper plasmid construct by restriction analysis.

2.6.3 Preparation of plant genomic DNA

Plant material (green leaf piece about 0.5 cm^2) was grind in 400 µl extraction buffer (200 mM Tris-HCl pH 7.5; 250 mM NaCl; 25 mM EDTA; 0.5% SDS), centrifuged 5 min 14,000 rpm at RT, and DNA was precipitated from 300 µl supernatant with isopropanol (1:1 v/v) by centrifugation for 5 min 14,000 rpm at RT. Pellet was washed twice with 100 µl 70% ethanol, dried and resuspended in 100 µl TE buffer. For PCR analysis 1-2 µl were used.

2.6.4 Agarose gel electrophoresis and isolation of DNA fragments

DNA was subjected to electrophoresis using 1.0 to 2.0% agarose gels containing ethidium bromide at final concentration of 0.5 µg/ml. Gels were cast and run in TAE buffer (40 mM Tris, 5 mM sodium acetate, 1 mM EDTA, adjusted to pH 7.8 with glacial acetic acid)
1Kb Plus DNA Ladder (Invitrogen) was routinely used as size marker.
Gel pieces containing desired DNA fragment were excised from the agarose gel. DNA was then isolated using GFX™ DNA and Gel Band Purification Kit (Amersham), according to the manufacturer's instructions.

2.6.5 DNA-Sequencing

Plasmids for sequencing were purified by PEG-precipitation (Sambrook and Russell, 2001), and were sequenced with Dideoxy-Method described by Sanger *et al.* (1977) using Capillarsequencer ABI PRISM® 310 Genetic Analyzer (Applied Biosystems, USA). Sequencing reactions were prepared with BigDye® Termionator v1.1 Cycle Sequencing Kit, Applied Biosystems. Primers used for sequencing are listed in table 2.2 (below).

Name	description	Sequence 5'→3'
T3	pBluescript KS	AATTAACCCTCACTAAAGGG
T7	pBluescript KS, pGEM, pET 28a	GTAATACGACTCACTATAGGGC
SP6	pGEM	ATTTAGGTAGACACTATAGAA
T3 univ primer	pET 28a	GGATCGAGATCTCGATCCCGC
M13	pET 28a	GTAAAACGACGGCCAGT
UG-ATPS-int1	wild type and mutagenized PTS expression constructs internal primer	CACAGGCCTACTCTTCCCACAA
UG-PETT7-ter	wild type and mutagenized PTS expression constructs internal primer	GCTAGTTATTGCTCAGCGG
INT FOR	wild type and mutagenized PTS expression constructs internal primer	CGTCACCGTCGTCTCAATCT
INT REV	wild type and mutagenized PTS expression constructs internal primer	CTTACCAAACAGAGCAACATCAGG

Table 2.2 Primers used for sequencing

2.6.6 Bioinformatics tools, protein sequences alignment

Computer analysis of DNA and protein sequences was performed using the DNASTAR package (Madison, USA) (www.dnastar.com) and VectorNTI (version 10; Invitrogen).
GenBank was searched for plant ESTs encoding full-length or partial homologues to *A. thaliana* PTS (gi:15239721) using the tblastn program (E-value cutoff 10-30). EST-encoded amino acid sequences with homology to *A. thaliana* PTS that were supported by at least two independent EST sequences were aligned with annotated PTS sequences from plants, algae, fungi, and bacteria by using the ClustalX program (version 1.82) (Chenna *et al*., 2003) with the Gonnet weight matrix and penalties for gap opening and extension of 10.0 and 0.2, respectively.

2.7 Constructs for plant overexpression of *E. coli* and *A. thaliana* pantothenate synthetase proteins

The *panC* ORF was initially amplified from genomic DNA of *E. coli* using the primer pair:
ECpanC FOR 5'-CGCGCCTCGAGGAGGAGTCACGTTATGTTAATTATCGAAACC-3
ECpanC REV 5'- GCGCGTCTAGATTACGCCAGCTCGACCATTTT-3'.
Primers carried *Xho*I and *Xba*I restriction site (underlined), and the corresponding restriction fragment was cloned into *Xho*I/*Xba*I cut pBluescript, yielding pECPTS plasmid from which plant expression constructs were derived.

2.7.1 Cytosolic construct (pUG-DCC)

The *E. coli panC* ORF (855 bp) was amplified from pECPTS plasmid using the primer pair:

ECpanC *Nco*I FOR:

5'-CGCC*ATGG*CTTTAATTATCGAAACCCTGCCGCTGCTGCGTCAGCAAATT**AGA AGA**CTGCGTATGGAAGGCAAG**AGA**GTGGCGCTGGTGCCT**ACT**ATGGGTAA-3',

ECpanC *Pml*I REV: 5'-CGCGCCACGTG*TTA*CGCCAGCTCGACCAT-3'

that introduced a silent nucleotide change at position 87 (C→A), in order to remove a internal *Nco*I restriction site. Additional Ala codon (GCT) was introduced after start codon in order to facilitate cloning. Codons which were adjusted to Arabidopsis are in bold, *Nco*I and *Pml*I restriction site are underlined, start and stop codons are in *italic*.

The PCR product was cloned into *Sma*I-cut pBluescript KS, and the desired sequence was confirmed by sequencing.

In order to construct expression plasmid, the pCambia 1202 vector was modified by removing the GUS gene located between *Nco*I/*Pml*I. The *Nco*I/*Pml*I fragment containing the *panC* ORF was then cloned into the modified pCambia 1202 vector, yielding the pUG-ARC plasmid. In the pUG-ARC plasmid, the *panC* gene is under the control of the 35S CaMV promoter (see results, Fig. 3.8 C).

2.7.2 Plastidic construct (pUG-ARC)

Leader peptide of rubisco small subunit 3b (At5g3840) was amplified from cDNA library (CD4-33 available at Arabidopsis Biological Resource Centre) from immature seeds (5-13 days after flowering) of *A. thaliana* ecotype Col-2 using primer pairs:

Rub *Afl*III FOR GCGCGAC*ATGT*CTTCCTCTATGTCTTCCTCCG-3', and

Rub *Afl*III REV GCGCGACATGTTCGACGTCACTAAGGTCAGGG-3',

carrying *Afl*III restriction sites (underlined). PCR product was cloned into *Sma*I-cut pBluescript, sequence was confirmed by sequencing and 241 bp.*Afl*III-cut fragment was cloned into *Nco*I-cut pUG-ARC plasmid, in frame with the *panC* gene, yielding pUG-DCC plasmid (see results, Fig. 3.8 B). The proper orientation of the insert was determined by restriction analysis.

2.7.3 Mitochondrial construct (pUG-BHC)

The targeting sequence of the mitochondrial HSP60 chaperon (At3g23990 - was amplified from the cDNA library (CD4-33 see above) using the primers:

mHSP FOR: 5'- CGGCCAC*ATG*TATCGTTTCGCTTCTAACCT-3'

mHSP REV: 5'- CCCAACTTTGCTCAATCACGAC-3'

The PCR product was cloned into *Sma*I-cut pBluescript, sequence was confirmed by sequencing and a 180 bp *Afl*III/*Nco*I-cut fragment (*Nco*I restriction site placed on amplified genomic fragment of the sequence) was cloned into *Nco*I-cut pUG-ARC plasmid, in frame with the *panC* gene, yielding pUG-DHC plasmid (see results, Fig. 3.8 A). The proper orientation of the insert was determined by restriction analysis.

2.7.4 Reporter construct (pRJ-PSPRO)

The *A. thaliana* PTS promoter region (531 bp upstream ATG codon) was amplified using primers pair:

5'-GCGCGGAATTCATTCTGTGTTTTCTTGTGTAT-3'

and 5'-GCGCGGCCATGGTCGGAAAATTGAGATTGT-3'

carrying *EcoR*I and *Nco*I restriction sites (underlined). The amplified fragment was cloned into *Sma*I-cut pBluescript. The *EcoR*I/*Nco*I fragment from the resulting plasmid was cloned into *EcoR*I/*Nco*I-cut pRJ plasmid, yielding pRJ-PSPRO. The pRJ plasmid was derived from pCambia 1305.1 by removing the *EcoR*I/*Nco*I fragment containing the CaMV 35S promoter (see results, Fig. 3.19).

2.8 Construct for overexpression of *E. coli* pantothenate synthetase protein in *E. coli*

2.8.1 *E. coli* PTS-N-terminal His-tag, ECPTS plasmid

A construct for expression of *E. coli* PTS with an N-terminal His-tag, the *panC* ORF contained in pECPTS was amplified using two sets of primers that introduced a silent nucleotide change A→G at position 112 bp of the *panC* ORF (nucleotide substitution was introduced into the *panC* ORF by overlap extension PCR, Ho *et al*., 1989) in order to remove an internal *Nde*I site:

Pair A: *Nde*I FOR (external): 5'- CGGCGCAT*ATG*TTAATTATCGAAACCCTGCCGC-3'

REV(internal):5'- GGCTTTGGCTTCGTCG**ACCAGCTTCATGTGGCCATCGTG**-3'

Pair B:

FOR (internal) 5'- GCCTACCATGGGTAACCTG**CACGATGGCCACATGAAGC TGGT**-3'

*Xho*I REV(external): 5'- GCGCGGCTCGAG*TTA*CGCCAGCTCGACCATTTTGTT GTCG-3'

Start and stop codons are in *italic,* overlap is **in bold**, the restriction sites *Nde*I and *Xho*I underlined. Three PCR reactions were carried: first two separate PCR amplifications were done using primer pair A and pair B. In the third PCR reaction, using external primers, about 50 ng of the products from above PCRs were combined. The fusion PCR product was cloned into pGEM-T, the *Nde*I/*Xho*I-fragment from the resulting plasmid was then inserted into pET28-a. In the resulting plasmid, the vector-encoded His-tag was fused in frame to the 5'-end of the inserted ORF (NH_2-MGSSHHHHHHSSGLVPRGSH- *E. coli* PTS), leading to the expression of N-terminal His-*E. coli* PTS. The resulted recombinant protein was 303 aa long and expected molecular mass was of 33.76 kDa.

The sequence of the construct was confirmed by sequencing expression plasmid.

2.8.2 Constructs for overexpression of *A. thaliana* wild type and mutagenized pantothenate synthetase proteins in *E. coli*

All expression constructs for wild type and mutagenized *Arabidopsis thaliana* PTS were derived from a cDNA corresponding to the single Arabidopsis gene encoding PTS (At5g48840) (Ottenhof *et al*., 2004). A full-length cDNA from *A. thaliana* encoding pantothenate synthetase (pJAR plasmid) was kindly provided by Dr. Alison Smith, University of Cambridge, UK.

2.8.2.1 *A. thaliana* PTS-Wild type (PTS)

The wild type *A. thaliana PTS* ORF was amplified from pJAR plasmid with primers:

PTS-full PET- FOR-5'- CGCGCAT*ATG*GAACCAGAAGTAATCAGAGACA-3'

PTS-full PET-REV-5'- CGCGGTCGAC*TTA*GAGAGAGACATTGATCTCAATG-3'

Restriction sites *Nde*I and *Sal*I are underlined start and stop codons are in *italic*. The overlap extension PCR product was cloned into pGEM-T and the *Nde*I/*Not*I-fragment from the resulting plasmid was then inserted into pET28-a. In this plasmid the N- terminal His –tag (20 aa, 2.18 kDa, NH_2-MGSSHHHHHHSSGLVPRGSH) was fused with complete *A. thaliana PTS* CDS (310 aa, 34.14 kDa). Stop codon was changed from TAG to TAA. Sequence of this plasmid was confirmed by sequencing. The recombinant product is 330 aa long and expected molecular mass is of 36.30 kDa.

This construct was used as a PCR template for generation of mutagenized PTS constructs.

2.8.2.2 PTS- Mut-1

In this expression plasmid position 98-132 (KNLYDYGGETKKINDGGGNGGRVVSCVEEGGLGHE) from *A. thaliana PTS* was replaced with position 94- 106 (SVKEIYPNGTETH) from *E. coli panC*.

The PTS external primers described above for the generation of *A. thaliana* PTS-wild type N-terminal His-tag were used in combination with the following sets of internal mutagenesis primers:

PTS-Mut1-FOR:

5'-**TCTGTTAAAGAAATTTATCCAAATGGTACTGAAACTCAT**ACTTGGATTA GGGTTGAGAGATTG-3'

PTS-Mut1-REV:

5'- **ATGAGTTTCAGTACCATTTGGATAAATTTCTTTAACAGA**TGGGTTAA AGACGACGACTTTACC-3'

Overlap marked in **bold**. The overlap extension PCR product was cloned into pGEM-T and the *Nde*I/*Not*I-fragment from the resulting plasmid was then inserted into pET28-a. In this plasmid the N- terminal His –tag (20 aa, 2.18 kDa, NH_2-MGSSHHHHHHSSGLVPRGSH) was fused with complete *A. thaliana PTS* CDS carrying internal replacement (288 aa, 32.00 kDa, stop codon changed from TAG to TAA). The recombinant product is 208 aa long and expected molecular mass of 34.16 kDa.

2.8.2.3 PTS-E132A

In this single replacement construct E (position 132) from *A. thaliana* PTS was replaced with A. The PTS external primers described above for the generation of PTS-wild type N-terminal His-tag were used in combination with the following sets of internal mutagenesis primers:

ATPS-E132A -FOR: 5'- **GGGTTAGGGCAT*GCG*ACTTGGATTAGG**GTT-3'

ATPS-E132A -REV: 5'- **CCTAATCCAAGT*CGC*ATGCCCTAACCC**ACC-3'

Ala codon is ***underlined***, overlap is **in bold**.

In this plasmid the N-terminal His- tag (20 aa, 2.18 kDa, NH_2-MGSSHHHHHHSSGLVPRGSH) was fused with complete *A. thaliana PTS* CDS carrying internal replacement (310 aa, 34.06 kDa, stop codon changed from TAG to TAA) The recombinant product is 330 aa long and expected molecular mass is of 36.24 kDa.

2.9 Genotyping of *pts-1* and *pts-2*

Genotyping of *pts* insertion lines was carried out using primers (Table 2.3) in combination as listed in Table 2.4 Obtained PCR product size was compared with expected size (Table 2.4).

Name	description	Sequence 5'→3'
WT FOR Salk_101901 (pts-1)	wild type allele amplification	GTTAGGGCATGAGACTTGGATTAG
WT REV Salk_101901	wild type allele amplification	ACTTTACCCTTTGCCTTTCTTCAT
T-DNA FOR Salk_101901 (pts-1)	T-DNA:flanking seq. amplification	TCTCGGGCTATTCTTTTGATTTAT
T-DNA REV Salk_101901	T-DNA:flanking seq. amplification	AGCCATGGCCAGTGACCTA
Salk_101901 LP	wild type allele amplification	CCAACAATGGGTTACCTCCAC
Salk_101901 RP	wild type allele amplification	CTCGTCCTGCAGATCCAACAA
LBb1	in combination with Salk_101901RP or Salk_094477 T-DNA:flanking seq. amplification	GCGTGGACCGCTTGCTGCAACT
Salk_094477 RP	wild type allele amplification	CGCATGGCTCACATCAAAACA
Salk_094477 LP	wild type allele amplification	CTGACGTCACCGTCGTCTCAA
35S constr FOR	plant overexpression construct	ATAAAGGAAAGGCCATCGTTGAA
ECpanC constr REV	plant overexpression construct	GCCTTCCATACGCAGTCTTCTAA

Table 2.3 primers used for genotyping

Primers pairs for *pts-1* locus	Amplified sequence	Expected PCR product size [bp]
pts-1 WT FOR + *pts*-1 WT REV	wild type allele	391
Salk_101909 LP + Salk_101909 RP	wild type allele	887
pts-1 T-DNA FOR + *pts-1* T-DNA REV	T-DNA:flanking seq.	420
Primers pairs for *pts-2* locus		
LP Salk_094477 + RP Salk_094477	wild type allele	931
LBb1 + Salk_094477	T-DNA:flanking seq	612

Table 2.4 Primer pairs and expected PCR product size in genotyping analysis of the *pts* loci

2.10 Protein techniques

2.10.1 Overproduction of *E. coli* PTS and *A. thaliana* PTS proteins

Expression plasmids were transformed into competent cells of *E. coli* strain BL21 (DE3) (Stratagene) by heat shock. The cells were grown at 37°C to an OD_{600} of 0.6 in dYT medium containing: 2% glucose, 4 mM $MgSO_4$, 10 mM KCl, 50 µg/ml kanamycin. In case of *A.*

thaliana PTS wild type and mutated protein, before expression induction culture was cooled into 20°C , IPTG was added (1 mM final concentration), and growth was continued for 30 h at 20ºC.

E. coli PTS expression was carried out at 37°C over night.

2.10.2 Protein purification

Cells (5-9g) were harvested by centrifugation at 4,500 x g for 10 min at 4°C, and resuspended in 20- 30 ml lysis buffer (50 mM NaH_2PO_4 (pH 8.0), 300 mM NaCl, 10 mM imidazole). Lysozyme was added (1 mg/ml) and the cells were incubated on ice for 30 min. After sonication and centrifugation (10,000 × g for 20 min), the cleared lysate was mixed with 1.5 ml Ni-NTA agarose for 1 h at 4°C. The mixture was transferred to a drip column and washed with 6 ml of wash buffer (50 mM NaH_2PO_4 (pH 8.0), 300 mM NaCl 20 mM imidazole). His-tag protein was eluted with 2.4 ml of elution buffer (50 mM NaH_2PO_4 (pH 8.0), 300 mM NaCl, 250 mM imidazole). The eluate was dialysed exhaustively against 50 mM Tris-HCl (pH 8.0), 0.1 mM DTT. The precipitate was removed by centrifugation. Aliquots of purified proteins were snap-frozen in liquid nitrogen and stored in -70°C. Typical yields of *A. thaliana* PTS proteins were 10 mg per litre of culture.

His-tagged *E. coli* PTS was expressed and affinity purified following essentially the same procedure except that cultures were grown in DYT medium at 37°C and cells were harvested 16 h after induction.

2.10.3 Protein quantification

Protein was assayed according to the method of Bradford (1976). The Bio-Rad Protein reagent was used to determine protein concentration using the assay in accordance with the manufacturer's instructions. Bovine serum albumin was used as a standard.

2.10.4 Preparation of crude protein extract from fresh and lyophilized plant material for western blot analysis

100 mg of FW leaves were placed in eppendorf, frozen in liquid nitrogen and grinded to fine powder. Powdered tissue was suspended in 1 volume (100 µl) of homogenization buffer (50 mM Tris-HCl (pH 8.0), 100 mM potassium acetate, 1 mM EDTA, 1 mM DTT, 20% glycerol). Probes were centrifuged at maximum speed for 10 minutes at 4°C, supernatant was transferred into new eppendorf and protein concentration was determined using the Bradford assay. Protein samples were mixed with an equal amount of 2 times concentrated sample

buffer (100 mM Tris-HCl (pH 6.8), 4% SDS, 0.2% Bropophenol blue, 20% glycerol, 200 mM DTT). Proteins were separated using SDS-PAGE as described in 2.9.5.

Crude protein extract from lyophilised leaves was prepared as described below.
10 mg lyophilised leaves were extracted with 100 µl of extraction buffer (50 mM Tris-HCl (pH 9.0), 100 mM potassium acetate, 1 mM EDTA, 1 mM DTT, 1 mM PMSF) in eppendorf. Homogenized probes were centrifuged at maximum speed for 10 minutes at 4°C, supernatant was transferred into new eppendorf and protein concentration was determined using Bradford assay. Aliquots were frozen in liquid nitrogen and stored in -70°C.

2.10.5 SDS-polyacrylamide-gel-electrophoresis (SDS-PAGE)

This technique was used to follow the purification of PTS proteins and to estimate subunit molecular weights. SDS-PAGE was performed according to the procedure of Laemmli (1970). Separating and stacking gels and running buffer were prepared as described by Sambrook and Russell (2001).Volumes described below (Table 2.5) were sufficient to prepare 6 gels (7 x 10 x 0.75cm).

	12,5% separating	5% stacking
1M Tris-HCl, (pH 8.8)	7.5 ml	-
1M Tris-HCl, (pH 6.8)	-	625 µl
H_2O	2.7 ml	3.1 ml
10% SDS	200 µl	50 µl
30% Acrylamid	8.3 ml	835 µl
1% APS	1.3 ml	400 µl
TEMED	14 µl	4.5 µl

Table 2.5

The separating and stacking gels were left for polymerization for ca. 40 min. Gels were used immediately or stored up to 7 days at 4°C. Protein samples were incubated with an equal amount of 2 times concentrated sample buffer (100 mM Tris-HCl, pH 6.8, 4% SDS, 0.2% bromophenol blue, 20% glycerol, 200 mM DTT) and incubated at 100°C for 5-10 minutes, samples were centrifuged prior to loading. SDS gel (10 x 6 x 0.75 cm) electrophoresis was carried at 100 Volts in „Mighty-Small“appliance (Bio-Rad), in 1x PAGE-running buffer (25 mM Tris, 250 mM Glycine, 0.1% w/v SDS).
Gels were stained in solution contained 9 parts 50% (w/v) isopropanol, 1 part glacial acetic acid, 125 mg per litre each of Commassie brilliant blue R250 and G250 at room temperature

with gentle shaking. Gels were distained in 10% glacial acetic acid. Mark 12™ (Invitrogen) was routinely used as size marker.

2.10.6 MonoQ anion exchange chromatography

The PTS proteins samples was dialyzed against 50 mM Tris-HCl (pH 8.0 or 9.0) and loaded onto a MonoQ anion exchange column equilibrated in 50 mM Tris-HCl (pH 8.0 or 9.0). Proteins were eluted in a linear 0 - 0.5 M KCl gradient. Fractions containing PTS proteins were pooled, dialyzed against 50 mM Tris-HCl (pH 8.0 or 9.0), 0.1 mM DTT, aliquoted, snap-frozen in nitrogen and stored at -70°C.

2.10.7 Gel filtration

This technique was used to estimate the native molecular weight of affinity purified PTS proteins. Gel filtration chromatography was performed using a HiLoad 16/60 Superdex 200 column equilibrated in 50 mM Tris-HCl (pH 8.0), 100 mM KCl. Proteins were eluted in the same buffer at 0.5 ml/min. Standard proteins used for calibration were obtained from Sigma and subjected to gel filtration under the same conditions.

2.10.8 Thrombin digest of His-tag proteins

Wild type *A. thaliana* PTS His-tag protein was treated with thrombin in order to remove His-tag sequence. 6 mg of protein was treated with 24 NIH units of thrombin in 30 ml of thrombin cleavage buffer (20 mM Tris-HCl (pH 8.4); 150 mM NaCl; 2.5 mM $CaCl_2$). Reaction was carried out in room temperature for 1 h then dialyzed against 50 mM Tris-HCl pH 8.8; 1mM phenylmethylsulfonyl fluoride (PMSF). Separation of the products of the reaction was carried on MonoQ anion exchange 1ml column (Pharmacia) equilibrated in 50 mM Tris-HCl (pH 8.8). Proteins were eluted in a linear 0- 0.5 M KCl gradient. Fractions containing *A. thaliana* PTS were pooled, dialyzed against 50 mM Tris-HCl (pH 8.0), 0.1 mM DTT and stored at -70°C. Removal of the N-terminal His-tag was confirmed by SDS-PAGE.

2.10.9 Western Blotting

Proteins were separated on SDS-gels and electrotransfered onto a Nitrocellulose membrane using the SemiDry-Blotter (Bio-Rad) and western transfer buffer (48 mM Tris, 39 mM Glycine, 20% Methanol, 0.0375% SDS; Bjerrum and Schafer-Nielsen 1986). To confirm the transfer of the protein onto the nitrocellulose membrane, the membrane was stained with Ponceau S (Sigma), photographed and distained in ddH_2O. The membrane was blocked with

TST buffer (6.1 g/l Tris, 8.8 g/l NaCl, 0.5% v/v Tween 20, pH 7.0) for 1 h. Next, the membrane was incubated with TST buffer and anti-*E. coli* PTS antibody (1:2000 dilutions) for 1h, and then washed 3 times for 15 min with TST buffer. The secondary antibody, (goat anti-rabbit antibody (Cy5 labelled) IgG (1:3000 dilution)) was applied and membrane was incubated for 1h in darkness, washed 3 times for 5 min in TST buffer, and scanned with Red Fluorescence modules using the STORM Phosphoimager (Molecular Dynamics).

2.11 Enzyme assays for pantothenate synthetase

2.11.1 Spectrophotometric assay

PTS initial rate data were obtained using a coupled assay procedure essentially as previously described (Genschel *et al*., 1999). Pantothenate synthetase (PTS) activity was assayed spectrophotometrycally by coupling the formation of AMP to the reactions of myokinase, pyruvate kinase and lactate dehydrogenase. In this assay, the rate of pantothenate formation is proportional to the rate of NADH oxidation which is followed at 340 nm.

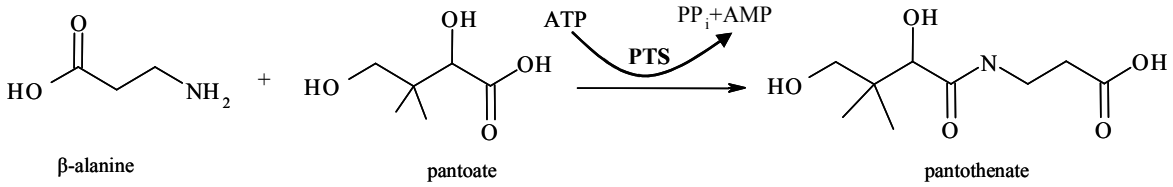

PTS	pantoate + β-alanine + ATP	⟶	pantothenate + AMP + PPi
MK	AMP + ATP	⟶	2 ADP
PK	2 PEP + 2 ADP	⟶	2 pyruvate + 2 ATP
LDH	2 pyruvate + 2 NADH	⟶	2 lactate + 2 NAD^+

Fig. 2.1 Coupled assay for pantothenate synthetase. The pantothenate synthetase (PTS) assay described by Pfleiderer *et al*. (1960) couples AMP production of pantothenate synthesis with oxidation of NADH which can be monitored in a spectrophotometer. PTS catalyses the condensation of pantoate with β-alanine to pantothenate in a reaction that hydrolyses ATP to give AMP and pyrophosphate (PPi). Myokinase (MK), catalyses the production of 2 moles of ADP per mole of AMP released in pantothenate synthesis using ATP. Next pyruvate kinase (PK) generates 2 moles of pyruvate and ATP per 2 moles of phosphoenylopyruvate (PEP) and ADP. Then, lactate dehydrogenase (LDH) reduces 2 moles of pyruvate to yield 2 moles of lactate and oxidizes in a stoichiometric manner, NADH to NAD^+. There are 2 molecules of NADH consumed for every molecule of pantothenate formed.

The standard assay contained 100 mM Tris-HCl (pH 8.0), 10 mM $MgSO_4$, 10 mM $(NH_4)_2SO_4$ (from coupling enzymes), 10 mM Na_2ATP, 0.5 mM potassium D-pantoate, 5 mM β-alanine, 1 mM potassium phosphoenolpyruvate, 0.3 mM NADH, myokinase (8 units), pyruvate kinase (12 units), lactate dehydrogenase (12 units), and 20 µg of assayed protein and was made up to a volume of 900 µl with ddH_2O. These components were assembled into a 1 ml plastic cuvette with a light path of 1 cm. Except for pantoate, the assay components were mixed and incubated at 25°C for 15 min. The reactions were initiated by the addition of prewarmed into 25°C potassium D-pantoate (100 µl of 5 mM solution). Assay was mixed immediately by pipetting up and down few times. When β-alanine was the varied substrate (replaced by pantoate in the assay mix), β-alanine instead of D-pantoate was used to initiate the assay. A_{340} was followed for 5 – 10 min at 25°C using a Beckman DU 640 spectrophotometer with electronic data collection and a circulating water bath. In this coupled assay, two molecules of NADH (ε_{340} = 6220 M^{-1} cm^{-1}) are oxidised per molecule of pantothenate formed.

The purified PTS enzymes used in this study gave no background activity when one of the three substrates was absent. PS activity is calculated from absorbance decrease (ΔABS/min) as follows:

Δ_C PA/min = Δ_CAMP/min

Δ_C PA/min = -0.5 · Δ_CNADH/min

Δ_C PA/min = 0.5 ΔABS/min · ε $NADH^{-1}$ · V · 1 cm

Δ_C PA/min = ΔABS · 80.39 nmoles

PS activity [nmoles/min] = ΔABS/min · 80.39 nmoles

V is the final assay volume, always 1000 µl; Δ_C PA is the increase in pantothenate concentration; Δ_CAMP is increase in AMP concentration.

2.11.2 Isotopic assay

The pH dependency of PTS activity was studied by monitoring the conversion of [3-^{14}C]β-alanine into ^{14}C-pantothenate. This isotopic assay contained 100 mM buffer (MES-NaOH, pH 6.0-6.5; Tris-HCl, pH 7.0-9.5; AMP-HCl, pH 9.0-10.5; CAPS-NaOH, pH 10.0-11.0), 10 mM $MgSO_4$, 10 mM $(NH_4)_2SO_4$, 10 mM Na_2ATP, 0.5 mM potassium D-pantoate, 0.5 mM [3-^{14}C]β-alanine (18 mCi/mmol), and 4 µg *A. thaliana* PTS or 1 µg *E. coli* PTS in a final volume of 40 µl. The assay was initiated by the addition of D-pantoate. At 0.5, 1, 2, 3, 4, 5, and 6 min after initiation, 5 µl aliquots were removed from the reaction, immediately combined with 2 volumes of acetone, and frozen in liquid nitrogen.

In this isotopic assays, initial rates were calculated from progress curves of pantothenate formation (up to 50% completion) corrected for non-enzymatic activity by using the 'exact' numerical method described by Cornish Bowden (1975). Briefly, for each pair of points (t_i, p_i) and (t_j, p_j) on the progress curve, the parameters K_{ij}^{app} and V_{ij}^{app} were calculated from the following equations:

$K_{ij}^{app} = (t_i\, p_j - t_j\, p_i) / \{t_j \ln[p_\infty/(p_\infty - p_i)] - t_i \ln[(p_\infty - p_j)]\}$

$V_{ij}^{app} = \{p_i + K_{ij}^{app} \ln[p_\infty/(p_\infty - p_i)]\}/t_i$

Where p is the product concentration, p_∞ is the value of p at equilibrium (*i.e.* 0.5 mM, in this assay), and p_i and p_j are the concentrations of pantothenate at time i j, respectively.

p_i was calculated using the following equation,

$pi = \frac{p^* \times 0.5}{100}$, where p^* is the percentage of ^{14}C label associated with pantothenate at time *i*.

The initial velocity v_{ij} was estimated from the equation,

$v_{ij} = V_{ij}^{app}\, p_\infty / (K_{ij}^{app} + p_\infty)$ The median of all v_{ij} values was determined and used as the initial velocity v_0.

2.11.3 PTS activity in segregating transgenic Arabidopsis overexpressing *panC*

Crude protein extract from segregating population of Arabidopsis overexpressing *E. coli panC* gene, was assayed for pantothenate synthetase activity. This isotopic assay contained: 100 mM Tris-HCl buffer (pH 9.0), 11 mM $MgSO_4$, 15 mM $(NH_4)_2SO_4$, 10 mM Na_2ATP, 5 mM potassium D-pantoate, 0.5 mM [3-^{14}C]β-alanine (18 mCi/mmol), 0.8 µg/µl crude protein extract. The assay was initiated by the addition of D-pantoate. At 0.5, 1, 2, 3, 4, 6, 12, 24 and 36 min after initiation, 5 µl aliquots were removed from the reaction, immediately combined with 2 volumes of acetone, and frozen in liquid N_2.

2.11.4 Thin layer chromatography (TLC)

Precipitated protein from isotopic assays was removed by centrifugation at 14,000 rpm, 4°C for 5 min, and a 5 µl aliquot of the supernatant was spotted onto a silica gel 60 F_{254} TLC plate. Pantothenate and β-alanine were separated using dioxane-NH_3 (25%)-H_2O (9:1:4, v/v/v) as a mobile phase.

2.11.5 Quantification of the labled products in isotopic assays

The relative amounts of ^{14}C-label associated with β-alanine and pantothenate, respectively, were quantified using a Storm 860 phosphoimager (Molecular Dynamics) and corrected for non-enzymatic activity.

2.11.6 Stability of assayed proteins

The stability of PTS proteins was tested by using the isotopic assay. By comparing activity of PTS enzymes in freshly prepared assay mixture with activity after a 25-hours-incubation of the assay mixtures at 25°C. PTS activity was determined by monitoring conversion the conversion of [3-^{14}C]β-alanine into ^{14}C-pantothenate. This isotopic assay contained: 10 mM ATP; 10 mM $MgSO_4$; 0.5 mM [3-^{14}C]β-alanine (18 mCi/mmol); 10 mM Tris-HCl (pH 8.0); 10 mM $(NH_4)_2SO_4$; 0.5 mM potassium D-pantoate; 0.1 µg/µl enzyme. The assay was initiated by addition of D-pantoate and after 1; 2; 3; 4; 6 min an 5 µl aliquot was from the reaction, immediately combined with 2 volumes of acetone, and frozen in liquid N_2.

2.11.7 Pantothenate:β-alanine isotope exchange assay

The standard isotope exchange assay was carried out at 25°C and contained 100 mM MES-NaOH (pH 5.5), 10 mM NaAMP, 10 mM pantothenate, 0.5 mM [3-^{14}C]β-alanine (18 mCi/mmol), and 0.55 µg/µl *A. thaliana* PTS or *E. coli* PTS. After initiation of the assay by the addition of β-alanine, 5 µl aliquots were removed from the reaction at specified time points (1 – 24 h), combined with 2 volumes of acetone, and stored at -70°C. Separation of pantothenate and β-alanine, and quantification of ^{14}C-label were carried out as described above. Control reactions without enzyme were carried out following the same procedure. The pH dependency of the isotope exchange reaction catalysed by PTS was studied by replacing MES-NaOH (pH 5.5) by equimolar amounts of one of the following buffers: Sodium acetate, pH 4.5-5.0; MES-NaOH, pH 5.0-6.5; Tris-HCl, pH 6.5-9.0.

2.11.8 Reverse activity of pantothenate synthetase

PTS activity in the reverse direction was assayed by incubating *A. thaliana* PTS (15 µM) or *E. coli* PTS (16 µM) with 100 mM MES-NaOH (pH 5.5), 10 mM pantothenate, 0.17 mM [3-^{14}C]pantothenate (55 mCi/mmol), 10 mM NaAMP, 2 mM Na_4PP_i, 10 mM $MgSO_4$, and 10 mM KCl. Aliquots of 5 µl were removed 1 h, 8 h, and 23 h after initiation of the reaction with enzyme. Separation of pantothenate and β-alanine, and quantification of ^{14}C-label were

carried out as described above. The percentage ^{14}C-label associated with β-alanine was corrected for non-enzymatic activity.

2.12 Kinetic analysis of *A. thaliana* and *E. coli* PTS proteins

Initial velocity data were fitted to four rate equations by least-squares non-linear regression. The rate equations used were the Michaelis-Menten equation (Eq. 1), the Hill equation (Eq. 2), the rate equation for substrate inhibition resulting from an enzyme-substrate dead-end complex (Eq. 3) (Segel, 1975), and a generalized rate equation in the form of a 2:2 rational polynomial (Eq. 4) (Schulz, 1994),

$$v_0 = \frac{V_{max}[S]}{K_m + [S]} \qquad \text{Eq. 1}$$

$$v_0 = \frac{V_{max}[S]^h}{K_{0.5}^h + [S]^h} \qquad \text{Eq. 2}$$

$$v_0 = \frac{V'_{max}[S]}{K'_m + [S](1 + [S]/K_{si})} \qquad \text{Eq. 3}$$

$$v_0 = \frac{\alpha_1[S] + \alpha_2[S]^2}{1 + \beta_1[S] + \beta_2[S]^2} \qquad \text{Eq. 4}$$

where, v_0 is the initial velocity, [S] is the concentration of the variable substrate, V_{max} is the maximum velocity, K_m is the Michaelis constant, $K_{0.5}$ is the substrate concentration required for half-maximal velocity, h is the Hill coefficient, and K_{si} is the substrate inhibition constant. The coefficients α_1, α_2, β_1, and β_2 are not directly meaningful but the maximum velocity at saturating [S] and the initial rate at very low [S] can be defined as $V_{max} = \alpha_2/\beta_2$ and $v_0 = \alpha_1[S]$, respectively (Schulz, 1994). Substrate inhibition is observed when $\alpha_1\beta_2 > \alpha_2\beta_1$ (Schulz, 1994). In this case, the substrate concentration leading to the actual maximum velocity is given by Eq. 5, which was obtained by differentiating Eq. 4, setting $dv_0 / d[S] = 0$, and rearranging.

$$[S]_{opt} = \frac{\alpha_2 + \sqrt{\alpha_2^2 - \alpha_1(\alpha_2\beta_1 - \alpha_1\beta_2)}}{(\alpha_1\beta_2 - \alpha_2\beta_1)} \qquad \text{Eq. 5}$$

The true maximum velocity (v_{opt}) is the velocity defined by Eq. 4 when $[S] = [S]_{opt}$. The non-inhibitory and, if applicable, inhibitory substrate concentrations at which $v_0 = 0.5\ v_{opt}$ are defined by Eq. 6,

$$[S]_{0.5} = \frac{1}{\frac{\alpha_1}{v_{opt}} - \frac{\beta_1}{2} \pm \sqrt{\left(\frac{\beta_1}{2} - \frac{\alpha_1}{v_{opt}}\right)^2 + \frac{2\alpha_2}{v_{opt}} - \beta_2}} \qquad \text{Eq. 6}$$

which was obtained from Eq. 4 by setting $v_0 = v_{opt}/2$ and rearranging. The extra-sum-of-squares F-test ($\alpha = 0.05$) was used to determine which rate law among Eqs. 1 – 4 was most likely to describe the observed velocity data.

Exchange velocities for the transfer of [3-^{14}C]β-alanine into pantothenate were calculated using Eq. 7 (Segel, 1975),

$$v^* = \left(\frac{[A][P]}{[A]+[P]}\right)\left(\frac{1}{t}\right)\ln(1-F) \qquad \text{(Eq. 7)}$$

where v^* is the initial exchange velocity, [A] and [P] are the concentrations of β-alanine and pantothenate, respectively, and F is the fraction of isotopic equilibrium attained at time t. As there is no label in pantothenate at time zero, F is given by the ratio P^*/P_∞^*, where P* and P_∞^* are the fractions of ^{14}C-label in pantothenate at time t and at isotopic equilibrium, respectively. Plots of ln(1 - F) versus t were linear and the slope was used to obtain v^*.

Chapter 3

Genetic analysis of T-DNA insertions in *A. thaliana PTS*, overexpression of *E. coli panC* in *A. thaliana*, and expression profile of *A. thaliana PTS*

3.1 Introduction

Arabidopsis thaliana is a model plant that is widely used to elucidate gene function including genes involved in vitamin metabolic pathways**.** Sequence homology can be helpful in predicting gene function; however, there are many genes without homology to functionally characterized genes. Furthermore, although sequence homology can reveal general functions, the precise function performed by a specific gene product cannot necessarily be determined from sequence homology alone (Session *et al*., 2002). Insertional mutagenesis has proven to be a powerful tool for generating knockout mutations in Arabidopsis. In both forward and reverse genetic approaches, the function of a gene is typically assigned to a specific biological process by analysing the phenotypic consequences of altering that gene's activity. In forward genetics, mutant analysis provides reliable means to assign gene function. However, one mutation often only describes part of the function of a gene, and only through analysis of numerous alleles can one identify the gene function (Hirschi, 2003).

Reverse genetics is a strategy to determine a particular gene's function by studying the phenotypes of individuals with alterations in the gene of interest. Reverse genetics is an essential component of functional genomics programs aimed at the functional characterization of large numbers of genes (Sessions *et al*., 2002). Arabidopsis reverse genetics has been aided by the establishment, by different groups, of large numbers of T-DNA and transposon insertion mutant collections (Azpiroz-Leehan and Feldmann, 1997; Krysan *et al*., 1999; Parinov *et al*., 1999; Speulman *et al*., 1999; Tissier *et al*., 1999; Scholl *et al*., 1999; Wilson *et al*., 1999; Parinov and Sundaresan, 2000; Sussman *et al*., 2000;). The Arabidopsis Biological Resource Center (ABRC) of the Ohio State University (http://aims.cps.msu.edu/aims) (Scholl *et al*., 1999) in cooperation with Nottingham Arabidopsis Stock Center (NASC; http://nasc.nott.ac.uk) (Wilson *et al*., 1999) are organizing the collection, preservation and distribution of transgenic seeds from some of these collections. Mutations in genes of interest can be identified by PCR screening of pooled mutant populations and confirmed by hybridization (Krysan *et al*., 1996). Positive pools are screened sequentially until an individual mutant line is identified (Winkler *et al*., 1998, Sussman *et al*., 2000). An alternative method is to sequence regions flanking insertion sites in individual plants thereby determining

large numbers of insertion sites in advance (Parinov *et al*., 1999; Tissier *et al*., 1999; Alonso *et al*., 2003) (http://signal.salk.edu/tabout.html).

3.2 The *Arabidopsis thaliana* gene for pantothenate synthetase (*PTS*)

To identify Arabidopsis genes potentially involved in pantothenate biosynthesis, the Blastn and Blastp algorithm was employed. The sequences of *Lotus japonicus* and *Oryza sativum* encoding PTS (Genschel *et al*., 1999) were used to search the entire Arabidopsis genome for homologous genes. In this way an Arabidopsis homologue, At5g48840 (gi: 30695550) was identified. Using the same approach Ottenhof *et al*. (2004) identified the same Arabidopsis gene.

3.2.1 Molecular characterisation of *PTS* gene (At5g48840)

Pantothenate synthetase (PTS) catalyses the final step of condensation of β-alanine and pantoate to pantothenate. It is encoded in *Arabidopsis thaliana* by At5g48840 (*PTS*), a single copy gene, located on the fifth chromosome. It consists of four exons. The translation start is preceded by 37 bp of untranslated region (UTR), the last 251 bp of the fourth exon is also UTR (Fig. 3.1). The *PTS* coding sequence encodes a polypeptide of 310 residues with a predicted molecular weight of 34.2 kDa, and theoretical izoelictric point (IP) of 6.1. *A. thaliana* PTS is a cytosolic protein (Ottenhof *et al*., 2004). In common with other plant PTSs, *A. thaliana* PTS does not have any organellar targeting sequence (Ottenhof *et al*., 2004).

A. thaliana PTS has 39% amino acid sequence similarity to the *E. coli* orthologue. It is 66% and 62% similar to counterparts from *Lotus* and rice, respectively. PTS is highly conserved across bacterial and eukaryotic organisms. *E. coli* PTS shows greater than 40% and > 50% sequence identity in local Blast alignments with PTS from fungi and plants, respectively (Genschel, 2004). This conservation is also pronounced by the fact that *PTS* form *Yeast*, *L. japonicus* and *O. sativa* were able to functionally complement an *E. coli* mutant lacking *panC* (Genschel *et al*., 1999). Moreover, eukaryotic and bacterial PTS sequences share the pantoate-beta-alanine ligase domain signature (PF02569) (Bateman *et al*., 2004). However, it was previously noted that plant PTS sequences posses an insertion of approximately 20 amino acids that precedes the domain that is involved in dimerization of the protein subunits in *E. coli* PTS (von Delft *et al*., 2001).

3.2.2 Molecular characterization of Salk T-DNA insertion mutants

To study At5g48840 (*PTS*) gene function in Arabidopsis, the T-DNA mutant collection of the Salk Institute (http://www.arabidopsis.org/Blast/) was searched for availability of corresponding mutants. Two T-DNA insertion lines in this gene were available: Salk_101909 (*pts-1*) and Salk_594477 (*pts-2*). These lines were analysed during this work.

The exact insertion point into the *PTS* gene in both Salk lines was determined by amplification and sequencing of the flanking region of the left border of the pROK2 T-DNA. In case of *pts-1*, the T-DNA is located in the second exon at position 729 bp of the genomic DNA, and the *pts-2* insertion is in the first intron at the position *ca.* 665 bp (Fig. 3.1). In case of the *pts-2* allele the exact insertion point turned out to be located *ca.* 100 bp upstream of that inferred by Salk (published flanking sequence). Although this insertion is in the intron, this line was also analysed, as the 5.2 kb T-DNA fragment may be sufficient to disrupt the gene function (see discussion).

A

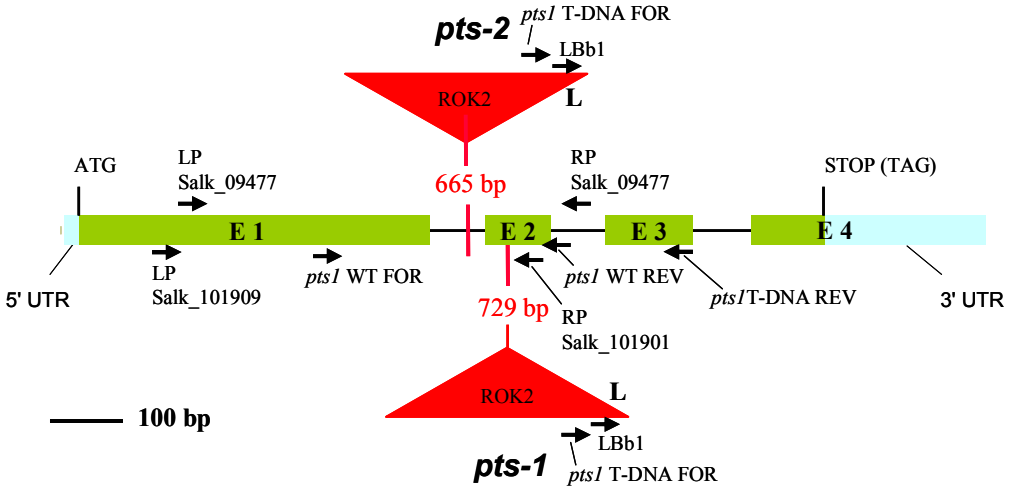

B

```
PTS genomic       711 > attgagattgtaggatcagatatagctagagaaaaagatgga > 753
PCR sequence   pts-1 > ttgtctaagcgtcaatttgatatagctagagaaaaagatgga
T-DNA left border 35 < ttgtctaagcgtcaatttgtttacaccataatata       < 1

PTS genomic       641 > agagattgtagagaatggtaagcctgatgttgctgtgtttgt > 682
PCR sequence   pts-2 > tcaatttgtttacaccacaatttctgatgttgctgtgtttgt
T-DNA left border 24 < tcaatttgtttacaccataatata                   < 1
```

Fig. 3.1 A. Exon/intron structure of the *A. thaliana PTS* gene. The *PTS* alleles carrying the T-DNA insertions Salk_101909 and Salk_094477 were named *pts-1* and *pts-2*, respectively. ROK2 is a 5.2 kbp T-DNA, arrows indicate primers location, L is the left border of the T-DNAs for which the precise integration sites was identified; E1, E2, E3 and E4, are exons; introns are depicted as a line; UTR, untranslated region. **B**, The locations of the insertion sites of the T-DNA in *pts-1* and *pts-2* mutants is based on sequencing of the T-DNA:flanking sequence (PCR sequence) and alignment analysis. In case of *pts-1* the exact insertion site was identified (position 729), while in case of *pts-2* allele insertion point was determined to be at *ca*. 665 bp. The exact insertion point could not be precisely defined as a 6-base pare fragment with similarity to both genomic

and T-DNA was identified between the *PTS* genomic sequence and T-DNA sequence (highlighted in black). The perfect mach of flanking:*PTS* to genomic DNA or T-DNA is highlighted in grey.

Typically, genotyping was carried with two sets of primers. The first set was specific for the left border of the T-DNA and corresponding flanking genomic sequence. In this case, a positive PCR result indicated the presence of the T-DNA, while a negative result (no amplification) was characteristic of the wild type form of the gene. The second primer pair was specific for the genomic sequence of the *PTS* gene. A negative result with this set of primers indicated the presence of the T-DNA in this region, and was characteristic of *PTS* knockout mutant plant. A positive result indicated that the plant carried at least one copy of the wild type allele. Information from both PCR analyses allowed to determine the genotype of analysed plants, *i.e*. when only wild type genomic DNA fragment could be amplified this indicated a wild type plant. In case of heterozygous plant in both PCR reactions DNA amplification was observed. In *PTS* knock out plants, only the T-DNA fragment could be amplified and negative result was observed when primers specific to the wild type form of the gene were used.

3.2.3 Phenotypical characterisation of *pts-1* and *pts-2*

Starting from *PTS/pts-1* and *PTS/pts-2* plants, F1 progeny were generated by self-pollination. Twenty-four F1 plants from *PTS/pts-1* and fifteen plants from *PTS/pts-2* were grown and genotyped by PCR (Table 3.2). No one *pts-1/pts-1* or *pts-2/pts-2* was identified among the F1 progeny. This suggested that homozygous mutant plants were unable to germinate. It was hypothesised that *pts-1* and *pts-2* are recessive mutations. To check this assumption a Chi-square (χ^2) statistical test was done. Based on the to genotyping result (Table 3.2), two phenotypic classes were tested (wild type and heterozygous). The resulting χ^2 values for analysed F1 population of selfed *PTS/pts-1* and *PTS/pts-2* are 3 and 1.25, respectively which is below the critical χ^2 value (χ^2_{95} = 3,841; with one degree of freedom), that means that data are in good agreement with the expected values for the segregation of a single recessive gene (3:1 segregation).

Heterozygous *PTS*/*pts-1* and *PTS*/*pts-2* plants showed wild-type phenotypes with regard to plant size, colour, leaf and flower development. However, a seed-defective phenotype was observed. Selfed *PTS*/*pts-1* and *PTS*/*pts-2* individuals produced normal-sized and shrunken seeds in mature siliques (Fig. 3.2).

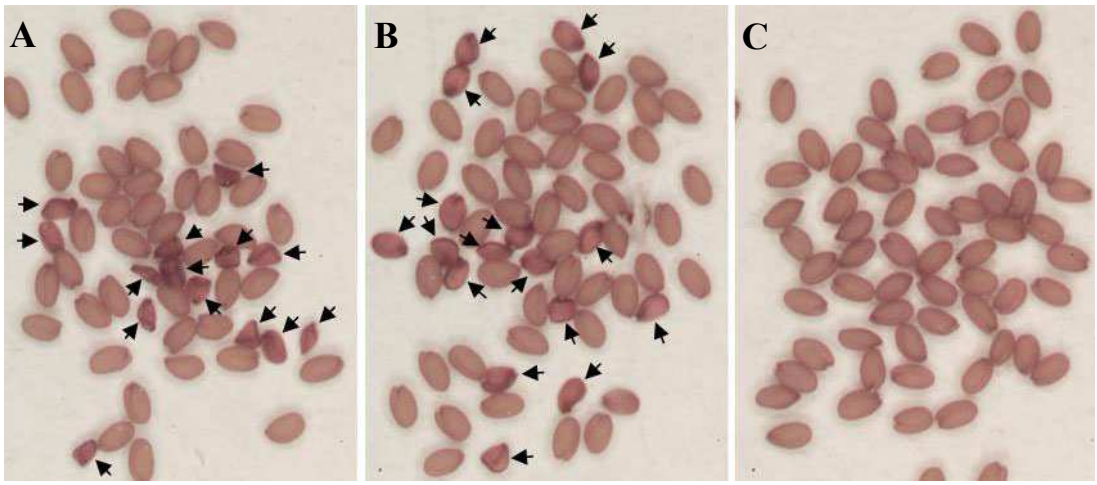

Fig. 3.2 Seed defective phenotype of *pts-1* and *pts-2*. Representative seeds sample from heterozygous *PTS*/*pts-1* (A) and *PTS*/*pts-2* plants (B), and wild type (C). Seeds with lethal phenotype are indicated by arrows.

Before the greening stage, developing seeds in selfed *PTS/pts-1* and *PTS/pts-2* plants appeared similar in colour and size. After the greening stage (*i.e.,* late heart to torpedo stages of embryo development), abnormal seeds become readily distinguishable as white seeds compared with the wild-type green seeds. The mutant seeds then became brownish and eventually dried out. To determine the frequency of mutant seeds, siliques from each F1 plant were scored for the number of mutant and wild-type seeds (Table 3.1). From each plant at least four siliques were analysed for the distribution of seed phenotypes. One-fourth of the seeds were shrunken, whereas the remaining seeds normal sized. The findings suggest that the shrunken-seed phenotype was associated with knock out of the *PTS* gene. Normal sized seeds represented *PTS*/*pts-1* or *PTS*/*pts-2* (two of four), and wild-type, *PTS/PTS* (one of four) individuals. All of the offspring from heterozygous for *PTS*/*pts-1* or *PTS*/*pts-2* plants produced seeds, one-fourth of which were shrunken. Segregation rate of *PTS*/*pts-1* and *PTS*/*pts-2* suggest that only one copy of T-DNA is present in the genome of heterozygous plants that this is inserted into *PTS*, and that *pts-1* and *pts-2* is a recessive mutation. A χ^2 tests for the two phenotypical classes (normal-sized and shrunken seeds) observed among F2 populations (seeds) were completely consistent with a single recessive mutation indicating that *pts-1/pts-1* or *pts-2/pts-2* seeds develop abnormally and are unable to germinate (Table 3.1).

segregation analysis of heterozygous *PTS*/*pts-1* offspring							
plant #	**genotype**	**№ of siliques**	**№ of seeds**	**№ of normal seeds**	**№ of shrunken seeds**	**% seed phenotype**	χ^2
1	*PTS/pts-1*	4	239	179	60	25.1	0.001
2	*PTS/PTS*	4	239	237	2	0.8	-
3	*PTS/PTS*	4	250	250	0	0.0	-
4	*PTS/pts-1*	4	214	165	49	22.9	0.505
5	*PTS/pts-1*	4	245	193	52	21.2	1.863
6	*PTS/PTS*	4	220	219	1	0.5	-
7	*PTS/PTS*	2	110	109	1	0.9	-
8	*PTS/pts-1*	4	178	131	47	26.4	0.187
9	*PTS/pts-1*	4	216	161	55	25.5	0.025
10	*PTS/pts-1*	4	232	173	59	25.4	0.023
11	*PTS/pts-1*	2	252	188	64	25.4	0.021
12	*PTS/PTS*	4	247	247	0	0.0	-
13	*PTS/pts-1*	4	185	139	46	24.9	0.002
14	*PTS/PTS*	4	204	198	6	2.9	-
15	*PTS/pts-1*	15	637	480	157	24.6	0.042
16	*PTS/PTS*	7	346	339	7	2.0	-
17	*PTS/pts-1*	8	378	285	93	24.6	0.032
18	*PTS/PTS*	15	610	585	25	4.4	-
19	*PTS/PTS*	4	158	156	2	1.3	-
20	*PTS/pts-1*	6	326	237	89	27.3	0.920
21	*PTS/PTS*	7	360	357	3	0.8	-
22	*PTS/pts-1*	8	373	275	98	26.3	0.323
23	*PTS/pts-1*	8	317	237	80	25.2	0.009
24	*PTS/pts-1*	4	191	135	56	27.7	1.901

genotype *PTS/PTS* 10 plants
PTS/pts-1 14 plants

segregation analysis of heterozygous *PTS*/*pts-2* offspring							
plant #	**genotype**	**№ of siliques**	**№ of seeds**	**№ of normal seeds**	**№ of shrunken seeds**	**% seed phenotype**	χ^2
1	*PTS/pts-2*	4	232	182	50	21.6	1.471
2	*PTS/pts-2*	4	276	207	69	25.0	0.000
3	*PTS/pts-2*	4	226	174	52	23.0	0.478
4	*PTS/pts-2*	4	251	197	54	21.5	1.626
5	*PTS/pts-2*	4	207	167	40	19.3	3.557
6	*PTS/pts-2*	4	218	171	47	21.6	1.376
7	*PTS/pts-2*	4	238	185	53	22.3	0.947
8	*PTS/PTS*	4	262	262	0	0.0	-
9	*PTS/PTS*	4	130	128	2	1.5	-
10	*PTS/pts-2*	4	210	167	43	20.5	2.292
11	*PTS/PTS*	4	244	244	0	0.0	-
12	*PTS/pts-2*	4	205	152	53	25.9	0.080
13	*PTS/PTS*	4	280	278	2	0.7	-
14	*PTS/pts-2*	4	146	106	40	27.4	0.447
15	*PTS/PTS*	4	254	253	1	0.4	-

genotype: *PTS/PTS* 5 plants
PTS/pts-2 10 plants

Table 3.1. Observed seed phenotype in segregating heterozygous *PTS*/*pts-1* and *PTS*/*pts-2* plants. The plants were genotyped. From each plant, seeds from at least 4 individuals siliques were collected and seeds with wild type and shrunken (lethal) phenotype were counted. The Chi-square statistical test (χ^2) was used to test the

hypothesis that the observed phenotype is caused by a single recessive allele. As the calculated χ^2 values of all heterozygous plants were below the critical χ^2 value ($\chi^2_{95} = 3.841$; with one degree of freedom), the results are reasonable for 3:1 segregation.

The mutation associated with *pts-1* or *pts-2* does not appear to interfere with pollen development or pollen-tube growth because mutant seeds were distributed randomly along the length of heterozygous siliques and segregation ratios were not significantly different from those expected for a single recessive mutation. Mutant seeds in the top half of the siliques were found with a frequency of 25.5% and in the base half of the siliques with a frequency of 25.2% (18 siliques analysed). For an example of a silique used for this analysis see Fig. 3.5B, below. Moreover, pollen grains obtained from *PTS*/*pts-1* and *PTS*/*pts-2* plants also appeared normal (data not shown).

3.3 Development of *pts-1/pts-1* seeds

The development of normal-size seeds and shrunken seeds in *PTS/pts-1* plants was examined by light microscopy using Nomarski optics. All the normal-sized seeds developed at a rate comparable with that of a wild-type plant. To characterise the nature of the seed lethality associated with *pts-1* and *pts-2*, wild-type and mutant embryos from siliques of heterozygous *pts-1* and *pts-2* plants were analysed at various stages of seed development. Embryos from abnormal seeds were compared with embryos from normal seeds from the same silique. While embryos with wild-type phenotype in a silique from *PTS/pts-1* plants reached globular stage (Fig. 3.3 C), the mutant embryos were at preglobular stage (Fig. 3.3 B). When embryos with wild-type phenotype reached heart-stage (Fig. 3.3 F), mutant embryos were still at preglobular stage of development (Fig. 3.3 E). Even when other embryos in the silique reached the early-torpedo stage (Fig. 3.3 I), mutant embryos showed no progress in development (Fig. 3.3 H). Despite arrested embryo development of seeds harbouring *pts-1/pts-1* embryos, endosperm development appeared normal until late heart stage of corresponding normal development (Fig. 3.3 A, D, G). Seeds from heterozygous *PTS/pts-2* were treated similarly, the same terminal phenotype of *pts-2/pts-2* embryos was observed (not shown). After torpedo stage, the endosperm and integuments started to dry out and disintegrate. In the mature silique, mutant seeds were visible as shrunken brown seeds.

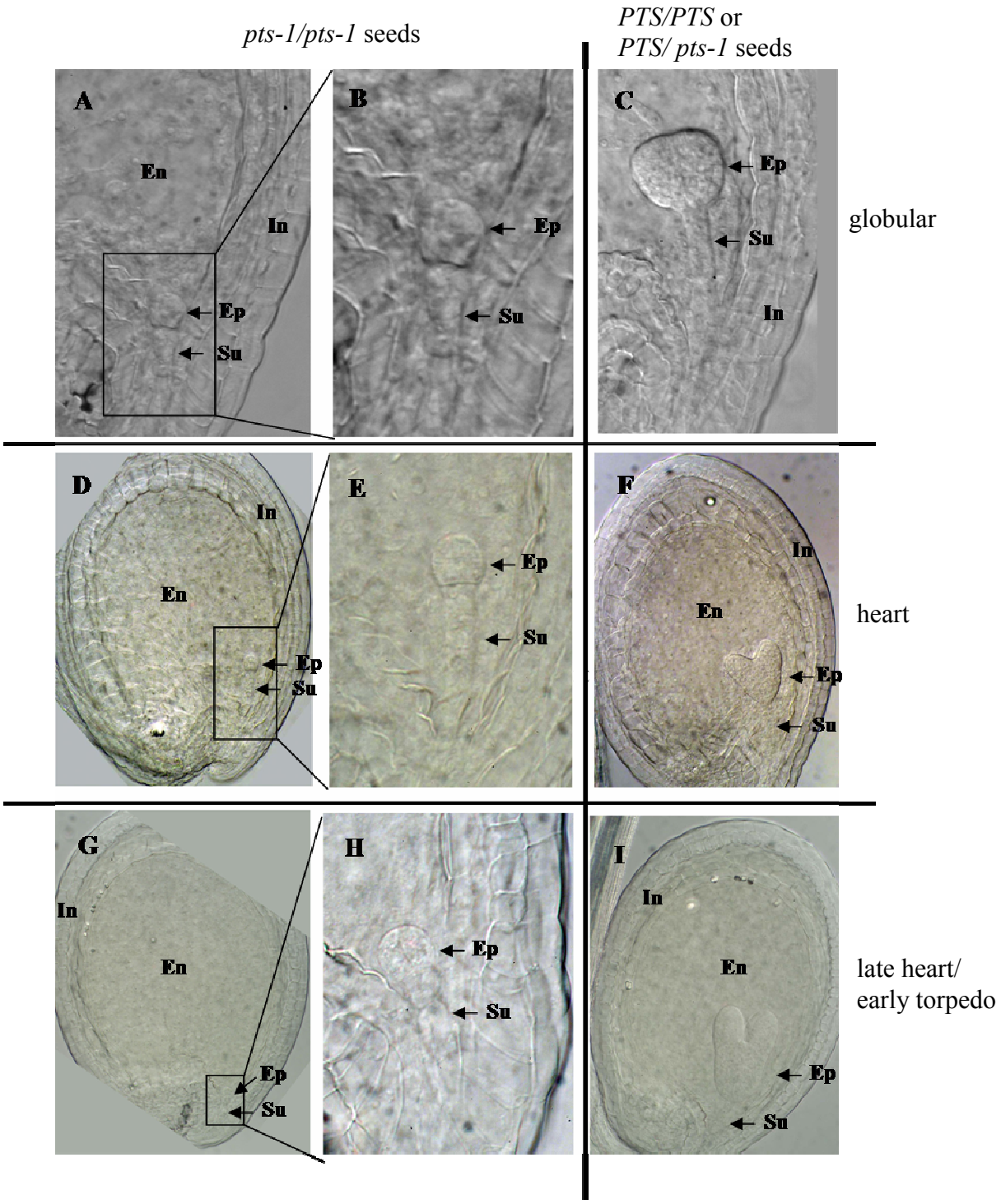

Fig 3.3 Development of wild type and abnormal seeds in siliques of selfed *PTS*/*pts-1* plants. Seeds from heterozygous *PTS*/*pts-1* plants were cleared with Hoyer's solution and examined under microscope with Nomarski optics at various stages of seed development. For each developmental stage, wild-type and mutant seeds from the same siliques were compared. B, E, H show higher magnifications of boxed mutant embryos in A, D, G respectively and represents proembryo at 2 cells of the embryo development. Terminal phenotypes of *pts-1*/*pts-1*were determined in heterozygous siliques at the globular to late heart stages of normal embryo development. In later stages of normal embryo development, ovules harbouring mutant embryos, turned brown and dried out causing observation impossible. In, integuments layers, Ep, embryo proper, En, endosperm, Su, suspensor.

All identified mutant embryos were arrested at preglobular stage of embryogenesis, after two divisions of the zygote. Apical cell and suspensor were formed from two cells (Fig. 3.4) Observed terminal phenotype was consistent from seed to seed and was the same in both *pts* lines.

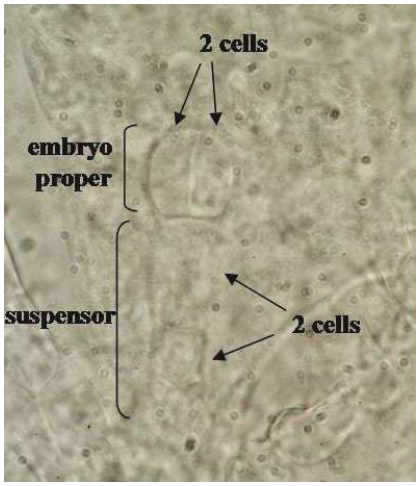

Fig 3.4 Typical terminal phenotype of *pts-1*/*pts-1* embryos. Embryo of *pts* knock-out plants stops to develop after division of apical and basal cell. Embryo proper of *pts-1/pts-1* mutants is visible as two clearly distinguishable cells although it can not be excluded that it consists of four cells. Suspensor is visible as 2 cells.

Based on the above, the following experiments were carried out with *pts-1* only.

3.4 Chemical rescue of *pts-1/pts-1* mutants

The aim of this experiment was to confirm the function of the *PTS* gene in pantothenate biosynthesis. *PTS* knock-out plants presumably lack de novo pantothenate synthesis which results in arrested embryo development. The organisation of coenzyme A pathway (chapter 5.1, Fig. 5.1) suggests that pantothenate or any of the downstream intermediates (provided that they are taken up) complement the *pts* mutation because it is currently assumed that only coenzyme A is biologically active. To test this hypothesis heterozygous *PTS/pts-1* plants were subjected to chemical treatment with pantothenate and pantetheine. It is known that pantothenate kinase can phosphorylate pantetheine (Abiko, 1975). Therefore the effect externally applied pantetheine on *pts-1* knock-out mutants should be the same as pantothenate.

3.4.1 Effect of exogenous pantothenate or pantehteine supplied by spraying on seed development in *PTS/pts-1* plants

Heterozygous *pts-1* plants were grown on soil in standard growth conditions. As soon as inflorescences appeared, plants were sprayed daily with 1% pantothenate (42 mM) or 1% pantetheine (18 mM). Mature siliques were analyzed under binocular, to see the effect of the treatment on seeds development. Both pantothenate and pantetheine could complement the defective phenotype of *pts-1/pts-1* mutant seeds (Fig 3.5). In case of plants treated with 1% pantothenate, normal seed development was observed (Fig. 3.5C) as in wild type plants (Fig. 3.5 A). Heterozygous *pts-1* plants without treatment showed 25% lethal-seeds phenotype (Fig. 3.5 B). Pantetheine also complemented the knock out mutation of the *PTS* gene (Fig. 3.5 D). Nevertheless, the treatment affected the siliques. The end of siliques treated with pantetheine became necrotic much faster than the rest of the siliques. Seeds developed in that part of the siliques were also affected. Their development was interrupted as soon as the surrounding tissues became necrotic. This effect may be attributed to the presence of DTT (36 mM) in pantetheine solution, (which is apparently toxic to plant at higher concentration). Externally applied (spraying) pantothenate and pantetheine supported normal seed development in siliques of *PTS/pts-1* plants. It is not clear how these supplements were available to the developing embryo in the analysed plants. One explanation is that pantothenate and pantetheine diffused throughout the silique tissue and then became available for the developing embryo. Another possibility is that the supplements were actively transported (see discussion).

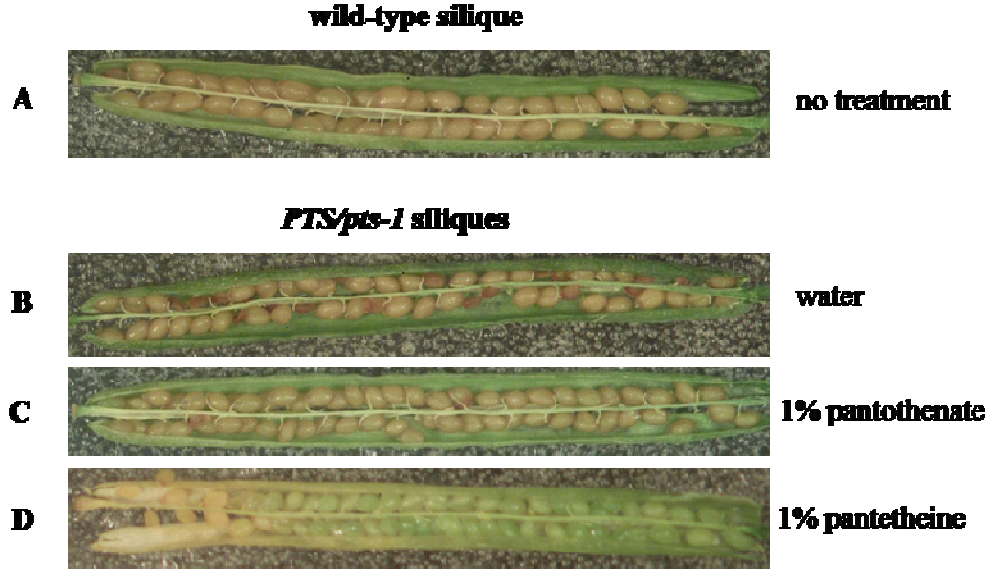

Fig. 3.5 Comparison of seed phenotypes in siliques of wild type Arabidopsis (A) and heterozygous *PTS/pts-1* plants, sprayed daily with water (B), 1% pantothenate (C), 1% pantetheine (D).

3.4.2 Effect of exogenous pantothenate supplied in the growth medium

The question addressed by this experiment was whether or not pantothenate can be transported through the vascular system and support the development of *pts-1/pts-1* seeds. Heterozygous *pts-1* plants were grown on ½ MS medium with 10 mM pantothenate as supplement. Siliques in mature plants were analysed for seed development. Clearly, pantothenate in the nutrient medium supported seed development (Fig. 3.6). In the siliques of these plants some unfertilized ovules were identified (not shown). It was probably due to *in vitro* cultures conditions. Generally, plants were developing normally but were weaker, possibly due to high humidity.

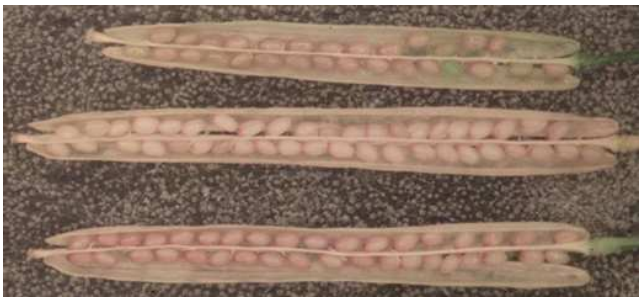

Fig. 3.6 Seed development in heterozygous *PTS/pts-1* plant (mature siliques) grown on ½ MS medium supplemented with 10 mM pantothenate. Absence of aborted seeds indicates that pantothenate present in medium can support normal seed development.

3.4.3 Pantothenate supports the complete developmental cycle of *pts-1/pts-1* plants

Seventy-five seeds from a selfed *PTS/pts-1* plant that was sprayed with pantothenate were germinated on ½ MS medium containing 1% sucrose and 10 mM pantothenate. Out of 66 seeds that germinated (88%), 34 seedlings were genotyped by PCR. Among them 8 *pts-1* homozygous seedlings were identified. This is in good agreement with the expected frequency of *pts-1/pts-1* seeds (25%). Three *pts-1/pts-1* individuals were then singled out and transferred onto fresh ½ MS medium in small plastic buckets. Another three *pts-1/pts-1* seedlings were transferred to soil. One plant grown in the plastic buckets was additionally sprayed every second day with 10 mM pantothenate. All plants grown on soil were watered with 10 mM pantothenate. All of the *pts-1/pts-1* plants grown on media developed normally and set seeds. There was no visible effect on the plant, which was additionally sprayed with 10 mM pantothenate. Plants transferred into soil were not able to develop. Watering with 10 mM pantothenate could not support normal development. Soon after the seedlings were transferred into soil they stopped to grow and eventually dried out (Fig. 3.7).

Fig. 3.7 Homozygous *pts-1/pts-1* seedlings were grown on ½MS medium or in soil. The ½ MS medium contained 10 mM pantothenate and the plants in soil were watered with 10 mM pantothenate. The *pts-1/pts-1* seedlings were identified by PCR (see above for details).

A wide range of pantothenate concentrations *in vitro* were tested (0.1, 0.5, 1.0, 5.0, 10.0 mM) to determine the minimum that is sufficient to support the growth of *PTS* knock-out plants. In all cases, *pts-1/pts-1* seeds germinated at a comparable rate and had wild type phenotype. Nevertheless, some of the seeds did not germinate (data not shown). This phenomenon was attributed to the viability of homozygous seeds, which clearly goes down within time. After about tree months of storage only a few percent of seeds germinated even if supplemented with 10 mM pantothenate. No one homozygous *pts-1* seed germinated when not supplemented with pantothenate.

From these experiments it is concluded that spraying with pantothenate (42 mM) can support normal seed development in heterozygous *PTS/pts-1* plants (section 3.4.2). In this way *pts-1* knock-out seeds were generated, which could be further grown *in vitro* into mature *pts-1* knockout plants producing normal seeds when pantothenate (10 mM) is supplemented in medium (section 3.4.3). The above experiments also clearly show that pantothenate can be transported in Arabidopsis plants *via* the root system into developing embryos, in sufficient quantities for complete morphogenesis and production of viable seeds. However, homozygous *pts-1/pts-1* plants could not be grown on soil when watered with 10 mM pantothenate.

3.5 Overexpression of *E. coli* pantothenate synthetase in Arabidopsis in different compartments

Increasing the level of pantothenate in *A. thaliana* by overexpressing a gene for pantothenate synthetase requires a concern about the organization of the whole pantothenate (and coenzyme A) biosynthetic pathway. The question arose whether overexpression of pantothenate synthetase in the cytosol would lead to increased level of pantothenate or would lead to higher level of coenzyme A, as all of the enzymes converting pantothenate into coenzyme A are located in the cytosol (Kupke *et al*., 2003). Overexpressing *panC* in plastids or mitochondria probably would omit that possible obstacle because enzymes metabolizing pantothenate have not been detected there (Tilton *et al*., 2006). Nevertheless, this raises the question whether there are substrates for pantothenate synthetase present in those compartments. In all cases the source of β-alanine is not known. It has been reported that in mitochondria pantoate is produced (Ottenhof *et al*., 2004). In plastids, in turn, pantoate production has not been detected. In both cases it can not be excluded that both pantoate and β-alanine are transported into this compartments. Therefore, in this study an attempt to overexpress *E. coli panC* gene in different compartments was undertaken to generate *A. thaliana* transgenic plants with increased level of pantothenate.

One of the methods to express a protein in mitochondria or plastids in higher plants is the use of known sequence encoding for leading peptide. Logan and Leaver (2000) successfully generated stable transgenic *A. thaliana* lines expressing GFP targeted to the mitochondria using signal sequence from the *Arabidopsis thaliana* cDNA encoding for mitochondrial chaperonin CPN-60. Similar studies (Nawrath *et al*., 1994) showed that a sequence encoding for plastidic transit peptide can be used for targeting genes into plastids in Arabidopsis. In this study to overexpress the *E. coli* PTS protein in plastids and mitochondria, similar strategy was employed.

3.5.1 Generation of the *A. thaliana* overexpressing constructs

To express *E. coli* PTS in different compartments, three plant-overexpressing constructs were generated, as described in materials and methods. As a starting point, the binary vector pCambia 1201 (http://www.cambia.org) was modified by removing a 2048 bp sequence between the *Nco*I and *Pml*I restriction sites yielding the plasmid pUG. To express the *panC* gene in the cytosol the full length *panC* ORF was cloned in the pUG plasmid, under the control of the CaMV 35S promoter (for details see materials and method) yielding a pUG-ARC plasmid. To target *panC* in plastids or mitochondria, targeting sequences from rubisco

small subunit 3b (At5g38410) and mitochondrial HSP60 chaperon targeting sequence (At3g23990) were inserted at the 5' end of the *panC* gene, on the pUG plasmid, respectively, generating pUG-DCC and pUG-BHC constructs (Fig. 3.8). The DNA sequence of cloned *panC* gene and targeting sequences were confirmed by sequencing.

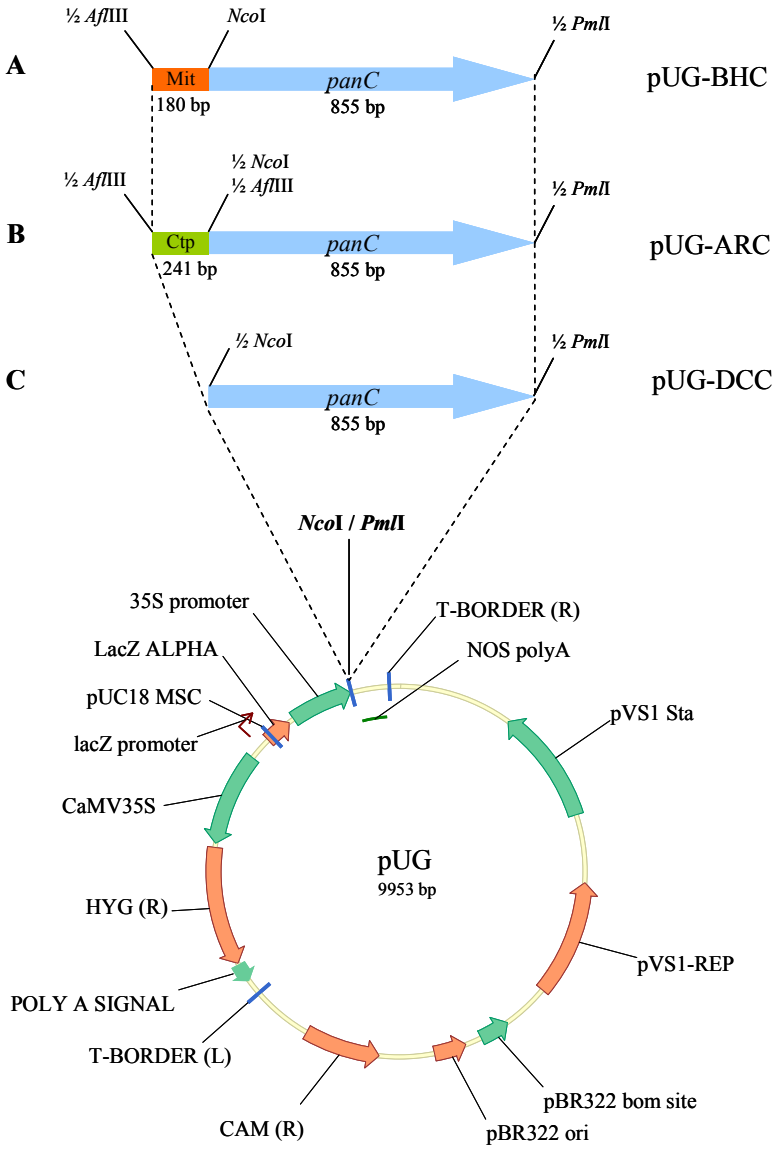

Fig. 3.8 Generation of constructs for the overexpression of *E. coli panC* in different *A. thaliana* compartments. The *panC* ORF was amplified from *E. coli* genomic DNA using a specific primers pairs carrying *Nco*I and *Pml*I restriction sites allowing cloning of the *panC* in pUG plasmid via corresponding restriction sites at the front of CaMV35S promoter. In this way pUG-DCC plasmid was generated (C). This plasmid was then used for generation of constructs for overexpression of the *panC* in different compartments in Arabidopsis. To target *panC* into chloroplasts Arabidopsis rubisco small subunit (3b) targeting sequence was amplified from cDNA library with specific primers carrying *Afl*III restriction site and corresponding 241 bp restriction fragment was cloned into pUG-DCC plasmid via *Nco*I site, resulting in the pUG-ARC construct (B). The proper orientation of the targeting sequence in this construct was determined by restriction analysis (data not shown). For mitochondrial expression, Arabidopsis mitochondrial chaperon (HSP60) targeting sequence was amplified from cDNA library with specific primers, and a 180 bp long *Afl*III/*Nco*I fragment was cloned into pUG-ARC plasmid via *Nco*I site generating pUG-BHC plasmid (A).

3.5.2 Analysis of transgenic *A. thaliana* carrying overexpression constructs

Wild type *Arabidopsis thaliana* Col-0 were transformed by infiltration method with *Agrobacterium* harbouring one of three abovementioned constructs in the binary plasmid vector. The T-DNA portion contained the cassette and the *hptII* hygromicin resistance gene. Seeds from infiltrated plants were screened on ½ MS selective medium containing hygromicin. Using this strategy, T1 transformants were recovered: a single transformant carrying cytosolic overexpressing construct (pUG-DCC), ten individuals with mitochondrial (pUG-BHC) and six with plastidic (pUG-ARC). The presence of the transgene was confirmed by PCR (Fig. 3.9). Progeny (T2) from these lines were also resistant to hygromicin.

The segregating plants carrying pUG-DCC construct were analysed for PTS expression in western-blot analysis. In addition, PTS activity in this population was measured (section 3.5.3.) as well as pantothenate level (section 3.5.4). Moreover, heterozygous plants carrying the pUG-DCC construct were used later as a pollen donor for complementation experiment (section 3.6.1).

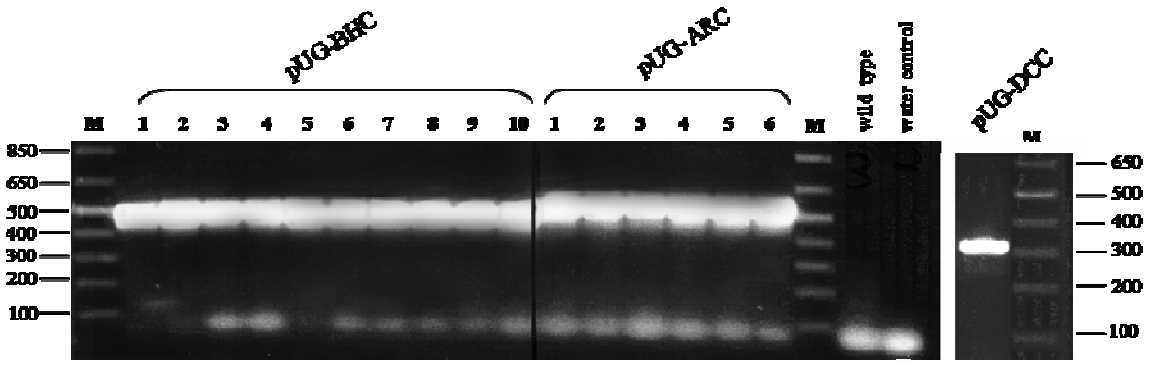

Fig. 3.9 Genotyping analysis of selected resistant transgenic plants carrying *panC* overexpressing constructs. All selected transformants where analysed by PCR where flanking fragment of CaMV35S promoter and the *panC* gene were amplified yielding PCR product of 485 bp, in case of plants with mitochondrial construct (pUG-BHC), 563 bp in case of plastidic construct (pUG-ARC), and 305 bp cytosolic (pUG-DCC). M, size marker. See materials and method chapter for details.

Transgenic plants carrying constructs for cytosolic, plastidic and mitochondrial overexpression were identified as described above. These plants were self pollinated and the offspring plants were grown to maturity and seeds were collected. Seeds were germinated on medium containing hygromicin for the selection of plants carrying the overexpression construct. On the basis of germination rate genotype of the parents was determined, allowing identification of homozygous seed pools. Selected homozygous seeds pools were then grown on soil and leaves were analysed for expression of the *E. coli* PTS protein. Western blot analysis showed that PTS was not expressed in plants carrying the pUG-BHC or pUG-ARC

constructs. However, plants carrying the pUG-DCC construct showed expression of *E. coli* PTS (Fig. 3.10).

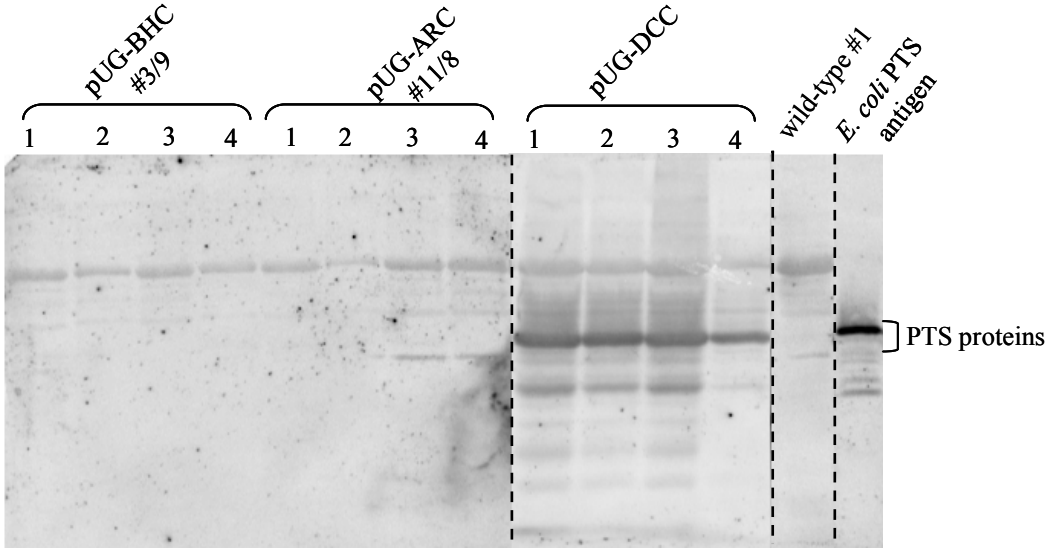

Fig. 3.10 Western blot analysis of selected homozygous transgenic plants carrying *panC* overexpressing constructs. 20 µg of plant protein (crude extract) and 50 ng antigen were analysed. Proteins were separated by SDS-PAGE, blotted onto nitrocellulose membrane. Membranes with transferred proteins were incubated with *E. coli* PTS antibody and goat anti-rabbit antibody (Cy5 labelled), scanned with Red Fluorescence modules using STORM PhosphorImager. Four offspring of homozygous plants carrying pUG-BHC, pUG-ARC and pUG-DCC construct were analysed. Only plants carrying pUG-DCC construct expressed E. coli PTS protein. No *E. coli* PTS expression could be observed in protein extract from wild-type. The difference in band size between pUG-DCC and *E. coli* PTS antigen is due to the fact that antigen protein, in contrast to overexpressing constructs, contain His-tag extension of 2.16 kDa.

3.5.3 Analysis of the expression level of the *E. coli* PTS protein and PTS activity in Arabidopsis plants overexpressing *panC* in the cytosol

Offspring of transgenic, heterozygous *A. thaliana* overexpressing *E. coli* PTS (genotype *panC/ –*) in the cytosol were grown. Ten randomly chosen F1 plants (4-5 week old) were analysed for expression of *E. coli* PTS and pantothenate synthetase activity. Western blot analysis revealed the presence of *E. coli* PTS proteins expressed at different levels in eight out of ten F1 plants (Fig. 3.11 C). The amount of detected *E. coli* PTS protein was then quantified using ImageQuant software. Calculated values represent the median out of four independent western blots. Among the F1 population little or no *E. coli* PTS expression was observed in three lines (Fig. 3.11 C and D #1; #3; #5), intermediate amounts in four lines (Fig. 3.11 C and D #2;# 6; #7; #9) and high amounts in three lines (Fig. 3.11 C and D #4; #8;#10). This finding might correspond to zero, one and two allelic doses of the *panC* transgene. This would be consistent with the expected segregation of the *panC* transgene in the F1 plants.

The F1 plants were also tested for pantothenate synthetase activity in crude protein extract. Observed PTS activity correlated positively with *E. coli* PTS levels (Fig. 3.11 E). The same tree groups were distinguishable: plants with PTS activity below detection limit, (#1; #3; #5); plants with intermediate PTS activity ranging 17- 47 mmol/min/mg (#2;# 6; #7; #9); and plants with the highest PTS activity ranging 171-230 mmol/min/mg (#4; #8;#10). The observed activity was due to the presence of the *E. coli* PTS protein, but not to endogenous *A. thaliana* PTS, because no PTS activity was detected in wild-type plants.

The detection limit of the PTS assay employed in this experiment was estimated based on detection limit of ^{14}C- labelled pantothenate. A conservative threshold based on 2% [^{14}C]–β-alanine converted into pantothenate within 36 minutes was used to estimate the increase of PTS activity in transgenic plants compared with wild type plants. Transgenic plants carrying the *panC* transgene showed 50 to 660- fold higher extractable PTS activity than wild type controls. As it is a lower estimate, the actual increase caused by *panC* could be even higher.

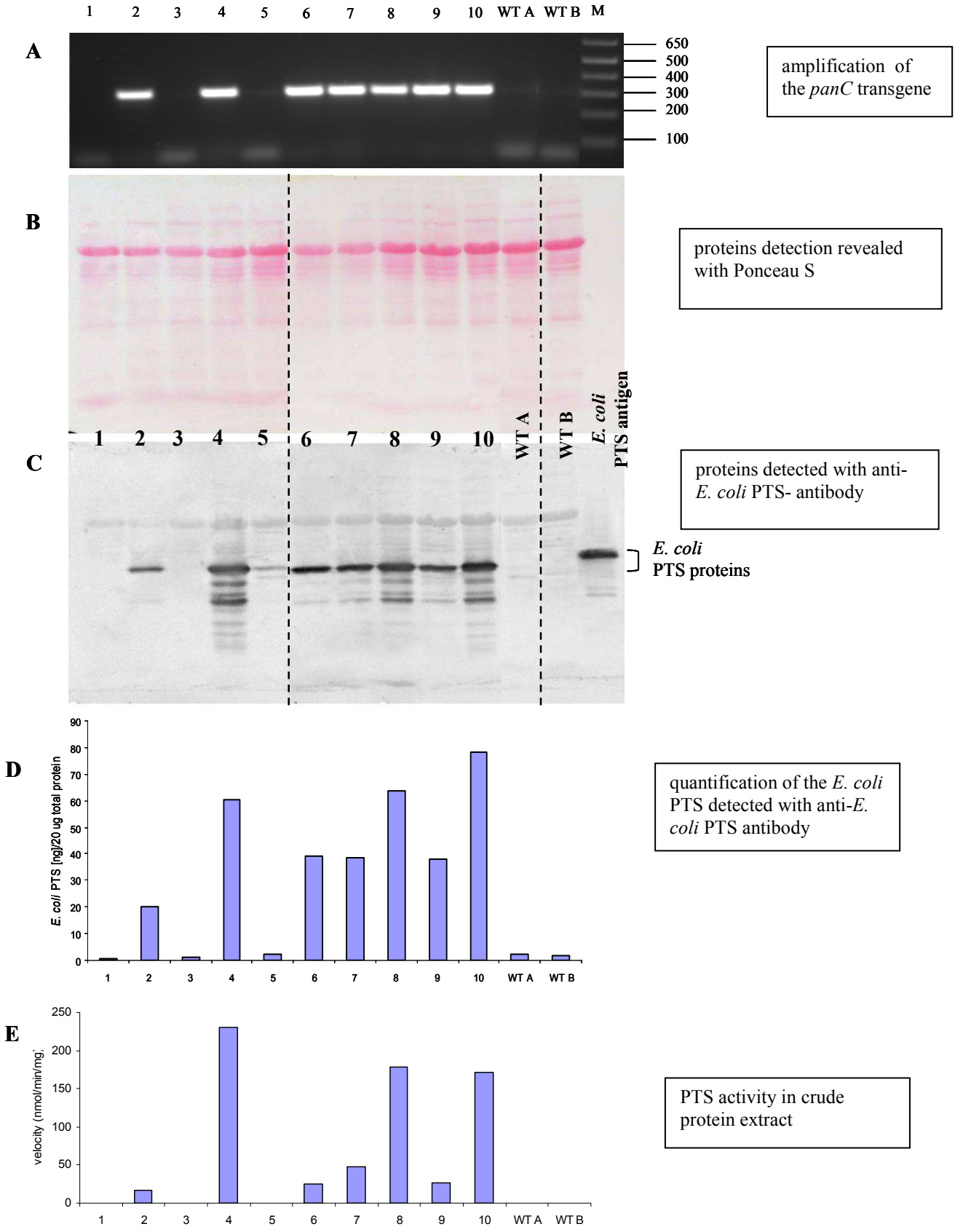

Fig. 3.11 Analysis of segregating transgenic *A. thaliana* overexpressing *E. coli* PTS (in cytosol). Plants were grown on soil to maturity (beginning of flowering); green leaves from each plant were collected and pooled. Pools were subdivided: (i) fresh green leaves were used to prepare crude protein extract for western blot analysis

and measuring PTS activity, (ii) second part was lyophilised and lyophilised leaves were extracted for pantothenate quantification.
A: Genotyping analysis in which a 306 bp fragment was amplified using a primer pairs specific to a CaMV 35S promoter region and the *panC* on the expression plasmid pUG-DCC. WT A and WT B are wild-types (negative controls); #4.7 and #4.9 are positive controls (genotype *pts-1 pts-1/panC* –); M, size marker (bands size in bp). For details, see materials and methods section.
B: Western blot analysis. In each western analysis, 20 µg of plant protein from each plant (total protein-crude extract) and 50 ng antigen (for details see materials and methods), as a reference, were analysed. Proteins separated by SDS-PAGE gel, blotted and the membranes were stained in Ponceau S solution to confirm the transfer. Thick bands visible after staining is rubisco (large subunit, 55 kDa), antigen is not visible as 50 ng of protein is below detection limit for Ponceau S solution. Segregating *A. thaliana* overexpressing the *panC* in cytosol (#1 to #10), WT A and WT B, are wild-type plants.
C: Detection of *E. coli* PTS proteins in western analysis. Membranes with transferred proteins were incubated with *E. coli* PTS antibody and goat anti-rabbit antibody (Cy5 labelled), scanned with Red Fluorescence modules using STORM PhosphorImager (for details see material and methods). Different *E. coli* PTS expression level in analysed segregating population visible as thick band (pointed with arrow). No *E. coli* PTS expression could be observed in protein extract from wild-type plant.
D: Quantification of *E. coli* PTS protein in crude protein extract. The amount of the proteins was determined using ImageQuant software. Calculated values (in ng/20µg of total protein) represent median of four independent western blots. Segregating population revealed 3 plants with wild-type like phenotype (lines #: 1; 3; 5), 3 plants with the highest expression level (lines #: 4; 8;10), and 4 plants with relative low expression level (lines #: 2; 6; 7; 9).
E: PTS activity in crude protein extracts. Radiolabeled assay in which 40 µg (50 µl assay) of soluble protein (crude extract) was assayed for pantothenate synthetase activity. Initial rates were calculated from progress curves of pantothenate formation using the numerical method described by Cornish Bowden, (1975), for details see materials and methods.

3.5.4 Analysis of pantothenate level in segregating Arabidopsis overexpressing *E. coli* PTS in cytosol

Lyophilised leave tissue from segregating transgenic *A. thaliana* overexpressing *E. coli* PTS (the same material as above) were extracted as described in materials and method. The quantification of pantothenate was carried by Dr. Rychlik (Institut für Lebensmittelchemie der TUM in Garching).

Segregating plants overexpressing *E. coli* PTS contained an active PTS protein. This was demonstrated by PTS activity assay (Fig. 3.11 E and 3.12 A)). The detected activity was positively correlated with the amount of *E. coli* PTS protein detected (Fig 3.11D). Nevertheless there is no correlation between PTS activity, and the level of pantothenate detected in segregating plants overexpressing *E. coli* PTS. As shown in Fig. 3.12 B the R^2 value is very low.

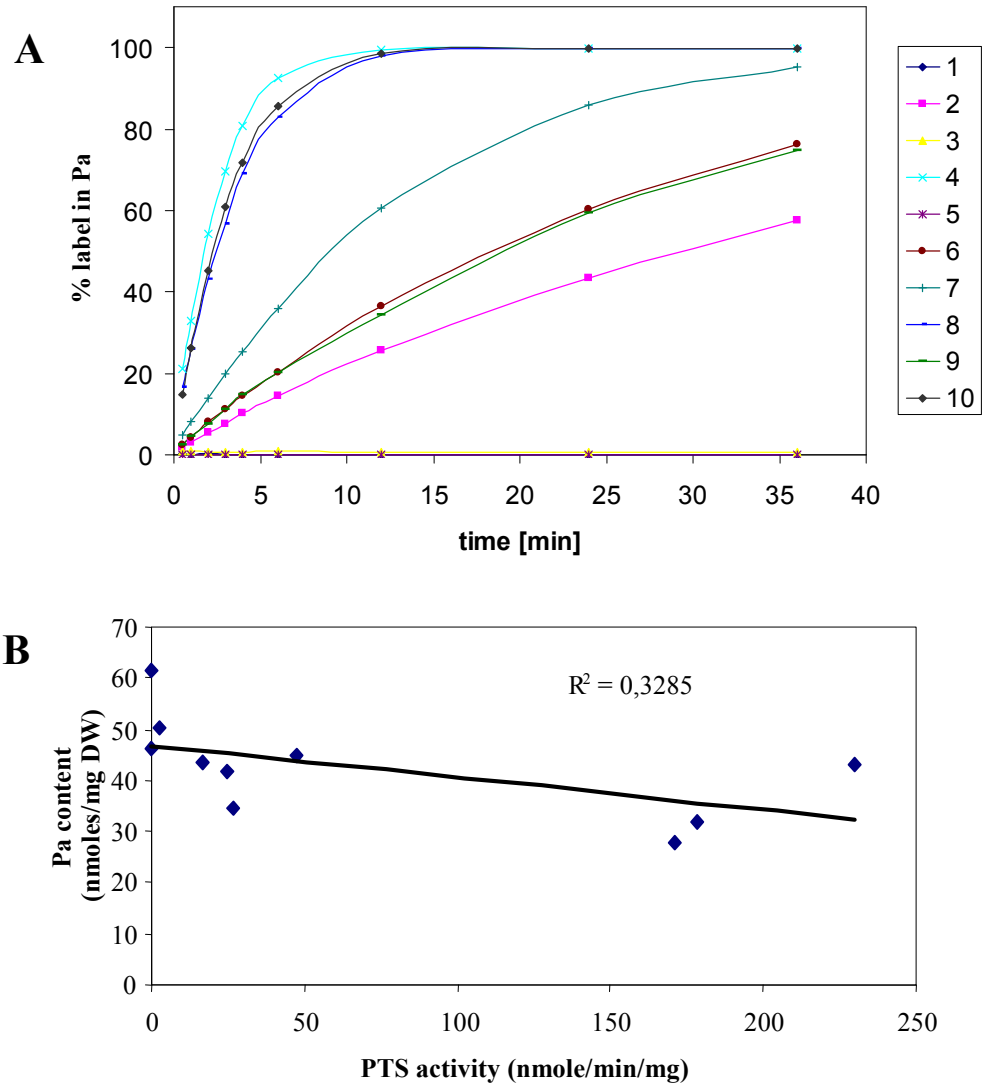

Fig. 3.12 A, Extractable PTS activity in transgenic *A. thaliana* overexpressing PTS was assayed using isotopic assay and measuring % of β-alanine converted into pantothenate. This assay (50 µl) contained 0.5 mM β-alanine, 10 mM ATP, 5 mM pantoate, 10 Mm $MgSO_4$, 15 mM $(NH_4)_2SO_4$, 100 mM Tris-HCl (pH 9.0), 40 µg extracted soluble protein. Numbering consistent with Fig.3.11
B, Correlation between detected PTS activity and the level of pantothenate in segregating transgenic *A. thaliana* plants overexpressing the *E. coli* PTS protein in the cytosol.

This result shows that even a large increase in cytosolic PTS activity does not lead to elevated levels of pantothenate in *A. thaliana* leaves. Moreover, this result is consistent with the recent report of Chakauya *et al.* (2006), who met no success when trying to increase pantothenate level in *A. thaliana* by overexpressing *A. thaliana PTS* gene (see discussion).

3.6 Genetic complementation of *PTS* knock-out plants

3.6.1 Generation of *pts-1* mutant plants functionally complemented by *panC*

The question addressed in this part of the project was whether the *E. coli panC* gene can complement the *pts-1* mutation. If it was the case, *PTS* could be assumed to have the same function as *panC*. Moreover, if *panC* could complement the lack of plant *PTS* it should be possible to isolate plants with knock-out of *PTS*, and a copy of the *panC* gene (*pts-1 pts-1*/ *panC* –).

Genetic complementation was performed by crossing heterozygous *PTS/pts-1* plants with an *A. thaliana* line overexpressing *E. coli* PTS as a pollen donor. The ecotype of both plants was Col-0 (Fig. 3.13). In case of the plant carrying the *panC* gene it was not possible to determine the copy number of the *panC* gene, because this plant line was generated by *Agrobacterium*-mediated T-DNA transformation. Therefore, the insertion point in the Arabidopsis genome is not known and has not been investigated. Consequently it was not possible to distinguish homozygous and heterozygous plants with respect to the *panC* transgene.

P *PTS pts-1 / – –* **x** *PTS PTS / panC –*

F1

♀ \ ♂	***PTS panC***	***PTS -***	***PTS panC***	***PTS -***
PTS –	*PTS PTS / panC –*	*PTS PTS / – –*	*PTS PTS / panC –*	*PTS PTS / – –*
PTS –	*PTS PTS / panC –*	*PTS PTS / – –*	*PTS PTS / panC –*	*PTS PTS / – –*
pts-1 –	*PTS pts-1 / panC –*	*PTS pts-1 / – –*	*PTS pts-1 / panC –*	*PTS pts-1 / – –*
pts-1 –	*PTS pts-1 / panC –*	*PTS pts-1 / – –*	*PTS pts-1 / panC –*	*PTS pts-1 / – –*

PCR selected *PTS pts-1 /panC –* (double heterozygous) individuals were selfed:

PTS pts-1 /panC – **x** *PTS pts-1 /panC –*

F2

♀ \ ♂	***PTS panC***	***PTS*** –	***pts-1 panC***	***pts-1*** –
PTS panC	*PTS PTS / panC panC*	*PTS PTS / – panC*	*pts-1 PTS / panC panC*	*pts-1 PTS / – panC*
PTS –	*PTS PTS / panC –*	*PTS PTS / – –*	*pts-1 PTS / panC –*	*pts-1 PTS / – –*
pts-1 panC	*PTS pts-1 / panC panC*	*PTS pts-1 / – panC*	*pts-1 pts-1 / panC panC*	*pts-1 pts-1 / – panC*
pts-1 –	*PTS pts-1 / panC –*	*PTS pts-1 / – –*	*pts-1 pts-1 / panC –*	*pts-1 pts-1 / – –*

Fig. 3.13 Crossing scheme showing the strategy to generate homozygous *pts-1* plants complemented with *E. coli panC,* which encodes for pantothenate synthetase.
P: heterozygous *PTS/pts-1* plants (genotype *PTS pts-1 / – –*), were pollinated with pollen from a transgenic plant which is wild type with respect to the *PTS* gene but overexpressing *panC* gene. According to the genetic crossing scheme, in the **F1**, four out of sixteen individuals should be double heterozygous, *i.e.* individuals that are heterozygous for both *panC* and *pts-1* (*PTS pts-1 / panC –*, in blue). These plants were identified by PCR and self-pollinated. Among the second generation (**F2**) of the plants it was expected that *pts-1* knock out plants could be identified only if they posses a copy of the *panC* gene (in red). This prediction was later confirmed by genotyping of the F2 population.

Among first generation (F1), plants which are double heterozygous for *pts-1* and *panC* gene were identified by PCR (genotype *PTS pts-1/panC* –). These plants (3 individuals) were then self-pollinated and their offspring was screened for *PTS* knock-out. Ten offspring plants from each of three F1 plants were genotyped (Fig. 3.14). All of them had wild type phenotype. Among them, two homozygous *pts-1* individuals were identified (#4.7 and #4.9). Both of them carried also a copy of the *panC* gene. No one knock-out of *PTS* plant without a copy of the *panC* gene was identified which is evidence that *panC* can functionally complement the *PTS* knock out mutation. This supports the view that in Arabidopsis there is no additional pathway leading to pantothenate. Western analysis of self pollinated complemented plants was done to check expression of the *E. coli* PTS protein (section 3.6.3).

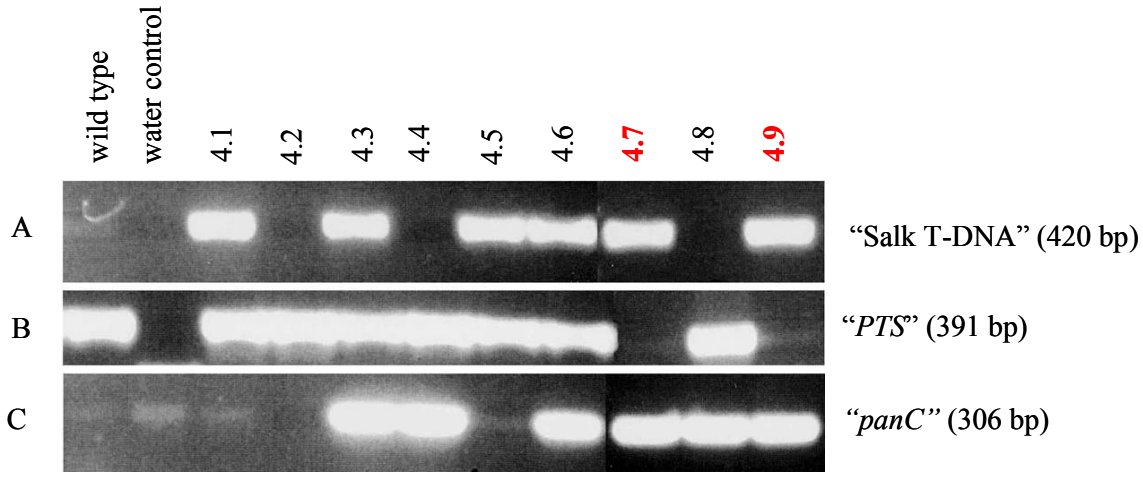

Fig. 3.14. Representative sample of genotyping analysis of the offspring of self pollinated double heterozygous plants in respect to *pts-1* and *panC* genes (genotype *PTS pts /panC* –), identified among F1 generation. Those plants were generated by crossing heterozygous *PTS*/*pts-1* plant, which is wild-type in respect to *panC* (genotype *PTS pts-1 / – –)* and transgenic Arabidopsis overexpressing *panC* gene, a heterozygous plant which is wild-type in respect to *PTS* gene (genotype *PTS PTS / panC* –), (for details see Fig. 3.13).
A: PCR of a 420 bp fragment of Salk T-DNA,
B: PCR of a fragment of the *PTS* locus;
C: PCR of a 306 bp fragment of the *panC* gene.
Amplification of the "Salk T-DNA" fragment indicate that a plant carry at least one copy of the T-DNA, likewise amplification of the *panC* fragment. Negative result of the amplification of a *PTS* fragment indicate knock-out of that gene. Five classes of genotype can be distinguished:
1st: wild type, line 4.2:
2nd: heterozygous *pts-1* plants without *panC* gene copy, plants #4.1; #4.5;
3rd: plants with *panC* gene and wild type *PTS* gene, plants #4.4; #4.8
4th: heterozygous *pts-1* plants carrying *panC* gene, plants #4.3; #4.6
5th: homozygous *pts-1* plants with *panC* gene, plants #**4.7**; #**4.9**. This class represents the complementation of *pts-1* mutation by *panC* gene and is of particular interest.

3.6.2 Analysis of the offspring of *pts-1* knock-out plants complemented by the *panC*

Offspring of two *pts-1* knock-out plants (described in section 3.6.1) complemented by *panC* (#4.7 and #4.9) were grown. All of them had wild-type phenotype with regard to plant size, colour, leaf and flower development (Fig. 3.15).

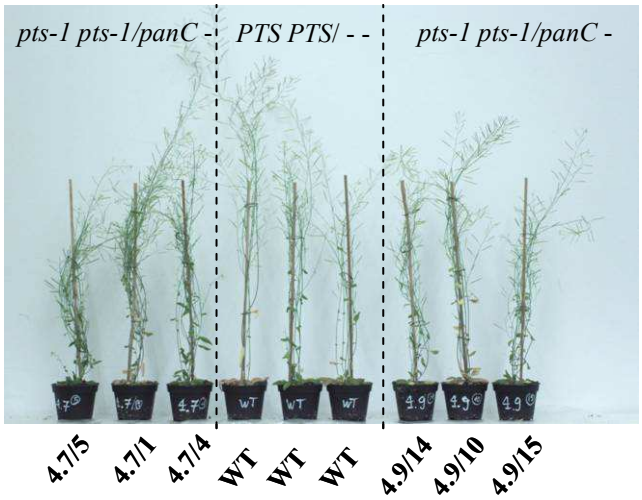

Fig. 3.15 Complementation of *pts-1* knockout by *panC*. Representative phenotype of the offspring of #4.7 (4.7/5; 4.7/1; 4.7/4) and #4.9 (4.9/14; 4.9/10; 4.9/15) lines, WT- wild type Col0 plants. All complemented plants had wild-type phenotype.

Genotyping analysis showed all of the individuals were homozygous in *pts-1* and had a copy of the *panC* gene (Fig. 3.16). This confirmed the genotype of the parents plants (#4.7 and #4.9).

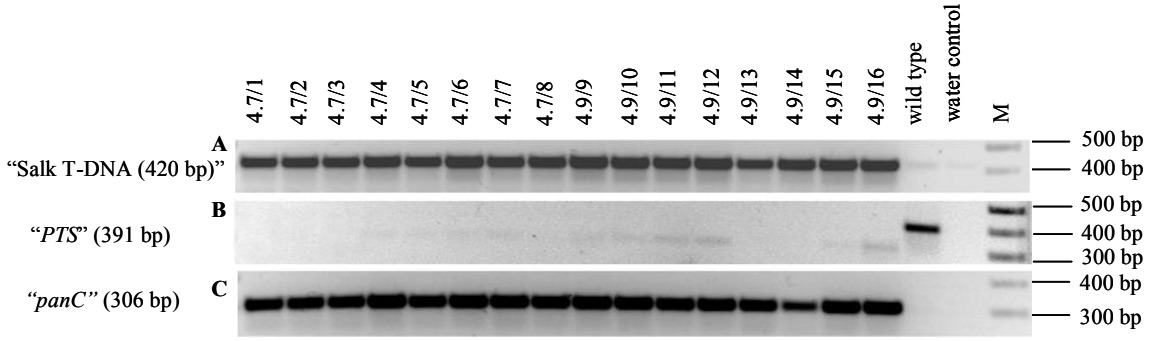

Fig. 3.16 Genotyping analysis of the offspring of *pts-1* knockout plants complemented by *panC* gene. All of the offspring of 4.7 and 4.9 mother plants were homozygous in *pts-1* which is reflected by the presence of "Salk T-DNA" band (A) and the absence of "*PTS*" band (B) and all of the analysed mutants had also copy of the *panC* gene (C), M- size marker.

Taken together, these results suggest that the activity of the *panC* transgene complements the loss of *PTS* gene function. The Arabidopsis *PTS* gene has therefore the same function as the *E. coli panC* gene. Given the ability of *E. coli* PTS enzyme to complement *A. thaliana* mutant lacking PTS, the enzymes seems to be conserved across phylogenetically distant organisms.

3.6.3 Western blot analysis of *pts-1* knockout plants complemented by the *panC* gene

Offspring of the selected *pts-1* plants complemented with the *panC* gene were analysed for expression of the *E. coli* PTS protein coming from the *panC* transgene. Four plants for each line (#4.7 and #4.9) were analysed. All of the analysed plants complemented by *panC* showed expression of the *E. coli* PTS protein (Fig. 3.17). No one plant lacking *E. coli* PTS was identified. This finding supports previous results that the *pts-1* mutation is lethal, unless complemented by pantothenate supplements or by introducing a gene that encodes a functional PTS. This is also pronounced by the fact that analysis of the seeds obtained by selfing #4.7 and #4.9 plants showed ≈25% seed lethal phenotype suggesting that they are heterozygous with respect to the *panC* gene (data not shown). This is also evidence for heterozygocity of *panC* in lines #4.7 and #4.9. The integration event of the T-DNA carrying *panC* in genome of transgenic Arabidopsis is not known, and was not investigated.

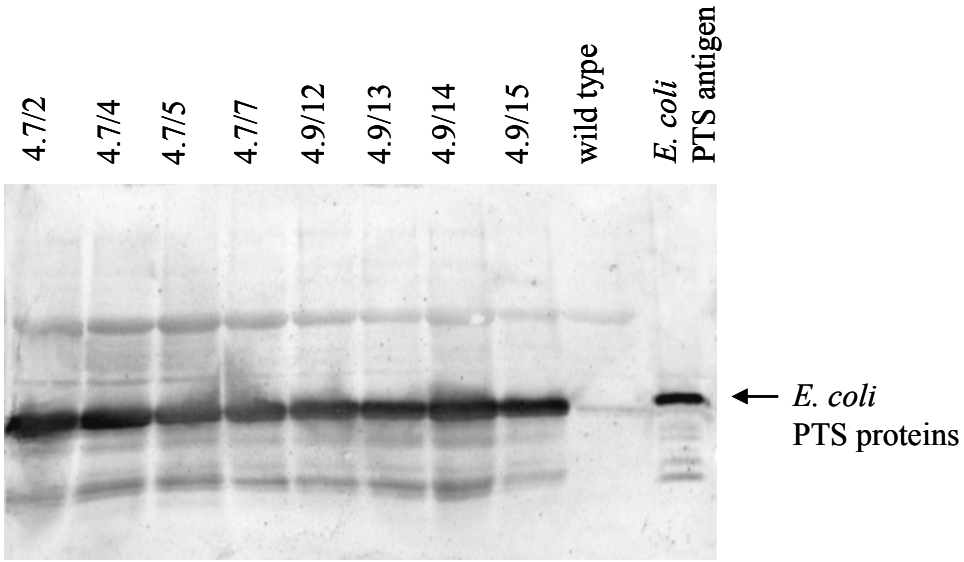

Fig 3.17 Western blot analysis of homozygous *pts-1* plants complemented by the *panC* gene. Fifteen µg of crude protein extract and 50 ng of *E. coli* PTS antigen were run on a 12.5% SDS gel and blotted on nitrocellulose membrane. The membrane with transferred proteins was incubated with the *E. coli* PTS antibody (generated as described in materials and methods) and a goat anti-rabbit antibody (Cy5 labelled), and scanned with Red Fluorescence modules using a STORM PhosphorImager (for details see material and methods).

3.7 Tissue specific expression of the *A. thaliana PTS* gene

3.7.1 Analysis of publicly available microarray data

To investigate the expression of *A. thaliana PTS*, publicly available microarray data were analyzed (https://www.genevestigator.ethz.ch/) (Zimmermann *et al*., 2004). According to Fig. 3.18 A, *A thaliana PTS* is expressed (at low level) throughout the whole plant development. The *PTS* expression at early stages of embryogenesis and flower development was of particular interest as *pts* mutants are embryo-lethal. Therefore, available datasets for flower development, and its constituents as well as early stages of siliques development and immature seeds were analysed in more detail. No data was available for embryo development alone. As is shown in Fig. 3.18 B, *PTS* is expressed during development in each flower structure, with the lowest in the stamen and the highest in the carpel. In case of mature pollen, the signal suggests that there is no *PTS* expression. Expression level seems to be at comparable level before and after fertilization (flower development at stage 12 and 15, respectively). During early stages of embryogenesis (zygote until torpedo stage) *PTS* is expressed in whole siliques, but the level of expression in embryo at that time is not known. Interestingly in immature seeds harbouring embryos at torpedo stage until early green cotyledon stage, *PTS* is apparently not expressed as detected signal was very low and the p-value indicated that the signal was not significantly higher than background.

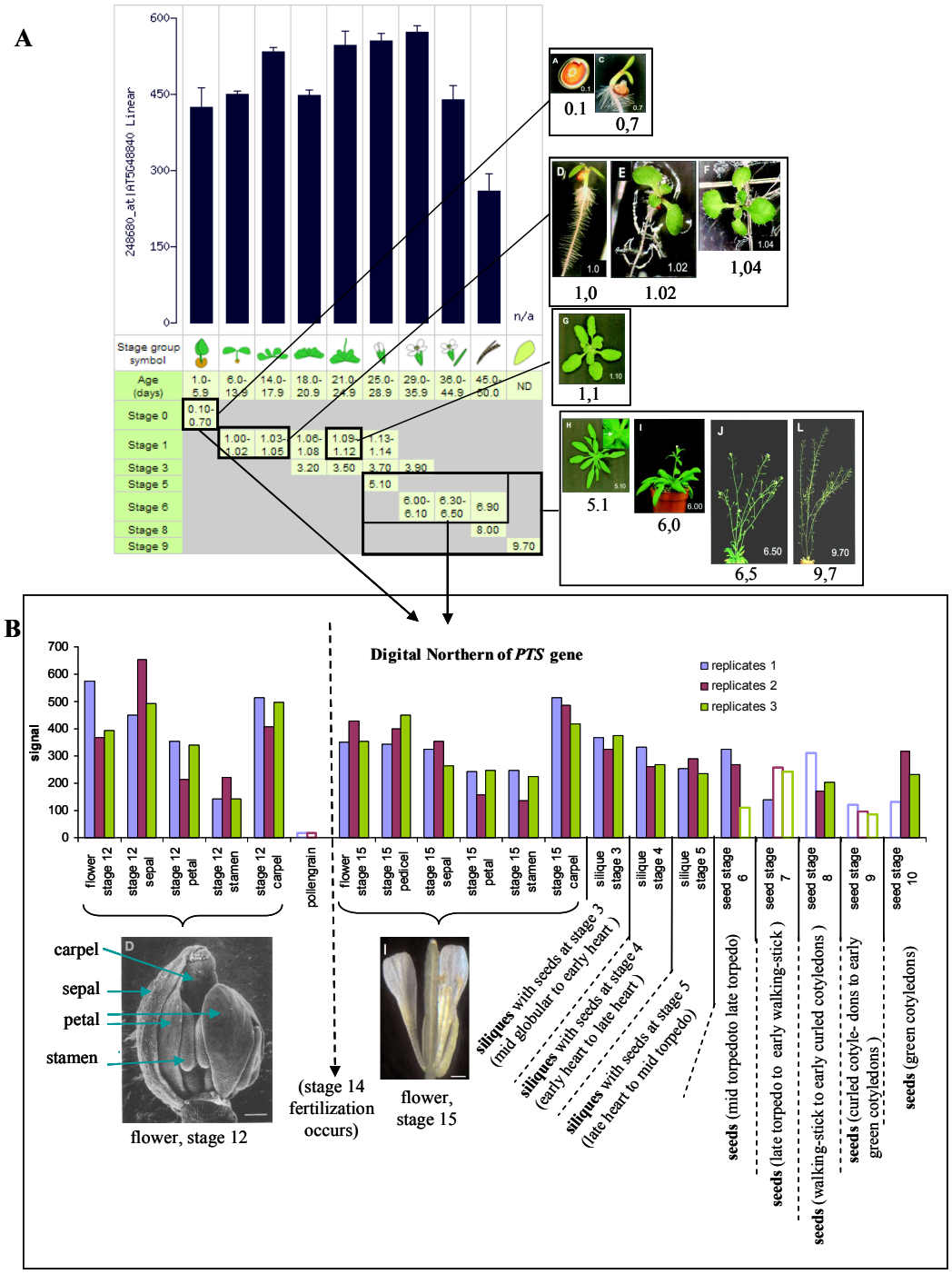

Fig. 3.18 AtGenExpress microarray data were analysed using the Genevestigator tools GeneAtlas (A) and Digital Northern (B).

A: PTS expression throughout *A. thaliana* development. Each black bar represents average signal intensity for the developmental stage described in a chart underneath. Corresponding representative growth stages are shown (Boyes *at al.*, 2001). For two digits description see materials end methods (section 2.3). Briefly, stage 0, germination; stage 1, leaf production; stage 3, rosette growth; stage 5, inflorescence emergence; stage 6, flowering; stage 8, silique ripening.

B: The Digital Northern of *PTS* for flowers (whole flowers, sepals, petals, stamens, carpels, mature pollen), siliques and seeds at early stages of development. Embryo developmental events in siliques and seeds are indicated below. In most cases three representatives datasets were available for each plant organ analysed. Open symbols indicate absent or marginal calls ($p > 0.06$; "signals not significantly higher than background"), closed symbols indicate present calls ($p = < 0.06$; "signals significantly higher than background").

3.7.2 *A. thaliana* PTS promoter driven GUS, expression profile

To gain a deeper insight into the tissue-specific expression of *PTS*, a 531 bp (upstream of ATG codon) promoter region was analysed. Reporter construct, pRJ-PTSpro, was created based on pCambia 1305.1 vector (http://www.cambia.org), where *Eco*RI/*Nco*I fragment carrying CaMV 35S promoter was removed and replaced with amplified *PTS* promoter region (Fig. 3.19). In this reporter construct promoter region is cloned at the front of the GUSPlus gene (*uidA*; encoding the β-glucuronidase). The construct was introduced into wild type *Arabidopsis thaliana* Col-0 by floral dip method as described in materials and methods.

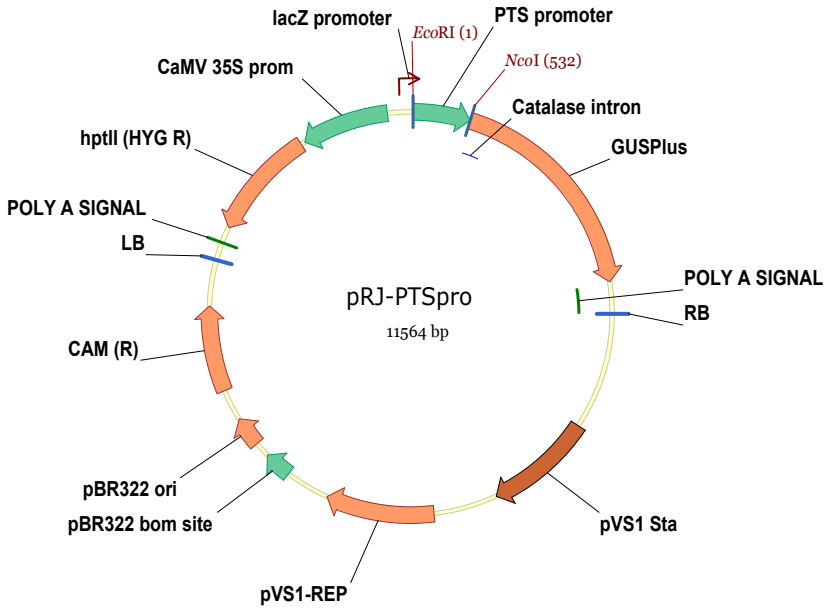

Fig. 3.19 Reporter construct carrying GUS driven by promoter region of Arabidopsis *PTS* (P_{AtPTS} promoter) (see above for details).

Seeds from transformed plants were screened on selective medium containing hygromicin. In this way 14 transgenic plants were selected. The presence of the transgene was confirmed by restriction analysis (data not shown). GUS histochemical staining showed that PTS is expressed ubiquitously (Fig. 3.20- right hand panel). Gus activity was detected ubiquitously throughout development from young seedlings till plant maturity. In flowers, GUS activity was detected in petals, sepals. In stamen (stage 12 of flower development) GUS expression was not detected. Interestingly in carpel expression was restricted to the stigma (Fig. 3.20 C). The results were compared with the data available at Genevestigator using the GeneAtlas and Digital Northern (above) and the Meta-Analyzer (https://www.genevestigator.ethz.ch) (below), tools for the analysis of *PTS* expression in different organs of the whole adult Arabidopsis plant (Fig. 3.20-left hand side). Generally, those analyses were consistent with

the GUS staining results. Surprisingly, in digital expression analysis, *PTS* expression was detected in low level in stigma whereas GUS staining shows that this part of the flower stains with the highest intensity (Fig. 3.20C). Moreover in young flowers at stage 12 stamens do not stain, whereas at stage 15 stamens stain with high intensity (Fig.3.20 B and D). Immature seeds in selfed homozygous P_{AtPTS}::GUS plants were analysed form several individuals but gave no reproducible results. In some cases all immature seeds showed week staining, in another only few seeds stained or not at all. Nevertheless, mature seeds (collected from ≈ 8 week old plant) never stained.

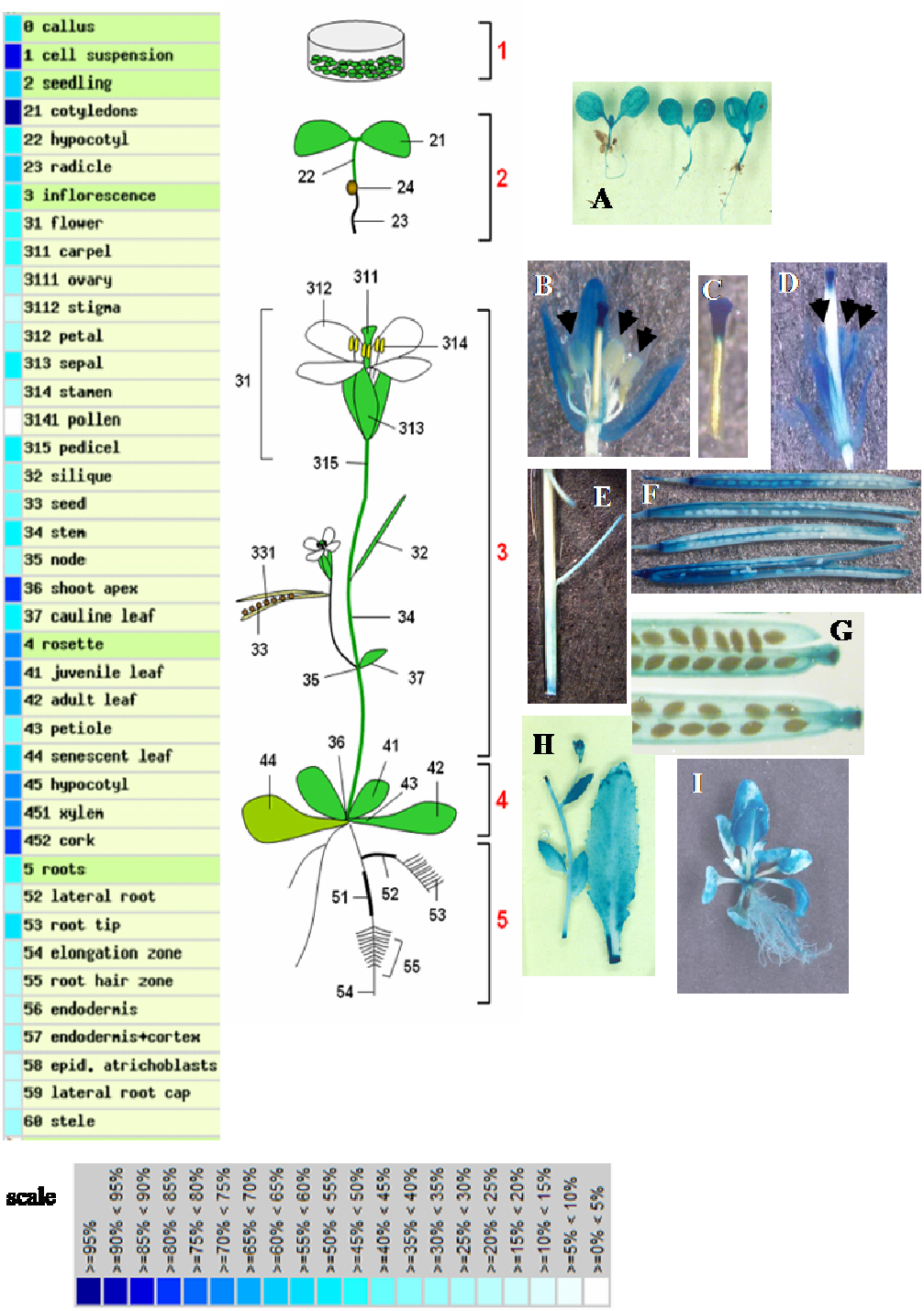

Fig. 3.20 Expression profile of *PTS* obtained using Meta-Analyzer (left hand side panel) and histochemical staining of plants carrying P_{AtPTS}::GUS construct (right hand side panel). Results are given as heat maps in blue/white coding (absolute signal values)
For the blue-white scheme, all gene-level profiles were normalized for colouring such that for each gene the highest signal intensity obtains value 100% (dark blue) and absence of signal obtains value 0 % (white).
A-J Histochemical location of *PTS* promoter driven GUS in transgenic Arabidopsis plants. A, five-day-old seedlings; B, flower at stage 12; C, carpel; D, flower stage 15; E, stem; F, immature siliques; G, mature silique; H, stem, cauline leaf, adult leaf; I, four-week old plant with roots.

3.8 Conclusions

In this work, a new *emb* (embryo specific) mutant, altered in pantothenate biosynthesis, is reported. The results demonstrate that the *pts-1* and *pts-2* mutations of Arabidopsis disrupt the gene that encodes for pantothenate synthetase. The pattern of inheritance indicated a single recessive mutation responsible for the observed defects in seed development. The fact that *PTS/pts* heterozygous plants produce 25% lethal seeds suggests that the seed coat and integuments, in heterozygous plants, do not provide sufficient pantothenate for *pts/pts* embryo to complete morphogenesis, even though the surrounding tissues contain one copy of the wild type allele. A selective elimination of mutant *pts* homozygotes takes place.

The Arabidopsis *pts* mutant described is an auxotroph, requiring pantothenate supplementation for growth. Pantothenate, when supplied externally can be apparently translocated in sufficient quantities to complete normal embryo development in *pts-1/pts-1* seeds.

Apparently, the pantothenate demand of *pts-1/pts-1* embryos can also be met in transgenic plants expressing the bacterial *panC* transgene. The fact that the *E. coli panC* gene complements the *pts-1* mutation also proves that the bacterial and plant PTS enzymes are functionally conserved.

PTS is expressed ubiquitously at low level throughout the whole Arabidopsis development analysed. The expression profile of *PTS* in embryo alone is not known.

The pattern of morphogenesis observed in *pts* homozygous embryos demonstrates that disrupting an essential metabolic function such as pantothenate biosynthesis can have developmental consequences that may resemble defects in pattern formation (see discussion). Developmental consequences similar to the *pts* mutation were observed and described in Arabidopsis (see discussion) *bio* mutants (Schneider *et al*., 1989; Patton *et al*., 1998), *atsufE* mutants (Xu and Moller, 2006), *hal3* mutants (Rubio *et al*., 2006). Many other mutants which result in embryo lethality have been reported (Meink and Sussex, 1979; Meinke, 1982, 1985; Kyjovska *et al*., 2003; McElver *et al*., 2001; Tzafrir *et al*., 2004).

Chapter 4

Kinetic analysis of wild type and mutant forms of *A. thaliana* PTS

4.1 Introduction

Biosynthesis of coenzyme A from pantothenate proceeds by the same route in bacteria, eukaryotes, and, in all likelihood, in archea (Genschel, 2004). There is evidence that the synthesis of coenzyme A from pantothenate is mainly controlled by pantothenate kinase, *i.e.* at the step after PTS in the coenzyme A biosynthetic pathway. Pantothenate kinase is feedback inhibited by coenzyme A or coenzyme A thioesters in bacteria, fungi, plants, and animals. This property is thought to constitute a universal mechanism for the control of intracellular coenzyme A levels (Rock *et al*., 2003). *E. coli* produces pantothenate in large excess over the amount incorporated into coenzyme A, and excess of pantothenate is excreted into the medium, suggesting that pantothenate biosynthesis proceeds largely unregulated (Jackowski and Rock, 1981). The regulation of pantothenate synthesis in plants has not been studied but is unlikely to depend on continuous excretion of excess pantothenate because this would require an elaborate transport system. The aim of this study was to evaluate the regulatory potential of *A. thaliana* PTS based on steady-state kinetic analysis.

In *E. coli*, pantothenate is synthesized in three steps from ketoisovalerate and β-alanine and this pathway is conserved in plants and fungi (Ottenhof *et al*., 2004; Genschel, 1999) (section 1.2.4). Pantothenate synthetase (PTS, pantoate-β-alanine ligase, EC 6.3.2.1) converts pantoate, β-alanine, and ATP into pantothenate, AMP and PP_i (Miyatake *et al*., 1979). The kinetic mechanism of *E. coli* PTS (Miyatake, 1979) and *M. tuberculosis* PTS (Zheng and Blanchard, 2001) was determined to be Bi Uni Uni Bi Ping Pong. The reaction was suggested to proceed via an enzyme bound pantoyl adenylate intermediate that is formed in the first half reaction from ATP and pantoate, and reacts with β-alanine to give pantothenate and AMP in the second half reaction (Maas, 1960). Pantoyl adenylate is subject to rapid hydrolysis in solution, but stable analogs could be demonstrated as kinetically competent intermediates of *E. coli* PTS (Wieland *et al.*, 1963). Binding of ATP precedes binding of pantoate, and release of pantothenate precedes release of AMP (Scheme 4.1). The kinetic mechanism of *E. coli* PTS (Miyatake *et al.*, 1979) and *Mycobacterium tuberculosis* PTS (Zheng and Blanchard, 2001) was also consistent with Scheme 4.1.

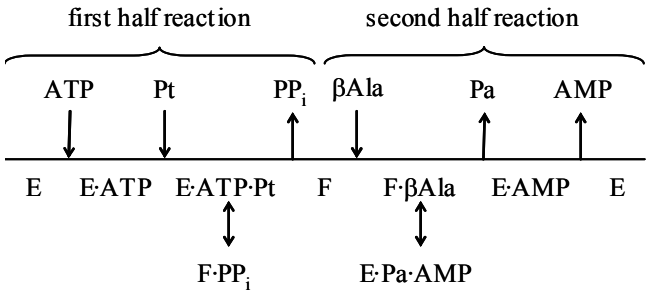

Scheme 4.1. Cleland diagram of the kinetic mechanism of *E. coli* pantothenate synthetase (EC 6.3.2.1) (Miyatake *et al.*, 1979). In this ordered Bi Uni Uni Bi Ping Pong system, Michaelis-Menten kinetics are strictly obeyed, irrespective of the variable substrate and at all cosubstrates levels (Segel, 1975). *E*, enzyme; *F*, enzyme-pantoyl adenylate complex; *Pt*, pantoate; *βAla*, β-alanine; *Pa*, pantothenate

The crystal structure of *E. coli* PTS (von Delft *et al.,* 2001) showed that the enzyme is a homodimer. Each subunit consists of two well-defined domains which are connected by a flexible hinge region. The active site is found in the N-terminal domain which forms a Rossmann fold, and structural elements involved in the dimerization form an insertion in this domain. *M. tuberculosis* PTS was crystallized in presence of various substrates, and the resulting structures confirmed pantoyl adenylate as the reaction intermediate that is protected from hydrolysis by tight binding within the active site cavity (Wang and Eisenberg, 2003, 2006).

PTS is highly conserved across bacterial and eukaryotic organisms, and *E. coli* shows greater than 40% and greater than 50% sequence identity in local Blast alignments with PTS from fungi and plants, respectively (Genschel, 2004). PTS belongs to the HIGH superfamily of nucleotidyltransferases, and is thus related to class I aminoacyl-tRNA synthetases (Aravind *et al*., 2002). Aminoacyl-tRNA synthetases attach amino acids to their cognate tRNA in a two-step process by ATP activation of the amino acids and subsequent transfer to the tRNA (Fersht, 1999). The first half-reactions of PTS and aminoacyl-tRNA synthetase are analogous in that both enzymes utilize ATP to form an acyl adenylate intermediate and release PP_i.

In accordance with PTS form *E. coli* or *M. tuberculosis*, PTS from *L. japonicus* exists as a homodimer. However, the *L. japonicus* enzyme showed significant substrate inhibition above 0.5 mM pantoate (Genschel *et al*., 1999) while bacterial pantothenate synthetases follow hyperbolic kinetics through (Miyatake, 1979; Zheng and Blanchard, 2001). The kinetic constants reported for *E. coli* PTS are vary significantly (Table 4.1). The discrepancies among the kinetic values reported may be partially due to differences in the enzyme preparations and different assay procedures.

reference	assay conditions	pantoate K_m [mM]	β-alanine K_m[mM]
Mass, 1952	25°C	1.52 - 3.54	0.38 - 0.74
Miyatake *et al*., 1979	pH 10.0, 30°C	0.063	0.15
Pfleiderer *at al*., 1960	pH 8.6, 25°C	0.66	2.1

Table 4.1 *E. coli* PTS kinetic constants reported by different authors.

During this study, overexpression and purification of PTS enzymes from *E. coli* and *A. thaliana* was undertaken in order to make available sufficient amounts of enzyme protein for enzymological and kinetic analysis. Data on the affinity and specificity for substrates and the pH-dependence of the reaction *in vitro* may help to understand the role of PTS *in vivo*. Moreover, characteristics of *A. thaliana* and *E. coli* PTS enzymes in this study could be directly compared. Apart from kinetic analysis, pure recombinant *E. coli* PTS was also used as an antigen to raise antibodies which were used to monitor the complementation of *PTS* knockout mutation by the *panC* gene (see above).

4.2 Alignment of pantothenate synthetases, conserved active site residues and divergent dimerization contacts in the PTS protein family

PTS from *E. coli* was shown to be a homodimeric enzyme and its crystal structure was reported (von Delft *et al*., 2001). The enzyme consists of two well-defined domains, which are connected by a flexible hinge region. The active site and dimerization region are found in the N-terminal domain which forms a Rossmann fold. Within the Rossmann domain, structural elements of the dimerization are inserted between the β3 and α3 structural elements of *E. coli* PTS (von Delft *et al.,* 2001). The hinged C-terminal domain is thought to form a lid that regulates access to the active site. PTS from *M. tuberculosis* was also a dimeric protein with a crystal structure similar to that of *E. coli* PTS (Wang and Eisenberg, 2003). *M. tuberculosis* PTS was crystallized in presence of various substrates, and the resulting structures confirmed pantoyl adenylate as the reaction intermediate that is protected from hydrolysis by tight binding within the active site cavity (Wang and Eisenberg, 2003, 2006).

Crystal structural analyses of PTS from *E. coli* and *M. tuberculosis* have previously afforded a detailed picture of the active site and the dimerization in these enzymes. Fifteen active site residues with various functions in catalysis were identified in the liganded structures of *M. tuberculosis* PTS (Wang and Eisenberg, 2003, 2006), and 6 of these active site residues were confirmed by kinetic analysis of the respective Ala mutants (Zheng *et al.*, 2004). The structure of *E. coli* PTS (von Delft *et al.*, 2001) revealed 11 residues specifically

involved in forming dimerization contacts, and the key structural elements of dimerization are conserved between *E. coli* and *M. tuberculosis* PTS. These functionally important residues were mapped onto an amino acid sequence alignment containing PTS homologues from bacteria, fungi, and plants (Fig. 4.1 A). In this alignment, all active site residues of *M. tuberculosis* PTS are strictly conserved, indicating that bacterial and eukaryotic pantothenate synthetases share an identical reaction mechanism. Although none of the residues involved in the dimerization of *E. coli* PTS is fully conserved, the majority of these residues are functionally conserved between plants, fungi, and *E. coli* (Tryp-134, Ile-135, Arg-154, Asn-165, Asp-191, Leu-192, and Phe-194 in *A. thaliana* PTS). This suggests that the overall design of the dimer interface is largely conserved in the PTS protein family. Among the remaining unconserved residues at the dimer interface, two position in *A. thaliana* PTS (Glu-132, and Arg-136) are conserved in plants but distinct from the corresponding residues in fungi or bacteria, and this pattern can be taken as an indication that these residues are involved in specialized subunit interactions occurring only in plant pantothenate synthetases. The alignment also shows that PTS sequences from plants and euascomycete fungi contain specific insertions relative to *E. coli* PTS, respectively.

In order to reveal the structure of the plant-specific insertion, which was previously noted to precede the dimerization domain of *E. coli* PTS (von Delft *et al.*, 2001), residues in the dimerization region that is situated between the β3 and the α3 structural elements of *E. coli* PTS were re-aligned. In addition, EST-encoded, partial PTS sequences from a range of angio- and gymnosperm plants were included in the alignment. A cDNA clone for PTS was identified in an EST library of the bryophyte *Physcomitrella patens* (Nishiyama *et al.*, 2003) and the full-length sequence was obtained (gi:84871839). Finally, the alignment includes gene models for PTS from the chlorophyte *Chlamydomonas reinhardtii* and the rhodophyte *Cyanidioschyzon merolae*. The resulting alignment (Fig. 4.2 B) shows that the insertion in plant PTS sequences is framed by the structural elements αD and βD. The insertion varies, relative to *E. coli* PTS, between 15 amino acids in *Allium cepa* and 32 amino acids in *Saruma henryi*, and is absent from all known bacterial or fungal PTS homologues. The inserted residues are poorly conserved except for the ^{122}SCVE^{125} motif. The alignment also reveals the conserved motif ^{131}HETWIRVER^{139}, which is present in PTS sequences from plants and algae, but not outside the Viridiplantae kingdom. This motif coaligns with the βD strand, which forms an intersubunit antiparallel β sheet and is central to the dimerization of bacterial PTS (von Delft *et al.*, 2001; Wang and Eisenberg, 2003). It is possible, therefore, that the ^{131}HETWIRVER^{139} motif is equally important for the dimerization of plant pantothenate

synthetases. Interestingly, the ^{131}HETWIRVER^{139} motif contains basic residues (His-131 and Arg-139) and acidic residues (Glu-132 and Glu-138) in a symmetrical fashion. This may be important because repulsion between like-charged residues flanking the predicted βD strand may have a role in intersubunit communication. A similar arrangement of like-charged residues was not detected in non-plant PTS sequences.

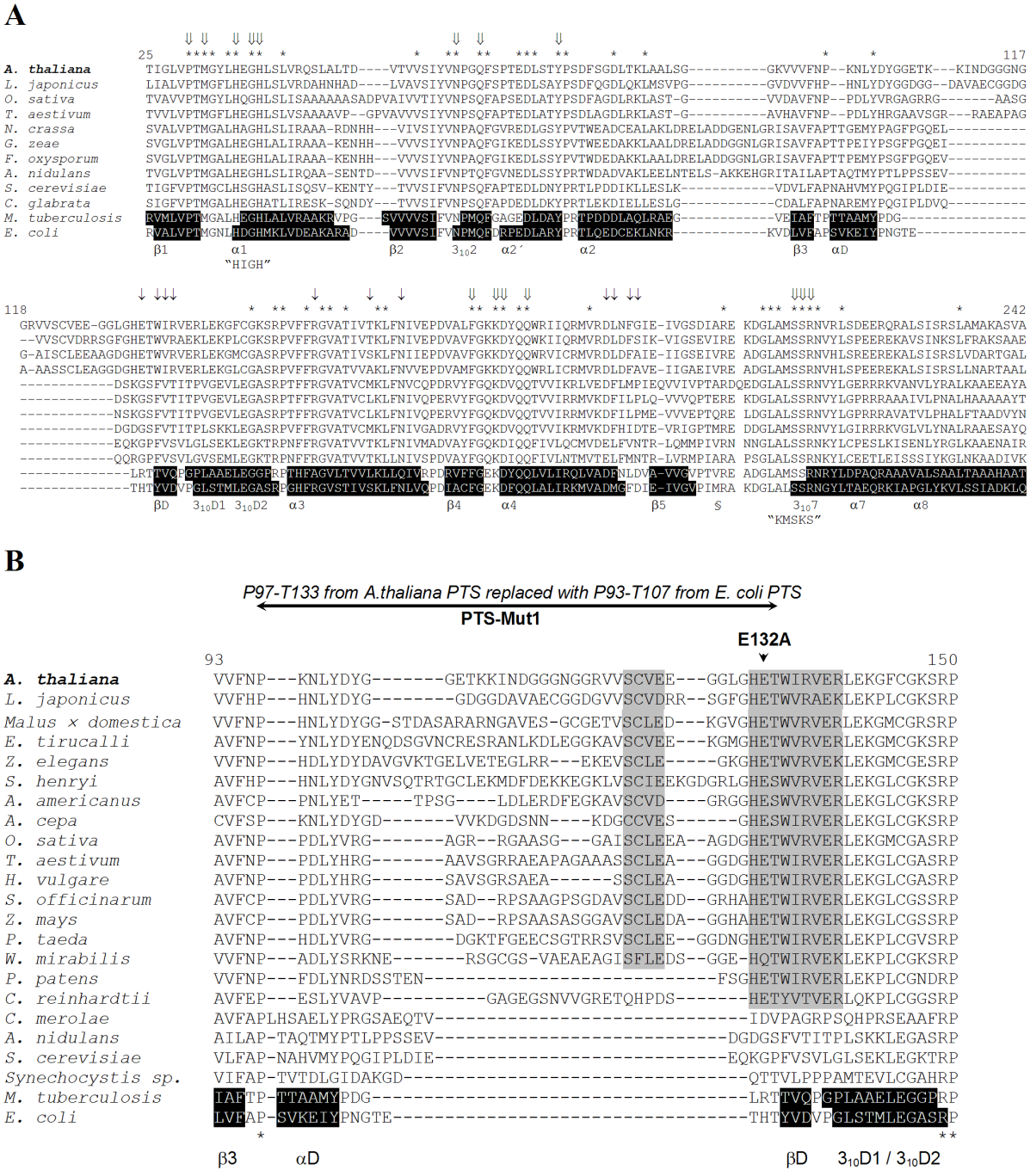

Fig. 4.1 Multiple sequence alignment of PTS proteins from plants, algae, fungi, and bacteria. (**A**) Mapping of residues with established functional roles in PTS from *E. coli* or *M. tuberculosis.* Active site residues (⇓) with various functions in catalysis, residues involved in dimerization (↓), and the "HIGH" and "KMSKS" sequence motifs, which characterize the HIGH superfamily of nucleotidyltransferases, were previously identified by crystal structural analysis of *E. coli* PTS (von Delft *et al.*, 2001) and *M. tuberculosis* PTS (Wang and Eisenberg, 2003, 2006). The secondary structural elements of *E. coli* and *M. tuberculosis* PTS are highlighted in black and

numbered according to von Delft *et al.* (2001). Strictly conserved residues (*) and the start of the N-terminal domain (§) are indicated.
(**B**) Re-alignment of the residues in the dimerization region. The ^{122}SCVE^{125} and ^{131}HETWIRVER^{139} motifs from *A. thaliana* PTS, which are conserved in plant PTS sequences, are highlighted in grey. The two PTS mutants analyzed in this study, PTS-E132A and PTS-Mut1, are indicated. The alignment contains annotated PTS sequences from *A. thaliana* var. Columbia (gi:9758883), *L. japonicus* (gi:2292921), *O. sativa* (gi:50920129), *A. nidulans* (gi:67515847), *C. glabrata* (gi:49526388), *F. oxysporum* (gi:14595008), *G. zeae* (gi:46116690), *S. cerevisiae* (gi:37362661), *N. crassa* (gi:85105428), *E. coli* (gi:16128126), *M. tuberculosis* (gi:15610738), and *Synechocystis* sp. (gi:16330757). Also included are conceptual translations of full-length cDNAs for PTS from *T. aesitvum* (gi:32128941) and *P. patens* (gi:84871839). Algal PS sequences correspond to gene models from *C. reinhardtii* (e_gwH.7.153.1, available at http://www.jgi.doe.gov/) and *C. merolae* (CMH138C; Matsuzaki *et al.*, 2004). The remaining plant PTS sequences were derived from public EST sequences as described in Materials and Methods.

4.2.1 Generation of PTS mutants

To evaluate the functional role of the divergent dimerization insertion in plant pantothenate synthetases, PTS mutants were constructed and their catalytic properties were compared with those of wild-type PTS. In one of the mutants (PTS-Mut1), the entire plant specific insertion occurring between the strictly conserved Pro97 and the βD strand was removed by replacing the amino acids Pro97 through Thr133 with Pro93 through Thr 107 from *E. coli* PTS (Fig. 4.1B). The resulting *A. thaliana* PTS-Mut1 is a hybrid with the region between β3 and βD coming from *E. coli* PTS (Fig. 4.1 B). *A. thaliana* PTS-Mut1 enzyme is shorter than wild-type *A. thaliana* PTS by 22 residues. The second PTS mutant carries a single amino acid change (E132A) within the ^{131}HETWIRVER^{139} motif.

4.2.2 Sequence analysis of PTS expression plasmids

The expression plasmids for *A. thaliana* PTS and PTS mutants were derived from a cDNA for PTS that had been amplified from a cDNA library of *A. thaliana* ecotype Landsberg erecta (Ottenhof *et al*., 2004). DNA sequencing of the expression plasmids revealed a non-silent T → G nucleotide change at position 432 of the PTS coding sequence (CDS) in this cDNA when compared with the annotated CDS of PTS from the ecotype *Columbia* (gi: 30695550), and this polymorphism was confirmed by inspection of the Monsanto *Landsberg erecta* sequence collection (available at http://www.arabidopsis.org/Cereon). The *Columbia* and *Landsberg erecta* alleles of PTS encode Phe (TTT) and Leu (TTG) at amino acid 144, respectively. No further polymorphism was found (Fig. 4.2). Interestingly, the *Landsberg erecta* allele is more similar to PTS sequences from other plants, which encode Leu or Met at this position (Fig. 4.1 A).

```
Col: 1       atggaaccagaagtaatcagagacaaagactctatgagaaaatggtctcgagccatgaga 60
             ||||||||||||||||||||||||||||||||||||||||||||||||||||||||||||
Ler: 3462    atggaaccagaagtaatcagagacaaagactctatgagaaaatggtctcgagccatgaga 3403

Col: 61      tcacaaggcaagaccattggtttagtaccaacaatgggttacctccacgaaggtcactta 120
             ||||||||||||||||||||||||||||||||||||||||||||||||||||||||||||
Ler: 3402    tcacaaggcaagaccattggtttagtaccaacaatgggttacctccacgaaggtcactta 3343

Col: 121     tctctcgttcgtcaatcactagccctcactgacgtcaccgtcgtctcaatctacgtcaat 180
             ||||||||||||||||||||||||||||||||||||||||||||||||||||||||||||
Ler: 3342    tctctcgttcgtcaatcactagccctcactgacgtcaccgtcgtctcaatctacgtcaat 3283

Col: 181     ccaggccaattctctcccactgaagacctctccacatacccatctgatttctccggcgat 240
             ||||||||||||||||||||||||||||||||||||||||||||||||||||||||||||
Ler: 3282    ccaggccaattctctcccactgaagacctctccacatacccatctgatttctccggcgat 3223

Col: 241     ctcactaagctcgcggctctttccggtggtaaagtcgtcgtctttaacccaaaaaacctc 300
             ||||||||||||||||||||||||||||||||||||||||||||||||||||||||||||
Ler: 3222    ctcactaagctcgcggctctttccggtggtaaagtcgtcgtctttaacccaaaaaacctc 3163

Col: 301     tatgattacggcggtgagacgaagaagataaacgacggtggtggtaatggtgggagggta 360
             ||||||||||||||||||||||||||||||||||||||||||||||||||||||||||||
Ler: 3162    tatgattacggcggtgagacgaagaagataaacgacggtggtggtaatggtgggagggta 3103

Col: 361     gtgagttgtgtggaggaaggtgggttagggcatgagacttggattagggttgagagattg 420
             ||||||||||||||||||||||||||||||||||||||||||||||||||||||||||||
Ler: 3102    gtgagttgtgtggaggaaggtgggttagggcatgagacttggattagggttgagagattg 3043

Col: 421     gagaaaggtTTTcgtgggaagagtaggcctgtgttctttagaggtgttgctactattgtt 480
             |||||||||||||||||||||||||||||||||||||||||||||||||||||||||||||
Ler: 3042    gagaaaggtTTGcgtgggaagagtaggcctgtgttctttagaggtgttgctactattgtt 2983

Col: 481     actaagctttttaatattgttgagcctgatgttgctctgtttggtaagaaagattatcaa 540
             ||||||||||||||||||||||||||||||||||||||||||||||||||||||||||||
Ler: 2982    actaagctttttaatattgttgagcctgatgttgctctgtttggtaagaaagattatcaa 2923

Col: 541     caatggaggattatacagagaatggt 566
             |||||||||||||||||||||||||
Ler: 2922    caatggaggattatacagagaatggt 2897
```

Fig. 4.2 Alignment of the annotated CDS of *PTS* (partial) from the ecotype Columbia (gi: 30695550) with genomic sequence from the ecotype Landsberg erecta revealed a non-silent T → G nucleotide change at position 432. This single nucleotide polymorphism is boxed. The Columbia and Landsberg erecta alleles of *PTS* encode Phe and Leu at amino acid 144, respectively. Col, Columbia ecotype; Ler, Landsberg erecta ecotype.

4.2.3 Expression, purification, and properties of *A. thaliana* PTS

A. thaliana PTS was overproduced in *E. coli* as a hexahistidine-tagged protein and purified using Ni^{2+} affinity chromatography. Typical yields of PTS proteins were above 10 mg per litre of culture. The subunit molecular mass of *A. thaliana* PTS determined by SDS-PAGE was ca. 37 kDa (Fig. 4.3) which is consistent with the predicted molecular mass of the His-tagged protein (36.3 kDa). *A. thaliana* PTS eluted from the Superdex 200 gel filtration

column in a single peak, and the corresponding native molecular weight of 71,000 suggests that PTS exists as a homodimer in solution (Fig. 4.4).

In order to test whether the hexahistidine-tag affects enzymatic activity, an aliquot of the PTS enzyme without His-tag was prepared by thrombin digest (Fig. 4.3) and further purified by anion exchange chromatography as described in materials and methods (2.9.6). The specific activity of affinity purified *A. thaliana* PTS was 2.14 ± 0.05 µmol min^{-1} mg^{-1} (n = 3) in the standard assay. The specific activity of PTS lacking the His-tag (2.05 ± 0.02 µmol min^{-1} mg^{-1}, n = 3) was similar to that of His-tagged *A. thaliana* PTS. This indicates that the His-tag does not interfere with the catalytic activity of *A. thaliana* PTS. This is supported by the structure of *M. tuberculosis* PTS, which showed that the N and C termini are away from the active site cavity and unlikely to affect pantothenate synthesis (Wang and Eisenberg, 2003).

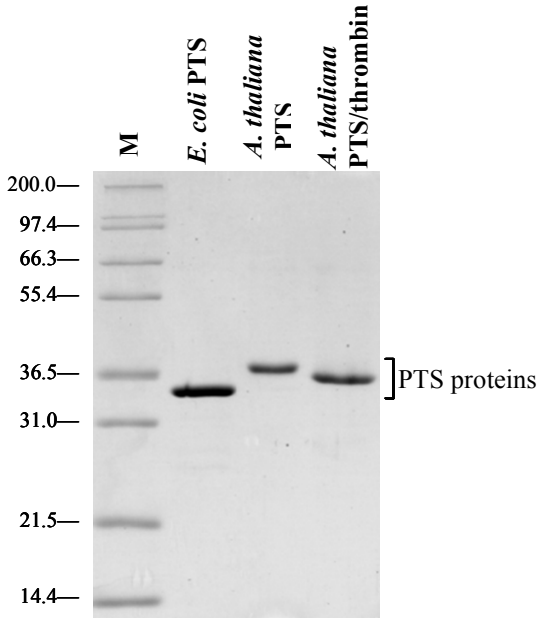

Fig 4.3 Purification of *E. coli* PTS and *A. thaliana* PTS proteins. SDS-PAGE analysis of His-tagged *E. coli* and *A. thaliana* PTS proteins after Ni^{2+} affinity chromatography. PTS/thrombin, PTS after thrombin digest and further purification by anion exchange chromatography. M, molecular weight marker

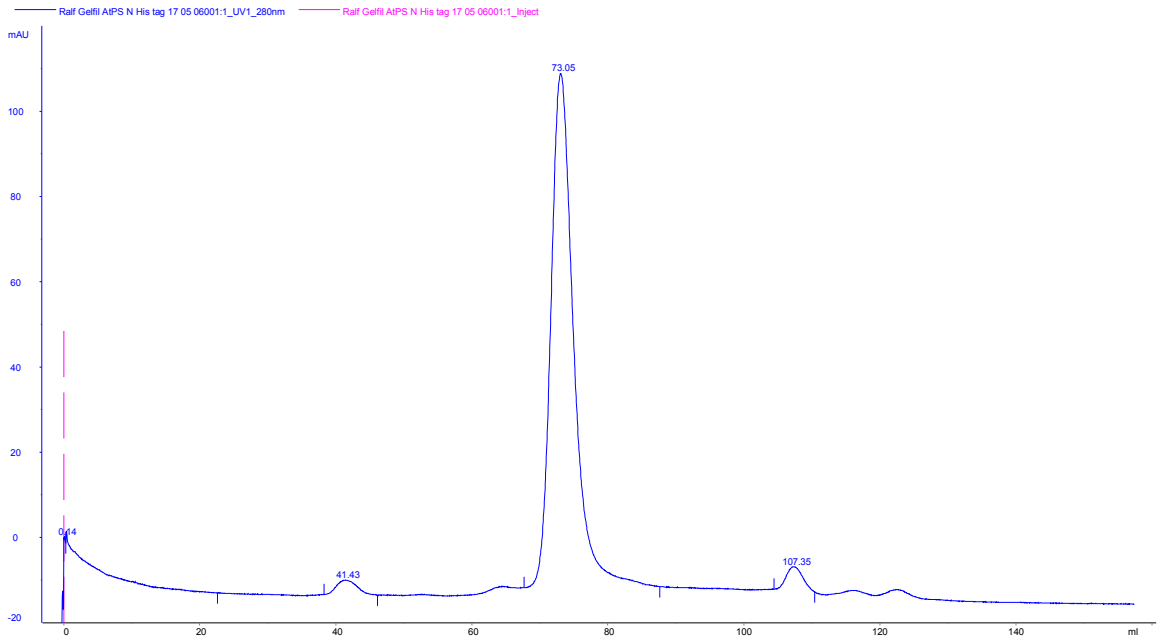

Fig. 4.4 Gel filtration profile of *A. thaliana* PTS His-tag protein. A HiLoad 16/60 Superdex 200 column was equilibrated in 50 mM Tris-HCl (pH 8.0), 100 mM KCl. PTS proteins and standards for calibration were eluted in the same buffer at 0.5 ml/min. *A. thaliana* PTS was eluted in a single peak, and the corresponding native molecular weight of 71,000 suggests that *A. thaliana* PTS exists as a homodimer in solution.

4.2.4 Expression, purification, and properties of *E. coli* PTS

E. coli PTS was also expressed with an N-terminal His-tag and purified following the same strategy as for *A. thaliana* PTS. The subunit and native molecular mass of recombinant *E. coli* PTS as judged by SDS-PAGE and gel filtration (data not shown) was ca. 34 kDa (Fig. 4.3). This is consistent with the predicted subunit size of His-tagged *E. coli* PTS (33.8 kDa) and confirms that the enzyme is a homodimer as was reported previously (von Delft *et al.*, 2001). Interestingly, it was not possible to obtain *E. coli* PTS enzyme in an active form when the enzyme was fused to a C-terminal His tag (data not shown).

4.2.5 Expression and purification of mutagenised PTS

PTS-Mut1 and PTS-E132A were overexpressed with an N-terminal His-tag and purified by affinity chromatography, respectively (Fig. 4.5). The subunit molecular masses were in good agreement with their predicted sizes (34-36 kDa by SDS-PAGE). The native molecular weights of these enzymes were estimated by gel filtration and lay between 68,000 and 73,000, indicating that the enzymes were dimers in solution. This result also shows that the mutation in the dimerization region of *A. thaliana* PTS did not affect the dimeric subunit structure.

Initial velocities were obtained at varying pantoate or β-alanine concentrations as described for *A. thaliana* PTS.

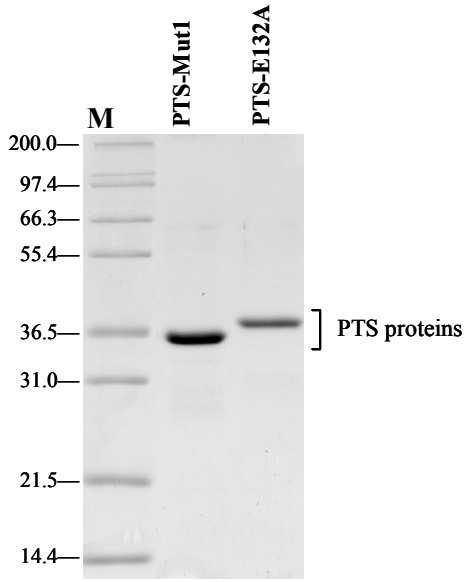

Fig. **4.5** Purification of mutagenised PTS proteins: PTS-Mut1 and PTS-E132A. SDS-PAGE analysis of His-tagged mutated proteins after Ni^{2}+ affinity chromatography. M, molecular weight marker.

Affinity purified, His-tagged PTS proteins were used in all enzyme assays reported below. When the enzyme was stored at 4°C or -70°C, no loss of activity was observed over a period of one week or six months, respectively

4.2.6 Stability of the enzymes

The stability of the enzymes was analysed using the isotopic assay (forward direction). The activity of bacterial and plant PTS proteins in forward direction was determined at 0 and 24 hours after incubation with the assay mixture at 25°C in Tris-HCl (pH 8.0) buffer. The assay was initiated with pantoate and the reaction was followed by analysing the conversion of [^{14}C]-β-alanine into pantothenate as described in materials and methods (2.11.6). The survival of enzyme activity after 24 hours is indicative of protein stability. Incubation of up to 24 hours at 25°C had little effect on the activity of the *E. coli* PTS as only 4.5% loss of activity was observed. *A. thaliana* PTS enzyme was less stable and 30% loss of activity was observed (0.83 µmol/min/mg at t = 0 and 0.58 µmol/min/mg after 24 hours) (Fig. 4.6).

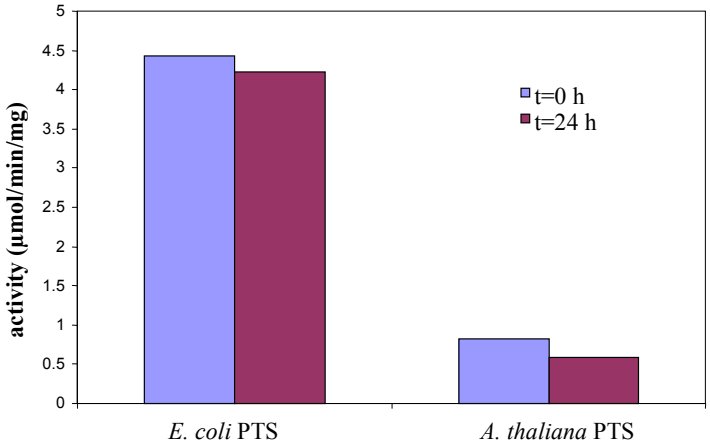

Fig. 4.6 Stability of *E. coli* and *A. thaliana* PTS at 25°C. Activities of *E. coli* and *A. thaliana* PTS were determined immediately after assembling the assay (t = 0) or after 24 hours preincubation time at 25°C (t = 24 h). Standard reactions contained: 100 mM Tris-HCl (pH 8.0) 10 mM $(NH_4)_2SO_4$; 10 mM $MgSO_4$; 10 mM ATP; 0,32 mM β-alanine; 0,18 mM [^{14}C]-β-alanine; 0,05 µg/µl *E. coli* PTS or 0.1 µg/µl *A. thaliana* PTS. Reactions were initiated by addition of 0.5 mM pantoate and the fraction of ^{14}C-labeled pantothenate formed was measured at 0.5, 1, 2, 3, 4, 5, and 6 min.

4.3 Radioisotope assays

4.3.1 Sensitivity and linearity of ^{14}C-label detection system

Two isotopic assays were used in this work. In the forward direction, the activity of PTS proteins was assayed by monitoring the synthesis [^{14}C]-pantothenate from [^{14}C]-β-alanine and pantoate. The reverse exchange assay is based on monitoring the exchange between pantothenate and [^{14}C]-β-alanine in the presence of the PTS enzyme. The products of isotopic assays were separated using thin layer chromatography (TLC) plates, and exposed on Phosphor Screen for radioactivity detection. The amounts of ^{14}C label associated with β-alanine and pantothenate were quantified using a Storm 860 PhosphorImager. To test the linear response of this system for ^{14}C label, a dilution series of [3-^{14}C]-β-alanine was spotted on TLC plates and exposed on Phosphor Screen for 3 hours or 18 hours. Two exposure times were tested to determine whether the Phosphor Screen reaches saturation after longer exposure time, affecting the quantification. The amount of detected label was corrected for the background. In Fig. 4.7 detected signals (arbitrary unit) correspond to the amounts of ^{14}C label (nCi) analysed on the Phosphor Screen. Judging from the R^2 value (in both cases $R^2 > 0.999$), the detection was linear between 0.083 and 16.6 nCi. Because from each radioactive assay a 16.6 nCi aliquot was analysed on TLC plates (per time point), the established linear range correspond to between 0.5% and 100% of radioactivity analysed (Fig. 4.7). Exposure time turned out to have no influence for quantification of the amount of ^{14}C-lable analysed.

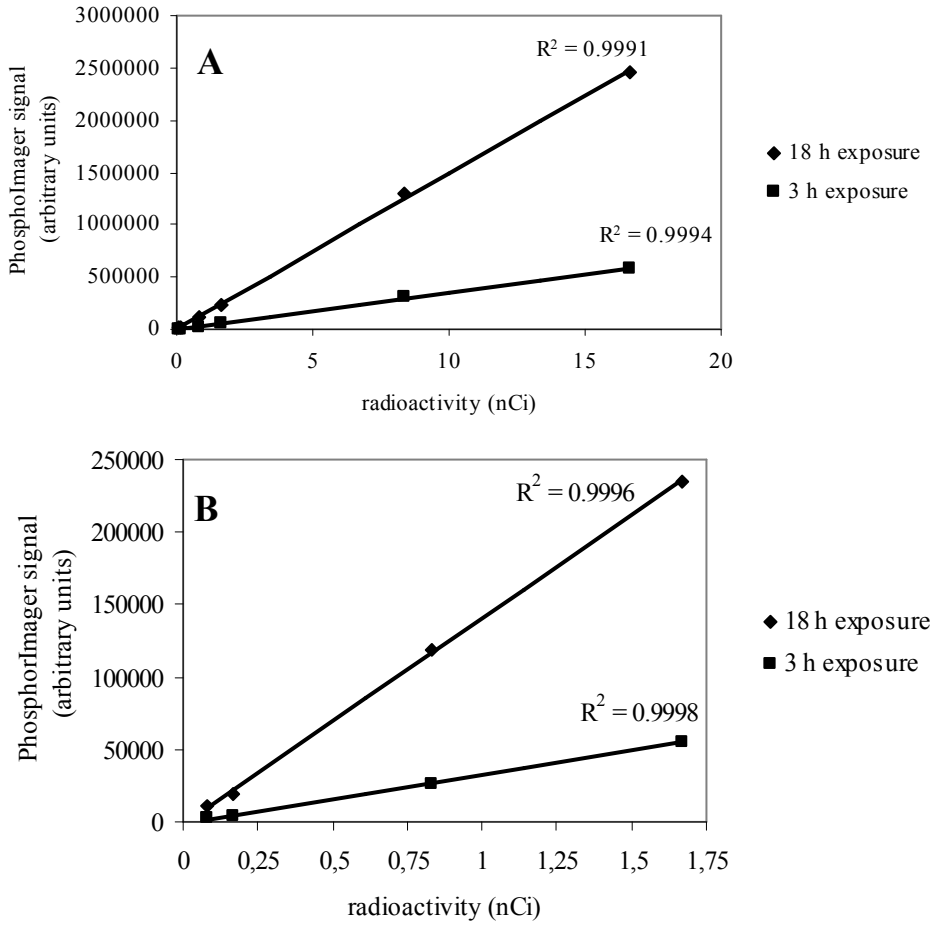

Fig 4.7 ^{14}C label detection by PhosphorImager. Exposure for 3 hours and 18 hours were tested. PhosphorImager signal is the response of Phosphor Screen for ^{14}C label determined on Storm 860 PhosphorImager. Dilution series of [3-^{14}C]-β-alanine contained: 16.6, 8.33, 1.66, 0.83, 0.16, 0.08 nCi (see text for details). B is directly derived from A where only four data points (corresponding to the lowest ^{14}C label amounts analysed) are included.

4.3.2 The effect of pH on *A. thaliana* and *E. coli* PTS activity

Based on the conservation of catalytic residues, (section 4.2) *A. thaliana* PTS is expected to catalyze the formation of pantothenate by the same reaction mechanism that was previously established for bacterial PTS (Scheme 4.1). In order to obtain experimental evidence supporting this prediction, *A. thaliana* PTS and *E. coli* PTS were compared with respect to the pH dependence of two reactions, the formation of pantothenate and the isotope exchange between pantothenate and β-alanine.

The activity of *A. thaliana* PTS and *E. coli* PTS in the forward direction was assayed at pH 5.5-11.0 by monitoring the incorporation of [^{14}C]-β-alanine into pantothenate (Fig. 4.8 A). Assays were carried out as described in materials and methods, using 100 mM MES, Tris-HCl, AMP or CAPS buffers.

Optimal activity of *A. thaliana* PTS and *E. coli* PTS occurred in Tris-HCl at pH 9.0 and in CAPS buffer at pH 10, respectively, which is in agreement with the previously reported optimum for *E. coli* PTS (pH 10, Miyatake *et al*, 1979). Generally, the activity of both enzymes was high at alkaline pH and low at neutral or acidic pH. At optimum pH, *A. thaliana* PTS and *E. coli* PTS had turnover rates of 0.5 s^{-1} and 2.0 s^{-1} in this assay, respectively. More importantly, the enzymes had little or no activity at neutral or acidic pH, and the largest change of activity occurred between pH 7.5 and 8.0 whereas activity at pH 9.0 was only slightly higher than at pH 8.0 (Fig. 4.8 B). Based on this result, the standard assay for PTS was carried out at pH 8.0, allowing for efficient operation of the coupling enzymes and nearly optimal activity of PTS enzymes.

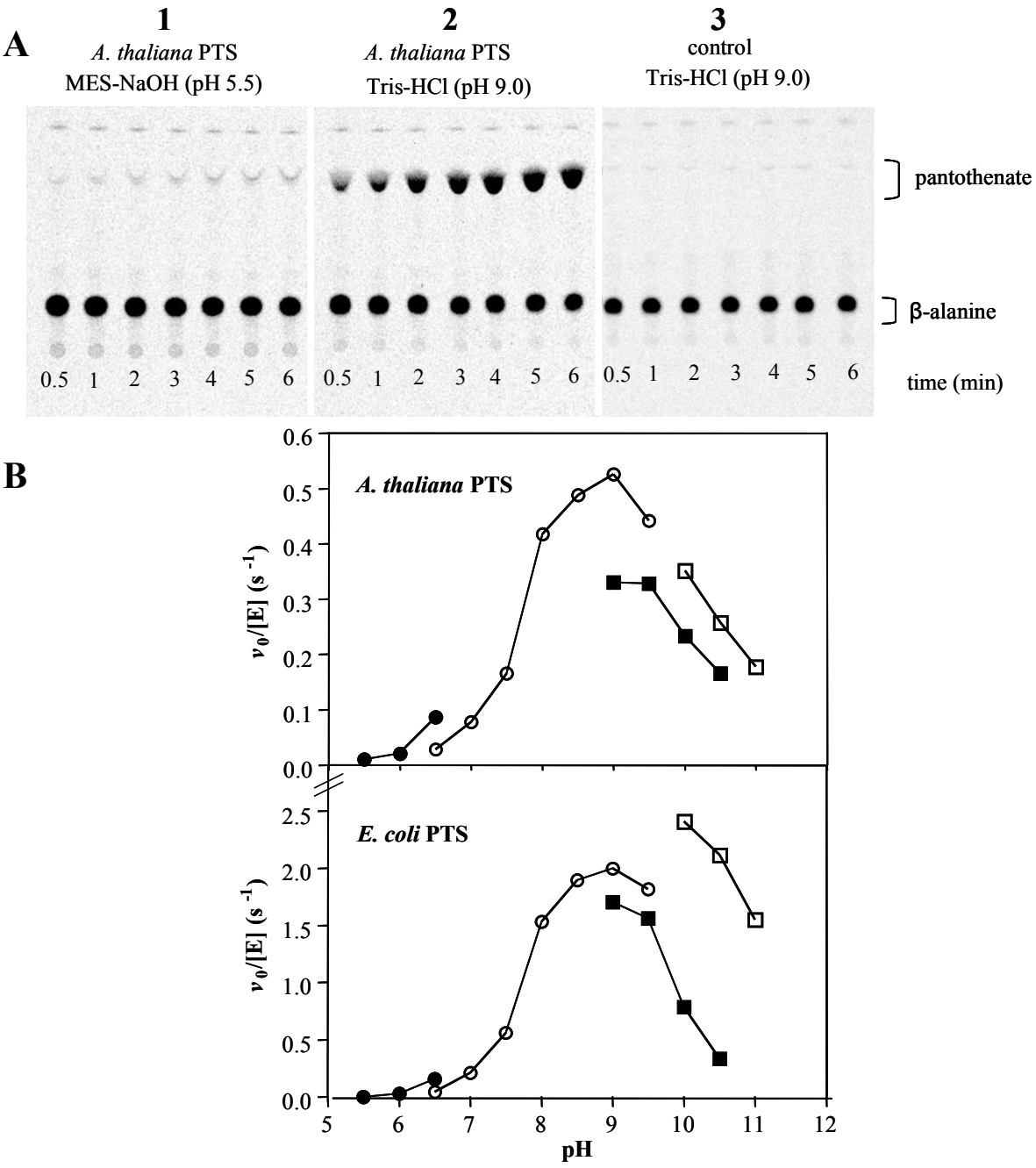

Fig. 4.8 A The pH dependency of *A. thaliana* PTS enzyme. An example of TLC-separation of the ^{14}C- labelled β-alanine and pantothenate, the product of the forward PTS reaction in MES-NaOH (pH 5.5) and Tris-HCl (pH 9.0) buffer. A control reaction was carried out in Tris-HCl buffer (pH 9.0) and was like the others but without enzyme. The data from panels 1 and 2 were used to calculate one data point (initial velocity v_0) each in Fig. 4.8 B. Indicated time points: 0.5, 1, 2, 3, 4, 5, and 6 min after initiation of the reaction. For details see materials and methods.

B The effect of pH on *A. thaliana* PTS and *E.* coli PTS. PTS proteins were assayed in the forward direction by monitoring the incorporation of [^{14}C]β-alanine into pantothenate. The substrates ATP, pantoate, and β-alanine were present at concentrations of 10 mM, 0.5 mM, and 0.5 mM, respectively. MES-NaOH (●), Tris-HCl (○), AMP-HCl (■), or CAPS-NaOH (□) buffers were present at a concentration of 100 mM, and the final pH of each assay mixture was verified. Each data point (initial velocity v_0) was derived as described above.

4.3.3 pH optima of the reverse exchange reaction catalysed by *A. thaliana* and *E. coli* PTS

The second reaction used to probe the reaction mechanism of *A. thaliana* PTS was the isotope exchange between pantothenate and β-alanine. In agreement with the kinetic mechanism in Scheme 4.1, *A. thaliana* and *E. coli* PTS catalysed the isotope exchange between [3-^{14}C]β-alanine and pantothenate in the presence of AMP. Both PTS enzymes catalyzed the exchange between [3-^{14}C]β-alanine and pantothenate in the presence of AMP with a pH optimum of 5.5. Again, the pH profile was very similar in both enzymes (Fig. 4.9 A and 4.9 B). At the pH optimum, similar isotope exchange rates (5 to 6 × 10^{-2} min^{-1}) were observed for *A. thaliana* and *E. coli* PTS, respectively. A tenfold lower exchange rate was reported for *M. tuberculosis* PTS (Zheng and Blanchard, 2001), presumably owing to the sub-optimal pH of 7.8 employed in that study.

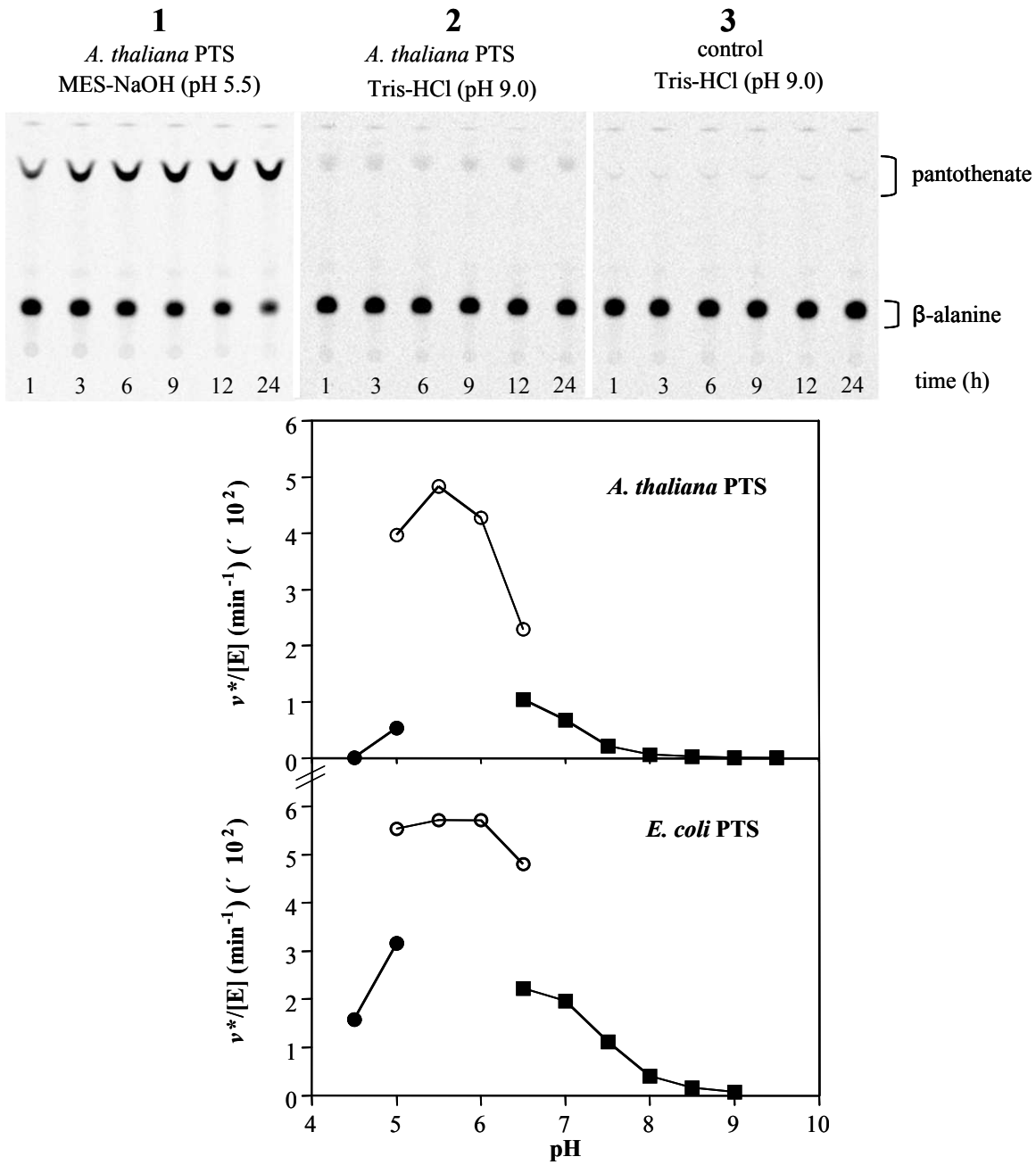

Fig. 4.9 A, The effect of pH on the isotope exchange between [^{14}C]β-alanine and pantothenate catalysed by *A. thaliana* PTS. An example of TLC-separation of β-alanine and pantothenate. Reverse PTS reaction was carried in MES-NaOH (pH 5.5) and Tris-HCl (pH 9.0) buffer. Control reaction was carried out in Tris-HCl buffer (pH 9.0) and was like the others but without enzyme. The data from panels 1 and 2 were used to calculate one data point (initial velocity v_0) each in Fig. 4.9 B. Indicated time points: 1, 3, 6, 9, 12, and 24 hours. For details, see materials and methods.

B, The effect of pH on the isotope exchange between [^{14}C]β-alanine and pantothenate catalysed by *A. thaliana* and *E. coli* PTS enzymes. The isotope exchange was assayed in the presence of 0.5 mM β-alanine, 10 mM pantothenate, and 10 mM AMP. Sodium acetate (●), MES-NaOH (○), or Tris-HCl (■) buffers were present at a concentration of 100 mM and the final pH of each assay mixture was verified. Each data point (initial velocity v_0) was derived as described above.

4.3.4 Comparison between reaction mechanism of *A. thaliana* and *E. coli* PTS

Scheme 4.1 predicts that the exchange reaction proceeds via the pantoyl adenylate intermediate and that binding of pantothenate occurs only in presence of AMP, as was previously demonstrated for PTS from *M. tuberculosis* (Zheng and Blanchard, 2001). Thus, the molecular exchange between β-alanine and pantothenate should have an absolute requirement for AMP. When AMP was removed from the exchange reaction or replaced with an equimolar amount of cAMP, the exchange rates of both *A. thaliana* PTS and *E. coli* PTS were reduced by approximately 50-fold or 20-fold, respectively (Fig. 4.10). Thus, hydrolysis and re-synthesis of the amide bond in pantothenate depend on AMP. When cAMP was used as a non-reactive analogue of AMP, the inability of cAMP to promote the pantothenate:β-alanine exchange supports the direct involvement of AMP in the catalytic process. As both AMP and cAMP are sodium salts, control reactions contained sodium to ensure equal ionic strength in all assays (Fig. 4.10).

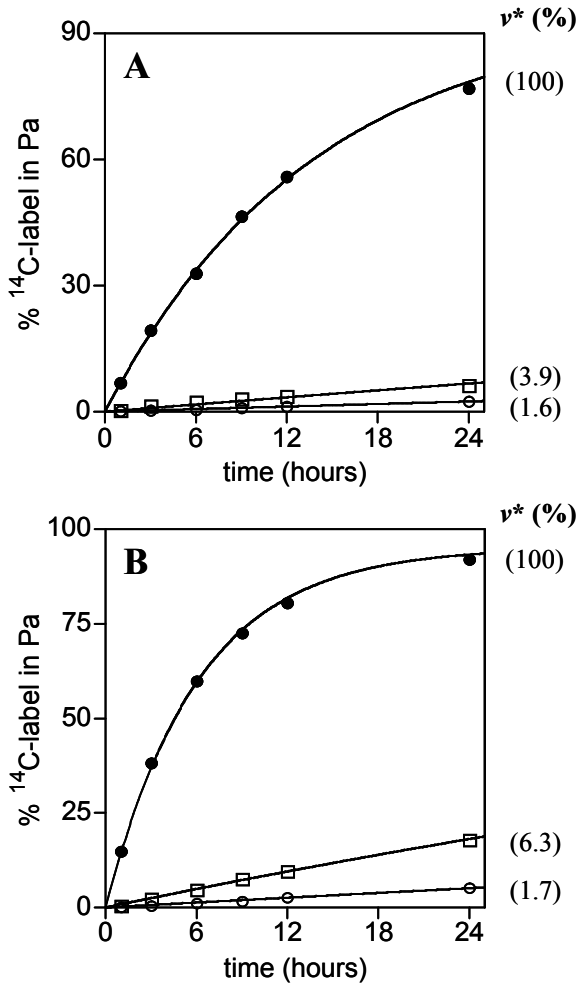

Fig. 4.10 Dependence of the pantothenate:β-alanine exchange on AMP. *A. thaliana* PTS (**A**) and *E. coli* PTS (**B**) were assayed for the exchange between [^{14}C]β-alanine and pantothenate in the presence of 0.5 mM β-alanine and 10 mM pantothenate at pH 5.5. Additionally, individual reactions contained 10 mM Na-AMP (●), 10 mM Na-cAMP (□), or 10 mM NaCl (○). For each reaction, the transfer of ^{14}C-label from β-alanine to pantothenate that

occurred over 24 hours was fitted to the exponential form of Eq. 7. The fraction of exchange activity remaining after removal of AMP is given in percent. The reactions catalyzed by *A. thaliana* and *E. coli* PTS in the presence of 10 mM AMP correspond to exchange rates of 3.6×10^{-2} min^{-1} and 6.8×10^{-2} min^{-1}, respectively. v^*, initial exchange rate.

To detect possible deviations from Scheme 4.1 or differences between the kinetic mechanisms of *A. thaliana* and *E. coli* PTS, the molecular exchange between [^{14}C]-β-alanine and pantothenate was also characterized in the presence of varying amounts of ATP or pantoate. Based on scheme 4.1, ATP should compete with AMP for binding to the free enzyme and pantoate should bind only to the enzyme-ATP complex. Therefore, the pantoate:β-alanine exchange should be inhibited by ATP and unperturbed by pantoate. However, increasing concentrations of pantoate inhibited the exchange reaction (Fig. 4.11)

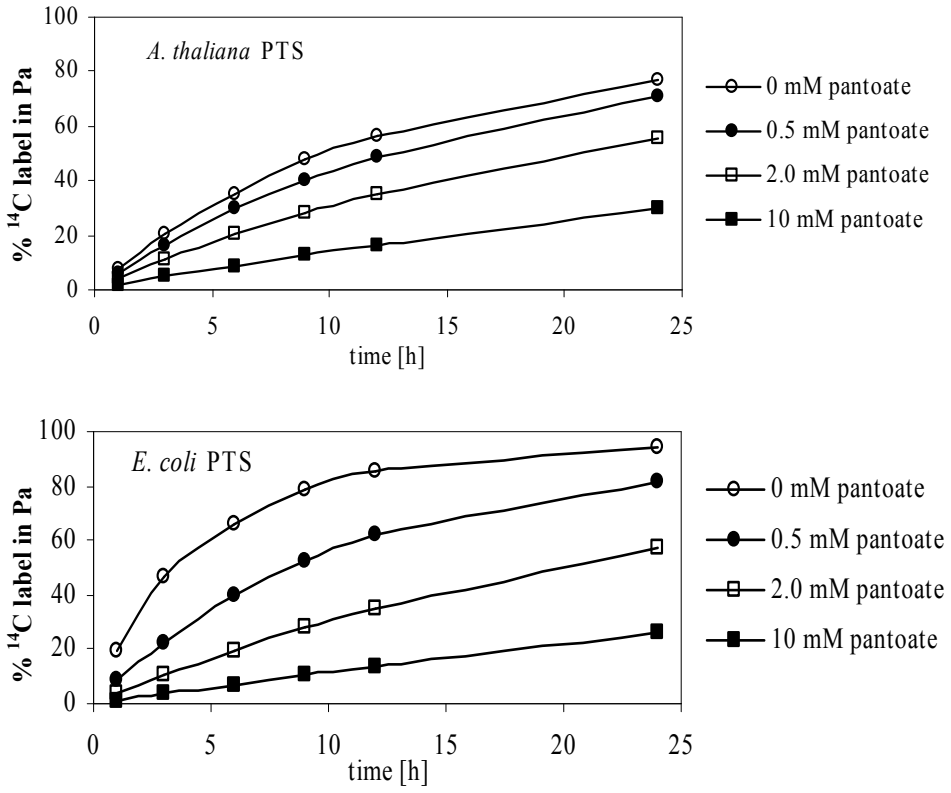

Fig. 4.11 Inhibition of the pantothenate:β-alanine exchange reaction by pantoate. The reaction contained 0.55 µg/µl *A. thaliana* or *E. coli* PTS, 10 mM PA, 0.5 mM β-alanine, 100 mM MES (pH 5.5), and 10 mM AMP.

The observed inhibition caused by pantoate is unexpected for *E. coli* PTS because of the ordered kinetic mechanism. Moreover, these data show that pantoate can bind in the absence of ATP. Binding of pantoate alone in the active site was previously demonstrated for PTS from *M. tuberculosis*, and this might be the basis for the inhibitory effect of pantoate on the exchange reaction catalyzed by *A. thaliana* and *E. coli* PTS enzymes.

No conclusion was reached with respect to the effect of ATP on the pantothenate:β-alanine exchange because, when MgATP was added to the standard reaction, the appearance of ^{14}C-labeled pantothenate with time did not conform to Eq. 7 (not shown). The most likely explanation is that, in presence of MgATP, the overall forward and reverse exchange reactions occurred simultaneously due to contamination of pantothenate with pantoate. Using the coupled and isotopic assays for PTS in the forward direction, it was found that the commercial pantothenate preparation used in this study contained just below 1 mol% pantoate, *i.e.* the standard reverse exchange reaction contained approximately 0.1 mM pantoate. Similar results were obtained with other commercially available pantothenate preparations.

4.3.5 Reverse reaction of PTS

The pantoyl adenylate intermediate of the reaction catalysed by PTS can enter two separate reactions with either PP_i to form pantoate and ATP or with β-alanine to form pantothenate and AMP (Scheme 4.1). According to scheme 4.1, PP_i should compete with β-alanine for pantoyl-adenylate (first half reaction). *E. coli* PTS was reported to efficiently catalyze the pyrophosphorolysis of pantoyl adenylate analogues (Wieland, 1963), and the *γ-O*-methyl-analogue of pantoyl adenylate was turned over at a rate of 10 min^{-1} (estimated from data reported by Wieland, 1963). Likewise, *M. tuberculosis* PTS catalyzed the pantoate-dependent positional isotope exchange between ATP and PP_i at rates of up to 5 min^{-1} (Williams *et al*., 2003). Therefore, under conditions that allow the formation of the pantoyl adenylate intermediate from AMP and pantothenate, the addition of PP_i would be expected to enable net hydrolysis of pantothenate. Indeed, in the presence of 10 mM [^{14}C]-pantothenate, 10 mM AMP, and 2 mM PP_i and at pH 5.5, both enzymes formed small amounts of [^{14}C]-β-alanine (Fig. 4.12). Alternatively, when the assay was carried out as described above but at 100 mM Tris-HCl (pH 7.5), negligible amounts of labelled β-alanine were formed (data not shown).

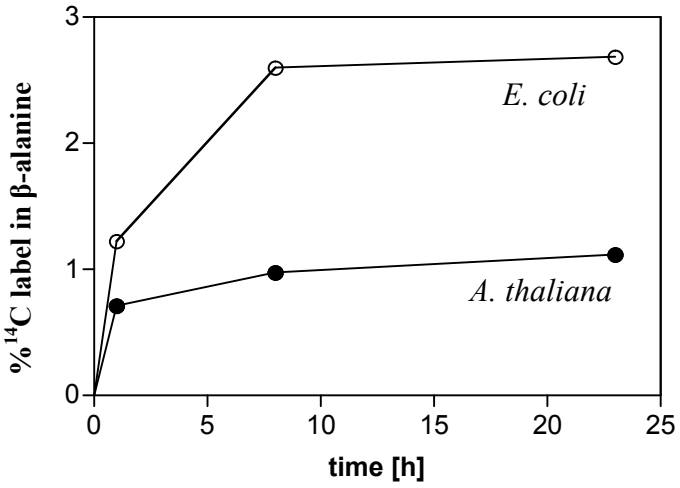

Fig. 4.12 PTS activity in the reverse direction was assayed by incubating *A. thaliana* PTS (15 µM) or *E. coli* PTS (16 µM) with 100 mM MES-NaOH (pH 5.5); 10 mM pantothenate, 0.17 mM [3-^{14}C]pantothenate (55 mCi/mmol, 10 mM NaAMP, 2 mM Na_4PP_i, 10 mM $MgSO_4$, and 10 mM KCl. The percentage ^{14}C-label associated with β-alanine was corrected for non-enzymatic activity.

In summary, the behaviour of *A. thaliana* and *E. coli* PTS supports the view that these enzymes share an identical two-step reaction mechanism with pantoyl adenylate as the key reaction intermediate as shown in Scheme 4.1. This view is supported by the conserved pH optima of the overall PTS reaction and the isotope exchange, respectively. Furthermore, based on the PTS sequence alignment (section 4.2) bacterial and eukaryotic active site residues are conserved suggesting the reaction mechanism is conserved within the pantothenate synthetase protein family.

4.4 Allosteric properties of *A. thaliana* PTS

Allostery is explained by the coupling of conformational changes between two widely separated binding sites. Allosteric proteins have identical (homotropic) or different (heterotropic) ligands. One term tightly linked to allostery is "cooperativity". This describes the interactions of binding processes of ligands to proteins with multiple binding sites (Ricard and Cornish-Bowden, 1987). The binding of one ligand increases (positive cooperativity) or decreases (negative cooperativity) the affinity of the protein toward the second ligand. Two binding sites may be on the same polypeptide chain (though in different domains), or in different subunits. It has been shown that allostery plays a role in controlling metabolism either through positive feedback regulation or inhibition (Koshland and Hamadani, 2002). After the importance of conformational changes was recognized, two different theories (models) of the cooperative mechanism were postulated. In 1965 Monod *et al*. proposed a

"plausible model on the nature of allosteric transition" (the "concerted" or "MWC" model). The MWC model suggested that allosteric proteins are symmetric oligomers with identical protomers. Each protomer exists in at least two conformational states (tense, T; relaxed, R) with different affinities for ligands (Monod *et al*., 1965). The basic assumption of the model is that the protein interconverts between two conformations, R and T, in a concerted manner. Subunits in the oligomers cannot exist in a hybrid form such as TR. Koshland *et al*. (1966) challenged the MWC model and proposed their sequential hypothesis (the "KNF" or "sequential" model). In the sequential model, subunits change conformation, one at a time. Thus, a hybrid form such as TR can exist in the sequential model. Here the binding of a ligand will change conformation of a protomer without affecting the neighbouring subunits. Both theories fit positively cooperative enzymes, however only the KNF theory fit negatively cooperative enzymes (Koshland and Hamadani, 2002). In most allosteric proteins, homotropic effects seem to be best accounted for by the MWC model while heterotropic effects are better described by the KNF model (Stryer, 1988). Eigen (1967) combined the MWC and KNF extreme models leading to a general model. However, decades of research have lead to the conclusion that the exact mechanisms by which allostery is achieved may span a broad range, and can be extremely different from each other (Gunasekaran *et al*., 2004).

The majority of allosteric proteins are presumably metabolic enzymes which act as control devices for flux alterations in metabolic pathways (Helmstaedt *et al*., 2001). Enzymes are regulated predominantly by heterotropic effectors modulating the catalytic turnover rates in a positive and/or negative fashion. Positive effectors often abolish cooperativity, resulting in Michaelis-Menten-like kinetics in substrate saturation assays, whereas negative acting ligands decrease catalytic efficiency either by decreasing the substrate affinity or by altering the intrinsic k_{cat} values (Segel, 1993).

4.4.1 Initial rate kinetic analysis of *A. thaliana* PTS

Initial velocities of PTS were obtained using the coupled enzyme assay. Pantoate was varied between 0.01 – 20.0 mM at fixed ATP concentrations ranging from 1 – 10 mM and at either 0.5 mM or 5.0 mM β-alanine, respectively. Similarly, β-alanine was varied between 0.02 – 10.0 mM at fixed pantoate concentrations ranging from 0.1 mM to 50 mM, and at either 2 mM or 10 mM ATP. No background activity was observed when one of the three substrates was absent. Given that ATP is a substrate of both pantothenate synthetase and myokinase, one of the coupling enzymes, the assay was confirmed to be linear with the amount of PTS at 1 mM and 10 mM ATP, respectively. The addition of up to 100 mM KCl or

5 mM pantoyl lactone to the standard assay had no effect on activity, suggesting that changes in PTS-activity caused by varying concentrations of potassium D-pantoate are not due to the concomitant variation in the concentration of K^+ or residual amounts of pantoyl lactone.

The bacterial PTS was found to obey hyperbolic kinetics for all substrates (Miyatake, 1979; Zheng and Blanchard, 2001) as is expected in a Bi Uni Uni Bi Ping Pong kinetic mechanism. The *E. coli* PTS enzyme strictly obeys Michaelis-Menten behaviour towards each of its substrates, *i.e.* ATP, pantoate, and β-alanine. However, initial rate kinetic analysis revealed that *A. thaliana* PTS deviates from Michaelis-Menten kinetics.

In the absence of a rate equation that can globally explain allosteric effects in a terreactant enzyme such as *A. thaliana* PTS, each substrate-velocity curve was analyzed separately. Individual sets of rate data were fitted to the Michaelis-Menten equation, the Hill equation, an equation for substrate inhibition resulting from dead-end complexes, and generalized rate equation in the form of a 2:2 rational function (Equations 1-4). The rate law most likely to explain the rate data was selected for each substrate-velocity curve (F test, $\alpha = 0.05$), enabling the detection of different types of kinetic behaviour and the estimation of apparent kinetic parameters (Table 4.4). For details, see Materials and Methods (2.12).

The most obvious non-Michaelis-Menten behaviour was inhibition at elevated levels of the substrate pantoate, *i.e.* the rate of PTS passed through a maximum (v_{opt}) as pantoate was increased (Fig. 4.13). The true maximum rate, which is attained at the optimal pantoate concentration, correlated positively with the levels of both cosubstrates ATP and β-alanine, and reached 1.5 s^{-1} when the latter were present at 10 mM and 5 mM, respectively (Table 4.2).

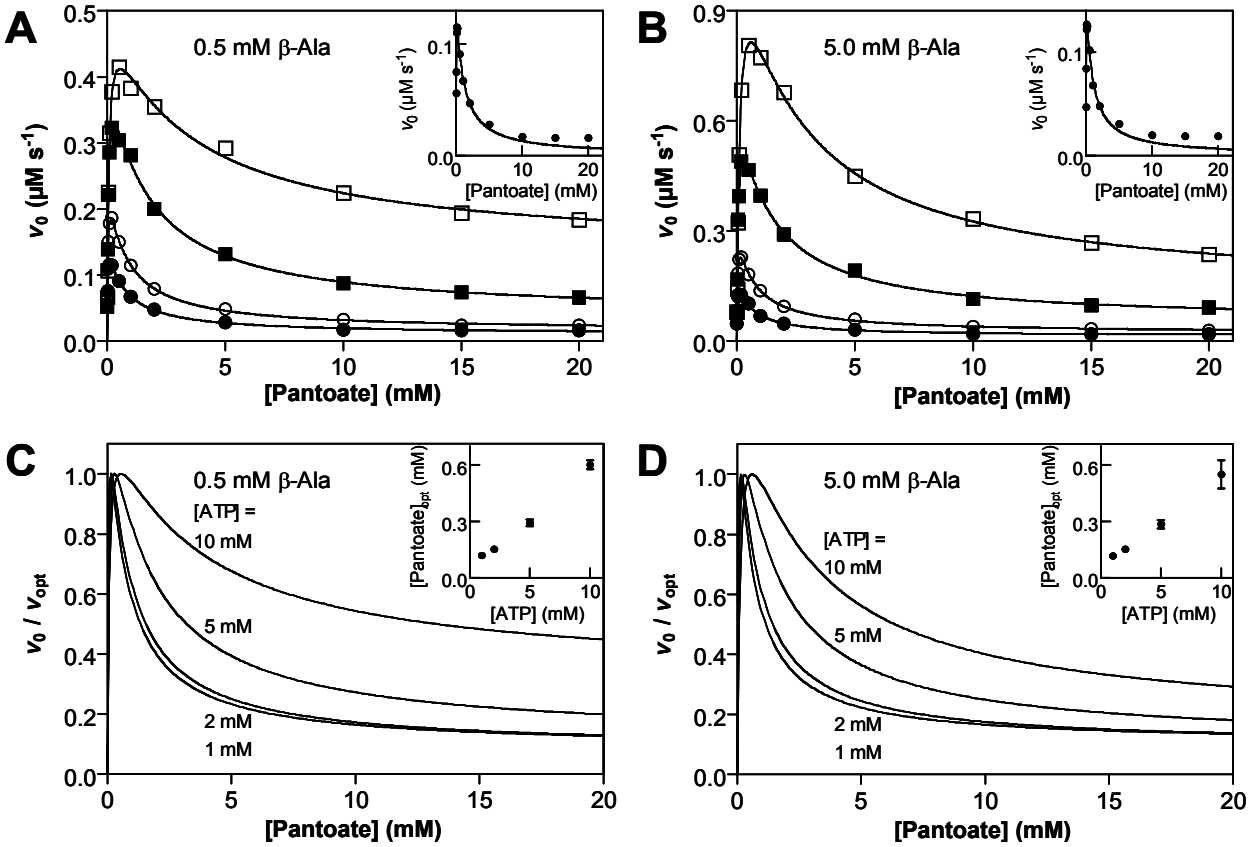

Fig. 4.13 Initial rate plots for *A. thaliana* PTS. Initial rates of PTS were obtained by using the coupled enzyme assay with pantoate as the variable substrate (0.01 mM - 10 mM) in the presence of 0.5 mM β-alanine (***A***) or 5.0 mM β-alanine (***B***). ATP was present in the assay at fixed concentrations of 1 mM (●), 2 mM (○), 5 mM (■), and 10 mM (□). Individual sets of rate data were fitted to the preferred rate law (Equation 4), yielding values for α_1, α_2, β_1, and β_2, which were used to calculate $[pantoate]_{opt}$ and v_{opt} for each curve. Initial rates normalized to v_{opt} were fitted to Eq. 4 and the resulting curves are shown with data points omitted for clarity (***C, D***). The insets show initial rate data fitted to Eq. 3 (*A, B*) and the variation of $[pantoate]_{opt}$ with the concentration of ATP (*C, D*). See Table 4.4 for apparent kinetic constants derived from the curve fits in *A* and *B*.

The apparent type of substrate inhibition was diagnosed using plots of initial rate normalized to the true maximal rate that occurs at $[pantoate]_{opt}$ (Fig. 4.13C and 4.13D) (MacRae and Segel 1991). These plots show that substrate inhibition is competitive with respect to ATP. At inhibitory concentrations of pantoate, the relative activity (v_0/v_{opt}) of *A. thaliana* PTS increases as [ATP] is increased, and $[pantoate]_{opt}$ increases continuously with [ATP] (insets in Figs. 4.13 C and 4.13 D). In contrast, $[pantoate]_{opt}$ is not significantly different at 0.5 mM or 5.0 mM β-alanine, respectively (Table 4.2), which implies noncompetitive substrate inhibition with respect to β-alanine. In this case, β-alanine should have no effect on v_0/v_{opt}. As indicated by the pantoate concentrations that cause 50% inhibition relative to optimal activity and the degree of inhibition reached at saturating pantoate (Table 4.2), this may be true at fixed ATP levels of 1 mM – 5 mM. However, at 10 mM ATP, substrate inhibition relative to v_{opt} is clearly stronger at 5 mM β-alanine than at 0.5 mM β-alanine, which implies uncompetitive substrate inhibition with respect to β-alanine.

The inhibitory effect of pantoate on *A. thaliana* PTS is summarized in Table 4.2. At low [ATP], *i.e.* when substrate inhibition is particularly strong, pantoate becomes inhibitory above 0.1 mM and causes *ca.* twofold and tenfold inhibition relative to the maximal rate at 1 mM and saturating levels, respectively. The rate of *A. thaliana* PTS at the optimal pantoate concentration increases as [ATP] or [β-alanine] are increased, suggesting that the processes involving ATP and β-alanine are both partially rate limiting under this condition.

fixed cosubstrates	$[pantoate]_{opt}$ [a]	k_{opt} [b]	$[pantoate]_{i50}$ [c]	k_{opt}/k_{cat} [d]
	μM	s^{-1}	*mM*	
0.5 mM β-Alanine				
1 mM ATP	118 ± 4	0.21 ± 0.01	1.3	12 ± 2
2 mM ATP	152 ± 6	0.33 ± 0.01	1.5	12 ± 3
5 mM ATP	285 ± 22	0.59 ± 0.03	3.2	9 ± 3
10 mM ATP	550 ± 73	0.75 ± 0.03	13.3	3 ± 1
5.0 mM β-Alanine				
1 mM ATP	119 ± 6	0.24 ± 0.01	1.1	10 ± 2
2 mM ATP	153 ± 4	0.41 ± 0.01	1.4	11 ± 2
5 mM ATP	293 ± 18	0.89 ± 0.04	2.9	10 ± 3
10 mM ATP	601 ± 23	1.48 ± 0.03	6.4	6 ± 1

Table 4.2 Substrate inhibition of *A. thaliana* PTS by pantoate.
Initial rate data were obtained using pantoate as the varied substrate and fitted to Eq. 4 (Fig. 4.13). The best fit parameters of individual sets of rate data were used to calculate apparent constants.
[a]the pantoate concentration leading to optimal activity (Eq. 5).
[b]$k_{opt} = v_{opt}/[E]$, where [E] is the total concentration of *A. thaliana* PTS subunits.
[c]the pantoate concentration leading to 50% inhibition relative to optimal activity (Eq. 6).
[d]$k_{cat} = V_{lim}/[E]$, where [E] is the total concentration of *A. thaliana* PTS subunits.
The ratio k_{opt}/k_{cat} represents the fold-inhibition relative to optimal activity achieved by saturating pantoate concentrations.

Two diagnostic features show that substrate inhibition by pantoate is competitive with respect to the substrate ATP (MacRae and Segel, 1999). First the pantoate concentration leading to v_{opt} increased continuously with increasing ATP levels but was unaffected by β-alanine levels. Second, normalizing the initial rates of each substrate velocity-curve to the appropriate value of v_{opt} revealed that the relative activity of *A. thaliana* PTS at inhibitory concentrations of pantoate correlated positively with the ATP concentration. Thus, substrate inhibition by pantoate was the most pronounced at low ATP levels (1 - 2 mM), where saturating pantoate lead to turnover numbers as low as 0.02 s^{-1} and caused 90% inhibition relative to optimal activity. However, substrate inhibition by pantoate is unlikely to function in the regulation of *A. thaliana* PTS activity *in vivo*. Non-inhibitory pantoate concentrations in the micromolar range led to half-optimal rates of *A. thaliana* PTS. 10- and 100-fold higher pantoate levels were required for optimal rates and for inhibition back to half-optimal rates, respectively (Table 4.2). Therefore, even if cellular pantoate levels were high enough to cause

substrate inhibition, a 10-fold change in pantoate concentration would cause at most a 2-fold change in *A. thaliana* PTS activity.

The type of kinetic response of *A. thaliana* PTS to β-alanine (Michaelis-Menten kinetics or negative cooperativity) depended on the fixed cosubstrates, *i.e.* on the levels of ATP and pantoate in the assay (Fig. 4.14). Generally, *A. thaliana* PTS followed Michaelis-Menten kinetics with respect to β-alanine when pantoate was present in excess over ATP. As is evident from the Hill plots in Fig. 4.14, 5 mM pantoate induced strong negative cooperativity for β-alanine in the presence of 2 mM ATP (h = 0.34) but not in the presence of 10 mM ATP (h = 1.04). However, in the latter case negative cooperativity for β-alanine became apparent when pantoate was raised to 50 mM (h = 0.68).

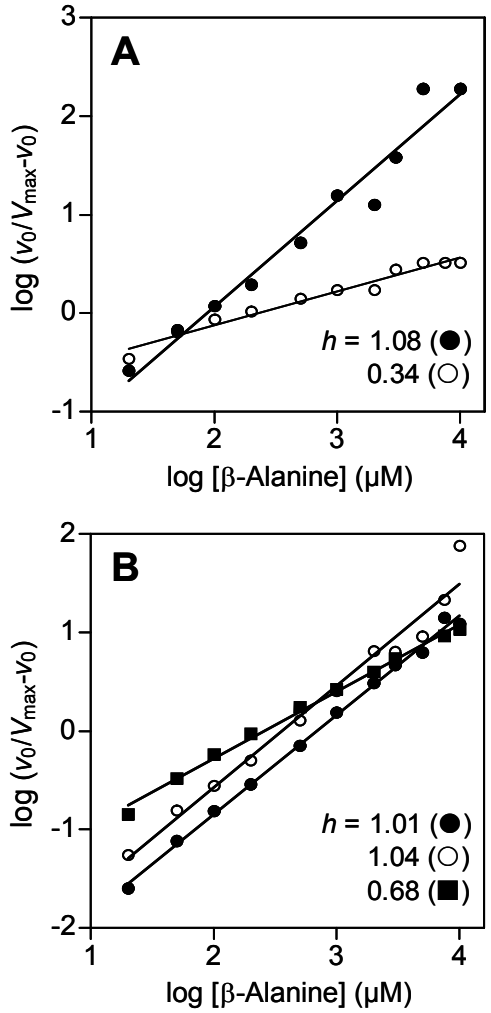

Fig. 4.14 *A. thaliana* PTS exhibits negative cooperativity for β-alanine at elevated pantoate concentrations. Initial rates were obtained by using the coupled enzyme assay with β-alanine as the variable substrate (0.02 mM – 10 mM) in the presence of 2 mM ATP (**A**) or 10 mM ATP (**B**). Pantoate was present at fixed concentrations of 0.5 mM (●), 5 mM (○), and 50 mM (■). Hill plots were constructed using the estimates of V_{max} defined in Table 4.4. h, Hill coefficient

Kinetic constants for *A. thaliana* PTS were calculated from the best fit parameters of the preferred rate law for each substrate-velocity curve (Table 4.3). The specificity constants (k_S) and catalytic constants (k_{cat}) derived in this way describe the linear behaviour of *A. thaliana* PTS at very low and saturating concentrations of the varied substrate, respectively. Thus, the reported values for k_S and k_{cat}, which are apparent constants at specific cosubstrates concentrations, may be compared across different models and irrespective of the kinetic behaviour at intermediate concentrations of the varied substrate.

varied substrate and fixed cosubstrates[a]		preferred rate law	k_{cat}[b]	k_S[c]
			s^{-1}	$M^{-1}\ s^{-1}$ ($\times 10^3$)
pantoate (varied substrate)				
0.5 mM β-alanine	1 mM ATP	Eq. 4[d]	0.018 ± 0.004	15 ± 1
	2 mM ATP	Eq. 4[d]	0.027 ± 0.006	16 ± 1
	5 mM ATP	Eq. 4[d]	0.069 ± 0.027	16 ± 1
	10 mM ATP	Eq. 4[d]	0.242 ± 0.076	15 ± 1
5.0 mM β-alanine	1 mM ATP	Eq. 4[d]	0.025 ± 0.006	13 ± 1
	2 mM ATP	Eq. 4[d]	0.039 ± 0.006	18 ± 1
	5 mM ATP	Eq. 4[d]	0.093 ± 0.032	20 ± 2
	10 mM ATP	Eq. 4[d]	0.235 ± 0.039	16 ± 1
β-alanine (varied substrate)				
2 mM ATP	0.1 mM Pantoate	Eq. 1	0.42 ± 0.005	4.6 ± 0.3
	0.5 mM Pantoate	Eq. 1	0.36 ± 0.004	4.1 ± 0.3
	5.0 mM Pantoate	Eq. 2	0.1 ± 0.2	4.4 ± 1.7
10 mM ATP	0.1 mM Pantoate	Eq. 1	1.1 ± 0.01	2.4 ± 0.2
	0.5 mM Pantoate	Eq. 1	2.2 ± 0.02	3.2 ± 0.1
	5.0 mM Pantoate	Eq. 1	1.1 ± 0.02	2.8 ± 0.2

Table 4.3 Apparent steady-state kinetic parameters of *A. thaliana* PTS enzyme.
[a]Initial rates were obtained by using the spectrophotometric, coupled enzyme assay. Pantoate was varied between 0.01 – 20.0 mM, and β-alanine was varied between 0.05 – 10.0 mM.
Individual sets of rate data were fitted to Eq. 1, 3 and 4, and the preferred rate law for each substrate-velocity curve was chosen using the F-test ($\alpha = 0.05$). Unless specified otherwise, catalytic constants (k_{cat}) and specificity constants (k_S) were calculated from the best fit parameters of the preferred rate law.
[b]$k_{cat} = V_{lim}/[E]$, where [E] is the concentration of PTS subunits. Eq. 1 and 4 simplify to $v_0 = k_{cat} \times [E]$ at high substrate levels.
[c]k_S is defined as k_{cat}/K_m and $\alpha_1/[E]$ in Eq. 1 and 4, respectively. Eq. 1 and 4 simplify to $v_0 = k_S \times [E] \times [S]$ at low substrate levels.
[d]In this curve fit to Eq. 4, $\alpha_1\beta_2 > \alpha_2\beta_1$ (95% confidence), indicating substrate inhibition (Schulz, 1994).

The catalytic constant for pantoate as the varied substrate ($k_{cat/pantoate}$) increases continuously as ATP is increased, which is consistent with competitive substrate inhibition, and is similar at 0.5 mM or 5.0 mM β-alanine, suggesting that the overall rate is determined by the first half reaction at saturating pantoate levels. The specificity constant for pantoate ($k_{pantoate}$) is not strongly affected by either ATP or β-alanine. The pattern of $k_{pantoate}$ at different cosubstrate levels is not in good agreement with the random path kinetic mechanism in Scheme 4.2B, which predicts that $k_{pantoate}$ increases to a maximum at saturating ATP levels

and is not affected by β-alanine. Replots of the same initial rate data for ATP as the varied substrate yield double reciprocal patterns that are consistent with competitive substrate inhibition (Fig. 4.15).

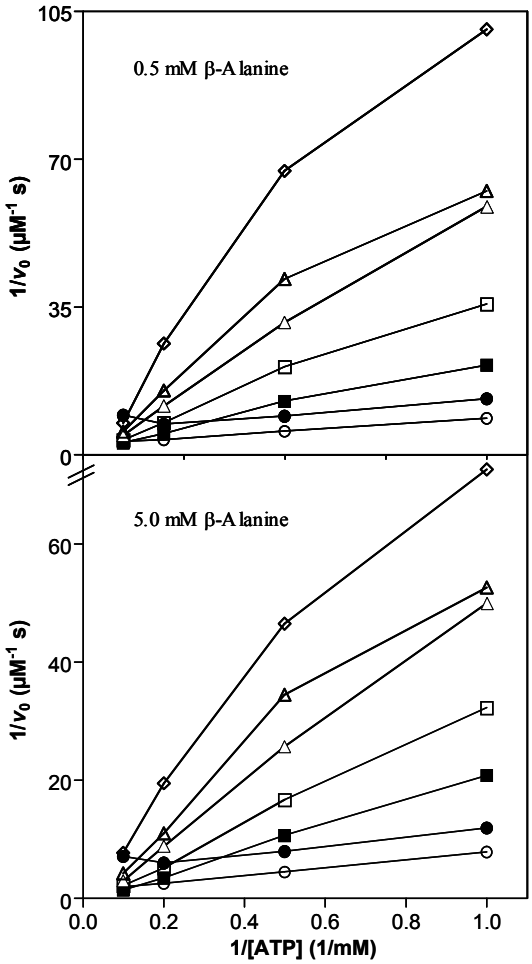

Fig. 4.15 Double reciprocal plots of *A. thaliana* PTS initial rates for ATP as the varied substrate. Initial rate data from Fig. 4.13 were replotted for ATP as the varied substrate at 0.5 mM or 5.0 mM β-alanine and at selected fixed pantoate concentrations of 0.02 mM (●), 0.1 mM (○), 2 mM (■), 5 mM (□), 10 mM (▲), and 20 mM (△). Values for V_{max} at saturating pantoate (◇) were obtained from the curve fits in Fig. 4.13. Individual sets of data points were connected for clarity but not fitted to a rate law.

Increasing levels of pantoate cause decreasing specificity constants for ATP (k_{ATP}), while the corresponding maximal rates are increasing or constant. It can be estimated, with equal results at 0.5 mM or 5.0 mM β-alanine, that k_{ATP} decreases by tenfold from 300 M^{-1} s^{-1} to 30 M^{-1} s^{-1} when pantoate is increased from 0.1 mM to 10 mM. However, saturation with pantoate does not seem to be associated with a significant further decrease of k_{ATP}. Thus, pantoate causes substrate inhibition by lowering the specificity constant for ATP. The limiting value for k_{ATP} at saturating pantoate can be interpreted as a property of either an allosteric dimer with two molecules of pantoate bound or an enzyme-pantoate complex (E·Pt in scheme 4.2B).

Likewise, high levels of ATP might decrease substrate inhibition either by repressing pantoate-induced negative subunit interactions or by enforcing the kinetically preferred path of substrate binding.

4.4.2 Consideration of modified kinetic mechanisms or allostery to explain the behaviour of *A. thaliana* PTS

The question arises whether the non-Michaelis-Menten kinetics of *A. thaliana* PTS are due to allostery, *i.e.* to interacting active sites, or have kinetic basis. Substrate inhibition and other non-hyperbolic responses can be explained by allosteric interactions between multiple catalytic sites, but may also arise for purely kinetic reasons (Segel, 1975). Therefore, allostery of the *A. thaliana* PTS dimer as well as kinetic cooperativity were considered as the basis for the kinetic behaviour of *A. thaliana* PTS. Two kinetic mechanisms with the ability to account for competitive substrate inhibition were derived based on the Ping Pong mechanism for bacterial PTS (Scheme 4.2).

Firstly, substrate inhibition may be caused by binding of pantoate to the free enzyme resulting in the formation of a catalytically inactive dead-end complex (E·Pt in Scheme 4.2A). In this case, substrate inhibition would be complete at saturating levels of pantoate, and the substrate-velocity curve for pantoate would be in the form of equation Eq. 3 (Segel, 1975).

Secondly, substrate inhibition may arise in steady-state random mechanisms with alternative paths of substrate binding if one path is significantly more favourable than the other (Segel, 1975). Thus, substrate inhibition in *A. thaliana* PTS might result from a kinetic mechanism like that shown in Scheme 4.2B, where the first half-reaction, that leads to the enzyme bound pantoyl adenylate intermediate (E´), corresponds to a bireactant random system. In this case, substrate inhibition would be incomplete at saturating levels of pantoate, and the substrate-velocity curves for pantoate would be in the form of equation Eq. 4 (Segel, 1975). Based on classical models of allostery, subunit interactions in dimeric enzymes also give rise to rate equations in the form of Eq. 4 (Segel, 1975). Consequently, individual curves of v_0 versus [pantoate] cannot be used to discriminate between allostery on the one hand and the random path kinetic mechanism in Scheme 4.2 B on the other.

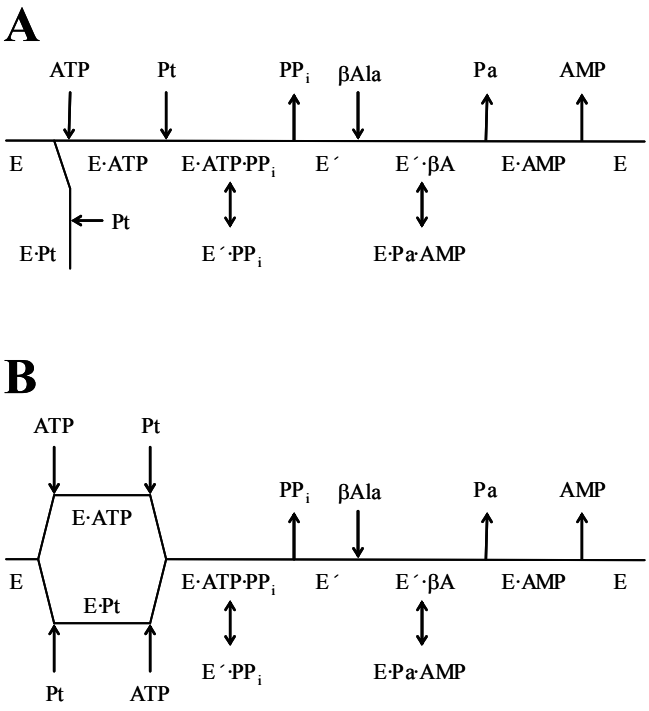

Scheme 4.2. Hypothetical kinetic mechanism for *A. thaliana* PTS. The kinetic mechanism in Scheme 4.1 was modified to account for competitive substrate inhibition. ***A***, Dead-end enzyme-pantoate (E·Pt) complex Bi Uni Uni Bi Ping Pong mechanism. ***B*,** Random ATP-pantoate Bi Uni Uni Bi Ping Pong mechanism *E*, enzyme; *F*, enzyme-pantoyl adenylate complex; *Pt*, pantoate; See text for details.

When pantoate was the varied substrate, Eq. 4 was the preferred model at all cosubstrates concentrations tested (F-test, p-values ≤ 0.01). Accordingly, the curve fits obtained using Eq. 4 (R^2 values 0.992 – 0.999) (Fig. 4.13 A and 4.13 B) are significantly better than the fits obtained with Eq. 3 (R^2 values 0.974 – 0.992). The inability of this Eq. 3 to accurately describe the initial rates of *A. thaliana* PTS is most obvious at low ATP levels. Eq. 3 describes a velocity curve that passes through a maximum and approaches zero at saturating substrate concentrations. However, as illustrated in the insets of Fig. 4.13 A and 4.13 B, the observed rates of *A. thaliana* PTS at high pantoate concentrations are higher than can be accommodated by equation Eq. 3. Thus, substrate inhibition is not due to the formation of a dead-end complex involving pantoate, and the mechanism in Scheme 4.2 A can be rejected. The response of *A. thaliana* PTS to pantoate discriminates against a dead-end mechanism but provides no basis to distinguish between interacting catalytic sites and random substrate binding. However, negative cooperativity with respect to β-alanine cannot be explained by alternative paths of substrate binding because β-alanine binds between two releasing steps. Generally, models for cooperativity in the absence of subunit interaction require that there are alternative modes of substrate binding and that the conversion of the enzyme-substrate complex into products is sufficiently fast to prevent equilibration between these modes

(Cornish-Bowden and Cardenas, 1987). To explain the observed dependence of cooperativity toward β-alanine on pantoate levels, the above condition for kinetic cooperativity would specifically require that increasing levels of pantoate accelerate the rate at which the enzyme-pantoyl adenylate complex (*F* in Scheme 4.1) reacts with β-alanine to give products. In other words, increasing pantoate levels would be predicted to raise the apparent specificity constant for β-alanine, which is, however, unaffected by pantoate (Table 4.4)

4.4.3 Initial rate kinetic analysis of PTS-Mut1

The kinetic behaviour of PTS-Mut1 was strongly altered compared with unmodified *A. thaliana* PTS. PTS-Mut1 showed no substrate inhibition at elevated pantoate concentrations and essentially hyperbolic kinetics with pantoate as the varied substrate (Fig. 4.16A). Apparent specificity constants for pantoate and β-alanine were lowered by approximately 15- to 30-fold, respectively, and limiting velocities at saturating pantoate were increased by three- to 20-fold (Table 4.4). The double reciprocal plot pattern for ATP as the varied substrate (Fig. 4.16B) reveals that increasing pantoate levels lead to increasing apparent specificity constants for ATP. It can be estimated that k_{ATP} of PTS-Mut1 reached 1200 $M^{-1}s^{-1}$ at 10 mM pantoate, a 40-fold increase compared with *A. thaliana* PTS. Fig. 4.16B also shows that PTS-Mut1 is subject to substrate inhibition at high ATP levels.

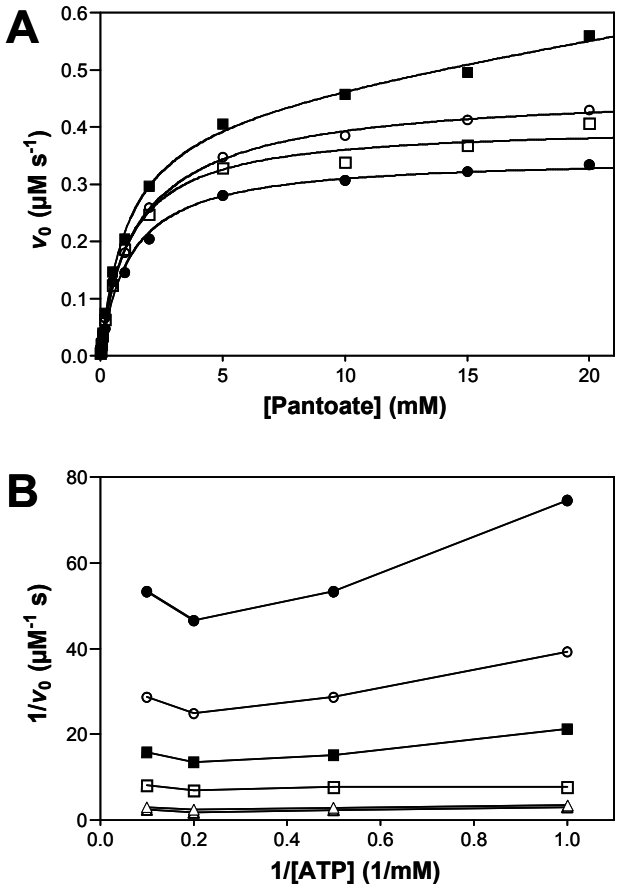

Fig. 4.16 Initial rate plots for PTS-Mut1. *A*, Primary plot of initial rates against pantoate concentration in the presence of 5.0 mM β-alanine and at fixed ATP levels of 1.0 mM (●), 2 mM (○), 5 mM (■), and 10 mM (□). Fitting individual sets of primary rate data to equations: 1(●, □) or 4 (○, ■) as the preferred rate law and absence of substrate inhibition at all ATP concentrations tested. See Table 4.4 for derived apparent kinetic constants. *B*, Double reciprocal plot of initial rates against [ATP]. Initial rate data from *A* were reploted for ATP as the varied substrate at selected fixed pantoate concentrations of 0.05 mM (●), 0.1 mM (○), 0.2 mM (■), 0.5 mM (□), 5 mM (▲), and 20 mM (△). Individual sets of data points were connected for clarity but not fitted to a rate law.

4.4.4 Initial rate kinetic analysis of PTS-E132A

The PTS-E132A mutation caused similar but weaker kinetic changes compared with those observed in PTS-Mut1. PTS-E132A showed substrate inhibition by pantoate of the same type (but reduced) as described above for *A. thaliana* PTS (Fig. 4.17 A and 4.17 B). However, the E132A change clearly reduced the inhibitory effect of pantoate (compare Figs. 4.13 D and 4.17 B) and led to fourfold higher values for $[pantoate]_{opt}$ and increased optimal activities. Specificity constants for pantoate and β-alanine were lowered by approximately two- and fourfold, respectively, and limiting velocities at saturating pantoate were increased by five- to sevenfold (Table 4.4). Substrate inhibition by ATP is evident at low pantoate levels below 1 mM (Fig. 4.17 C). The double reciprocal plot in Fig. 4.17 C also show that the specificity constant for ATP increased initially as pantoate was increased and decreased again at pantoate

levels above 0.5 mM. In addition, neither mutant showed negative cooperativity for β-alanine, not even at cosubstrate levels that caused strong negative cooperativity in *A. thaliana* PTS.

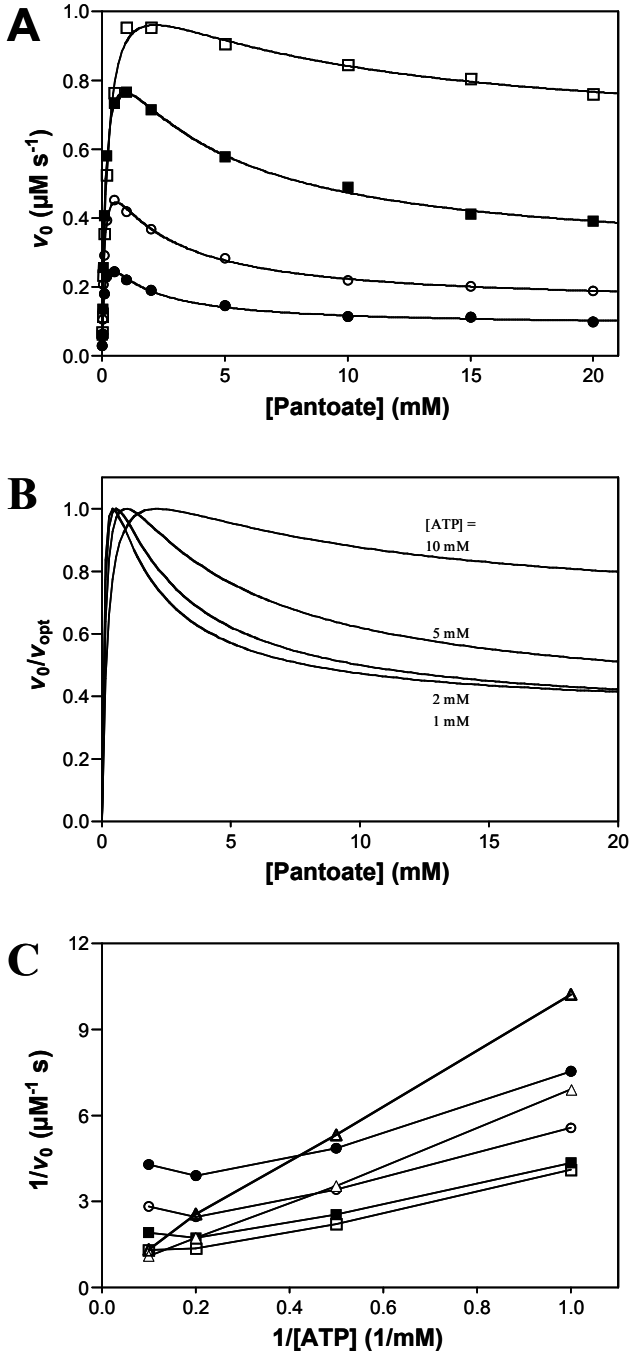

Fig. 4.17 Initial rate plots for PTS-E132A. ***A***, Primary plot of initial rates against pantoate concentration in the presence of 5.0 mM β-alanine and at fixed ATP levels of 1.0 mM (●), 2 mM (○), 5 mM (■), and 10 mM (□). Individual sets of rate data were fitted to the preferred rate law (Eq. 4), and $[pantoate]_{opt}$, v_{opt}, and apparent kinetic constants (Table 4.4) were calculated for each curve. ***B***, Initial rates normalized to v_{opt} were fitted to Eq. 4 and the resulting curves are shown with data points omitted for clarity. ***C***, Double reciprocal plot of initial rates against [ATP]. Initial rate data from *A* were replotted for ATP as the varied substrate at selected fixed pantoate concentrations of 0.05 mM (●), 0.1 mM (○), 0.2 mM (■), 0.5 mM (□), 5 mM (▲), and 20 mM (△). Individual sets of data points were connected for clarity but not fitted to a rate law.

enzyme, variable substrate, and fixed cosubstrates[a]		preferred rate law[b]	type of response[c]	h[d]	$k_{opt/app}$[e] (s^{-1})	$k_{cat/app}$[f] (s^{-1})	$[S]_{0.5/app}$[g] (mM)	$k_{S/app}$[h] (mM^{-1} s^{-1})
PTS								
pantoate (variable)								
0.5 mM β-alanine	1 mM ATP	Eq. 4	SI	-	0.21	0.018 ± 0.004	0.012	15 ± 1
	2 mM ATP	Eq. 4	SI	-	0.33	0.027 ± 0.006	0.016	16 ± 1
	5 mM ATP	Eq. 4	SI	-	0.59	0.069 ± 0.027	0.029	16 ± 1
	10 mM ATP	Eq. 4	SI	-	0.75	0.242 ± 0.076	0.044	15 ± 1
5.0 mM β-alanine	1 mM ATP	Eq. 4	SI	-	0.24	0.025 ± 0.006	0.014	13 ± 1
	2 mM ATP	Eq. 4	SI	-	0.41	0.039 ± 0.006	0.018	18 ± 1
	5 mM ATP	Eq. 4	SI	-	0.89	0.093 ± 0.032	0.034	20 ± 2
	10 mM ATP	Eq. 4	SI	-	1.48	0.235 ± 0.039	0.070	16 ± 1
β-alanine (variable)								
2 mM ATP	0.1 mM pantoate	Eq. 1	MM	-	-	0.42 ± 0.005	0.090	4.6 ± 0.3
	0.5 mM pantoate	Eq. 1	MM	-	-	0.36 ± 0.004	0.086	4.1 ± 0.3
	5.0 mM pantoate	Eq. 2	NC	0.31	-	0.16 ± 0.03	0.088	4.4 ± 1.7
10 mM ATP	0.1 mM pantoate	Eq. 1	MM	-	-	1.1 ± 0.01	0.47	2.4 ± 0.2
	0.5 mM pantoate	Eq. 1	MM	-	-	2.2 ± 0.02	0.68	3.2 ± 0.1
	5.0 mM pantoate	Eq. 1	MM	-	-	1.1 ± 0.02	0.38	2.8 ± 0.2
	50 mM pantoate	Eq. 2	NC	0.71	-	0.37 ± 0.01	0.21	3.0 ± 0.7
PTS-E132A								
pantoate (variable)								
5.0 mM β-alanine	1 mM ATP	Eq. 4	SI	-	0.45	0.15 ± 0.03	0.047	7.3 ± 0.4
	2 mM ATP	Eq. 4	SI	-	0.81	0.27 ± 0.04	0.058	11.0 ± 0.4
	5 mM ATP	Eq. 4	SI	-	1.39	0.50 ± 0.09	0.088	12.7 ± 0.4
	10 mM ATP	Eq. 4	SI	-	1.74	1.15 ± 0.86	0.16	9.2 ± 0.6
β-alanine (variable)								
2 mM ATP	0.5 mM pantoate	Eq. 1	MM	-	-	1.06 ± 0.02	0.94	1.1 ± 0.1
	5.0 mM pantoate	Eq. 1	MM	-	-	0.59 ± 0.01	0.48	1.2 ± 0.1
10 mM ATP	0.5 mM pantoate	Eq. 1	MM	-	-	2.7 ± 0.1	3.6	0.74 ± 0.05
	5.0 mM pantoate	Eq. 1	MM	-	-	4.9 ± 0.4	8.0	0.61 ± 0.10
PTS-Mut1								
pantoate (variable)								
5.0 mM β-alanine	1 mM ATP	Eq. 1	MM	-	-	0.59 ± 0.01	1.2	0.49 ± 0.05
	2 mM ATP	Eq. 2	NC	0.88	-	0.81 ± 0.01	1.4	0.72 ± 0.09
	5 mM ATP	Eq. 4[i]	NC	0.78	-	1.10 ± 0.06	1.7	0.70 ± 0.06
	10 mM ATP	Eq. 1	MM	-	-	0.69 ± 0.01	1.2	0.58 ± 0.05
β-alanine (variable)								
2 mM ATP	0.5 mM pantoate	Eq. 1	MM	-	-	0.27 ± 0.01	1.2	0.23 ± 0.03
	5.0 mM pantoate	Eq. 1	MM	-	-	1.27 ± 0.03	4.7	0.27 ± 0.02
10 mM ATP	0.5 mM pantoate	Eq. 1	MM	-	-	0.32 ± 0.02	2.8	0.11 ± 0.01
	5.0 mM pantoate	Eq. 1	MM	-	-	1.92 ± 0.07	14.1	0.14 ± 0.01

Table 4.4 Apparent steady-state kinetic behaviour and parameters of *A. thaliana* PTS and PTS mutants.

[a]Initial rates were obtained by using the spectrophotometric, coupled enzyme assay. Pantoate was varied between 0.01 – 20 mM, and β-alanine was varied between 0.02 – 10 mM.

[b]Individual sets of rate data were fitted to Eqs. 1 – 4, and the preferred rate law for each substrate-velocity curve was selected (F-test, $\alpha = 0.05$). Unless indicated otherwise, apparent kinetic parameters were calculated from the best fit parameters of the preferred rate law. [E] is the total concentration of PTS subunits in all calculations.

[c]MM, Michaelis-Menten kinetics; SI, substrate inhibition; NC, negative cooperativity. The types of response were classified according to the following conditions: Preference for Eq. 1 → MM; Preference for Eq. 4 and $\alpha_1\beta_2 > \alpha_2\beta_1$ (Schulz, 1994) → SI; preference for Eq. 2 and $h < 1$, or preference for Eq. 4 and $\beta_1 > (\alpha_1\beta_2/\alpha_2 + \alpha_2/\alpha_1)$ (Schulz, 1994) → NC.

[d]Where negative cooperativity (NC) was detected, the Hill coefficient h was estimated by fitting initial rate data to Eq. 2.

[e]Where substrate inhibition (SI) was detected, k_{opt} (true maximal rate) is equal to $v_{opt}/[E]$.

[f]$k_{cat} = V_{max}/[E]$.

[g]Where Michaelis-Menten behaviour (MM) was detected, $[S]_{0.5} = K_m$; where negative cooperativity (NC) was detected, $[S]_{0.5} = K_{0.5}$; where substrate inhibition (SI) was detected, $[S]_{0.5}$ is the substrate concentration where $v_0 = 0.5\ v_{opt}$ and was calculated using Eq. 6.

[h]$k_S = k_{cat}/K_m$ (specificity constant) where Michaelis-Menten behaviour (MM) was detected. In all other cases, k_S was estimated by fitting initial rate data to Eq. 4 and using the definition $k_S = \alpha_1/[E]$ (Schulz, 1994).

[i]k_{cat} was estimated by fitting initial rate data to Eq. 2.

4.4.5 Mutation in the subunit interface, conclusions

Substrate inhibition by pantoate could not be detected in PTS-Mut1 and was reduced in PTS-E132A (Fig. 4.16A and 4.17A). Also, neither mutant showed negative cooperativity for β-alanine at cosubstrates levels that caused strong negative cooperativity in wild-type *A. thaliana* PTS. Substrate inhibition by ATP was suppressed by pantoate and not detectable above 0.05 mM pantoate in *A. thaliana* PTS or above 0.2 mM pantoate in PTS-E132A, whereas it was apparent in PTS-Mut1 at pantoate concentration up to 20 mM.

The apparent kinetic parameters displayed by PTS-E132A and PTS-Mut1 reveal that the respective mutations in the dimerization region of *A. thaliana* PTS consistently led to increased maximum rates, whereas the corresponding substrate affinities and specificities were lowered. This effect was observed for both pantoate(Table 4.5) and β-alanine(Table 4.6) as the variable substrate. Given that the reaction rates at low and high substrate concentrations are determined by the specificity constant and K_{cat}, respectively, *A. thaliana* PTS will be more active than the PTS mutants at low concentrations of pantoate and β-alanine, whereas PTS-E132A and PTS-Mut1 will have superior turnover rates at intermediate and high levels of these substrates, respectively.

Enzyme	$[S]_{0.5/app}$ (mM)	$k_{cat/app}$ (s^{-1})	$k_{S/app}$ (mM^{-1} s^{-1})
PTS	0.018[b]	0.039	18
PTS-E132A	0.058[b]	0.27	11
PTS-Mut1	1.4	0.81	0.72

Table 4.5 Dependence of pantothenate synthesis on pantoate[a]
[a]At 2 mM ATP and 5 mM β-alanine (*cf.* Table 4.4).
[b]Pantoate concentration where $v_0 = 0.5\ v_{opt}$.

Enzyme	$[S]_{0.5/app}$ (mM)	$k_{cat/app}$ (s^{-1})	$k_{S/app}$ (mM^{-1} s^{-1})
PTS	0.088	0.16	4.4
PTS-E132A	0.48	0.59	1.2
PTS-Mut1	4.7	1.3	0.27

Table 4.6 Dependence of pantothenate synthesis on β-alanine[a]
[a]At 2 mM ATP and 5 mM pantoate (*cf.* Table 4.4).

The notion that *A. thaliana* PTS is optimized for catalysis at low pantoate levels is supported by the effect of pantoate on the apparent specificity constant for ATP ($k_{ATP/app}$) (Fig. 4.18). When pantoate was varied between 0.01 mM and 20 mM, $k_{ATP/app}$ passed through a maximum in the *A. thaliana* PTS, PTS-E132A, and PTS-Mut1 enzymes, and each form of PTS had superior values for $k_{ATP/app}$ in a different range of pantoate concentrations. Notably,

A. thaliana PTS had the highest specificity for ATP at pantoate levels below 50 µM. The pantoate concentration at which $k_{ATP/app}$ was maximal shifted from 0.05 mM to 0.2 mM and 10 mM in *A. thaliana* PTS, PTS-E132A, and PTS-Mut1, respectively. Concomitantly, the maximal values for $k_{ATP/app}$ increased from approximately 0.3 mM^{-1} s^{-1} in *A. thaliana* PTS to 0.5 mM^{-1} s^{-1} in PTS-E132A and 1.3 mM^{-1} s^{-1} in PTS-Mut1. This pattern of $k_{ATP/app}$ values is consistent with a stepwise reduction of competitive substrate inhibition by pantoate on mutation of the dimerization region in *A. thaliana* PTS. Also, it suggests that the heterotropic interactions between ATP and pantoate are balanced to achieve maximal specificity for ATP at low pantoate levels.

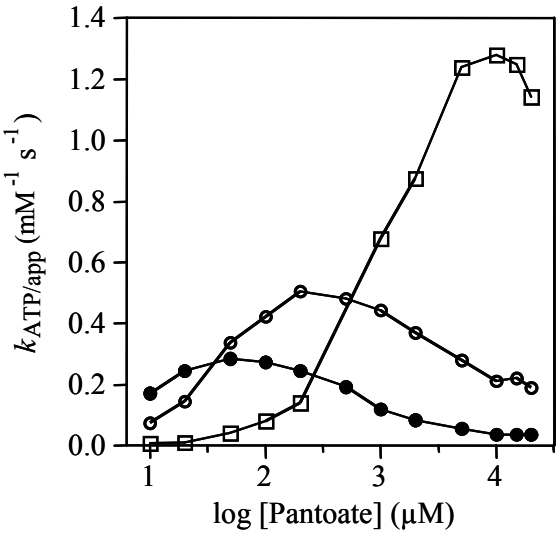

Fig. 4.18 The effect of pantoate on the apparent specificity constant for ATP ($k_{ATP/app}$) in *A. thaliana* PTS (●), PTS-E132A (○), and PTS-Mut1 (□). The plotted values for $k_{ATP/app}$ were estimated from double-reciprocal plots for ATP as the variable substrate and are for a fixed β-alanine concentration of 5 mM. *A. thaliana* PTS gave essentially identical values for $k_{ATP/app}$ in the presence of 0.5 mM β-alanine (not shown).

4.5 Conclusions

The pantothenate synthetases from *E. coli* and *M. tuberculosis* catalyze a two-step reaction that proceeds via a pantoyl adenylate intermediate as shown in Scheme 4.1 (Miyatake *et al*, 1979; Zheng and Blanchard, 2001). These enzymes can be assumed to be non-allosteric because they obeyed Michaelis-Menten kinetics, and crystal structures of *M. tuberculosis* PTS indicated that the active sites located on each of the two subunits are catalytically independent (Wang and Eisenberg, 2006). Alignment of bacterial and eukaryotes PTS sequences (Fig. 4.1) indicated high level of conservation of functional residues. This implied that the active site and the reactions mechanisms are conserved within the pantothenate synthetase protein family while the dimerization contacts have diverged substantially.

Scheme I predicts that the exchange reaction proceeds via the pantoyl adenylate intermediate and that binding of pantothenate occurs only in presence of AMP. Thus, the molecular exchange between β-alanine and pantothenate should have an absolute requirement for AMP. Indeed, analysis of *A. thaliana* and *E. coli* PTS indicated that pantoyl adenylate is the key reaction intermediate in both enzymes. Both enzymes catalyzed the isotope exchange between pantothenate and β-alanine in an AMP-dependent fashion and only negligible exchange occurred in the absence of AMP (Fig. 4.10). This strongly suggested that the Ping Pong mechanism of bacterial PTS is conserved in *A. thaliana* PTS. This view is supported by the conserved pH optima of the overall PTS reaction and the isotope exchange (Fig. 4.8 B and 4.9 B). However, initial rate studies of *A. thaliana* PTS revealed several deviations from hyperbolic kinetics. Most obviously, pantoate caused strong substrate inhibition (Fig. 4.13 A, B) and, at higher levels, negative cooperativity for β-alanine (Fig. 4.14). Both effects were suppressed by ATP, which conversely caused weak substrate inhibition that was suppressed by pantoate (Fig. 4.15). These observations cannot fully be accounted for by kinetic cooperativity, leaving allosteric interactions as the preferred explanation for the non-Michaelis-Menten behaviour of PTS. The PTS-E132A and PTS-Mut1 mutations in the dimerization region of PTS partially and fully removed substrate inhibition by pantoate, respectively, which was associated with a stepwise increase of substrate inhibition by ATP. The activity of PTS-Mut1 increased continuously when pantoate was increased at all ATP levels tested (Fig. 4.16 A), showing that substrate inhibition was abolished by the deletion of the insertion in the dimerization region. The mutations also eliminated the ability of pantoate to induce negative cooperativity for β-alanine.

Homotropic and heterotropic effects of pantoate therefore appear to be tightly coupled which is a classic tenet of allosteric systems (Monod *et al*, 1965). A general mechanism that

can explain rate enhancement through interacting sites presented in Scheme. 4.3 is based on half-of-the-sites reactivity where one subunit has little or no catalytic activity but instead is used to modulate catalysis on the other subunit (Fersht, 1975). Scheme 4.3 illustrates how this mechanism could account for key aspects of the kinetics of PTS.

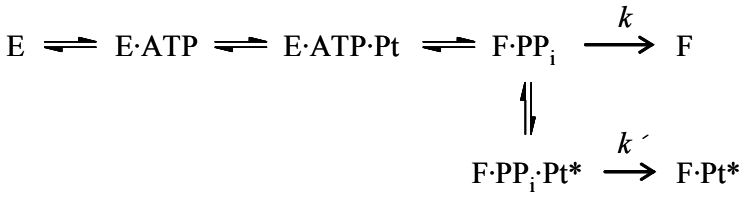

Scheme 4.3. Hypothetical mechanism for the allosteric interaction of pantoate with PTS. See text for details. *E*, enzyme; *F*, enzyme-pantoyl adenylate complex; *Pt*, pantoate; *Pt**, 'second site' pantoate

The basic assumption in Scheme 4.3 is that the formation of F·PP$_i$ (F represents the enzyme-bound pantoyl adenylate intermediate) from ATP and pantoate is energetically unfavourable, causing its steady-state concentration to be low. Strong binding of a second molecule of pantoate (Pt*) to F·PP$_i$ would then shift the equilibrium towards F·PP$_i$ and increase turnover. Substrate inhibition at elevated pantoate levels would follow from Scheme 4.3 if binding of Pt* to the second site significantly retards the release of PP$_i$ from F·PP$_i$ ($k' < k$). With these constraints, Scheme 4.3 can also explain negative cooperativity for β-alanine provided that the two forms of the pantoyl adenylate intermediate, F and F·Pt*, are not in equilibrium. Assuming that Pt*competes with ATP for binding to the second site, Scheme 4.3 also provides a basis to explain the heterotropic interactions between these substrates.

The PTS-E132A and PTS-Mut1 mutations in the dimerization region of PTS decreased the enzyme's specificity for pantoate and β-alanine and increased the corresponding values for $k_{cat/app}$ (Table 4.4). Thus, PTS-E132A and PTS-Mut1 are tuned for optimal activity at increasingly higher concentrations of pantoate and β-alanine, respectively.

Chapter 5
Discussion

5.1 Pantothenate synthesis in *Arabidopsis thaliana*

In this work, a new *emb* (embryo specific) mutant, altered in pantothenate biosynthesis, is reported. The Arabidopsis *pts* mutant described is an auxotroph, requiring pantothenate supplementation for growth. Embryo-lethal mutants are blocked in a particular step of the process necessary for embryo viability and development and are maintained as heterozygotes. Embryo-defective mutants differ in their terminal phenotypes, extent of abnormal development, allele strength, nature of underlying mutation, size and colour of aborted seeds and embryos, efficiency of transmission through male and female gametes, capacity to produce mutant seedlings. Embryo phenotypes are remarkably consistent from seed to seed in some mutants and exhibit considerable variations in others (Tzafrir *et al*., 2004). Some embryo-defective mutants may represent weak alleles of genes required for gametogenesis, or knock-out of genes whose products are compensated in part by contributions from surrounding maternal or paternal tissues (Springer *et al*., 2002).

Pantothenate synthetase is encoded in the Arabidopsis genome by At5g48840, a single copy gene (Ottenhof *et al*., 2004). Two Salk lines with a T-DNA insertion in pantothenate synthetase, *pts-1* and *pts-2,* were analysed in this work. The exact insertion point was determined by sequencing of the fragment flanking the T-DNA insertion. In case of *pts-2,* the insertion point turned out to lie in the first intron. The question arose whether 5.2 kbp of T-DNA insertion in the intron is sufficient to disrupt the gene function. The observed seed-lethal phenotype in the *pts-1* and *pts-2* insertion lines was apparently caused by single T-DNA insertions in the At5g48840 gene, respectively. Potential second T-DNA insertion in both Salk lines do not contribute to the observed phenotype, although its presence was not investigated. Both insertions showed the same segregation pattern, *i.e*. 25% seed-lethal phenotype, suggesting that the observed effect is due to a single recessive gene locus (only one copy of T-DNA insertion in heterozygous plant) and both T-DNA insertions efficiently disrupt the *PTS* gene function. The seed-lethal phenotype supports the assumption that in Arabidopsis there is only one pathway leading to pantothenate.

Mapping the distribution of aborted seeds in siliques of selfed heterozygotes has been used to identify mutations that interfere with both embryogenesis and pollen-tube growth (Meinke, 1982, 1985). In case that gametophytic expression of the *PTS* gene would be

required for normal pollen-tube growth, aborted seeds would be rarely found at the base of a heterozygous silique because mutant pollen tubes would show a competitive growth disadvantage. Nevertheless this is not the case in *pts-1* and *pts-2* mutants as mutant seeds were distributed randomly along the length of heterozygous siliques (section.3.4.1), and, on the basis of χ^2 statistical testing, segregation ratios were not significantly different from those expected for a single recessive mutation (Table 3.2). Thus, even the complete loss of pantothenate synthesis in mutant pollen grains does not appear to interfere with pollen-tube growth.

Examination of cleared mutant seeds with Nomarski optics revealed that embryo development was arrested in very early stages of embryogenesis. Despite arrested embryo development, endosperm development of seeds harbouring *pts-1* or *pts-2* embryos appeared normal until late heart stage of normal development (Fig. 3.3). The fact that *PTS/pts-1* and *PTS/pts-2* heterozygous plants produce 25% defective seeds indicates that the seed coat and integuments do not provide sufficient pantothenate for *pts-1/pts-1* or *pts-2/pts-2* embryos to complete morphogenesis, even though the surrounding tissues contain one copy of the wild type allele. This defect was, in all likelihood, not caused by another linked mutation because it disappeared in heterozygous plants treated externally with pantothenate (section 3.4) or grown on pantothenate-supplemented media (section 3.4.2). Moreover, those two independent insertions with equal defective phenotype are strong evidence against a linked mutation. The question arises why heterozygous maternal tissue does not supply pantothenate to developing *pts* zygotes. The possible explanation could be that pantothenate synthesised in plant cells is immediately converted into coenzyme A, which is not transported. Moreover, pantothenate transport in plants has not been investigated yet, leaving this only for speculations. Bearing in mind the whole spectra of biochemical processes in which coenzyme A is involved, it is not surprising that coenzyme A deficiency (resulting directly from pantothenate deficiency) has tremendous consequences, leading to embryo death.

Despite the absence of pantothenate synthesis, both male and female gametophyte develop normally. Fertilisation takes place, indicating that pollen is able to develop pollen tube and embryo sac is formed properly. Moreover, after fertilization there are two cell divisions of the zygote, leading to the formation of the two-cell proembryo and the two-cell suspensor. This is leading to the conclusion that there is enough pantothenate and coenzyme A in both male and female gametophyte and later in fertilised ovules to support initial embryo formation (at which it is formed of two cells of embryo proper and two cells of suspensor) (Fig. 3.4). It is striking that embryo proper and suspensor stop to develop at that particular

phase of development. The observed pattern of final phenotype is consistent in all mutants analysed. This "synchronisation" of cell division after which they stop to divide is astonishing. In Arabidopsis, after fertilization the zygote divides asymmetrically yielding a smaller apical and a larger basal cell (Mansfield and Briaty, 1991). These two cells differ profoundly in their internal composition and in their subsequent division patterns. The apical cell contains dense cytoplasm and is the site of very active protein synthesis, whereas the basal cell and its descendants are highly vacuolated (Berleth and Chatfield, 2002). From this point outwards, *pts* mutants are capable to carry on only one cell division, which terminates embryo development. Apparently, after this final cell division pantothenate/coenzyme A pool is depleted to such extend, or consumed completely that further development is impossible and the ovules containing such embryos are then aborted.

The observed arrested embryo development in *pts-1* and *pts-2* embryos demonstrates that disrupting a general metabolic function, such as pantothenate synthesis, can have developmental consequences that may resemble defects in pattern formation. This supports the conclusion that defects in cell division pattern are not necessarily the result of mutations in genes that play a direct role in the regulation of morphogenesis (Meinke, 1996). Embryogenesis is a complex process during which a cascade of changes, orchestrated by different gene expression pattern takes places. Important genes in embryogenesis are often also expressed in vegetative tissues. Many embryo-defective mutants are likely to be altered in a basic or so-called housekeeping function which first become essential during early stages of development.

Embryogenesis mutants have been attributed to alteration in transcription factors and associated proteins (Aida *et al*., 1997; Grossniklaus *et al*., 1998; Hardthe and Berleth, 1998; Li and Thomas 1998; Lotan *et al*., 1998), in metabolic enzymes (Patton *et al.,* 1998; Lukowitz *et al*., 2001); in transport and trafficking proteins (Lukowitz *et al.,* 1996; Assaad *et al*., 2001), in factors required for replication and translation (Springer *at al*., 1995; Tsugeki *et al*., 1996), in proteins with other essential functions (Jang *et al*., 2000; Schrick *et al*., 2000; Boisson *et al*., 2001). *pts* falls into the class of mutants with defect in metabolic enzymes.

Recently an Arabidopsis mutant impaired in coenzyme A biosynthesis has been reported (Rubio *et al*., 2006). It has been demonstrated that disrupting genes encoding for 4'-phosphopantothenoyl-cysteine decarboxylase an intermediate enzyme in coenzyme A biosynthetic pathway, lead to embryo lethality (see Fig. 5.1 C). In plants, every step of coenzyme A biosynthesis from pantothenate is catalyzed by monofunctional enzymes. In Arabidopsis *HAL3A* (At3g18030) encodes for 4'-phosphopantothenoyl-cysteine

decarboxylase and it has been demonstrated that the product of the *HAL3B* (At148605) plays the same, but redundant, catalytic role as *HAL3A* (Rubio *et al*., 2006). Double homozygous mutants are lethal, with arrested embryo development at the early/midglobular stage (Fig. 5.1 C), showing that de novo coenzyme A biosynthesis by the embryo is required for embryogenesis (Rubio *et al*., 2006). Recently Tilton *et al*. (2006) showed that also pantothenate kinase activity is crucial for embryogenesis in Arabidopsis. Arabidopsis has two functional pantothenate kinases (encoded by *AtPANK1* and *AtPANK2*; Tilton *et al*., 2006) which phosphorylate pantothenate to 4'-phosphopantothenate. Knock-out mutation of either *AtPANK1* or *AtPANK2* did not inhibit plant growth whereas *pank1-1/pank2-1* double knockout mutations were embryo lethal (Fig. 5.1 B). It was shown that *pank1-1/pank2-1* double mutant seeds were aborted in early stages of development, and no embryo could be discerned in the remains of the aborted seeds (Fig. 5.1 B). In addition, it has been demonstrated that only one of the *AtPANK* enzymes is necessary and sufficient for producing adequate coenzyme A levels, and no other enzyme can compensate for the loss of both isoforms (Tilton *et al*., 2006).

Similar to the *pts* knock out mutation (Fig. 5.1 A), the embryo from double *hal3a/hal3b* and *pank1-1/pank2-1* double mutants are arrested at early stages of embryogenesis. The *pts* mutation, in comparison with *hal3a/hal3b* double mutants, is more severe, as the embryo reaches a less advanced stage of embryogenesis (two-cell proembryo) (Fig. 5.2 E). This is enigmatic because on the basis of the coenzyme A biosynthetic pathway, the lack of pantothenate would be expected to have the same consequences as the lack of the 4'-phosphopantetheine, the product of the reaction catalysed by *HAL3A* and *HAL3B* genes. Although the observed effect of the lack of synthesis of either pantothenate or 4'-phosphopantetheine is striking, it is not clear why the lack of the latter allows embryo to reach early/midglobular stage, while absence of pantothenate synthesis allows the embryo to reach only two-cell preglobular stage. Yet, it is plausible that pantothenate might have a second function, *e.g*. in cell cycle regulation. This could explain the difference between *pts* and *hal3a/hal3b* mutants. Apparently, when the residual amount of coenzyme A present in *hal3a/hal3b* zygote is titrated below certain threshold by early cell divisions, then further development is arrested (Rubio *et al*. 2006). This argument, as discussed above, could also be true for *pts* embryo mutants. On the basis on the organization of coenzyme A biosynthetic pathway it would be expected that *pts* knock out embryos would reach a more advanced stage of development than those of *hal3a/hal3b*, as pantothenate is synthesized three enzymatic

steps before 4'-phosphopantetheine, so there should be higher total amounts of precursors of coenzyme A.

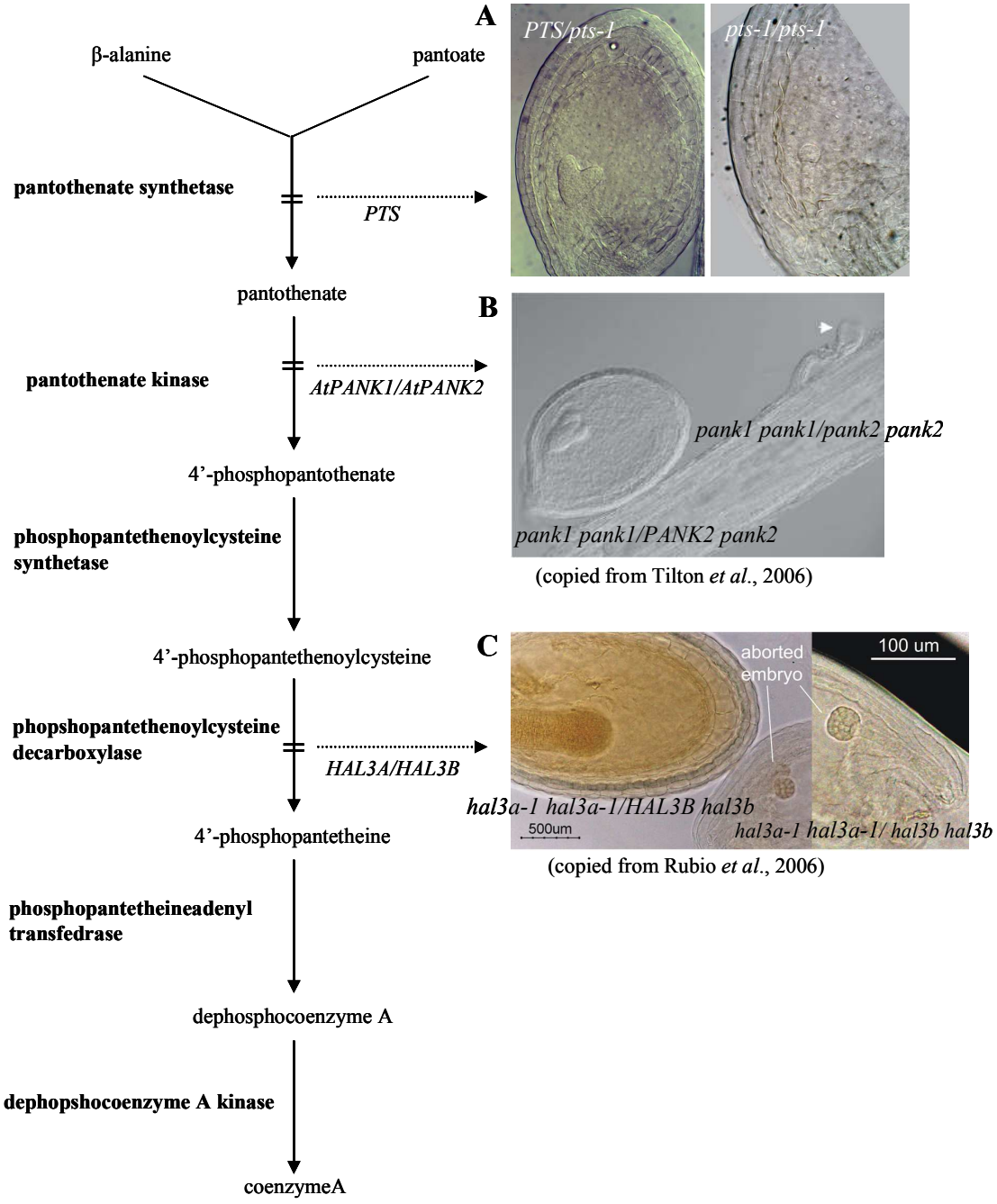

Fig. 5.1 Organisation of coenzyme A biosynthetic pathway. Effect of mutation in genes encoding: **A**, pantothenate synthetase; homozygous *pts-1/pts-1* are embryo lethal, with arrested embryo development at preglobular stage of embryogenesis (this study) (*cf* Fig. 5.2E); **B**, pantothenate kinase, knock-out mutation of either *AtPANK1* or *AtPANK2* did not inhibit plant growth, whereas *pank1-1/pank2-1* double knockout mutation is embryo lethal (Tilton *et al*., 2006); **C**, phosphopantethenoylcysteine decarbpxylase, *hal3a-1 hal3a-1/HAL3B hal3b* plants had a viable embryos (torpedo stage at the picture) and *hal3a-1 hal3a-1/hal3b hal3b* embryos were aborted at the early/midglobular stage (Rubio *et al*., 2006). All compared seeds in each A, B, C came from the same silique. See text for details.

5.2 Comparison of *pts* with other *emb* mutations

Embryo lethality, caused by a defect in metabolic enzymes were observed and characterised also in *bio* mutants of *Arabidopsis thaliana*. The *bio-1* mutant, the first plant auxotroph resulting in embryo lethality (Schneider *et al*., 1989), was shown to be defective in the synthesis of the biotin precursor 7,8-diaminopelargonic acid (Shellhammer and Meinke, 1990). Likewise the *bio-2* mutant which was shown to be defective in the final step of biotin synthesis the conversion of dethiobiotin to biotin (Patton *et al*., 1998). Plants, bacteria and certain fungi are capable of synthesizing biotin directly from chemical intermediates, while animals and most fungi require it for growth (Koser, 1968). Consequently, mutations that prevent biotin synthesis lead to severe consequences in the organism. Arrested *bio-2* embryos remain white or pale yellow-green throughout development. They often reach a globular or heart shape prior to desiccation (Fig. 5.2 A, C), and consistently fail to germinate at maturity, while *bio-1* embryos reached more advanced cotyledon stage (Patton *et al*., 1998). While deficiency of biotin synthesis in *bio* embryos leads to malformations (elongation) of embryo cells in comparison with the wild type, *pts* mutant embryos seem to develop normally considering pattern formation and general shape (Fig. 5.2 E). Moreover, *bio* mutants vary in the final phenotype observed (globular to cotyledon stage), while *pts* mutant final phenotype is consistent from seed to seed.

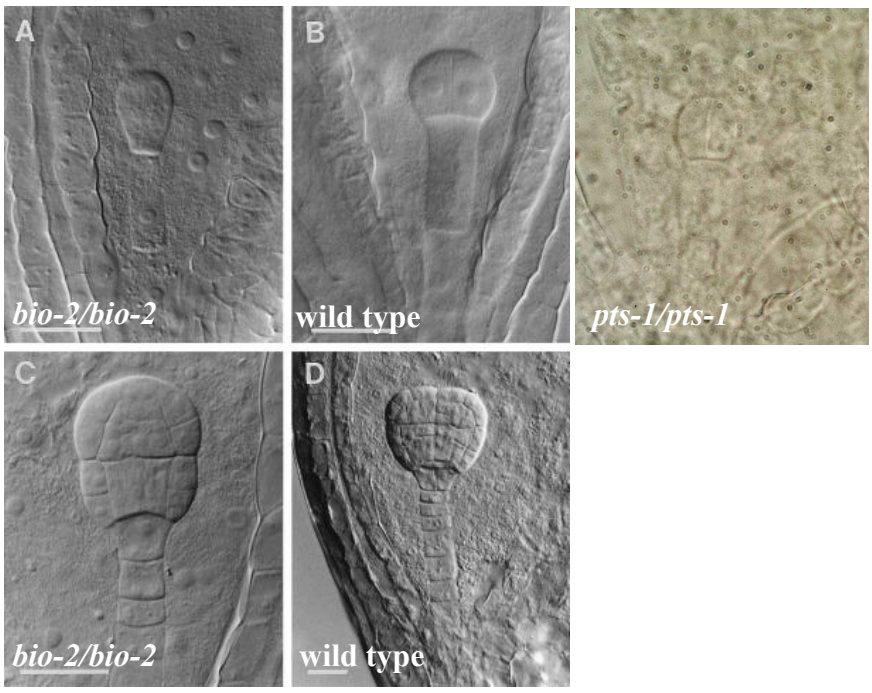

Fig. 5.2 Early defects in development of *bio-2* embryos (Patton *et al*., 1998) compared with arrested development of *pts-1*. A and C, immature bio-2 mutant seeds. Note the unusual elongation of the apical cell (A) and the embryo proper (C) (in mutant seeds). B and D, wild type seeds at proembryo (B) and late-globular (D) stages. E, typical terminal phenotype of *pts-1* embryo. Note that phenotype of *pts-1* embryo does not differ from

that observed for wild type proembryo (B). The *pts-1* mutation disrupt embryogenesis to a greater extent than the *bio-2*.

So far, only six genes have been identified (At1g48175, At1g76060, At3g48470, At4g26500, At5g21140, At5g22370) whose knock out results in embryo lethal mutants with development arrested at preglobular stages of embryogenesis (Tzafrir *et al*., 2004). Only one of them, At4g26500 (*AtSufE*), has been described (Xu and Moller, 2006). It was shown that At4g26500, a single copy gene, is an essential activator of plastidic and mitochondrial desulfurases in *A. thaliana* (Xu and Moller, 2006). Two T-DNA insertions in At4g26500 have been characterised, which resulted in an identical phenotype characterised by retarded development. At the WT two-four cell stage (Fig. 5.3 a), mutant embryos had only reached initial zygote division (Fig. 5.3 b), and at the WT eight-cell stage (5.3 c), the mutants embryos had only reached the four-cell stage (5.3 d). Those mutant embryos never progress beyond the preglobular eight-cell stage (Fig. 5.3 d) (Xu and Moller, 2006).

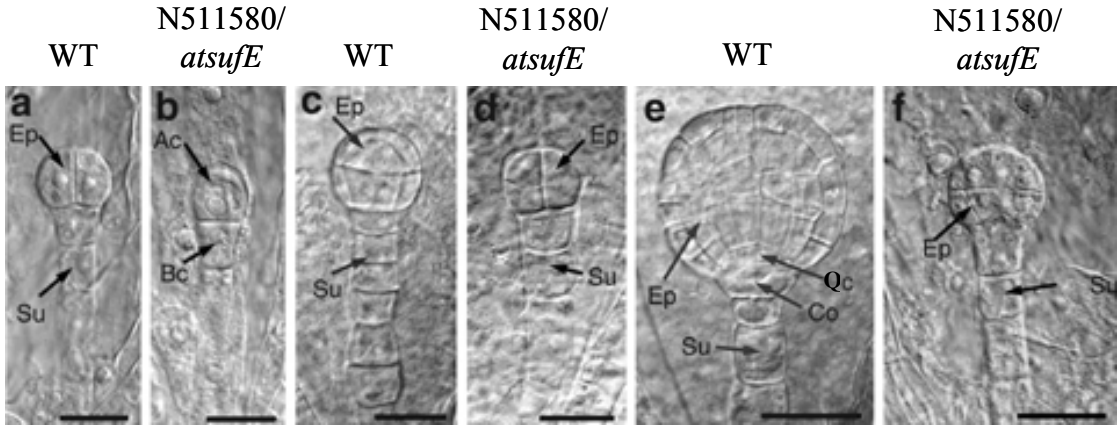

Fig. 5.3 In Arabidopsis AtSufE deficiency results in arrested embryo development. Microscopy of wild type (WT) and homozygous aborted seeds from the same heterozygous N511580 at (a, b) the two-four cell stage, (c, d) the eight-cell stage and (e, f) the globular stage. Ep, embryo proper; Su, suspensor; Ac, apical cell; Bc, basal cell; Qc, prospective quiescent center; Co, prospective columella siliques (copied from Xu and Moller, 2006).

It was estimated that there are 500 to 1000 *EMB* genes in *A. thaliana* genome (Franzmann *et al*., 1995; McElver *et al*., 2001). Tzafrir *et al*. (2004) identified dataset of 250 EMB genes, which represent about 25% to 50% of the total. As mentioned above, knock out of six of them results in arrested embryo development at preglobular stage of embryogenesis. One strategy for uncovering additional *EMB* genes might be to focus on reverse genetics of specific pathways or protein complexes for which at least one knockout is known to result in embryo defect (Tzafrir *et al*., 2004). For example, as described above, mutants disrupted in two different steps of biotin synthesis are embryo lethal (Patton *et al*., 1998) therefore, disruption of the remaining steps should also result in embryo abortion unless, and these steps are

encoded by two or more functionally redundant genes. Such redundancy has been mentioned here in the coenzyme A biosynthetic pathway, where *HAL3B* has redundant to HAL3A role (Rubio *et al*., 2006). Consequently, knock out of *HAL3A* alone has no phenotype. Likewise, coenzyme A knock-out disrupting a gene encoding for single component of a large protein complexes, which are known that disruption of a single component result in seed phenotype, are candidates to reveal another *emb* genes. Remaining members of such complex might be promising candidates for reverse genetic analysis (Tzafrir *et al*., 2004). Also, using comparative approach embryo-defective mutants identified in other plant species could be explored (Tzafrir *et al*., 2004).

5.3 Chemical complementation

To confirm the function of the *PTS* gene heterozygous *PTS/pts-1* plants were subjected to chemical treatment with pantothenate or panthteine (section 3.4). On the basis of the organization of the coenzyme A pathway (Fig. 5.1), it was expected that mutant plants defective in pantothenate biosynthesis also lack 4'-phosphopantethiene. Therefore, supplementation with pantothenate should restore coenzyme A biosynthesis pathway. It has been demonstrated that pantothenate kinase can phosphorylate pantetheine (Abiko, 1975), therefore, also supplementation with this chemical should restore coenzyme A biosynthesis pathway in *pts* mutants. Indeed, when pantothenate or pantetheine were externally applied by spraying, they supported normal seed development in siliques of selfed heterozygous *PTS/pts-1* plants. It is not clear how those supplements were available to the developing seeds. One explanation is that pantothenate and pantetheine diffused through the silique tissue and then became available for the developing seeds. Another possibility is that those supplements were actively transported. Clearly, pantothenate can be transported through the vascular system in *pts* mutants. This was demonstrated by supplementation of this chemical into growth medium (section 3.4.2 and 3.4.3). However, the complementation by spaying may or may not work via vascular transport.

5.4 Genetic complementation

The question addressed by this analysis was whether the *panC* gene, which encodes PTS in *E. coli*, can rescue plants lacking a functional *PTS* allele (section 3.6), *i.e.* whether it is possible to generate viable *pts-1/pts-1* plants complemented by *panC*. A transgenic line of *Arabidopsis thaliana* overexpressing the bacterial *panC* gene was generated. This plant was then used as a pollen donor in a cross with a *pts-1* segregating line to generate *pts-1* knock out

plants complemented with the *E. coli panC* gene. In a PCR-based screen such plants were identified. The *E. coli* panC gene turned out to rescue *pts-1/pts-1* mutants (section 3.6). No one plant lacking *PTS* gene was identified indicating selective elimination of *pts-1* homozygotes. This finding is consistent with the assumption that *pts-1/pts-1* plants lack PTS activity. Segregation rate and observed seed lethal phenotype (one of four) among homozygous *pts-1* plants complemented by *panC* gene suggest that those plants are heterozygous for *panC*. The analysis was complicated by the fact that the *panC* gene donor plant was generated by *Agrobacterium*-mediated transformation, so the insertion point in Arabidopsis genome of T-DNA carrying *panC* expression cassette is unknown. Consequently, it was impossible by PCR approach (section 3.6.1) to determine the number of copies of the *panC* gene in complemented *pts-1* knock out plants. Nevertheless, the bacterial gene was expressed in Arabidopsis in functional form. This was confirmed by western-blot analysis and by the fact that the *panC* transgene was able to complement the *pts-1* mutation. The fact that the *E. coli panC* gene complements the *pts-1* mutation also proves that the bacterial and plant enzyme encoded by these genes are functionally conserved.

The complementation experiment along with pantothenate-chemical rescue of homozygous *pts-1* plants supports the view that plants poses only one pathway leading to pantothenate. However, the presence of additional biosynthetic pathway leading to pantothenate cannot be finally excluded. The second pathway leading to pantothenate may exist but pantothenate synthesised via this hypothetical route may not be sufficient to meet pantothenate requirements in *pts-1/pts-1* mutants. However, considering the embryo terminal phenotype of the *pts* mutants (section 3.3), this seems unlikely.

5.5 Plants overexpressing the *E. coli panC* gene

Wild type *Arabidopsis thaliana* Col-0 were transformed by infiltration method with *Agrobacterium* harbouring a binary plasmid vector whose T-DNA portion contained the *E. coli panC* gene under the CaMV 35S promoter and the *hptII* hygromicin resistance gene. Three different versions of this construct were generated (Fig. 3.8)

Plastidic or mitochondrial signal peptides for the rubisco small subunit (3b) and the mitochondrial chaperon protein (HSP60) were used for plastidic and mitochondrial expression, respectively. Seeds from infiltrated plants were plated of ½ MS selective medium containing hygromicin. A single T1 transformant carrying the cytosolic overexpressing construct, ten T1 plants with the mitochondrial, and six T1 plants with the plastidic construct were recovered. Progeny (T2) from these lines were also resistant to hygromicin. The

presence of the transgene was confirmed, in all selected resistant plants, by PCR. During this analysis the T-DNA containing fragment of the 35S promoter and/or sequence for target peptide and fragment of the *panC* gene were amplified. Although the transgene was detected (Fig. 3.9), western-blot analysis showed that only plants carrying cytosolic construct expressed *E. coli* PTS (Fig. 3.10). There are several possible explanations. First, on the basis of PCR-based genotyping analysis, it is not known whether the complete sequence of the expression cassettes, required for functional expression of *panC* is present in the analysed transgenic plants. All expression plasmids were partially sequenced. In this analysis a fragment of the *panC* gene and targeting sequences were confirmed. It is also unlikely that incomplete T-DNA or mutation in ORF took place because the lack of the expression was observed in 10 and 6 independent transformants carrying mitochondrial and plastidial constructs, respectively. A more likely explanation is that silencing took place.

There are two kinds of gene silencing. Firstly, transcriptional gene silencing (TGS), which results from promoter inactivation, and secondly, post-transcriptional gene silencing (PTGS), which occurs when the promoter is active but the mRNAs fails to accumulate (reviewed in Stam *et al*., 1997). Even though this difference suggests two distinct silencing mechanisms, the two seems to be related, in particular when one invokes interaction between homologues DNA sequences (reviewed in Stam *et al*., 1997). Transgene silencing cannot be explained by a single mechanism. Multiple mechanisms involving DNA-DNA, DNA-RNA, or RNA-RNA interactions may be evoked (Fagard and Vaucheret, 2000). TGS can be triggered in *cis* or in *trans*. *Cis*-acting elements may be endogenous heterochromatin surrounding the transgene locus, endogenous repeat and methylated elements located close to the transgene locus, transgene-genomic junctions that disturb chromatin organization, or particular arrangements of transgene repeats that create heterochromatin locally (reviewed in Fagard and Vaucheret, 2000). *Trans*-acting elements may be allelic or ectopic homologues loci that potentially transfer their epigenetic state by direct DNA-DNA pairing or protein-mediated DNA-DNA interactions, or ectopic transgene or nuclear DNA viruses that produce a diffusible signal (aberrant RNA, PTGS-targeted viral RNA) that potentially imposes an epigenetic silent state by interaction with the homologous promoter of target transgenes (reviewed in Fagard and Vaucheret, 2000). PTGS, like TGS, can occur in *cis* (only the RNA transcribed from silencing source is degraded), simultaneously in *cis* and *trans* (RNA transcribed from the silencing source and all homologous RNA are degraded), or in *trans* (only RNA that is homologous to RNA transcribed from the silencing source is degraded, but not the RNA transcribed from the source) (Fagard and Vaucheret, 2000).

The *panC* and *PTS* sequence similarity seems to be too low to induce silencing. Nevertheless, if silencing takes place, then it is PTGS occurred in *cis,* because apparently only the transgene is silenced. In case where both RNAs from transgene and homologues locus were silenced it would lead to lethality, as it has been discussed above that *pts* knock-out is lethal. This hypothesis can be rejected because all plants carrying above constructs were viable, although it should be noted that transcript level was not analysed. In the opposite situation, *i.e*. when the transgene would initiate PTGS leading to the degradation of the homologues RNA from endogenous genes (co-suppression), such transgenic plants should express the transgene which could then potentially complement the lack of PTS protein. This could be the case for plants expressing *panC* in the cytosol, where expression of the *E. coli* PTS was observed, but was not observed in plants expressing *panC* in the plastids and mitochondria as no *E. coli* PTS protein was detected in western blot analysis (Fig. 3.10).

The major difference between the plants expressing *panC* in the cytosol on one hand and the plants expressing *panC* in the plastids and mitochondria on the another is the presence of the Arabidopsis targeting sequences. Considering that transgenic plants expressed the *E. coli* PTS in the cytosol, the targeting sequences were the most likely to be responsible for the lack of expression. An attractive model explaining PTGS invokes an effect of highly expressed transgenes, as it could be the case in transgenic *A. thaliana* overexpressing *panC* in plastids or mitochondria (under the control of CaMV35S promoter). In this model, the transgenes produce so much RNA that the level exceeds a critical threshold thereby triggering a mechanism that specifically removes all homologous RNAs irrespective of their source (Stam *et al*., 1997). This mechanism is plausible considering the targeting sequences were of Arabidopsis origin. The overexpression of those Arabidopsis signal peptides (rubisco 3b small subunit and mitochondrial chaperonin 60) in transgenic Arabidopsis plants could reach that hypothetical threshold leading to silencing. However, this would be in contradiction to report by Logan and Leaver (2000) who successfully targeted GFP into mitochondria using the Arabidopsis mitochondrial chaperonin 60 signal sequence.

5.6 Evolution of allostery in plant pantothenate synthetases

Two lines of evidence support conclusion that the allosteric properties of PTS are conserved in all plant pantothenate synthetases. First, the characteristics of substrate inhibition by pantoate are similar for the PTS enzymes from Arabidopsis (this study), *Lotus japonicus* (Genschel *et al*., 1999). Second, all available plant PTS sequences contain a dimerization region characterized by an insertion relative to *E. coli* PTS and the ^{131}HETWIRVER^{139} motif,

both of which are important for allosteric interactions in PTS. PTS arose in the bacterial domain and was inherited, presumably independently, by plants and fungi (Genschel, 2004). Subsequent selection for and maintenance of a divergent dimerization region in the plant lineage of the PTS protein family indicate that the associated allosteric properties have an important role in the biosynthesis of pantothenate in plants. This leads to the question in which way allostery of plant pantothenate synthetases might be physiologically relevant. Allostery of PTS has two important consequences for catalysis, *i.e.* increased catalytic efficiency at low pantoate levels and substrate inhibition at elevated pantoate levels. Although pantoate has not been determined in plants, it can be argued that the latter enzymatic feature is not important *in vivo*. If the concentration of pantoate in the cytosol, where PTS is localized (Ottenhof *et al*., 2004), was within the range where substrate inhibition is significant (*i.e.* above 0.1 mM) it would need to change by at least 10-fold in order to cause a 2-fold change in *A. thaliana* PTS activity (Table 4.4). Thus, inhibition of *A. thaliana* PTS by pantoate is unlikely to constitute an efficient regulatory mechanism. On the other hand, if cytosolic pantoate levels were well below 0.1 mM, substrate inhibition would be negligible while the high specificity of PTS for pantoate would benefit the overall rate of pantothenate synthesis.

Pantothenate biosynthesis in plants is more complex than in bacteria in that the pathway is compartmentalized, and it can be speculated that allostery arose in plant pantothenate synthetases as an adaptation to this compartmentation. The committed step of pantothenate biosynthesis in plants, the formation of ketopantoate from 2-ketovalerate, takes place in the mitochondria (Ottenhof *et al*., 2004). Even though the reductase responsible for converting ketopantoate into pantoate is still unknown in plants, sequestration of the committed step is consistent with a scenario where pantoate accumulates in the mitochondria and pantothenate synthesis is controlled and limited by the supply of pantoate to the cytosol. In this hypothetical model, the specific catalytic properties of plant pantothenate synthetases have no regulatory function but allow robust synthesis of pantothenate from low amounts of pantoate. The conservation of active site residues in pantothenate synthetases from bacteria, plants, and fungi (Fig. 4.1A) suggests that the active site does not easily tolerate mutations. Consequently, active site mutations may not have been available during the evolutionary process that led to the divergent catalytic properties of plant pantothenate synthetases. It appears that plant pantothenate synthetases nicely fit an earlier prediction (Conway *et al*., 1968) that optimization of catalytic properties is preferably achieved by adjusting allosteric subunit interactions when the active site has little or no freedom to evolve.

5.7 Is there a parallel pathway leading to pantothenate?

Analysis of the Arabidopsis genome for genes and proteins homologous to the *E. coli* gene for ketopantoate reductase (*panE*) and its product indicated no significant hits (Ottenhof *et al*., 2004). It is possible that the plant ketopantoate reductase has diverged in its sequence from the microbial counterparts and hence comparative sequence analyses could not identify them. The identity of the enzyme that carries out the reduction step in pantothenate biosynthesis in the cytosol remains elusive.

As it was described in section 1.2.2, results shown by Julliard (1994), suggested the existence of parallel pathway from α- ketoisovalerate to pantothenate in plant cells. This pathway was suggested to proceed via ketopantoyl-lactone, and pantoyl lactone (left-hand branch in Fig 5.4).

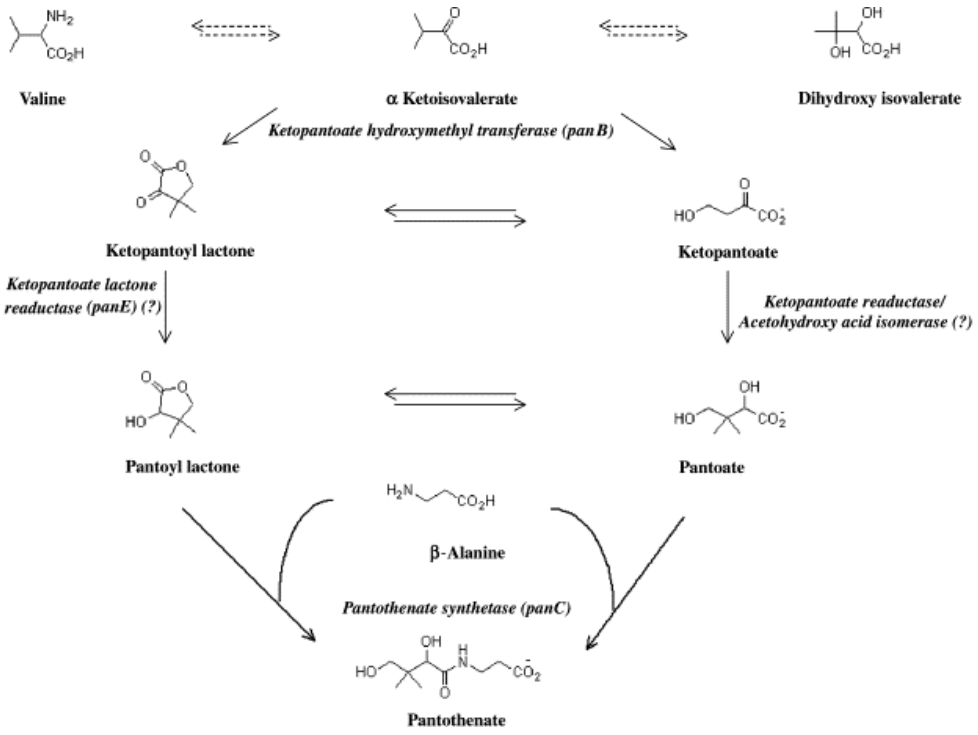

Fig. 5.4 A suggested route of pantothenate synthesis in plants (copied from Raman and Rathinasabapathi, 2004). Direct evidence for the participation of the enzymes marked with a question mark is not available. Se text for details.

Ketopantoyl-lactone reductase, believed to convert ketopantoyl-lactone to pantoyl-lactone was partially purified and characterized from spinach (*Spinacia oleracea*) leaves (Julliard, 1994). This study suggested that this enzyme may be involved in pantothenate synthesis since pantoyl-lactone, the putative product of the reaction and not pantoate, was required for the appearance of pantothenate in the presence of β-alanine, ATP–Mg and chloroplast stroma

(Julliard, 1994). The partially purified enzyme showed Michaelis–Menten type kinetics for the following compounds: ketopantoyl-lactone (K_m = 26 μM), isatin (K_m = 10 μM), bornanedione (K_m = 12.5 μM), and 8-bromobornanedione (K_m = 15 μM). Lower K_m values for the latter three substrates (compounds that are common substrates of short chain dehydrogenase/reductases), together with the fact that the enzyme it had low specific activity indicate that ketopantoyl reductase identified in this study might not be specific for the pantothenate synthetic pathway alone, *i.e.* the enzyme is probably a non-specific dehydrogenase (Chakauya *et al*., 2006). Furthermore, as its product is pantoyl-lactone, it is unlikely to be involved in pantothenate biosynthesis mediated by *PTS* -encoded pantothenate synthetase, because the latter cannot use pantoyl-lactone as substrate (Genschel *et al*., 1999). Surprisingly, Rathinasabapathi and Raman (2005) reported a significant increase in pantothenate levels in tomato leaf discs fed with pantoyl-lactone (see section 5.7). This supports the view that there is an alternative pathway located in the chloroplast that involves a pantoyl lactone- dependent pantothenate synthetase. An argument against a parallel pathway to pantothenate is the embryo-lethal phenotype of the *pts* mutants plants. The knock-out of *PTS* (section 3.3) indicate that no any other enzyme can assure synthesis of pantothenate in quantities which are sufficient to support normal development. Therefore, parallel pathway leading to pantothenate seems to be unlikely.

5.8 Overproduction of pantothenate in plants

In this work it has been demonstrated that overexpression of *E. coli panC* in cytosol in transgenic *A. thaliana* led to increased PTS activity but did not lead to increased pantothenate levels. This result is consistent with the recent report of Chakauya *et al*. (2006) who met with no success when trying to elevate pantothenate level in *A. thaliana* by overexpressing the *A. thaliana PTS* gene. The above results suggest that PTS activity is not limiting the pantothenate level, consequently PTS is not a target for improving the vitamin content in *A. thaliana*. As discussed above kinetic data indicate that *A. thaliana* PTS seems to be tuned to catalyse pantothenate synthesis very efficiently at low substrate concentrations and substrate inhibition (pantoate) presumably does not play a role in regulation of pantothenate level *in vivo*. Therefore, the limiting factors for pantothenate synthesis are probably substrates, not the activity of PTS. Recently it has been demonstrated that overexpression of *E. coli panD* gene encoding L-aspartate-α-decarboxylase in tobacco lead to increased level of β-alanine (1.2 to 4- fold) and pantothenate (3.2 to 4.1- fold) (Fouad and Rathinasabapathi, 2006). This result suggests that β-alanine availability is limiting pantothenate synthesis in tobacco leaves. This

result is in contradiction with an earlier study of Rathinasabapathi and Raman (2005). When excised leaves of *L. latifolium*, *Phaseolus vulgaris*, *Lycopersicon esculentum* and *Citrus* x *paradisi* where incubated in nutrient medium supplemented with 1mM β-alanine, pantothenate level did not increase significantly in any of these species (Rathinasabapathi and Raman, 2005). Interestingly, exogenous supply of 1 mM pantoyl lactone to excised leaves significantly increased pantothenate levels in the leaves from all the four species (Rathinasabapathi and Raman, 2005). Pantoyl lactone, inside the plant cell, could be expected to yield pantoate *via* hydrolysis. Activities of ketopantoyl lactone reductase and a pantoyl lactone-dependent pantothenate synthetase were known in spinach (Julliard, 1994), but no direct evidence is available for a biosynthetic pathway leading to pantothenate via the lactone forms of ketopantoate and pantoate in any organism (Ottenhof *et al*., 2004). In a time-course experiment, wherein tomato leaflets were supplied with pantoyl lactone, pantothenate increased linearly (from ≈ 2 to ≈ 11 nmol g^{-1} f.wt after 24 hours) (Rathinasabapathi and Raman, 2005). Also, when tomato leaflets were supplied with 1 mM D-pantoate for 24 hours, pantothenate level increased significantly (to ≈ 90 nmol g^{-1} f.wt) (Rathinasabapathi and Raman, 2005). Such increases were not observed for negative controls or β-alanine-supplied leaflets although β-alanine uptake was observed (≈ 300 nmol of β-alanine g^{-1} f.wt) (Rathinasabapathi and Raman, 2005). In the light of this experiment, Rathinasabapathi and Raman (2005) suggest that pantoate could be rate-limiting for pantothenate synthesis in leaf tissue in the species examined. An alternative explanation proposed by the authors for increased pantothenate levels following the supply of pantoyl lacton was that pantoyl lactone or its derivatives reduced coenzyme A synthesis by inhibiting pantothenate kinase, thus elevating the free pantothenate levels. These explanations are not mutually exclusive, but regulation of plant pantothenate kinase by pantoyl lactone or its derivatives has not been tested (Falk and Guerra, 1993).

In the light of the above studies it seems promising to increase pantothenate level in plants by overexpressing bacterial enzymes producing substrates for pantothenate synthetase, *i.e.* ketopantoate hydroxymethyltransferase, ketopantoate reductase and aspartate decarboxylase. The source of β-alanine in plants has not been determined but *E. coli* aspartate decarboxylase has been shown to be active in transgenic tobacco overexpressing this protein (Fouad and Rathinasabapathi, 2006). Ketopantoate reductase, in turn, has not been identified in plants yet. Overexpressing both *E. coli* enzymes (ketopantoate reductase and aspartate decarboxylase) would be expected to increase pantothenate level to higher level than overexpressing those proteins alone. Moreover, it has been reported that tobacco plants overexpressing *E. coli*

aspartate decarboxylase were more resistant to heat stress than wild type plants (Rathinasabapathi and Raman, 2005). It would be desirable to determine whether the reported termotolerance is attributed to increased β-alanine level or pantothenate.

Taking together the results of this work, a new model of the regulation of pantothenate production in plants can be proposed (Fig. 5.5). The key steps limiting pantothenate production in plants seem to be the enzyme that supply pantoate and β-alanine. Of these enzymes, only KPHMT has been described in plants so far. *A. thaliana* pantothenate synthetase is not a regulatory enzyme. It is tuned to catalyse the synthesis of pantothenate very efficiently at physiological substrate concentrations. Therefore, the enzyme is not a target for engineering a transgenic plant overproducing the vitamin.

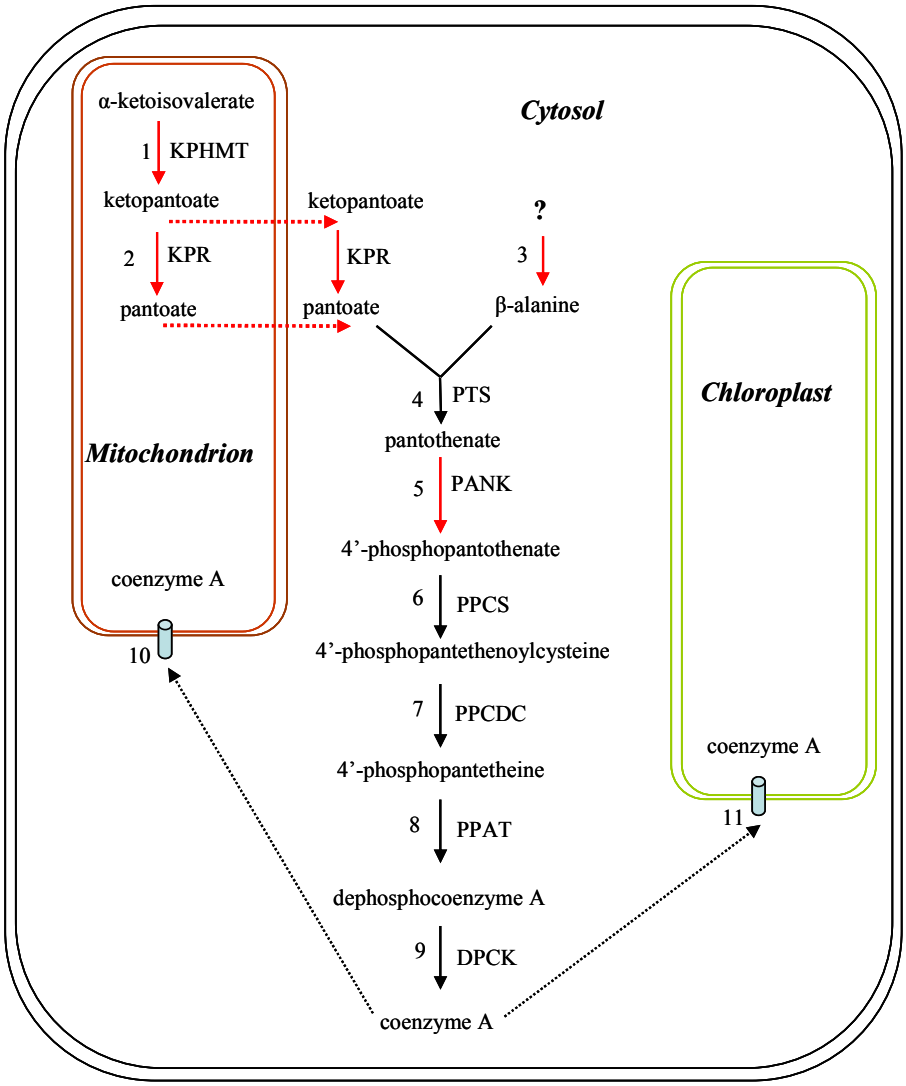

Fig. 5.5 Proposed model for pantothenate and coenzyme A biosynthesis in the plant cell.
Limiting steps in the pathway are shown by red arrows. Individual reaction or transport steps are numerated, and the evidence for each step is listed below.
1, Jones *et al*. (1994), Ottenhof *et al*. (2004)*;
2, No plant KPR has yet been identified in plants and it is unclear whether ketopantoate or pantoate is exported from the mitochondrion. Jones *et al*. (1994), Coxon *et al*. (2005), Matak-Vinkovic *et al*. (2001); Lobley *et al*. (2003), Kallberg *et al*. (2002), Chakauya *et al* (2006).
3, The source of β-alanine in plants is not known, although several routes have been proposed. Raman and Rathinasabapathi (2004), Coxon *et al* (2005), Awai *et al*. (1995, 2004), Duhaze *et al*. (2003), Chakauya *et al*. (2006), Rathinasabapathi (2002), Ottenhof *et al*. (2004), White *et al*. (2001)
4, this study, Sahi *et al*. (1988), Genschel *et al*. (1999), Ottenhof *et al*. (2004)*, Falk and Guerra (1993), Kupke *et al*. (2003)
5, Pantothenate kinase has a regulatory properties as it is feedback inhibited by coenzyme A and coenzyme A esters therefore, it represents rate-determining step in coenzyme A biosynthesis (Vallari *et al*., 1987). Tilton *et al*. (2006), Kupke *et al* (2003)
6, Kupke *et al*. (2003)
7, Kupke *et al*. (2003), Rubio *et al*. (2006),
8, **9**, Kupke *et al*. (2003)
10, A transporter for coenzyme A has been reported in potato mitochondria (Neuburger *et al*., 1984; Yang *et al*., 1994). Since coenzyme A is transported into mitochondria a mitochondrial site of coenzyme A synthesis may not be necessary.
11, Evidence exists that chloroplasts also have coenzyme A import capability (Savage and Post-Beittenmiller, 1994).
* subcellular location of the protein has been confirmed.

Chapter 6

Bibliography

Aberhart, D.J., Russell, D.J. (1984) Steric course of ketopantoate hydroxymethyltransferase in *Escherichia coli. J. Am. Chem. Soc*. **106**, 4902-4906.

Abiko, Y. (1975) in Metabolic Pathways pp 1-25, Academic Press, New York

Aida, M., Ishida,T., Fukaki, H., Fujisawa, J., Tasaka, M. (1997) Genes involved in organ separation in Arabidopsis: an analysis of the *cup-shaped cotyledon* mutant. *Plant Cell* **9**: 841-857.

Airas R.K., (1988) Pantothenases from pseudomonas produce either pantoyl lactone or pantoic acid. *Biochem. J*., **250**: 447-451

Albert, A., Dhanaraj, V., Genschel, U., Khan, G., Ramjee, M.K., Pulido, R., Sibanda, B. L., von Delft, F., Witty, M.,. Blundell, T.L., Smith A.G., Abell, Ch. (1998) Crystal structure of aspartate decarboxylase at 2.2 Å resolution provides evidence for an ester in protein self−processing. *Nature Structural Biology* **5**: 289 – 293.

Alonso, J.M., Stepanova, A.N., Leisse, T.J,, Kim C.J., Chen, H., Shinn, P., Stevenson, D. K, Zimmerman, J., Barajas, P., Cheuk, R., Gadrinab, C., Helle,r C., Jeske, A., Koesema, E., Meyers, C.C., Parker, H., Prednis, L., Ansari, Y., Choy, N., Deen., H., Geralt, M., Hazari, N., Hom, E., Karnes, M., Mulholland, C., Ndubaku, R., Schmidt, I., Guzman, P., Aguilar-Henonin, L., Schmid, M., Weigel, D., Carter, D. E., Marchand, T., Risseeuw, E., Brogden, D., Zeko, A., Crosby, W. L., Berry, C. C., Ecker, J. R. (2003) Genomewide insertional mutagenesis of *Arabidopsis thaliana*. *Science* **301**: 653–657.

Arabidopsis Genome Initiative (2002) Analysis of the genome sequence of the flowering plant *Arabidopsis thaliana*. *Nature*, **408**: 796-815.

Aravind, L., Anantharaman V, Koonin, E.V. (2002) Monophyly of class I aminoacyl tRNA synthetase, USPA, ETFP, photolyase, and PP-ATPase nucleotide-binding domains: implications for protein evolution in the RNA. *Proteins* **48:** 1-14

Assaad, F., Huet, Y., Mayer, U., Jurgens, G. (2001) The cytokinesis gene *KEULE* encodes a Sec1 protein that binds the syntaxin KNOLLE. *J. Cell Biol*. **152**: 531-544.

Awal, H.M.A., Yoshida, I., Doe, M., Hirasawa, E. (1995) 3-Aminopropionaldehyde dehydrogenase of millet shoots. *Phytochemistry* **40**: 393–395.

Azpiroz-Leehan, R., Feldmann, K.A. (1997) T-DNA insertion mutagenesis in Arabidopsis: Going back and forth. *Trends Genet*. **13:** 152–159.

Begley, T.P., C. Kinsland, E. Strauss. (2001) The biosynthesis of coenzyme A in bacteria. *Vitam. Horm*. **61**: 157–171.

Berleth, T., and Chatfield, S. (2002) Embryogenesis: pattern formation from a single cell. The Arabidopsis Book. *American Society of Plant Biologist.*

Biou, V., Dumas, R., Cohen-Addad, C., Douce, R., Job, D., Pebay-Peyroula, E. (1997) The crystal structure of plant acetohydroxy acid isomeroreductase complexed with NADPH, two magnesium ions and a herbicidal transition state analog determined at 1.65 A resolution. *EMBO J.* 16: 3405-3415.

Bjerrum, O. J., Schafer-Nielsen, C. (1986) Buffer systems and transfer parameters for semidry electroblotting with a horizontal apparatus. In: Dunn M J. editor. Electrophoresis 86. Weinheim, Germany: VCH; 1986. pp. 315–327.

Boyes, D.C., Zayed, A.M., Ascenzi, R., McCaskill, A.J., Hoffman, N.E., Davis, K.R., Gorlach, J.(2001) Growth stage-based phenotypic analysis of Arabidopsis: a model for high throughput functional genomics in plants. *Plant Cell*. **13**:1499-510.

Bradford, M.M (1976) A rapid and sensitive method for quantitation of microgram quantities of protein utilizing the principle of protein-dye-binding. *Anal Biochem* **72**:248-54.

Brown, G.M., (1959) The metabolism of pantothenic acid *J.Biol. Chem.* **234**: 370-378.

Bullock, W.O., Fernandez, J.M., Short, J.M. (1987) XL1-Blue: A high efficiency plasmid transforming rec A *Escherichia coli* strain with beta-galactosidase selection. Biotechniques **5**: 376 - 379.

Chakauya, E., Coxon, K.M., Whitney, H.M., Ashurst, J.L., Abell, C., Smith A.G., (2006) Pantothenate biosynthesis in higher plants: advances and challenges. *Physiol. Plant*. **126**: 319-329.

Chassagnole, C., Diano, A., Letisse, F., Lindley, N.D. (2003) Metabolic network analysis during fed-batch cultivation of *Corynebacterium glutamicum* for pantothenic acid production: first quantitative data and analysis of by-product formation. *J. Biotechnol*. **104:** 261-72.

Chaudhuri, B.N., Sawaya, M.R., Kim, C.Y., Waldo, G.S Park, M.S., Terwilliger, T.C. and. Yeates, T.O. (2003) *Structure (London)* **11**: 753.

Chenna, R., Sugawara, H., Koike, T., Lopez, R., Gibson, T.J, Higgins, D.G., Thompson, J.D. (2003) Multiple sequence alignment with the Clustal series of programs. *Nucleic Acids Res* **31:** 3497-3500.

Cornish-Bowden, A. (1975) The use of the direct linear plot for determining initial velocities. *Biochem J* **149:** 305-312.

Cornish-Bowden, A., Cardenas ML (1987) Co-operativity in monomeric enzymes. *J Theor Biol* **124:** 1-23.

Conway, A., Koshland, D.E.Jr., (1968) Negative cooperativity in enzyme action. The binding of diphosphopyridine nucleotide to glyceraldehyde 3-phosphate dehydrogenase. *Biochemistry* **7:** 4011-4023.

Coxon, K.M., Chakauya, E., Ottenhof, H.H., Whitney, H.M., Blundell, T.L., Abell, C., Smith, A.G., (2005) Pantothenate biosynthesis in higher plants *Biochem. Soc. Trans.* **33**: 743-746.

Cronan, J.E., (1980), β-alanine synthesis in *Escherichia coli*. *J. of Bacter.* **141**: 1291-1297.

Cronan, J.E.Jr., Little, K.J., Jackowski, S. (1982) Genetic and biochemical analyses of pantothenate biosynthesis in *Escherichia coli* and *Salmonella typhimurium. J. Bacteriol.* **149:** 916–922.

Cronan, J.E., Jr (1980) Beta-alanine synthesis in *Escherichia coli*. J. Bacteriol. **141**: 1291-1297.

Cronan, J.E.Jr., Little, K.J., Jackowsk, S. (1982) Genetic and biochemical analyses of pantothenate biosynthesis in *Escherichia coli* and *Salmonella typhimurium. J. Bacteriol.* **149:** 916–922.

Dakshinamurti, K., Bhagavan, N.H. eds (1985) *Biotin. Ann NY Acad Sci* **447:** 1–441.

Duhaze, C., Gagneul, D., Lepor, L., Larher, R.F., Bouchereau, A. (2003) Uracil as one of the multiple sources of b-alanine in Limonium latifolium, a halotolerant β-alanine betaine accumulating *Plumbaginaceae*. *Plan.t Physiol. Biochem.* **41**: 993–998.

Dusch, N., Pühler, A., Kalinowski, J., (1999) Expression of the *Corynebacterium glutamicum panD* Gene Encoding l-Aspartate-α-Decarboxylase Leads to Pantothenate Overproduction in *Escherichia coli*. *Appl Environ Microbiol*.**65**: 1530–1539.

Eigen, M. (1967) Kinetics of reaction control and information transfer in enzymes and nucleic acids. Nobel Symp 1967;5:333–369.

Elischewski, F., Pühler, A., Kalinowski, J. (1999) Pantothenate production in *Escherichia coli* K12 by enhanced expression of the *panE* gene encoding ketopantoate reductase. *J. Biotechnol*. **75**: 135-146.

Fagard, M., Vaucheret, H. 2000 (Trans)gene silencing in plants: how many mechanisms? *Annu Rev Plant Physiol Plant Mol Biol*. **51**:167-194

Falk, K.L., Guerra, D.J., (1993) Coenzyme A biosynthesis in plants: partial purification and characterization of pantothenate kinase from spinach. *Arch. Biochem. Biophys.* **301**: 424-430.

Fersht, A.R. (1975) Demonstration of two active sites on a monomeric aminoacyl-tRNA synthetase. Possible roles of negative cooperativity and half-of-the-sites reactivity in oligomeric enzymes. *Biochemistry* **14:** 5-12.

Fersht, A.R., Wilkinson, A.J., Carter, P., Winter. G. (1985) Fine structure-activity analysis of mutations at position 51 of tyrosyl-tRNA synthetase. *Biochemistry* **24:** 5858-5861.

Fersht, A. R. (1999) *Structure and mechanism in protein science*, W. H. Freeman & Co, NewYork.

Fouad, W.M., Rathinasabapathi, B. (2006) Expression of bacterial L-aspartate-alpha-decarboxylase in tobacco increases beta-alanine and pantothenate levels and improves thermotolerance. *Plant Mol Biol*. **60**:495-505.
Frodyma, M.E., Downs, D. (1998) The *pan*E gene, encoding ketopantoate reductase, maps at 10 minutes and is allelic to *apbA* in *Salmonella typhimurium*. *J. Bacteriol*. **180**, 4757-4759.

Genschel, U., Powell, C.A., Abell, C., Smith, A.G. (1999) The final step of pantothenate biosynthesis in higher plants: cloning and characterization of pantothenate synthetase from *Lotus japonicus* and *Oryza sativum* (rice). *Biochem. J*. **341:** 669–678.

Genschel, U. (2004) Coenzyme A biosynthesis: reconstruction of the pathway in archaea and an evolutionary scenario based on comparative genomics. *Mol. Biol. Evol.,* **21**: 1242-1251.

Gerdes, S.Y., Scholle, M.D., D'Souza, M., Bernal, A., Baev, M.V., Farrell, M., (2002) From Genetic Footprinting to Antimicrobial Drug Targets Examples", *J Bacteriol*. **184**: 4555–4572.

Goodhue, C.T., Snell, E.E. (1966) The bacterial degradation of pantothenic acid. Over-all nature of the reaction. *Biochemistry*. **5**: 393-398.

Grossniklaus, U., Vielle-Calzada, J.P., Hoeppner, A.A., Gagliano, W.B. (1998) Maternal control of embryogenesis by *MEDEA* a *polycomb* group gene in Arabidopsis. *Science* **280**: 446-450.

Gunasekaran, K., Ma, G., Nussinov, R. (2004) Is allostery an intrinsic properyo of all dynamic proteins? *Proteins: Structure, Function, and Bioinformatics* **57**: 433–443.

Hardtke, G.C., Berleth, T. (1998) The Arabidopsis gene *MONOPTEROS* encodes a transcription factor mediating embryo axis formation and vascular development. *EMBO J.* **17**:1405-1411.

Helmstaedt, K., Kramppmann, S., Braus, G, H. (2001) Allosteric regulation of catalytic activity: Escherichia coli Aspartate transcarbamoylase versus Yeast chorismate mutase. *Microbiology and Molecular Biology Reviews*, **65**: 404-421.

Hirschi, K.D. (2003) Insertional mutants: a foundation for assessing gene function. *Trends in Plant Science* **8**: 205–208.

Ho, S.N., Hunt, H.D., Horton, R.M., Pullen, J.K, Pease, L.R. (1989) Site-directed mutagenesis by overlap extension using the polymerase chain reaction. *Gene* **77:** 51-59.

Huh, W.K., Falvo, J.V., Gerke, L.C., Carroll, A.S., Howson, R.W., Weissman, J.S., O'Shea, E.K. (2003) Global analysis of protein localization in budding yeast. *Nature* 16: 686-689.

Jackowski, S., Rock, C.O. (1981) Regulation of coenzyme A biosynthesis. *J. Bacteriol.,* **148:** 926–932.

Jackowski, S.,. Alix, J.H.J. (1990) Cloning, sequence, and expression of the pantothenate permease (panF) gene of *Escherichia coli*. *Bacteriol* **172**: 3842–3848.

Jang, J. C., Fujioka, S., Tasaka, M., Seto, H., Takatsuto. (2000) Acritical role of sterols In embryogenic pattering and meristem programming revealed by the *fackel* mutant of *Arabidopsis thaliana. Genes Dev*. **14**: 1471-1484.

Jones, C., E., Brook, J., M., Abell, C., Smith, A., G., (1993) Cloning and sequencing of the *Escherichia coli panB* gene, which encodes ketopantoate hydroxymethyltransferase, and overexpression of the enzyme. *J Bacteriol*; **175**: 2125–2130.

Jones, C. E., Dancer, J. E., Smith, A. G. Abell, C. (1994) Evidence for the pathway to pantothenate in plants. *Can. J. Chem*. **72**: 261-263.

Julliard, J.H. (1994) Purification and characterization of oxypantoyl lactone reductase from higher plants: role in pantothenate synthesis. *Bot. Acta*. **107**: 191–200.

Kleinkauf, H. (2000) The role of 4'-phosphopantetheine in the biosynthesis of fatty acids, polyketides and peptides. *Biofactors*. **11**:91-2.

Konz, C., Schell, J. (1986) The promoter of TL-DNA gene 5 controls the tissue-specific expression of chimaeric genes carried by a novel type of *Agrobacterium* binary vector. *Mol. Gen. Genet*. **204:** 382-396

Koshland, D.E., Nemethy, G., Filmer, D. (1966) Comparison of experimental binding data and theoretical models in proteins containing subunits. Biochemistry **5**:365- 385

Koshland, D.E. Jr, Hamadani, K. (2002) Proteomics and models for enzyme cooperativity. *J Biol Chem* **277:** 46841-46844.

Koser, S. A. (1968)Vitamin Requirements of Bacteria and Yeasts. Springfield, Ill. : Thomas,.

Krysan, P.J., Young, J.C., Tax, F., and Sussman, M.R. (1996). Identification of transferred DNA insertions within Arabidopsis genes involved in signal transduction and ion transport. *Proc. Natl. Acad. Sci*. *USA* **93,** 8145–8150.

Krysan, P.J., Young, J.C. Sussman, M.R. (1999). T-DNA as an insertional mutagen in Arabidopsis. *Plant Cell* **11:** 2283–2290.

Kupke, T., Hernández-Acosta, P., Culiáñez-Macià, F.A. (2003) 4'-phosphopantetheine and coenzyme A biosynthesis in plants. *J. Biol. Chem.* **278**:38229-38237.

Kurtov, D., Kinghorn, J.R., Unkles, S.E. (1999) The *Aspergillus nidulans panB* gene encodes ketopantoate hydroxymethyltransferase, required for biosynthesis of pantothenate and coenzyme A. *Mol.Gen. Genet*. **262**: 115-120.

Kyjovska, Z., Repkova, J., Relichova, J. (2003) New embryo lethals in *Arabidopsis thaliana*: basic genetic and morphological study. *Genetica*. **119**: 317-25.

Laemmli, U. K. (1970) Cleavage of structural proteins during the assembly of the head of bacteriophage T4. Nature. **227**:680–685.
Leonardi, R., Zhang, Y.M., Rock, C.O., Jackowski, S. (2005) Coenzyme A: back in action. *Progress in lipid research*, **44**: 125-153.

Li, Z., Thomas, T. L. (1998) *PEI1*, an embryo-specific zinc finger protein gene required for heart-stage embryo formation in Arabidopsis. *Plant Cell* **10**: 383-398.

Lobley, C.M. Schmitzberger, F., Kilkenny, M.L., Whitney, H., Ottenhof, H.H., Chakauya E., Webb, M.E., Birch, L.M., Tuck, K.L, Abell, C., Smith, A.G., Blundell, T.L. (2003) Structural insights into the evolution of the pantothenate-biosynthesis pathway. *Biochem. Soc. Trans*. **31**:563-71.

Logan, D. C., Leaver, C. J. (2000) Mitochondria-targeted GFP highlights the heterogeneity of mitochondrial shape, size and movement within living plant cell. *Journal of Experimental Botany* **51**: 865-871.

Lotan, T., Ohto, M., Yee, K. M., West, M. A., Lo, R. (1998) Arabidopsis LEAFY COTYLEDONI is sufficient to induce embryo development in vegetative cells. *Cell* **93**: 1195-1205.

Lukowitz, W., Mayer, U., Jurgens, G. (1996). Cytokinesis in the Arabidopsis embryo involves the syntaxin-related *KNOLLE* gene product. *Cell* **84**: 61-71.

Margulis, L., (1970) Origin of Eukaryotic Cells. *Yale University Press, New Haven*.

Mass, W.K. (1952) Pantothenate studies. II. Evidence from mutants for interference by salicylate with pantoate synthesis. *J. Bacteriol*. **63**:227-232.

Mass. (1960) W.K., The biosynthesis of pantothenic acid, *ed. W. Umbriet and H. Molitor, New York,*.

Matak-Vinkovic, D., Vinkovic, M., Saldanha, S.A. (2001) Crystal structure of *Escherichia coli* ketopantoate reductase at 1.7 Å resolution and insight into the enzyme mechanism. *Biochemstry*, **40**: 14493-14500.

Matsuzaki, M., Misumi, O., Shin, I.T., Maruyama, S., Takahara, M., Miyagishima, S.Y., Mori, T., Nishida, K., Yagisawa, F., Nishida, K., Yoshida Y., Nishimura Y, Nakao S, Kobayashi T, Momoyama Y, Higashiyama T, Minoda, A, Sano, M., Nomoto, H., Oishi, K. *et al* (2004) Genome sequence of the ultrasmall unicellular red alga *Cyanidioschyzon merolae* 10D. *Nature* **428:** 653-657.

McElver, J., Tzafrir, I., Aux, G., Rogers, R., Ashby, C., Smith, K., Thomas, C., Schetter, A., Zhou, Q., Cushman, M.A., Tossberg, J., Nickle, T., Levin, J.Z., Law, M., Meinke, D., Patton, D. (2001) Insertional mutagenesis of genes required for seed development in *Arabidopsis thaliana*. *Genetics* **159**:1751-63.

MacRae, I.J., Sege,l I.H. (1999) Adenosine 5'-phosphosulfate (APS) kinase: diagnosing the mechanism of substrate inhibition. *Arch Biochem Biophys* **361:** 277-282.

Meinke, D.W. (1982) Embryo-lethal mutants of *Arabidopsis thaliana*: evidence for gametophytic expression of the mutant genes. *Theor Appl Genet* **63:** 381–386.

Meinke, D.W. (1985) Embryo-lethal mutants of *Arabidopsis thaliana*: analysis of mutants with a wide range of lethal phases. *Theor Appl Genet* **69:** 543–552.

Meinke, D. W., M. Sussex, I. M. (1979) Isolation and characterization of six embryo-lethal mutants of *Arabidopsis thaliana*. Dev. Biol. **72**: 62-72.

Meinke, D.W. (1986), Embryo lethal mutants and the study of plant embryo development. *Oxford Surv. Plant Mol. Cell Biol*. **3**: 122-165.

Merkamm, M., Chassagnole, C., Lindley, N.D., Guyonvarch, A. (2003) Ketopantoate reductase activity is only encoded by *ilvC* in *Corynebacterium glutamicum*. *J Biotechnol*.**104**: 253-60.

Merkel, W.K., Nichols, B.P. (1996) Characterization and sequence of the *Escherichia coli panBCD* gene cluster *FEMS Microbiol. Letters* **143**: 247-252.

Miller, S. L., G. Schlesinger (1993). Prebiotic syntheses of vitamin coenzymes: II. Pantoic acid, pantothenic acid, and the composition of coenzyme A. *J. Mol. Evol*. **36**:308–314.

Miyatake, K., Nakano, Y., Kitaoka, S., (1979) Pantothenate synthetase from *Escherichia coli Methods enzymol.* **62**: 215-219.

Monod, J., Wyman, J., Changeux, J.P. (1965) On the nature of allosteric transitions: a plausible model. *J. Mol. Biol.* **12:** 88-118.

Moriya, T., Hikichi, Y., Moriya, Y., Yamaguchi, T. (1997) Process for producing D-pantoic acid, D-pantothenic acid or salts thereof. Patent No. WO 97/10340.

Nawarth, C., Poirier, Y., Somerville, C. (1994) Targeting of the polyhdroxybutyrate biosynthetic pathwat to the plastids of *Arabidopsis thaliana* results in high levels of polymer accumulation. *Proc. Natl. Acad. Sci*. *USA* **91**: 12760- 12764.

Neuburger, M., Day, D. A., Douce, R. (1984) Transport of co-enzyme A in plant mitochondria. *Arch. Biochem. Biophys*. **229**: 253-258.

Nishiyama, T., Fujita, T., Shin, T., Seki, M., Nishide, H., Uchiyama, I., Kamiya, A., Carninci, P., Hayashizaki, Y., Shinozaki, K., Kohara, Y., Hasebe, M. (2003) Comparative genomics of *Physcomitrella patens* gametophytic transcriptome and *Arabidopsis thaliana*: implication for land plant evolution. *Proc Natl. Acad. Sci. USA* **100:** 8007-8012.

Nurmikko, V., Salo, E., Hakola, H., Makinen, K., Snell E.E. (1966) The bacterial degradation of pantothenic acid. II Pantothenate hydrolase. *Biochemistry* **5:**399-402.

Ottenhof, H.H., Ashurst, J.L., Whitney, H.M., Saldanha, S.A., Schmitzberger, F, Gweon, H.S., Blundell, T.L., Abell, C., Smith, A.G., (2004) Organisation of the pantothenate (vitamin B5) biosynthesis pathway in higher plants. *Plant* J. **37**:61-72.

Parinov, S., Sevugan, M., Ye, D., Yang, W., Kumaran, M., and Sundaresan, V. (1999). Analysis of flanking sequences from Dissociation insertion lines: A database for reverse genetics in Arabidopsis. *Plant Cell* **11:** 2263–2270.

Parinov, S. and Sundaresan, V. (2000) Functional genomics in Arabidopsis: Large-scale insertional mutagenesis complements the genome sequencing project. *Curr. Opin. Biotechnol*. **11:** 157–161.

Patton, A.D., Schetter, A.L., Franzmann, L.H., Nelson, K., Ward, E.R., Meinke, D.W. (1998) An embryo-defective mutant of Arabidopsis disrupted in the final step of biotin synthesis. *Plant Physiol*. **116**: 935-946.

Perez-Espinosa, A., Roldan-Arjona, T., Ruiz-Rubio, M. (2001) Pantothenate synthetase from *Fusarium oxysporum* f. sp. lycopersici is induced by alpha-tomatine. *Mol. Genet. Genomics* 265: 922-929.

Pfleiderer, G., Kreiling, A., Wieland, T. (1960) On pantothenic acid synthetase from *E. coli*. I. Concentration with the aid of an optical test. *Biochem Z.* **333**:302-307.

Powers, S.G., Snell, E.E. (1976) Ketopantoate hydroxymethyltransferase. II. Physical, catalytical and regulatory properties. *J. Biol. Chem*. **251**: 3786-3793.

Primerano, D. A., Burns, R. O. (1983) Role of acetohydroxy acid isomeroreductase in biosynthesis of pantothenic acid in *Salmonella typhimurium*. *J Bacteriol*. **153**: 259–269.

Raman, S. B., Rathinasabapathi, B. (2004) Pantothenate synthesis in plants. *Plant Science **167***:961-968.

Ramjee, M.K., Geschel. U., Abell, C., Smith, A.G. (1997) *Escherichia coli* L-aspartate-α-decarboxylase: preprotein processing and observation of reaction intermediates by electrospray mass spectrometry *Biochem. J*. **323**: 661-669.

Rathinasabapathi, B. (2002) Propionate, a source of β-alanine, is an inhibitor of β-alanine methylation in *Limonium latifolium*, *Plumbaginaceae J. Plant. Physiol*. **159**: 671-674.

Rathinasabapathi, B., Raman, S.B. (2005) Exogenous supply of pantoyl lactone to excised leaves increases their pantothenate levels. *Ann Bot (Lond)* **95**(6):1033-7.

Ravanel, S., Cherest, H., Jabrin, S., Grunwald, D., Surdin-Kerjan, Y., Douce, R., Rebeille, F. (2001) Tetrahydrofolate biosynthesis in plants: molecular and functional characterization of dihydrofolate synthetase and three isoforms of folylpolyglutamate synthetase in *Arabidopsis thaliana*. *Proc. Natl. Acad. Sci. U S A*. **18**:15360-15365.

Recsei, P.A., Huynh, Q.K., Snell, E.E. (1983) Conversion of prohistidine decarboxylase to histidine decarboxylase: peptide chain cleavage by nonhydrolytic serinolysis. *Proc. Natl. Acad. Sci. USA* **80**: 973-977.

Ricard, J., Cornish-Bowden, A. (1987) Co-operative and allosteric enzymes: 20 years on. Eur J Biochem. 1987 Jul 15:166(2):255–272.

Rock, C.O., Park, H.W., Jackowski, S. (2003) Role of feedback regulation of pantothenate kinase (CoaA) in control of coenzyme A levels in *Escherichia coli*. *J. Bacter.*, **185**: 3410-3415.

Rubio, S., Larson, T.R., Gonzalez-Guzman, M., Alejandro, S., Graham, I.A., Serrano, R., Rodriguez, P.L. (2006) An Arabidopsis mutant impaired in coenzyme A biosynthesis is sugar dependent for seedling establishment. *Plant Physiol*. **140**: 830-43.

Sahi, S. V., Saxena, P. K., Abrahams, G. D., King, J., (1988) Identification of the biochemical lesion in a pantothenate-requiring auxotroph *Datura innoxia* P. Mill. *J. Plant Physiol*. **133**: 277-280.

Saldanha, S.A., Birch, L.M., Webb, M.E., Nabbs, B.K., von Delft, F., Smith, A.G., Abell, C. (2001) Identification of Tyr58 as the proton donor in the aspartate-α-decarboxylase reaction. *Chem. Commun.* 1760-1761.

Sahm, H., Eggeling, L. (1999) D-Pantothenate Synthesis in *Corynebacterium glutamicum* and Use of *panBC* and Genes Encoding l-valine synthesis for D-pantothenate overproduction. *Appl. Environ. Microbiol*. **65**: 1973–1979.

Sambrook, J., Russell, D. W. (2001) Molecular cloning: a labolatory manual 3rd Ed. *Cold Spring Harbor Laboratory Press, Cold Spring Harbor, New York.*

Savage, L.J., Post-Beittenmiller, D. (1994) Phosphopantethenylated precursor acyl carrier protein is imported into spinach (*Spinacia oleracea*) chloroplasts. *Plant Physiol*. **104**: 989-995.

Schmitzberger, F., Kilkenny, M.L., Lobley, C.M., Webb, M.E., Vinkovic, M., Matak-Vinkovic, D., Witty, M., Chirgadze, D.Y., Smith, A.G., Abell, C., Blundell, T.L. (2003) Structural constraints on protein self-processing in L-aspartate-alpha-decarboxylase. *EMBO J*. **22**:6193-204.

Schneider, T., Dinkins, R., Robinson, K., Shellhamme, J., Meinke, D.W. (1989) An embryo-lethal mutant of *Arabidopsis thaliana* is a biotin auxotroph. *Dev. Biol.* **131:** 161–167.

Shellhammer, J., Meinke, D. (1990) Arrested embryos from the *bio1* auxotroph of *Arabidopsis thaliana* contain reduced levels of biotin. *Plant Physiol*. **93**: 1162–1167.

Scholl, R., Rivero, L., Crist, D., Ware, D., Davis, K. (1999) Progress of ABRC in obtaining new T-DNA stocks and preparing DNA from T-DNA populations for PCR screening**.** 10th International Conference on Arabidopsis Research: 4–8 July; The University of Melbourne, Australia. Abstracts can be downloaded from http://www.arabidopsis.org/abstract_australia.pdf

Schrick, K., Mayer, U., Horrichs, A., Kuhnt, C., Bellni, C. *et al*. (2000) FACKEL is a sterol C-14 reductase required for organized cell division and expansion in Arabidopsis embryogenesis. *Genes Dev*. **14**: 1471-1484.

Schulz, A.R. (1994) Non-hyperbolic enzyme kinetics. In *Enzyme Kinetics*, pp 133-165. Cambridge University Press.

Segel, I.H. (1975) *Enzyme Kinetics*. John Wiley & Sons, Inc, New York, USA.

Sessions, A., Burkea, E., Presting G., McElver, J., Patton, D., Dietrich, B., Hoa, P., Bacwaden, J., Ho, C., Clarke, J. D., Cotton, D., Bullis, D., Snell, Miguel, T. J., Hutchison, D., Kimmerly, B., Mitzel, T., Katagiri, F., Glazebrook, J., Law, M.,. Goff , S. A., (2002) A High-Throughput Arabidopsis Reverse Genetics System. *The Plant Cell*, **14**: 2985-2994.

Shimizu, S., Kataoka, M., Chung, M. C., Yamada, H. (1988) Ketopantoic acid reductase of *Pseudomonas maltophilia* 845. Purification, characterization, and role in pantothenate biosynthesis. *J. Biol. Chem.* **263**: 12077-12084.

Smith, C.M., Song, W.O. 1996 Comparative nutrition of pantothenic acid. *J. Nutr. Biochem*. **7**: 312-321

Sorokin, A., Azevedo, V., Zumstein, E., Galleron, N., Ehrlich, S.D., Serror, P,. **(**1996). Sequence analysis of the *Bacillus subtilis* chromosome region between the *serA* and *kdg* loci cloned in a yeast artificial chromosome. *Microbiology* **142:**2005–2016.

Speulman, E., Metz, P., van Arkel, G., B., Steikema, W.J., Pereira, A. (1999). A two component *Enhancer-Inhibitor* transposon mutagenesis system for functional analysis of the Arabidopsis genome. *Plant Cell* **11:** 1853–1866.

Springer, P.S., Holding, D.R., Groover, A., Yordan, C., Martienssen, R.A. (2000) The essential Mcm7 protein PROLIFERA is localized to the nucleus of dividing cells during the G1 phase and is required maternally for early Arabidopsis development. *Development* **127**: 1815–1822.

Springer, P. S., McCombe, W. R., Sundaresan, V., Martienssen, R. A. (1995) Gene trap tagging of PROLIFERA, an essential *MCM2-3-5*-like gene in Arabidopsis. *Science* **268**: 877-880.

Stam, M., Mol, J.M.N., Kooter, J.M. (1997) The silence of genes in transgenic plants. *Annals of Botany* **79**: 3-12.

Stolz, J. and Sauer N. (1999) The fenpropimorph resistance gene *FEN2* from *Saccharomyces cerevisiae* encodes a plasma membrane H+-pantothenate symporter. *J Biol Chem* **274**: 18747–18752.

Stolz, J., Caspari, T., Carr, A.M. and Sauer N. (2004) Cell division defects of *Schizosaccharomyces pombe* liz1– mutants are caused by defects in pantothenate uptake. *Eukaryot Cell* **3**: 406–412.

Stryer, L. (1988) Control of enzymatic activity, p. 233–259. *In* L. Stryer (ed.), Biochemistry, 3rd ed. W. H. Freeman & Co., New York, N.Y.

Studier, F.W. and Mofat, B.A. (1986) Use of bacteriophage T7 RNA polymerase to direct selective high-level expression of cloned genes. *J. Mol. Biol.* **189:** 113-130.

Sussman, M.R., Amasino, R.M., Young, J.C., Krysan, P.J., and Austin-Phillips, S. (2000) The Arabidopsis knockout facility at the University of Wisconsin-Madison. *Plant Physiol*. **124:** 1465–1467.

Teller, J.H., Powers, G.S., Snell, E.E. (1976) Ketopantoate hydroxymethyltransferase. I. Purification and role in pantothenate biosynthesis ", *J. Biol. Chem*. **251**: 3780-3785.

Tilton, G.B., Wedemeyer, W.J., Browse, J., Ohlrogge, J. (2006) Plant coenzyme A biosynthesis: characterization of two pantothenate kinases from Arabidopsis. *Plant Mol. Biol*. **61**:629-642.

Tissier, A.F., Marillonnet, S., Klimyuk, V., Patel, K., Torres, M.A., Murphy, G., and Jones, J.D. (1999) Multiple independent defective *Suppressor-mutator* transposon insertions in Arabidopsis: A tool for functional genomics. *Plant Cell* **11:** 1841–1852.

Tsugeki, R., Kochieva, E. Z., Fedorof, N. V. (1996) A transposon insterion in the Arabidopsis SSR16 gene causes an embryo-defective lethal mutation. *Plant J*. **10**: 479-489.

Tzafrir, I., Pena-Muralla, R., Dickerman, A., Berg, M., Rogers, R., Hutchens, S., McElver, J., Aux, G., Patton, D., Meinke, D. (2004) Identification of genes required for embryo development in Arabidopsis. *Plant Physiol*. **135**:1206-20.

Vallari, D.S. and Rock C.O. (1985) Pantothenate transport in *Escherichia coli. J. Bacteriol*., **162:** 1156–1161.

Vallari, D.S., Rock C.O. (1985) Isolation and characterization of *Escherichia coli* pantothenate permease (panF) mutants. *J Bacteriol.* **164**: 136–142.

Villari, D.S., Jackowski, S., Rock, C.O. (1987) Regulation of pantothenate kinase by coenzyme A and its thioesters *J. Biol. Chem.*, **262**: 2468-2471.

Vallari, D.S., Jackowski, S. (1988) Biosynthesis and degradation both contribute to the regulation of coenzyme A content in *Escherichia coli*. *J. Bacteriol*. **170**: 3961–3966.

von Delft, F., Lewendon, A., Dhanaraj, V., Blundell, T.L., Abell, C., Smith, A.G. (2001) The crystal structure of *E. coli* pantothente synthetase confirms it as a member of the cytidylyltransferase superfamily. *Structure* **9**: 439-450.

von Delft, F., Lewendon, A., Dhanaraj, V., Blundell, T.L., Abell, C., Smith, A.G. (2001) The crystal structure of *E. coli* pantothente synthetase confirms it as a member of the cytidylyltransferase superfamily. *Structure* **9**: 439-450.

von Delft F.*et al*. (2003), "Structure of *E. coli* ketopantoate hydroxymethyl transferase complexed with ketopantoate and Mg^{2+}, solved by locating 160 selenomethionine sites", *Structure* **11**: 985-996.

Wang, S., Eisenberg, D. (2003) Crystal structures of a pantothenate synthetase from *M. tuberculosis* and its complexes with substrates and a reaction intermediate. *Protein Sci* **12:** 1097-1108.

Wang, S., Eisenberg, D. (2006) Crystal structure of the pantothenate synthetase from *Mycobacterium tuberculosis*, snapshots of the enzyme in action. *Biochemistry* **45:** 1554-1561.

Webb, M.E., Smith, A.G., Abell, C. (2004) Biosynthesis of pantothenate. *Nat Prod Rep*. **21**: 695-721.

White, W.H., Gunyuzlu, P.L. and Toyn, J.H. (2001) *Saccharomyces cerevisiae* is capable of de novo pantothenic acid biosynthesis involving a novel pathway of β-alanine production from spermine *J. Biol. Chem.* **276**: 10794–10800.

Wieland, T., Loewe, W., Kreiling, A., Pfleiderer, G. (1963) [On pantothenic acid synthetase from *E. coli*. V. Pantoyladenylate as the acylating component in the enzymatic synthesis of pantothenic acid.] *Biochem Z* **339:** 1-7.

Williams, L., Zeng, R., Blanchard, J.S., Rauschel, F. M., (2003) Positional isotope exchange analysis of the pantothenate synthetase reaction. *Biochemistry*, **42**: 5108-5113.

Williamson, J.M., Brown, G.M. (1979) Purification and properties of L-Aspartate-alpha-decarboxylase, an enzyme that catalyzes the formation of beta-alanine in *Escherichia coli*. *J. Biol. Chem.* **254**: 8074-8082.

Wilson, F., Dennis, P., Hall, C., Kincaid, J., Kitchingman, S., Searle, K., Walsh, S., May, S. **N**.A.S.C. (Nottingham Arabidopsis Stock Centre). *10th International Conference on* Arabidopsis *Research: 1999 4–8 July; The University of Melbourne, Australia.* Abstracts can be downloaded from http://www.arabidopsis.org/abstract_australia.pdf

Winkler, R., Frank, M., Galbraith, D., Feyereisen, R., and Feldmann, K. (1998) Systematic reverse genetics of transfer-DNA-tagged lines of Arabidopsis. *Plant Physiol*. **118:** 743–750.

Xu, X.M., Moller, S.G. (2006) AtSufE is an essential activator of plastidic and mitochondrial desulfurases in Arabidopsis. *EMBO J*. 4: 900-909.

Yang, L.M., Fernandez, M.D., Lamppa, G.K. (1994) Acyl carrier protein (ACP) import into chloroplasts. Covalent modification by a stromal holoACP synthase is stimulated by exogenously added CoA and inhibited by adenosine 3', 5'-bisphosphate. *Eur J Biochem* **224**:743–750

Zheng, R., Blanchard, J.S. (2000) Identification of active sites residues in *E. coli* ketopantoate reductase by mutagenesis and chemical rescue *Biochemistry* **39**: 16244-16251.

Zheng, R., Blanchard, J.S. (2000) Kinetic and mechanistic analysis of the *E. coli panE*-encoded ketopantoate reductase. *Biochemistry* **39**: 3708-3717.

Zheng, R., Blanchard, J.S. (2001) Steady-state and pre-steady-state kinetic analysis of *Mycobacterium tuberculosis* pantothenate synthetase. *Biochemistry* **40:** 12904-12912.

Zheng, R., Dam, T.K., Brewer, C.F,, Blanchard, J.S. (2004) Active site residues in *Mycobacterium tuberculosis* pantothenate synthetase required in the formation and stabilization of the adenylate intermediate. *Biochemistry* **43:** 7171-7178.

Zimmermann, P., Hirsch-Hoffmann, M., Hennig, L., Gruissem, W. (2004) GENEVESTIGATOR. Arabidopsis Microarray Database and Analysis Toolbox. *Plant Physiol.* **136**: 2621-2632